Genetic Manipulation of Stomatal Patterning and Function to Optimise Leaf Gas Exchange

William Atkinson

Thesis submitted for the degree of
Doctor of Philosophy

School of Life Sciences
01/10/25
University of Essex

Abstract

Global food security depends on crops with enhanced productivity and resilience under increasingly variable environments to meet the growing demand. Photosynthetic carbon assimilation, a key determinant of yield, is often constrained by stomatal conductance, which governs CO_2 uptake and water loss. Under natural fluctuating light, slow stomatal responses cause lost carbon gain during increases and excess water loss during decreases, making stomatal behaviour a critical target for improving photosynthetic and water-use efficiency. This thesis investigates whether manipulating stomatal traits can alleviate diffusional limitations in strawberry (*Fragaria* × *ananassa*) and tobacco (*Nicotiana tabacum*).

Transgenic strawberry lines were generated to overexpress STOMAGEN (increasing stomatal density), guard cell-targeted Hexokinase (reinforcing closure), and both constructs. Complementary tobacco studies were carried out in two parts: lines overexpressing STOMAGEN, ictB (enhancing carbon assimilation), and their combination; and lines with guard cell-specific Hexokinase, plasma membrane H^+-ATPase (AHA2), and their combination to assess synergistic impacts on stomatal dynamics.

STOMAGEN increased stomatal density and clustering but did not enhance conductance, with clustering impairing responses. Hexokinase had little effect in strawberry, except partially rescuing stomatal response times in clustered lines, but in tobacco accelerated stomatal responses and photosynthetic induction. ictB improved PSII efficiency, with some additional enhancement observed in combination with STOMAGEN. AHA2 reduced photosynthesis and biomass without altering conductance

or kinetics. Most combinations showed no advantage over controls, with benefits being strongly environment-dependent and often failing to persist across generations.

These findings reveal the trade-offs of manipulating stomatal traits across species. The thesis highlights both the opportunities and constraints of engineering stomatal development and guard cell function as a strategy to improve carbon assimilation and water-use efficiency, providing a framework for future crop optimisation.

Acknowledgements

I would first like to express my deepest gratitude to my supervisors, Prof. Tracy Lawson, Dr. Andrew Simkin, and Dr. Graham Dow, for their guidance, support, and encouragement throughout my PhD. Their expertise, advice and guidance have been invaluable in shaping both this thesis and my development as a researcher.

I am also grateful to the staff and students at NIAB East Malling, whose technical assistance, resources, and camaraderie made much of this work possible. In particular, I would like to thank Erick Oliveria and Alexander Williams, both of whom I spent the first two years of this journey side by side with. At the University of Essex, I would like to thank the Plant Productivity group and fellow students for their insight, collaboration, and friendship during my time in the lab and beyond. In particular, I would like to thank Mengjie Fan and Piotr Kasznicki, whose friendship, support and guidance made my time at the university productive and enjoyable.

Finally, I owe the greatest thanks to my fiancée, whose patience, love, and constant support carried me through the most challenging moments of this journey.

Table of Contents

1. Introduction

1.1. The Need For Crop Improvement

1.1.1. Meeting The Calorie Demand Of The Growing Population

The global population is set to reach nearly 10 billion people by 2050, and thus crop production must increase alongside it to ensure food security (United Nations, 2019). To ensure food security, the yields of some staple crops, like wheat and rice, will have to increase by 70 – 100% to provide adequate supplies (FAO, 2015; Tilman and Clark, 2015). Food security is one of the pillars of a stable society, and the crop yield increase that we have experienced over the last 50 years has not only allowed for the rapid expansion of the global population but also been an effective tool for reducing poverty (Gulati, Fan and Dalafi, 2005; Pingali, 2012; Barrett, 2014). The reductions in poverty can be attributed to the resultant lowering of food prices from increased food production (Mehta, 2018). Global average caloric intake has increased in accordance with greater food availability due to reduced prices, which has been beneficial for the population in terms of health and life expectancy (Evenson and Gollin, 2003). The prevailing consensus within the scientific community is that increasing crop yields, rather than expanding arable land, is the most sustainable direction to meet the calorie demand of the growing population (Green *et al.*, 2005; Matson and Vitousek, 2006; Foley *et al.*, 2011; Phalan, Balmford, *et al.*, 2011; Phalan, Onial, *et al.*, 2011; Tscharntke *et al.*, 2012; Hulme *et al.*, 2013). Crop yield increases cannot be majorly focused on

increasing the yield of staple crops, as they may be rich in calories but are quite poor in micronutrient content (Graham, Welch and Bouis, 2001; Welch and Graham, 2004; Mayer, Pfeiffer and Beyer, 2008). The production of non-staple micronutrient-rich foods, such as fruits and vegetables, has not increased recently and their prices have risen, decreasing the nutrition available to poorer communities (Bouis, Eozenou and Rahman, 2011; Simkin, 2019). This demonstrates the need for further research into improving non-staple food crop productivity, ensuring cost reductions and greater availability of nutrition for everyone.

1.1.2. Addressing Hidden Hunger

Simply increasing the global calorie availability is insufficient to ensure an adequate quality of life for people around the world. Micronutrient deficiencies, often referred to as the 'Hidden Hunger', affect over 2 billion people and can have severe consequences on human health and can directly or indirectly lead to death (FAO, 2015; Hodge, 2016). Micronutrient deficiencies are most prevalent in developing countries, with pregnant women and children being the most vulnerable groups (Black *et al.*, 2013; Bailey, West and Black, 2015; Ritchie and Roser, 2017). Iron, iodine, folate, vitamin A, and zinc deficiencies are the most widespread micronutrient deficiencies and contribute to poor growth, intellectual impairment, perinatal complications, and increased risk of morbidity and mortality (Bailey, West and Black, 2015). For example, folate deficiency causes megaloblastic or macrocytic anaemia and increases the likelihood of pregnancies affected by neural tube defects (Bailey, West and Black, 2015;

Khan and Jialal, 2021). Folate deficiency in pregnancy has also been associated with low birth weight, preterm delivery, and foetal growth retardation (de Benoist, 2008; Tamura *et al.*, 2010). Another common micronutrient deficiency in low-income regions is Vitamin C deficiency. Vitamin C deficiency causes fatigue, lethargy, and mood changes (Mitra, 1971; Léger, 2008). Extreme Vitamin C deficiency can result in clinical scurvy, which is fatal if left untreated (Crandon, Lund and Dill, 2009). Vitamin C is also linked to proper immune function, with deficiencies possibly influencing the spread and severity of infectious disease (Thomas and Holt, 1978; Maggini, Wenzlaff and Hornig, 2010). Fruits are a food group that can be particularly high in micronutrients that are commonly deficient in the global population. Strawberries are high in both folate and Vitamin C, thus increasing the availability of the fruit and increasing the micronutrient content of the fruit could be a pragmatic effort to address this issue. It is imperative to address the Hidden Hunger that affects the most vulnerable people in the poorest countries to ensure them an adequate quality of life.

1.1.3. The Potential Effects Of Climate Change On Global Crop Production

Anthropogenic elevations in atmospheric carbon dioxide concentrations and the resultant changes to global climate will likely have dramatic effects on crop production. Atmospheric [CO_2] is forecast to reach 550 ppm by 2050 from the 420 ppm today (le Quéré *et al.*, 2009). This rise in atmospheric [CO_2] is predicted to produce a further 2 °C increase in global temperature, which will be accompanied by increased frequency and

severity of extreme weather conditions, droughts being of the greatest concern regarding crop production (Solomon *et al.*, 2007; Field and Barros, 2014). The rising temperature is predicted to decrease the grain yield of the staple crop wheat (Asseng *et al.*, 2015). Parry *et al*. (2004) suggested that the yield decrease caused by rising global temperatures may be offset by rising [CO_2], supported by evidence showing that increased [CO_2] can have a protective effect against heatwaves in semi-arid regions, actually increasing yield (Parry *et al.*, 2004; Fitzgerald *et al.*, 2016). Elevated [CO_2] in soybean, however, was unable to mitigate the yield losses caused by drought (Gray *et al.*, 2016). This evidence suggests that the effects of climate change will be differential based on a wide range of factors including crop species, region and local climate. Genetically improving photosynthesis in soybean has been shown to maintain seed yields under heat stress when grown under elevated [CO_2] (Köhler *et al.*, 2017). Genetically improving photosynthesis could aid in mitigating yield loss as a result of the predicted elevated temperatures of the future.

1.1.4. Summary

This introduction will explore how crop yields can be increased through the genetic enhancement of photosynthetic carbon assimilation, with a specific focus on the cultivated strawberry, *Fragaria x ananassa,* as an example of a commercially relevant and nutrient-rich crop to not only meet the calorie needs of the growing population but also address its micronutrient needs. Firstly, current successful genetic enhancements of photosynthesis will be described, after which new approaches to improve

photosynthesis through changes in stomatal density, as well as how changes to stomatal function could affect leaf gas exchange will be explored. The potential effect of such changes will be investigated using plants grown under elevated atmospheric CO_2 concentrations as a proxy for the genetic enhancement of photosynthesis. Finally, the research aims of this thesis will be outlined.

1.2. Efforts To Improve Crop Production

1.2.1. The Green Revolution And Its Plateau

Since the 1960's there has been a significant increase in crop productivity commonly referred to as the Green Revolution (Pingali, 2012). The rise in productivity has been in line with the population demand and has facilitated the exponential growth in the human population. One of the major contributors to the boom in productivity during the Green Revolution was the introduction of dwarfing traits into cereal crops, providing shorter, stronger stems that prevented the crops from lodging, allowing for greater grain yield (Hedden, 2003). The application and optimisation of synthetic fertiliser and pesticide regimes were also in part responsible for the increase in yield, however, the large dose application of fertiliser and pesticides had unforeseen consequences in terms of ecological damage, such as eutrophication and loss of species diversity (Pimentel *et al.*, 1992; Barrett, 1996; Matson *et al.*, 1997; Mineau, 2005; Mosier, Syers and Freney, 2013). The rate of increase in crop yield has declined between the periods of 1960-1980 to 1981-2000 in all regions except sub-Saharan Africa (Evenson and Gollin, 2003). This is of particular concern as it highlights the

plateauing of crop yield increases and that current yield increases are insufficient to meet the demand of the growing population (Ray *et al.*, 2013). Thus, action must be taken toward finding new ways to increase crop productivity rather than expanding farmed land to avoid further environmental damage (Green *et al.*, 2005; Matson and Vitousek, 2006; Foley *et al.*, 2011; Phalan, Balmford, *et al.*, 2011; Phalan, Onial, *et al.*, 2011; Tscharntke *et al.*, 2012; Hulme *et al.*, 2013).

1.2.2. Genetic Enhancement Of Photosynthesis

Crop productivity can be further improved through increasing photosynthetic carbon assimilation. Many of the parameters regarding biomass accumulation through photosynthesis are near their theoretical maxima, leaving the conversion efficiency, found to be only 30% of its theoretical maximum, to be the main target for yield improvement (Morgan *et al.*, 2005; Long *et al.*, 2006; Dermody *et al.*, 2008; Zhu, Long and Ort, 2010). A great body of literature regarding the genetic enhancement of photosynthetic carbon assimilation, with many avenues of research including but not limited to: protein/enzyme overexpression in the CBC, photorespiration and electron transport, and engineering C4 photosynthesis in C3 plants (please refer to these reviews for the protein/enzyme overexpression (South et al., 2018; Simkin, 2019; Simkin, López-Calcagno and Raines, 2019; Weber and Bar-Even, 2019) and research outlining strategies for C4 photosynthesis engineering (Schuler, Mantegazza and Weber, 2016; Yuanyuan Li *et al.*, 2017) for comprehensive reporting on the respective topics).

Genetically enhancing photosynthetic carbon assimilation by overexpressing key enzymes involved in the CBC has been a successful avenue of research in model and crop species alike. The rate-limiting steps of the CBC have been identified through computational modelling and gene knockout analysis on photosynthetic rates. A model developed by Zhu et al., (2007) predicted the enzyme concentrations needed to maximise photosynthesis, revealing the amounts of CBC enzymes SBPase and FBPA need to be increased (Zhu, de Sturler and Long, 2007). Furthermore, antisense studies of tobacco with reduced levels of SBPase showed that only slight reductions in enzymatic activity (>9%) were sufficient to reduce the maximum carbon assimilation, photosynthesis, growth rates and yield in tobacco (*Nicotiana tobacum*) (Harrison *et al.*, 1997, 2001; Ölçer, Lloyd and Raines, 2001; Lawson *et al.*, 2006). FBPA knockdowns showed reduced biomass phenotypes in potato lines with FBPA activity reductions of over 50% (Haake *et al.*, 1998, 1999). Both *in silico* and in vivo studies demonstrate the importance of these two enzymes and thus have made them prime targets for overexpression to eliminate the rate limitation they impose on the CBC.

SBPase overexpression has increased plant biomass in a variety of species, including crop species. Depending on the growth conditions, plants of the model species *Arabidopsis thaliana* overexpressing SBPase had a maximum of 23% increased biomass and 53% increased seed yield at seed harvest (Simkin *et al.*, 2017). SBPase overexpression in tobacco resulted in up to a 30% increase in leaf area and biomass under greenhouse conditions (Lefebvre *et al.*, 2005). Furthermore, tobacco overexpressing SBPase showed differential increases in yield of 12% and 23% at

atmospheric and elevated [CO_2] of 585 ppm, respectively, clearly demonstrating the effects of enhanced carbon availability. In the staple crop rice (*Oryza sativa*), a tripling of biomass relative to WT was seen under elevated temperature and salt stress (Feng, Han, *et al.*, 2007; Feng, Wang, *et al.*, 2007). Wheat grain yield was also increased by up to 40% when overexpressing SBPase under glasshouse conditions (Driever *et al.*, 2017). In one of the only genetic enhancements of fruiting crops, SBPase overexpression in tomato increased vegetative biomass by 30% and also had early-onset flowering and tolerance to chilling stress (Ding *et al.*, 2016). Unfortunately, the authors did not report the effect of the overexpression on fruit yield, however, as will be discussed in Section 1.6, the 25% increase in photosynthesis reported would likely confer fruit yield increases demonstrated through the proxy of CO_2 enrichment studies (Islam, Matsui and Yoshida, 1996; Hicklenton and Jolliffe, 2011; Khan, Azam and Mahmood, 2013). The literature regarding FBPA overexpression is not as extensive as SBPase, likely due to the smaller effect size it has on photosynthesis (Zhu, de Sturler and Long, 2007). Nonetheless, FBPA overexpression in Arabidopsis resulted in a maximum of 29% increase in biomass and a 36% increase in seed yield at seed harvest (Simkin *et al.*, 2017). Furthermore, tobacco overexpressing FBPA had up to 30% increased biomass at ambient [CO_2] and up to 120% increased biomass at elevated [CO_2] of 700 ppm (Uematsu *et al.*, 2012). This again clearly demonstrates the beneficial effect that increased carbon availability would have on plants overexpressing CBC enzymes.

The overexpression of multiple genes to enhance photosynthetic carbon assimilation has the potential to vastly exceed the yield benefits of their respective single gene overexpression, making multigene overexpression an excellent strategy to

maximise the yield benefits gained. In tobacco, the simultaneous constitutive overexpression of SBPase, FBPA and the cyanobacterial putative inorganic carbon transporter B, ictB, produced a maximal increase in dry weight of 103%, which was much greater than any of the other single gene and different combinations of double gene overexpression (Simkin *et al.*, 2015). The simultaneous leaf tissue-specific overexpression of SBPase, FBPA and the photorespiratory glycine decarboxylase-H protein in Arabidopsis resulted in a 71% increase in dry weight and a maximal increase in seed yield of 62%, again far exceeding any of the single gene overexpressions (Simkin *et al.*, 2017). Additionally, the simultaneous constitutive overexpression of the bifunctional FBP/SBPase (FBP/SBPase) and the algal cytochrome c_6 in tobacco increased above-ground biomass by 27% in field conditions, where their respective individual gene overexpression showed no significant difference to the controls (López-Calcagno et al., 2020). Interestingly, in the double gene overexpression, the authors found that at light intensities over 1000 µmol m^{-2} s^{-1}, stomatal conductance (g_{sw}) was significantly reduced, leading to an increase in intrinsic water use efficiency. Multigene overexpression of genes within the CBC and other genes implicated in improving photosynthesis appears to have a synergistic effect in improving favourable outcomes, such as increased yield, more so than simply overexpressing multiple genes in the CBC. This might suggest that targeting multiple genes involved in different photosynthetic processes may be more beneficial than only focusing on one process.

1.2.3. Alternative Methods Of Increasing Photosynthesis

RuBisCO, the enzyme responsible for the fixation of CO_2 in the CBC, is capable of both the desired carboxylation reaction and, in 25% of all reactions, fixes oxygen instead of CO_2, resulting in a toxic by-product, the processing of which results in CO_2 loss (Bauwe, Hagemann and Fernie, 2010; Peterhansel *et al.*, 2010). The incidence of the oxygenation reaction can make RuBisCO rate-limiting to the CBC (Parry *et al.*, 2013). A great deal of research has gone into resolving this inefficiency through genetic modification with varying degrees of success in terms of enhancing photosynthesis, such as increasing RuBisCO content, increasing RuBisCO's catalytic turnover rate, and both increasing and decreasing the rate of photorespiration (Suzuki *et al.*, 2007; Ishikawa *et al.*, 2011; South *et al.*, 2018). Modifying photorespiratory metabolism to reduce its negative impact on carbon assimilation has emerged as a promising approach to improving photosynthesis and plant productivity, as reviewed by South et al., 2018. Alternatively, when exposed to elevated atmospheric concentrations of CO_2, the rates of the carboxylation reaction increased, due to the greater availability of CO_2 (Sage, Way and Kubien, 2008). So in theory, if one could genetically increase the internal CO_2 concentration (C_i) in the leaf, then there would be increased rates of CO_2 fixation by RuBisCO, leading to a greater CO_2 assimilation rate (A).

One possible mechanism for doing so would be manipulating the stomatal density (SD) of the leaf, defined as the number of stomata per unit leaf area. The resistance of gas diffusion from the atmosphere to the chloroplast is one of the major limitations of A (Farquhar and Sharkey, 1982). Stomatal conductance (g_{sw}) is one of the major

determining factors of *A* (Wong, Cowan and Farquhar, 1979). Studies investigating the effect of increasing SD found that the leaves had greater g_{sw}, increased C_i and *A* than WT plants (Tanaka et al., 2013; Sakoda et al., 2020). The effect of SD on photosynthesis and biomass accumulation is controversial and appears to be somewhat dependent on the light intensity, with higher SD producing increased g_{sw} and *A* under high light conditions (Schlüter et al., 2003; Tanaka et al., 2013; Lawson and Blatt, 2014). Conversely, it has been reported that lowering SD produced higher growth rates and biomass production in constant light when the soil water content was limited, due to improved intrinsic water use efficiency (iWUE), the ratio of carbon gained through CO_2 assimilation and water lost via transpiration (Farquhar and Richards, 1984), and reduced metabolic cost of producing and maintaining the stomata (Doheny-Adams *et al.*, 2012). SD manipulation could prove an effective tool to enhance photosynthesis and plant growth, but will likely require optimisation depending on the environmental conditions and plant species to ensure maximal results. The full extent of manipulating SD will be thoroughly explored in the following section.

1.3. Manipulating Stomata To Improve Photosynthesis

1.3.1. Stomata Overview

Stomata are pores in the epidermal layer of cells of the aerial parts of plants, with the most frequent distribution found on leaves, the greatest densities being found on the lower abaxial side of leaves (Kirkham, 2014). The pore of a singular stoma is formed between a pair of kidney-shaped or dumbbell-shaped Guard cells (Kirkham,

2005). Stomata function to control the movement of gases between the external atmosphere and the internal leaf air spaces (Lawson and Morison, 2004). The guard cells control the stomatal aperture to maintain the optimal balance of CO_2 intake necessary for photosynthesis and water loss, which in combination determines the iWUE (Lawson et al., 2014; Hatfield and Dold, 2019). Plants must open their stomata to allow the influx of CO_2 for photosynthesis; however, water loss through transpiration is inevitable, with the vast majority of water a plant takes up (98%) being lost by evaporation (Morison, Stewart and Howell, 2003; Lawson, Caemmerer and Baroli, 2010).

Stomata open and close through changes in cell turgor (Heath, 1938). Generally, stomatal opening is in response to increasing or high light intensity, low [CO_2], high temperatures and low vapour pressure deficit (VPD). Change in guard cell turgor is driven by changes in osmolarity through the influx of organic and inorganic ions, such as K^+, Cl^-, $malate^{2-}$ and sucrose, that results in an influx of water into the cells (Heath, 1938; Fujino, 1967; Weyers, 1990; Willmer and Fricker, 1996; Blatt, 2000; Outlaw, 2010; Chen *et al.*, 2012; Hills *et al.*, 2012). In dark, low [CO_2] and high VPD conditions, the reverse happen, resulting in a loss of turgor and the closing of the aperture.

Stomatal function is measured as stomatal conductance (g_{sw}), defined as the maximum rate of gas flux through the stomata and measured as molar fluxes of water (mmol m^{-2} s^{-1})(Jeanguenin, Mir and Chaumont, 2017; Lawson and Vialet-Chabrand, 2019). Several stomatal characteristics dictate g_{sw}, including SD, stomatal aperture and pore depth, as well as environmental conditions, such as gas concentrations, relative

humidity and temperature that influence stomatal behaviour (Franks and Beerling, 2009; Lawson, Caemmerer and Baroli, 2010). Stomatal characteristics, such as density, size and distribution, vary between and within species, dependent on environmental growth conditions (Tichá, 1982; Weyers and Lawson, 1997; Weyers, Lawson and Peng, 1997). The fluctuations in environmental conditions will mean that g_{sw} will vary throughout the day (Buckley and Mott, 2013; Lawson, von Caemmerer and Baroli et al 2010). Under steady-state and non-limiting conditions, g_{sw} strongly correlates with *A* (Wong, Cowan and Farquhar, 1979). This has made stomatal gas diffusion an attractive target for engineering improved photosynthetic carbon assimilation due to the process being well understood in terms of physiology, physics, and multicellular patterning of the epidermis (Parlange and Waggoner, 1970; Farquhar and Sharkey, 1982; Lau and Bergmann, 2012; Tanaka et al., 2013).

1.3.2. Determining Epidermal Cell Fate- Epidermal Patterning Factor Genes

The epidermis of a plant shoot is comprised of multiple cell types, those being guard cells, pavement cells and trichome cells (Sachs, 1991). The meristemoid mother cell (MMC) lineage, from which guard cells are derived, are cells that are directly formed from a protodermal cell, which then begins to divide asymmetrically, forming the meristemoid and its sister cell (Geisler, Nadeau and Sack, 2000). Meristemoids are easily recognised due to their triangular shape and small size (Hara *et al.*, 2009). All cells derived from MMCs are known as stomatal lineage cells (Geisler, Nadeau and

Sack, 2000). Meristemoids can undertake amplifying divisions, where the cells perform one or two further rounds of asymmetrical division, resulting in a sister cell and another meristemoid. The meristemoid will go on to become an oval-shaped guard mother cell (GMC), which will itself divide symmetrically, forming a pair of guard cells (Hara *et al.*, 2009). The sister cell can undergo spacing cell divisions, where it will divide asymmetrically, producing a satellite meristemoid and its sister cell (Geisler, Nadeau and Sack, 2000; Nadeau and Sack, 2002; Bergmann and Sack, 2007). The sister cells are proliferative, producing pavement cells that make up the stomatal lineage ground cells (SLGCs) (Shpak *et al.*, 2005; Nadeau, 2009).

The patterning of stomata relies on cell-cell communication, with SD heavily relying on signals that promote or block the aforementioned asymmetric divisions defining stomatal development (Lampard, MacAlister and Bergmann, 2008). Epidermal patterning factor genes (EPFs) encode secreted peptide hormones with a conserved structure, having an N-terminal secretory signal peptide, followed by a predicted cleavage site and a mature peptide at the C-terminal end (Kondo *et al.*, 2010). EPFs play an important role in stomatal patterning and density, with their signals being mediated by a mitogen-activated protein kinase (MAPK) cascade (Bergmann, Lukowitz and Somerville, 2004; Wang *et al.*, 2007). EPFs are perceived by several receptors including three cell surface leucine-rich repeat receptor kinases, ERECTA (ER), ER-LIKE (ERL1) and ERL2, and one leucine-rich repeat receptor protein TOO MANY MOUTHES (TMM) that relay the signal into the cell (Nadeau and Sack, 2002; Shpak et al., 2005; Hara et al., 2007, 2009; Hunt and Gray, 2009; Abrash and Bergmann, 2010; Hunt, Bailey and Gray, 2010; Kondo et al., 2010; Sugano et al., 2009; Abrash, Davies and Bergmann,

2011; Lee et al., 2012; J. Lee et al., 2015; J. S. Lee et al., 2015; Lin et al., 2017; Qi et al., 2017).

EPF1 and EPF2 both act as negative regulators of stomatal development, with both having similar peptide structures and sharing the same receptors (J. Lee *et al.*, 2015; Lin *et al.*, 2017). EPF1 is expressed in late meristemoids, GMCs, and young guard cells and is involved in determining the plane of asymmetric cell division of meristemoids, as to follow the one-cell spacing rule (Geisler, Nadeau and Sack, 2000; Hara et al., 2007). EPF2 is expressed in early precursors, MMCs and early meristemoids, and acts to inhibit cells from adopting the MMC fate, which limits the number of MMCs (Hara *et al.*, 2009; Hunt and Gray, 2009). EPF1 associates with the ERL1–TMM receptor complex, and EPF2 associates with a preformed receptor complex consisting of ER and TMM (Lee *et al.*, 2012; Lin *et al.*, 2017; Qi *et al.*, 2017).

STOMAGEN/EPFL9 promotes stomatal development and is expressed in mesophyll cells (Hunt, Bailey and Gray, 2010; Kondo et al., 2010; Sugano et al., 2009; Ohki, Takeuchi and Mori, 2011; Lee et al., 2015; Lin et al., 2017). STOMAGEN and EPF2 directly compete for binding to the ER receptor complex, with STOMAGEN inhibiting the activation of downstream MAPK signalling that would inhibit stomatal development (Lee *et al.*, 2012; J. Lee *et al.*, 2015). STOMAGEN may also compete with EPF1 for the binding of ERL1, as the receptor can perceive STOMAGEN signalling (Qi *et al.*, 2017). The competitive binding of STOMAGEN with EPF1 and EPF2 to the same compartment created by the ER family and TMM is further supported by structural analysis (Lin *et al.*, 2017). External application of chemically synthesised STOMAGEN peptide retains its

function, promoting stomatal development and resulting in increased SD when plants were dipped into a solution containing the peptide (Kondo et al., 2010; Tanaka et al., 2013).

1.3.3. Using EPFs To Alter Plant Physiology

Changing the expression of the EPF genes can alter plant physiology and photosynthesis and can ultimately result in biomass changes. One of the prominent studies investigating the effects of increasing SD through overexpressing STOMAGEN is that of Tanaka et al. (2013). The authors investigated the effects of overexpressing STOMAGEN in Arabidopsis. In STOMAGEN overexpressing (ST-OX) lines, the authors found that SD was increased up to 372%, guard cells had significantly reduced cell length and stomatal Index (the percentage of total leaf cells that are stomata) was also increased compared to WT. ST-OX plants were shown to have significantly increased transpiration of 82%; however, there was only a trend towards decreased iWUE with no significant difference reported. In terms of photosynthesis, ST-OX had 72% increased g_{sw}, a parallel increase in C_i and under light-saturating conditions, the leaves had a 30% increase in *A*. Increased SD was also shown to affect the light response of photosynthesis under high light conditions, as ST-OX showed significant differences in *A* were seen in parallel at light intensities above 300 μmol $m^{-2}s^{-1}$ PPFD (photosynthetic photon flux density). The authors also found that the differences in *A* under ambient [CO_2] were not primarily due to carboxylation capacity, as the maximum carboxylation rate was not significantly enhanced in ST-OX; thus, the difference must be due to CO_2

diffusion. Additionally, the authors found a significant increase in maximum carboxylation rate in elevated [CO_2] conditions, which could be partially attributed to a non-significant increase in the electron transport rate. Interestingly, the 30% increase in *A* did not translate to significant differences in leaf area or whole plant biomass at 300 µmol $m^{-2}s^{-1}$ PPFD and ambient [CO_2]. The authors' concluding hypothesis was that higher SD resulted in a higher initial value of g_{sw} and then higher C_i, which would contribute to the rapid activation of RuBP regeneration and carboxylation in the CBC.

A follow-up study by Sakoda et al. (2020) was conducted to elucidate the effect of STOMAGEN overexpression and its increase in SD on Arabidopsis under fluctuating light (Sakoda *et al.*, 2020). In this study, the authors also included an EPF1 knockout line (*epf1*), which acted to produce a moderate increase in SD compared to ST-OX. ST-OX and *epf1* showed 268 and 46.5% higher SD than WT, guard cell length of ST-OX was 10% lower than that of WT, and the incidence of stomatal clustering was increased, over the near-zero in WT, in ST-OX and *epf1*, with ST-OX having greater clustering than *epf1*. ST-OX and *epf1* had higher g_{sw}, C_i, and *A*, as well as greater transpiration than WT at a high light intensity of 500 µmol $m^{-2}s^{-1}$ PPFD, resulting in lower iWUE. The higher SD lines, STO-OX and *epf1*, also had faster g_{sw} induction than the WT. The cumulative CO_2 assimilation in ST-OX was 58% higher, and in *epf1* was 79% higher than in the WT. Transpiration was also significantly higher, 194% in ST-OX and 139% in *epf1*. In terms of biomass, there was no significant difference in dry weight under constant light between ST-OX, *epf1* and WT, but under fluctuating light, *epf1* had 25.6% higher dry weight than WT, with no significant difference between ST-OX and WT. *Epf1* likely had higher cumulative CO_2 assimilation because having more stomata incurs a metabolic cost and

water uptake necessary for stomatal movement, potentially explaining the biomass increase seen with a moderate increase in SD shown by *epf1*. Fluctuating light conditions are more representative of field conditions, which could demonstrate that having a moderate increase in SD could produce greater biomass in well-watered conditions.

Alternatively, much research has focused on reducing stomatal density using epidermal patterning factor genes to improve iWUE. The overexpression of STOMAGEN antagonists, particularly EPF1, has been used to reduce SD and consequently improve iWUE. Overexpression of the native *Triticum aestivum* EPF1 in bread wheat reduced SD (Dunn *et al.*, 2019). Lines with a moderate reduction in SD reduced their water use whilst also maintaining *A*, leading to improved iWUE and maintaining yields similar to WT. Rice plants overexpressing OsEPF1 showed reduced SD, decreased g_{sw}, increased stomatal size, increased WUE and improved several measures of drought tolerance (Mohammed *et al.*, 2019). Rice with substantially reduced SD, produced again through EPF1 overexpression, had even greater drought tolerance (Caine *et al.*, 2019). The drought tolerance and reduced water loss should allow these plants to provide high yields in hotter, drier climates that are expected to be produced as a result of climate change. The ability to finely tune SD could provide an invaluable tool for designing crops that are specifically tailored to their growing environment to maximise productivity and minimise the influence of environmental factors.

1.3.4. Improving Stomatal Function

Understanding and exploiting natural variation in stomatal physiology and the mechanisms controlling this variation could be a useful tool when aiming to increase crop yields. Smaller stomata have been suggested to have faster movement kinetics, which would greatly aid in reducing the lag between mesophyll demands for CO_2 and stomatal response to these demands (Drake, Froend and Franks, 2013; Matthews, Vialet-Chabrand and Lawson, 2018). Stomata with slow movement kinetics respond poorly to dynamic environmental conditions, reducing their iWUE (Matthews, Vialet-Chabrand and Lawson, 2018). While changes in CO_2 demand occur within seconds, alterations in g_{sw} often take several minutes. This lag can substantially limit *A* and, under certain circumstances, result in decreased WUE (Barradas and Jones, 1996; Hetherington and Woodward, 2003; Lawson and Morison, 2004; Franks and Farquhar, 2007; Brodribb et al., 2009; Lawson, Caemmerer and Baroli, 2010; Vico et al., 2011; Lawson, Kramer and Raines, 2012; Drake, Froend and Franks, 2013; McAusland et al., 2016). This consequently makes improving stomatal movement dynamics a very attractive target to increase crop yields.

The overexpression of STOMAGEN and the consequent increase in SD has one major consequence: the increase in transpiration and thus the reduction in iWUE. As global water usage is set to double by 2030, attempts to increase photosynthetic carbon assimilation by increasing SD cannot be overly burdened by the increased transpiration and decreased WUE that this produces (Tanaka et al., 2013; Lawson and Blatt, 2014; Lawson and Vialet-Chabrand, 2019; Sakoda et al., 2020). One way to

mitigate reductions in iWUE caused by genetically increased SD would be to produce moderate increases in SD, as demonstrated by the aforementioned *epf1* knockout that produced increased biomass compared to WT when STOMAGEN overexpression did not (Sakoda *et al.*, 2020). An alternative method would be to improve the speed of stomatal response to environmental changes. The speed of stomatal response is controlled most notably by the capacity for solute transport and exchange with the surroundings and the speed that which the transport responds to environmental cues (Lawson and Blatt, 2014).

In the guard cells, the enzyme Hexokinase is a dual-function enzyme that mediates sugar sensing in addition to its catalytic hexose-phosphorylation activity (Moore et al., 2003; Rolland, Baena-Gonzalez and Sheen, 2006). It has been shown that sugars stimulate a guard cell-specific response mediated by Hexokinase and abscisic acid that leads to stomatal closure, likely due to a feedback inhibition mediated by sucrose, which is a direct product of photosynthesis (Kelly *et al.*, 2013). The authors hypothesise that when sucrose production exceeds its loading into the phloem, the surplus is carried to the stomata to activate the closure of the stomata to reduce water loss. The overexpression of Hexokinase in guard cells resulted in accelerated stomatal closure, leading to reduced g_{sw} without compromising photosynthesis, resulting in improved iWUE and enhanced growth in some cases (Kelly *et al.*, 2013; Lugassi *et al.*, 2015). Hexokinase guard cell-specific overexpression could work in tandem with STOMAGEN overexpression to aid in mitigating water loss. Hexokinase overexpression could also act synergistically with improving stomatal response to light induction due to the faster closing of the pore.

More recently, transgenic tomato and Arabidopsis plants overexpressing Hexokinase in their guard cells exhibit reduced transpiration and 20% higher WUE under normal conditions compared to WT, whilst maintaining comparable rates of *A* (Kelly *et al.*, 2019). The improved iWUE of these plants likely caused the slower response time to shorter periods of drought (3 days), which the authors' reason is due to their consistently lower transpiration rates, which allows the plants to gradually use and preserve soil water. Over longer drought periods (9-16 days), plants with guard cell Hexokinase expression had significantly reduced transpiration, greater plant fresh weight, greater leaf area and, for the Arabidopsis, had increased *A*. This study shows the potential benefit that guard cell Hexokinase expression can have in drought conditions. A recent field trial of tobacco plants overexpressing Hexokinase in the guard cells showed beneficial effects depending on the age of the plant and the proximity of precipitation events to gas exchange measurements (Acevedo-Siaca *et al.*, 2022). Guard cell Hexokinase overexpression was most likely to benefit older plants (20-leaf stage) under low precipitation conditions, with some plants having greater iWUE than the WT. This would be particularly beneficial in a commercial setting, as older crops are more likely to suffer yield loss due to drought stress (Farooq *et al.*, 2009). Conversely, under high precipitation conditions, younger plants (10-leaf stage) were most likely to benefit from guard cell Hexokinase overexpression, with these plants having the highest iWUE on days with the greatest precipitation. This could be particularly useful as increasing iWUE in young plants or seedlings, even under non-stress conditions, could help preserve soil water content, which could help buffer the plants from future water stress and its negative impacts on productivity (Acevedo-Siaca *et al.*, 2022). No significant differences were found between genotypes for net carbon assimilation.

These results show that guard cell-specific overexpression of Hexokinase can increase the stress tolerance of plants but can also act as a buffer against future water stress.

Improving stomatal opening speeds in response to changing environmental stimuli is also of great importance in terms of reducing stomatal limitations on plant growth and productivity. When activated by blue light, plasma membrane H^+-ATPase induces the hyperpolarisation of the membrane allowing the influx of K^+ through inward rectifying channels and the accumulation of K^+ induces the swelling of the guard cells and stomatal pore opening (Schroeder, Hedrich and Fernandez, 1984; Assmann, Simoncini and Schroeder, 1985; Shimazaki, Iino and Zeiger, 1986; Schroeder, Raschke and Neher, 1987; Kwak *et al.*, 2001). When the Arabidopsis plasma membrane H^+-ATPase gene AHA2 was overexpressed specifically in guard cells under the GC1 promoter, plants exhibited markedly enhanced stomatal opening, photosynthesis, and growth (Wang *et al.*, 2013). Transgenic lines showed significantly greater light-induced stomatal conductance and CO_2 assimilation, which translated into substantial biomass gains: fresh and dry weights were 42-63% higher than WT plants during vegetative growth, and reproductive biomass (stems, flowers, siliques, seeds) increased by 36-41% at flowering. These benefits were achieved without impairing closure, as responses to ABA and darkness remained intact, indicating that the manipulation selectively enhanced opening dynamics. However, the gains came at the expense of reduced intrinsic water-use efficiency (iWUE) under high light, due to greater water loss via transpiration. The positive effect of AHA2 overexpression has also been demonstrated in woody perennials. In hybrid aspen, guard cell–targeted expression of Arabidopsis AHA2 similarly enhanced stomatal opening and transpiration, leading to

significantly higher photosynthetic rates and >20% increases in stem elongation relative to WT (Toh *et al.*, 2021). Guard-cell-specific overexpression of AHA2 may be a useful strategy for improving stomatal opening kinetics in response to changes in light, especially if this results in a normal ABA-mediated closure response.

The overexpression of STOMAGEN produces many, importantly, smaller stomata (Tanaka et al., 2013). This reflects the general negative relationship between stomatal density and pore size, whereby increases in density are typically accompanied by reductions in individual stomatal dimensions (Franks, Drake and Beerling, 2009; Lawson and Blatt, 2014). Smaller stomata have been suggested to have faster movement kinetics, which would be beneficial for maximising *A* and iWUE in response to a dynamic environment (Drake, Froend and Franks, 2013). Further, the overexpression of both Hexokinase and H^+-ATPase could accelerate stomatal movement dynamics, which could potentially have a compounding effect if combined with the smaller stomata resulting from STOMAGEN overexpression. The combined overexpression of these three genes could work synergistically, improving g_{sw}, *A* and iWUE more than they would individually. Changes in the expression levels of genes involved in stomatal development and function could aid in improving photosynthesis, reducing water loss and improving biomass production.

1.4. Strawberry

1.4.1. Origins And Physiology

The cultivated strawberry, *Fragaria x ananassa*, is a member of the *Rosaceae* family, whose members are widely cultivated for their fruit. *F. x ananassa* was cultivated when octoploid members of the *Fragaria* family, *F. chiloensis* and *F. virginiana,* cross-pollinated, resulting in the octoploid modern cultivar (Davis, Denoyes-Rothan and Lerceteau-Köhler, 2007; Hancock, Sjulin and Lobos, 2008). Recently, however, more complex origins of the genome resulting from the hybridisation of three or four different species with different levels of ploidy have been proposed (Tennessen *et al.*, 2014; Sargent *et al.*, 2016). Cultivated strawberries exist primarily in two types based on their flowering habit: day-neutral and short-day. Day-neutral cultivars are a subtype of everbearing cultivars that fruit multiple times per season and are used to produce fruit throughout the summer and autumn (Pritts and Dale, 1989). Day-neutral cultivars are insensitive to photoperiod and continue to flower as long as temperatures are between 4 and 29 °C (Pritts and Dale, 1989). Day-neutral plants are established in the early spring, come into production in late June, and continue to fruit through the summer and autumn months (Pritts and Dale, 1989). Short-day cultivars, often referred to as June-bearers, are conversely limited by temperature and photoperiod for flowering (Durner *et al.*, 1984) but are successfully used to concentrate the majority of fruit production in a single annual period (Poling, 1993; Black, Enns and Hokanson, 2002; Stevens *et al.*, 2011). Short-day cultivars are typically planted in autumn, with the fruit being ready for harvest in June the following year (Durner *et al.*, 1984). The short-day

flowering habit is believed to be the natural state of most strawberry species (Darrow, 1966).

All *Fragaria* species are low-growing, herbaceous perennial plants that can grow clonally and have animal-dispersed fleshy accessory fruits (Johnson, Govindarajulu and Ashman, 2014). Strawberries have a short, thick stem known as the 'crown', from which buds form to produce leaves, flowers, stolons (runners), branch crowns and adventitious roots (Handley, 2008; Poling, 2012). *Fragaria* species leaves are evergreen and trifoliate, however, some variation can occur in a few different species (Kellerman, 1892; Hummer, Nathewet and Yanagi, 2009). An inflorescence (a cluster of flowers) is initiated in the apical meristem, from which the fruits form. Post-flower initiation, the uppermost axillary buds can form a vegetative extension of the crown, known as branch crowns. Branch crowns themselves can produce an inflorescence under the right conditions (Jahn and Dana, 1970; Guttridge, 1985). Axillary bud differentiation is also environmentally controlled, producing branch crowns under short-day conditions and stolons under long-day conditions (Darrow, 1966; Konsin, Voipio and Palonen, 2001). The growth of stolons results from the development of an internode, which extends from the mother plant. Continued growth is from a secondary node from which the runner plant will form (Handley, 2008; Poling, 2012). The strawberry fruit is an accessory fruit in the form of a swollen fleshy receptacle which bears the true botanical fruits, the achenes, embedded in its surface (Liston, Cronn and Ashman, 2014; Longhi *et al.*, 2014). Within the ovary wall of each achene lies the ovule, capable of developing into a new plant (Poling, 1993, 2012). The receptacle is comprised of an epidermal layer, a cortex and a pith. The cortex and the pith are segregated by vascular bundles

that supply nutrients to developing achenes (Pritts *et al.*, 1998). Cells in the cortex and pith are responsible for most of the receptacle growth, with the vast majority of the growth being caused by cell enlargement rather than cell division. Sugars, aromatic compounds and pigments all increase as the receptacle tissue grows and matures. Ripening lasts approximately 30 days, depending on environmental conditions (Pritts *et al.*, 1998; Handley, 2008). Both strawberry leaves and fruit possess kidney-shaped Guard cells, that when in a turgid state can lead to water loss from both sources (Wang *et al.*, 2014).

1.4.2. Economic Importance

Strawberries are a highly economically important horticultural crop, with the global fresh strawberry market valued at approximately USD 14.7 billion in 2024 and projected to continue growing over the coming decade (Mordor Intelligence, 2024). Global strawberry production reached around 10.5 million tonnes in 2023, with China accounting for approximately 40 % of total production, followed by the United States as the second largest producer (FAO, 2024). These two countries are also the largest consumers of strawberries worldwide, reflecting a close alignment between production and domestic demand. Europe accounts for roughly 10–12 % of global strawberry production, with Spain, Poland and Germany among the largest producers, and Germany, the United Kingdom and France representing the major consumer markets within the region (FAO, 2024). Strawberries are a particularly important fruit crop in the UK, where annual production is approximately 106 000 tonnes, and the retail value of

UK-grown strawberries has been estimated at around £650 million per year, making strawberries the most valuable fresh fruit crop in the UK market (GOV.UK, 2024).

1.4.3. Nutritional Importance

Strawberries are an important source of nutrition and beneficial phytochemicals for many people. Strawberries are a potent source of the essential micronutrient Vitamin C, containing 58.8 mg/100 g of fresh weight (Giampieri *et al.*, 2012). Vitamin C contributes to normal immune function and has important antioxidant properties necessary for the beneficial control of lipid peroxidation of cellular membranes (Bendich *et al.*, 1986; Carr and Maggini, 2017). The recommended daily allowance for Vitamin C is 90 and 75 mg for adult males and females respectively, meaning only 153 g of fresh strawberries is required to meet the upper limit (U.S. Department of Agriculture, 2018; National Institute of Health, 2021c).

Strawberries are also a good source of folate, containing between 20-25 µg/100 g of fresh weight. Folate is an essential micronutrient, being vital for cell division and homeostasis due to the essential role of folate coenzymes in nucleic acid synthesis, methionine regeneration, and in the shuttling, oxidation and reduction of one-carbon units required for normal metabolism and regulation (Bailey, 2009). The NIH recommends a daily intake of 400 µg/ day for adults, with this being increased to 600 µg for pregnant women (National Institute of Health, 2021a). 250 grams of strawberries is enough to meet 30% of the daily recommended allowance for Europe and the US (Giampieri *et al.*, 2012).

Magnesium is the fourth most abundant cation in the human body, being involved in over 300 reactions as a cofactor (al Alawi, Majoni and Falhammar, 2018). Strawberries are an excellent source of magnesium, with 144 g of strawberry providing over 20% of the 400-420 mg recommended daily intake for adults (Giampieri *et al.*, 2012; National Institute of Health, 2021b). Strawberries are an excellent source of many essential vitamins and minerals and would be a great addition to a healthy diet.

1.4.4. Commercial Production

1.4.4.1. Propagation

Conventionally, strawberries are propagated vegetatively from stolons; however, this produces a limited number of propagules, and these propagules are susceptible to disease, particularly soil-borne fungi (Dijkstra, 1993; Debnath, 2012a). To overcome these limitations, soilless propagation under aseptic conditions has been developed. Micropropagation is an in vitro tissue culture propagation system that can use a variety of different plant explant types, including node cultures (Bhatt and Dhar, 2000) and leaf, sepal and petiole explants (Debnath, 2005, 2011, 2015). Strawberry plants propagated using tissue culture can exhibit many undesirable traits, particularly changes in growth habits, such as greater branching, more crowns and stolons and increased vegetative growth compared to conventionally propagated plants (Debnath, 2009, 2012b, 2016). Meristem cultures are also possible (Nishi and Ohsawa, 1973; Whitehouse *et al.*, 2011), but they too fall prey to similar morphological changes that are typical of micro-propagated strawberries (Swartz, Galetta and Zimmerman, 1981; Cameron and

Hancock, 1986; Biswas *et al.*, 2009). Molecular treatments, for example, using the plant cytokine Kinetin, have been developed to mitigate the negative effects of tissue culture propagation and produce true-to-type plants (Naing *et al.*, 2019).

1.4.4.2. Production Methods

There are two predominant production systems used globally: matted rows and hills. In the matted row system, transplants are typically planted in the spring, with crowns developing during the summer months that produce runners (Hancock, Sjulin and Lobos, 2008). These runners are the primary yield component of this system and are allowed to spread throughout the rows with periodic training into narrow rows (Fernandez, Butler and Louws, 2001). Matted rows are conventionally used in climates with short summers and cold winters like continental Europe and North America, utilising short-day cultivars (Hancock, 1999). Depending on disease pressure, the crops are left in the ground for 3 to 7 years. Mechanical weeding and occasional pesticide use are the primary weed control mechanisms employed (Stevens *et al.*, 2011).

The hill system, more commonly referred to as plasticulture, uses crowns as the primary yield component, with runners being removed (Hancock, Sjulin and Lobos, 2008). Plasticulture has been primarily used in regions with warm winters and hot summers like California, Spain and Italy (Hancock, Sjulin and Lobos, 2008) but has also been adapted to cold climates due to benefits in yield and fruit quality (Fiola, Lengyen and Reichert, 1995; Poling, 1996; Fiola *et al.*, 1997; O'Dell and Williams, 2009). Plasticulture is an annual system, where transplants are planted in autumn, with harvest being approximately 6 months post-planting and plants being removed quickly

post-harvest (Fernandez, Butler and Louws, 2001). Much of the weed control is done by the plastic mulch, however, chemical fumigation, conventionally methyl bromide, is necessary to maximise yields (Larson, 1996; Pritts *et al.*, 1998). Chemical fumigation and annual cropping result in material costs being much larger over both short and long-term operations (Stevens *et al.*, 2011).

1.5. Genetic Resources For Improving Crop Production

A wide range of genetic resources can be exploited to improve crop production, including strategies targeting yield, stress tolerance, resource-use efficiency and photosynthesis. Improving photosynthesis, particularly through modification of gas exchange and carbon assimilation via stomata, represents one promising avenue for enhancing productivity. Although photosynthesis is only one of many potential targets for genetic crop improvement, it is particularly attractive due to its central role in determining plant growth and yield.

Many of the genetic tools used for crop improvement are broadly applicable across diverse traits, including enhanced tolerance to biotic and abiotic stresses, altered development and metabolic optimisation. Many commonplace regulatory sequences could be used towards this goal, particularly in the case of overexpression systems. The Cauliflower mosaic 35S promoter is a constitutive promoter widely used in overexpression systems in plants for many years (Amack and Antunes, 2020). The terminators of octopine synthase (OCS) and nopaline synthase (NOS) are widely used in plant molecular biology as generic terminator sequences and are often used in

overexpression constructs (Kado, Lai and Kelly, 2000). Another terminator, the heat shock protein 18.2 (HSP) terminator, was shown to increase transgene expression approximately 2-fold more than the NOS terminator, making it a particularly useful tool for overexpression constructs (Nagaya *et al.*, 2010).

Tissue-specific promoters are useful tools to restrict the expression of transgenes, especially when system-wide expression is detrimental to plant growth and development, a principle that is relevant to a wide range of crop improvement strategies. Several guard cell-specific promoters have been identified and developed to restrict gene expression to these cells and the stomata that they form. A truncated version of the ADP-glucose phosphorylase (AGPase) is a guard cell-specific promoter that has been developed, with the 300bp 5' proximal promoter fragment conveying guard cell-specific expression and has been used to express transgenes in the guard cells of potato, tobacco, and Arabidopsis (Müller-Röber *et al.*, 1994; Berger and Altmann, 2000). Another guard cell-specific promoter, the *Solanum tuberosum* KST1 promoter, has been developed to express only in guard cells by identifying the minimal promoter through deletion analysis and has been shown to successfully produce tissue-specific gene expression in 13 different plant species (Plesch, Ehrhardt and Mueller-Roeber, 2001; Sade *et al.*, 2014; G Kelly *et al.*, 2017). The KST1 promoter has been successfully used to express the gene Hexokinase (Kelly *et al.*, 2013; Lugassi *et al.*, 2015), which had been previously shown to inhibit the growth of the plants when expressed under the 35S constitutive promoter (Dai et al., 2002; Kelly et al., 2012), clearly demonstrating the benefits of transgene expression under the control of tissue-specific promoters.

A near-complete chromosome-scale assembly for *Fragaria* × *ananassa* was published in 2019 (Edger *et al.*, 2019). However, due to the lack of a whole-genome sequence, the genome of the diploid *F. vesca* is commonly used as a reference (Shulaev *et al.*, 2010; Tennessen *et al.*, 2013, 2014; Yongping Li *et al.*, 2017; Edger *et al.*, 2018).

CRISPR/Cas9 is a powerful molecular biology tool and is particularly useful in gene editing and targeted gene knockout applications. The first use of the CRISPR/Cas9 genome editing system in an octoploid species was achieved by Martín-Pizarro, Triviño and Posé in 2019 in *F.* × *ananassa*, clearly demonstrating the feasibility of gene editing in the cultivated strawberry regardless of its high ploidy (Martín-Pizarro, Triviño and Posé, 2019). The high ploidy of the cultivated strawberry's genome could also be a useful tool for generating a range of phenotypes when performing knockouts. Wilson et al. visually demonstrated a range of phenotypes when knocking out the marker gene phytoene desaturase in the octoploid *F.* × *ananassa* 'Calypso' (Wilson *et al.*, 2019). Together, these genetic resources provide a versatile toolkit for crop improvement and form the foundation for targeted manipulation of stomatal behaviour and photosynthesis in cultivated strawberry.

1.6. The Potential Effects Of Genetic Improvement Of Photosynthesis In Strawberry

1.6.1. Using CO_2 Enrichment As A Proxy For Improved Photosynthesis

Successful genetic manipulation of photosynthesis generally results in, as described in Section 1.2.2, increased yields of the crops in question; however, research regarding the genetic manipulation of photosynthesis in fruiting crops is limited, with little being known about the effect of the said manipulation on fruit (Bi *et al.*, 2013; Ding *et al.*, 2016). A proxy is required to elucidate the potential effects of genetic manipulation of photosynthesis would have on the fruit, in terms of yield and quality. CO_2 enrichment studies, where the plants receive elevated atmospheric [CO_2] (e[CO_2]), show increased levels of photosynthesis and biomass in many species, including fruiting crops (Ainsworth and Long, 2005, 2021). Another reason e[CO_2] is a useful proxy is that under e[CO_2] conditions, the carbon fixing enzyme RuBisCO has increased rates of the desired carboxylation reaction, reducing the rate limitation imposed by RuBisCO on the CBC (Sage, Way and Kubien, 2008; Parry *et al.*, 2013). These reasons make e[CO_2] a useful proxy, as it closely mimics improved carbon throughput in the CBC that genetic manipulation of photosynthesis aims to achieve.

1.6.2. Effect Of CO_2 Enrichment On Yield

Elevated CO_2 studies have produced a wide range of yield increases in the cultivated strawberry (*Fragaria x ananassa* Duch.), ranging from 1 - 51% in strawberry plants cultivated under e[CO_2] of 450 – 3000 ppm (Enoch, Rylski and Spigelman, 1976; Hartz, Baameur and Holt, 1991; Sung and Chen, 1991; Deng and Woodward, 1998; Bushway and Pritts, 2002; Wang, Bunce and Maas, 2003; Wang and Bunce, 2004; Sun *et al.*, 2012; Balasooriya *et al.*, 2018). The effects of e[CO_2] on the plants are also quite varied with increases in fruit number but no difference in individual fruit weight at 1000 ppm (Sung and Chen, 1991) and increases in individual fruit weight (Wang and Bunce, 2004), showing that there isn't a uniform change under e[CO_2] but generally an increase in yield.

The yield increases have been directly linked to increased photosynthetic rates and CO_2 assimilation in the strawberry leaves, giving further credence to the use of e[CO_2] as a proxy for genetic manipulation of photosynthesis (Sung and Chen, 1991; Keutgen, Chen and Lenz, 1997; Bunce, 2001; Bushway and Pritts, 2002; Balasooriya *et al.*, 2018; Li *et al.*, 2020). Optimal e[CO_2] of 600 ppm produced a CO_2 assimilation rate increase of up to 73% (Keutgen, Chen and Lenz, 1997). Further benefits can also be drawn from strawberry cultivation under e[CO_2] due to reduced fruiting time leading to increased annual yields (Enoch, Rylski and Spigelman, 1976; Bushway and Pritts, 2002).

1.6.3. Effects Of CO_2 Enrichment On Fruit

Respective fruit quality traits were also favourably altered in strawberries cultivated in e[CO_2] conditions. Increased content of reducing sugars have been described, accompanied by reduced contents of organic acids which would lead to a more palatable sense of the fruit flavour have been described (Wang and Bunce, 2004; Drewnowski *et al.*, 2012; Sun *et al.*, 2012). Wang and Bunce also reported increases in volatile organic compounds that are vital in producing the distinct "strawberry" flavour (Wang and Bunce, 2004). In addition to the flavour, vitamin C concentrations were increased by up to 13.3% accompanied by additional increases in antioxidant compounds (Wang, Bunce and Maas, 2003; Balasooriya *et al.*, 2019).

The evidence presented demonstrates the beneficial effects of cultivating strawberries under elevated atmospheric CO_2 concentrations and, by proxy, the potential effect that genetic enhancement of photosynthesis. Increases in yield, health-benefiting compounds and improved flavour show the important effects genetically enhancing photosynthesis can have towards meeting the global calorie demand and addressing the hidden hunger.

1.7. Research Aims

This thesis investigates strategies to overcome stomatal limitations on photosynthesis through targeted genetic manipulation. The overarching aim was to determine how altering stomatal development and guard cell behaviour influences gas exchange, photosynthesis, and growth in both a model species (*Nicotiana tabacum*,

tobacco) and a commercial crop (*Fragaria* × *ananassa*, strawberry). To address this, three complementary approaches were pursued: (i) increasing stomatal density to enhance CO_2 uptake capacity, (ii) improving stomatal responsiveness and kinetics by manipulating guard cell metabolism, and (iii) testing the feasibility of combining these traits to achieve additive benefits. Together, these research avenues were designed to evaluate the potential of stomatal engineering as a strategy to reduce diffusional constraints on photosynthesis and improve crop performance.

1.7.1. Strawberry: Increasing Stomatal Density And Manipulating Guard Cell Behaviour

In greenhouse-grown strawberry (*Fragaria* × *ananassa*), photosynthetic carbon assimilation is strongly limited by stomatal conductance, even when water supply is not limiting (Yokoyama *et al.*, 2023). To address this constraint, two genetic strategies were pursued. First, constitutive overexpression of STOMAGEN, under the control of the 35S CMV promoter, was used to increase stomatal density and thereby raise maximum potential g_{sw} (Tanaka et al., 2013; Sakoda et al., 2020). Second, guard cell-targeted overexpression of Hexokinase, under the control of the KST1 promoter, was employed to enhance stomatal closure responses, improving water-use efficiency by reducing unnecessary transpiration (Kelly *et al.*, 2013; Lugassi *et al.*, 2015). By combining both constructs in a stacked line, the aim was to test whether the benefits of increased stomatal capacity and improved closure control could be integrated, providing additive gains in CO_2 uptake while mitigating the water costs associated with higher stomatal density.

1.7.2. Tobacco: Increasing Stomatal Density And Improving Photosynthetic Capacity

Photosynthetic carbon assimilation is limited by both the supply of CO_2 through the stomata and its utilisation within the chloroplast. To address these constraints, two complementary genetic strategies were applied. Overexpression of the putative inorganic carbon transporter ictB has been shown to enhance photosynthetic efficiency and biomass across several C_3 species (Lieman-Hurwitz et al., 2003; Simkin et al., 2015; Yu Gong et al., 2015; Hay et al., 2017; Koester et al., 2021), while overexpression of STOMAGEN (EPFL9) increases stomatal density, raising maximum potential stomatal conductance and CO_2 uptake capacity (Tanaka et al., 2013; Sakoda et al., 2020). By combining these traits (both genes using the 35S CMV promoter), the aim was to test whether boosting carbon fixation capacity alongside increased CO_2 diffusion into the leaf could provide additive benefits for photosynthesis, water-use efficiency, and growth.

1.7.3. Tobacco: Manipulating Guard Cell Behaviour

Photosynthetic efficiency is often constrained by the slow kinetics of stomatal movements, which lag behind the rapid responses of mesophyll photosynthesis under fluctuating light (Lawson and Blatt, 2014; McAusland et al., 2016; Lawson and Vialet-Chabrand, 2019). To overcome this limitation, two complementary genetic strategies were pursued. Guard cell-targeted overexpression of the plasma membrane H^+-ATPase was used to accelerate stomatal opening and enhance CO_2 uptake (Wang *et al.*, 2013; Toh *et al.*, 2021), while overexpression of Hexokinase (HXK) in guard cells was

employed to reinforce closure through ABA-mediated signalling, reducing unnecessary water loss (Kelly *et al.*, 2013, 2019; Lugassi *et al.*, 2015, 2019; Acevedo-Siaca *et al.*, 2022). By combining these approaches (using the KST1 Guard cell specific promoter), the aim was to generate plants with stomata that open more rapidly during light increases and close more effectively under declining light or drought, thereby improving the coordination between stomatal behaviour and mesophyll demand to enhance both photosynthetic performance and water-use efficiency.

2. Methods

2.1. Construct Assembly

2.1.1. Module Design

All synthesised Level 0 modules were designed and codon optimised for expression under the control of either the Cauliflower mosaic virus 35S (35S) constitutive promoter or the Solanum tuberosum KST1 (KST1) guard cell-specific promoter, and terminated using the heat shock protein 18.2 (HSP), nopaline synthase (NOS) or octopine synthase (OCS) terminators (Kado, Lai and Kelly, 2000; Plesch, Ehrhardt and Mueller-Roeber, 2001; Dai *et al.*, 2002; Nagaya *et al.*, 2010; Amack and Antunes, 2020). The *Arabidopsis thaliana* sequence for STOMAGEN was obtained from Tanaka et al. (2013). The *Arabidopsis thaliana* sequence for Hexokinase 1 was taken from Kelly et al. (2013). The *Arabidopsis thaliana* sequence for Arabidopsis H+ATPase 2 (AHA2) was obtained from Wang et al. (2013). Codons were optimised to remove restriction sites for the enzymes used in GoldenGate cloning (BsaI and BbsI) using the Vector Builder Codon Optimisation Tool (Vector Builder, www.VectorBuilder.com).

2.1.2. Level 0 Module Synthesis And Preparation

Level 0 modules were synthesised by NBS Biologicals (NBS Biologicals, UK). Level 1 destination vectors, the assembled Kanamycin resistance Level 1 module and the Level 1 and 2 linkers were provided by the University of Essex (University of Essex, UK). The Level 2 destination vector was provided by Niab (Niab, UK).

2.1.3. Assembly Of Level 1 Modules

Level 1 constructs were assembled from Level 0 using the Golden Gate modular cloning method established by Weber *et al.*, 2011 (Weber *et al.*, 2011). 1 µL Level 1 destination vector (100 ng μl^{-1}), 1 µL of each Level 0 (containing the selected promoter, coding sequence, and terminator) (100 ng μl^{-1}), 1.5 µL of 10x NEB T4 buffer, 1.5 µl of 10x BSA, 1 µL NEB T4 DNA Ligase. Each reaction also contained 1 µL of the level-specific restriction enzymes BsaI and dH_2O to bring the reaction volume to 15 µL. The digestion and ligation were performed in a thermocycler using the following program: 25x cycles of 37 °C for 3 minutes and 16 °C for 4 minutes, 1x cycle of 50 °C for 5 mins and 1x cycle of 80 °C for 5 mins.

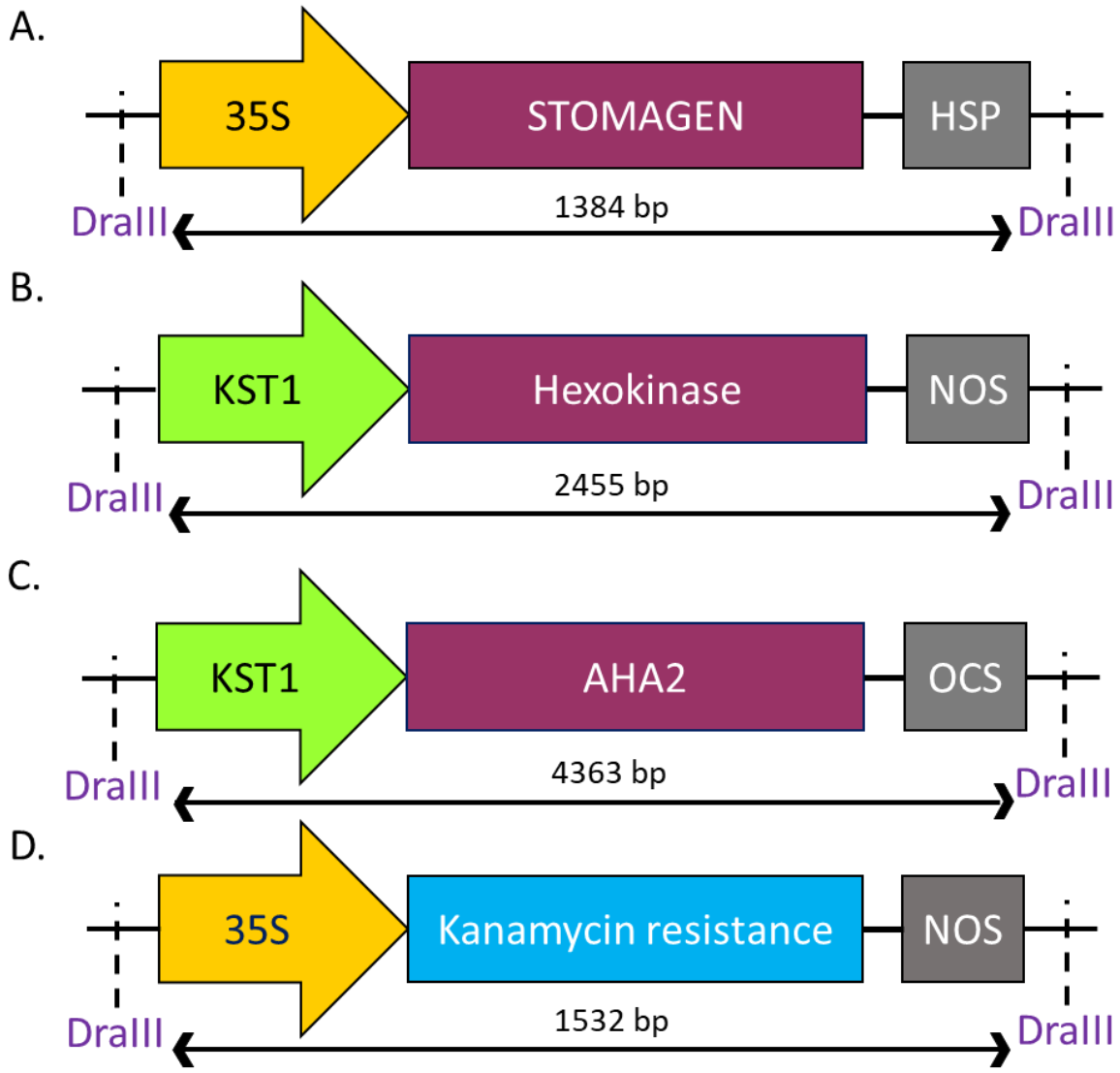

Figure 2.1. Schematic representation of assembled Level 1 modules. A) STOMAGEN under the control of the CaMV35S constitutive promoter and the Heat Shock Protein (HSP) terminator. B) Hexokinase under the control of the Solanum tuberosum Guard cell-specific promoter KST1 and the nolapine synthase (NOS) terminator. C) AHA2 under the control of the Solanum tuberosum Guard cell-specific promoter KST1 and the octopine synthase (OCS) terminator. D) Kanamycin resistance gene NPII under the control of CaMV35S constitutive promoter and the nolapine synthase (NOS) terminator. The insert site is flanked by DraIII restriction enzyme recognition sites, and the arrows depict the length of the insert.

2.1.4. Bacterial Transformation And Colour Selection

Following the assembly of Level 1 constructs, chemically competent *E. coli* cells (in-house-made DH5α cells) were transformed with each of the Golden Gate modules (Fig. 2.1) using the heat shock method of transformation (Froger and Hall, 2007). 4 µL of each Golden Gate module (100 ng μL^{-1}) was added to ice-thawed chemically competent E. coli cells (Top10 Thermo Fisher Scientific or in-house-made DH5α cells) and were tap mixed. The cells were placed on ice for 2 minutes before being transferred to a water bath/ heating block at 42 °C for 45 seconds, then immediately returned to the ice for an additional 2 minutes. 300 µL of Super Optimal Broth (SOB) was added to the cells, and they were left to incubate for 1 hour at 37 °C. After the incubation period, the cells were well mixed with a pipette before adding 100 µL of the broth to agar plates. Cells were grown on agar plates containing ampicillin (100 µg mL^{-1}), supplemented with X-gal and IPTG (1.5 µL mL^{-1}) to permit blue/white selection of colonies. Cells were incubated overnight at 37 °C. White colonies containing the putatively correctly assembled Level 1 module were isolated.

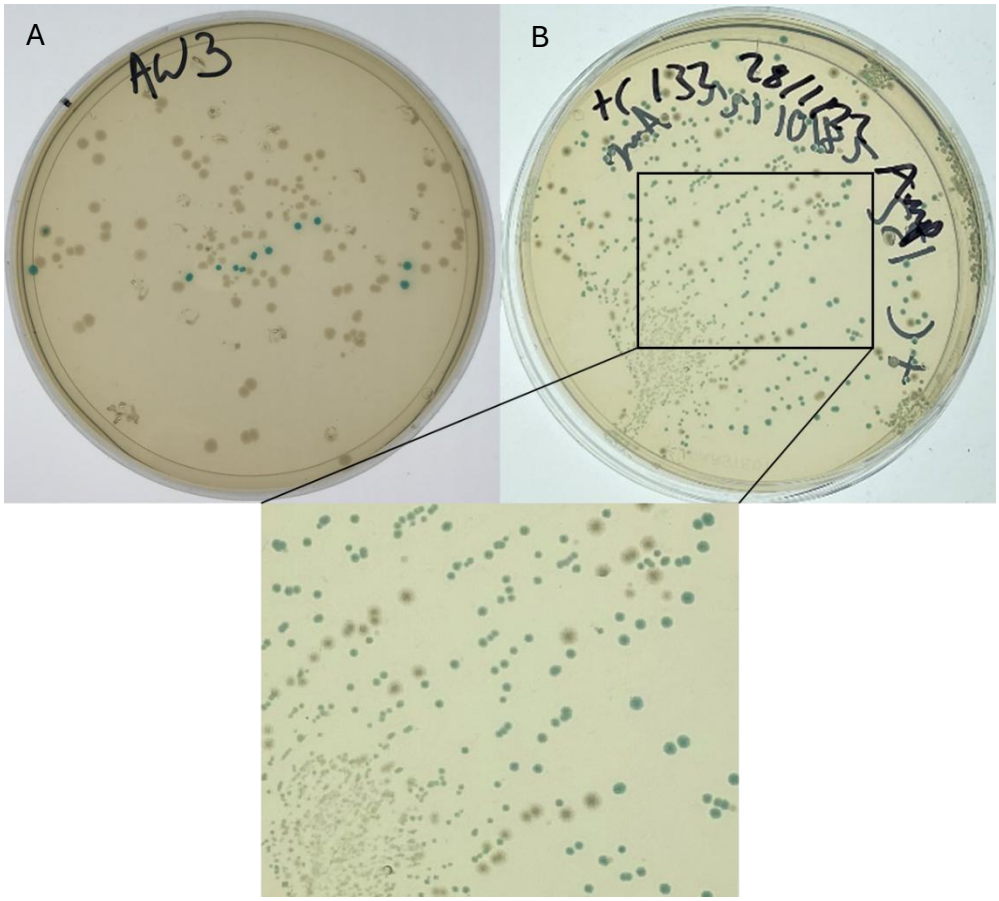

Figure 2.2. Blue/white selection of E. coli cells containing assembled Level 1 Golden Gate modules. Blue colonies contain only the Level 1 destination vector. White colonies contain the Level 1 destination vector with the inserted Level 0 modules. A) Blue/white selection of E. coli cells containing an assembled Level 1 construct. B) Negative control, displaying colonies containing the Level 1 destination vector 132, which still contains the Lac operon.

2.1.5. Plasmid Isolation And Quantification

Three independent colonies displaying the desired white phenotype were selected (Fig. 2.2). Overnight cultures of isolated single white colonies, collected using the colony picking method, were made and incubated overnight in approximately 5 mL of high salt LB broth containing 100 µg mL^{-1} of ampicillin (100 µg mL^{-1}) as a selectable marker.

Plasmids were extracted using a NucleoSpin® plasmid kit (Machery-Nagel) following the manufacturer's instructions, using sterile Milli-Q® Ultrapure water instead of the elution buffer. Extracted plasmid concentrations were measured using Nanodrop 1000 (ThermoFisher Scientific). Extracted plasmids were diluted to 100 ng μL^{-1} for further Golden Gate assemblies.

Level 1 plasmids were subject to DraIII restriction enzyme digestion to ensure correct assembly. The Level 1 vectors contain the restriction site CACNNNGTG for DraIII digestion. 17 µL of plasmid was incubated with 1 µL of DraIII and 2 µL of 10x rCutsmart buffer for 1 hour at 37 °C. Samples were run on a 1% agarose gel at 160 volts for 1 hour. Banding patterns were compared to the known sizes of the digested plasmid to confirm correct assembly.

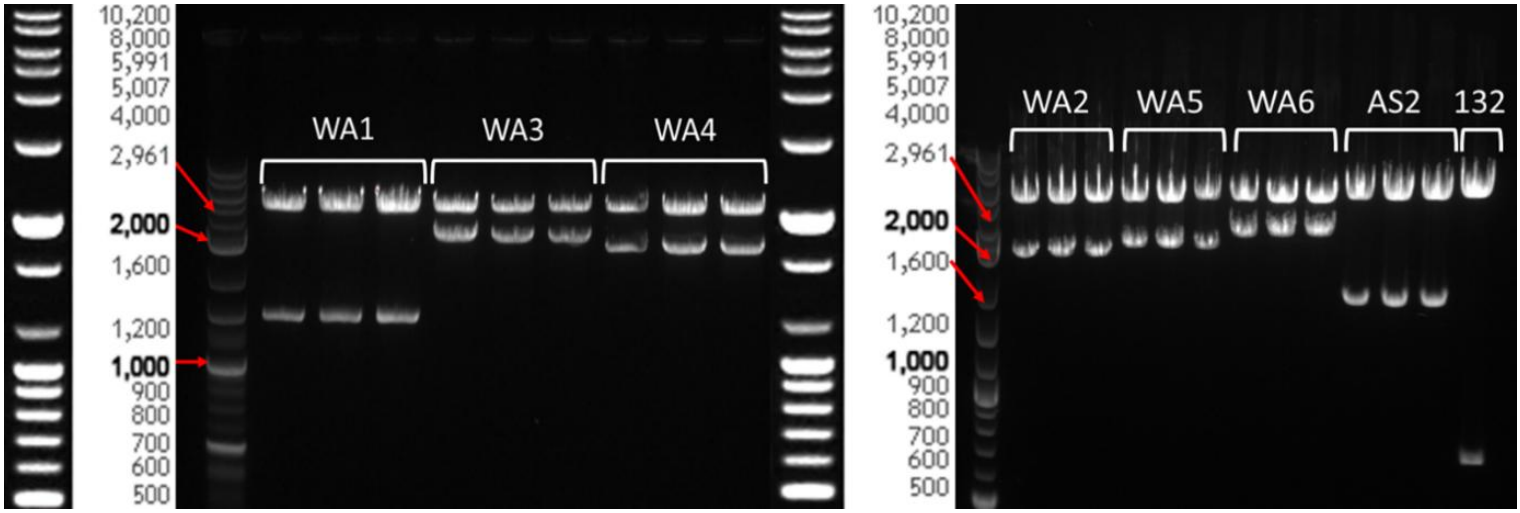

Figure 2.3. DraIII digestion of extracted plasmid from single colonies post-blue/white selection. The red arrows show the respective bands on the ladder. WA1 and WA2 represent the Level 1s depicted in Figure 2.1A and B. WA3 and 4 represent backup Level 1 constructs for Guard cell-specific overexpression of Hexokinase using an alternative ADP-Glucose Pyrophosphorylase promoter. WA5 and 6 represent the Level 1 constructs for Guard cell-specific overexpression of Hexokinase in position 3 for multigene assembly, using ADP-Glucose Pyrophosphorylase and KST1 promoters, respectively. AS2 represents Guard cell-specific overexpression of a MADS box transcription factor for an additional project. The arrows highlight the corresponding bands from the digestion chart to the left. The digestion of 132, the level 1 destination vector, acts as a positive control.

2.1.6. Assembly Of Level 2 Modules

Level 1 plasmids displaying the correct banding patterns were used for Level 2 assembly. Level 2 constructs were assembled as described in section 2.1.3 using the restriction enzyme BbsI, replacing BsaI. Following Golden Gate assembly as described (section 4.1.2), NEB® 10-beta Competent *E. coli* (High Efficiency) were transformed with 4 µL of each Level 2 assembly as described above. Cells were plated onto agar plates using kanamycin (100 µg mL^{-1}) for selection and incubated overnight at 37 °C.

Bacterial transformation and colour selection were carried out as described above. In brief, *E. coli* cells were transformed with the assembled Level 2 construct and were visually discriminated using red/white colour selection (Figure 2.4). Colonies presenting a red phenotype (Figure 2.4A) contain only the Level 2 destination vector with the still intact canthaxanthin biosynthesis operon. Following assembly, the canthaxanthin operon is replaced by the integration of the level 1 modules, resulting in white colonies (Figure 2.4B). White colonies were selected and had their plasmids extracted.

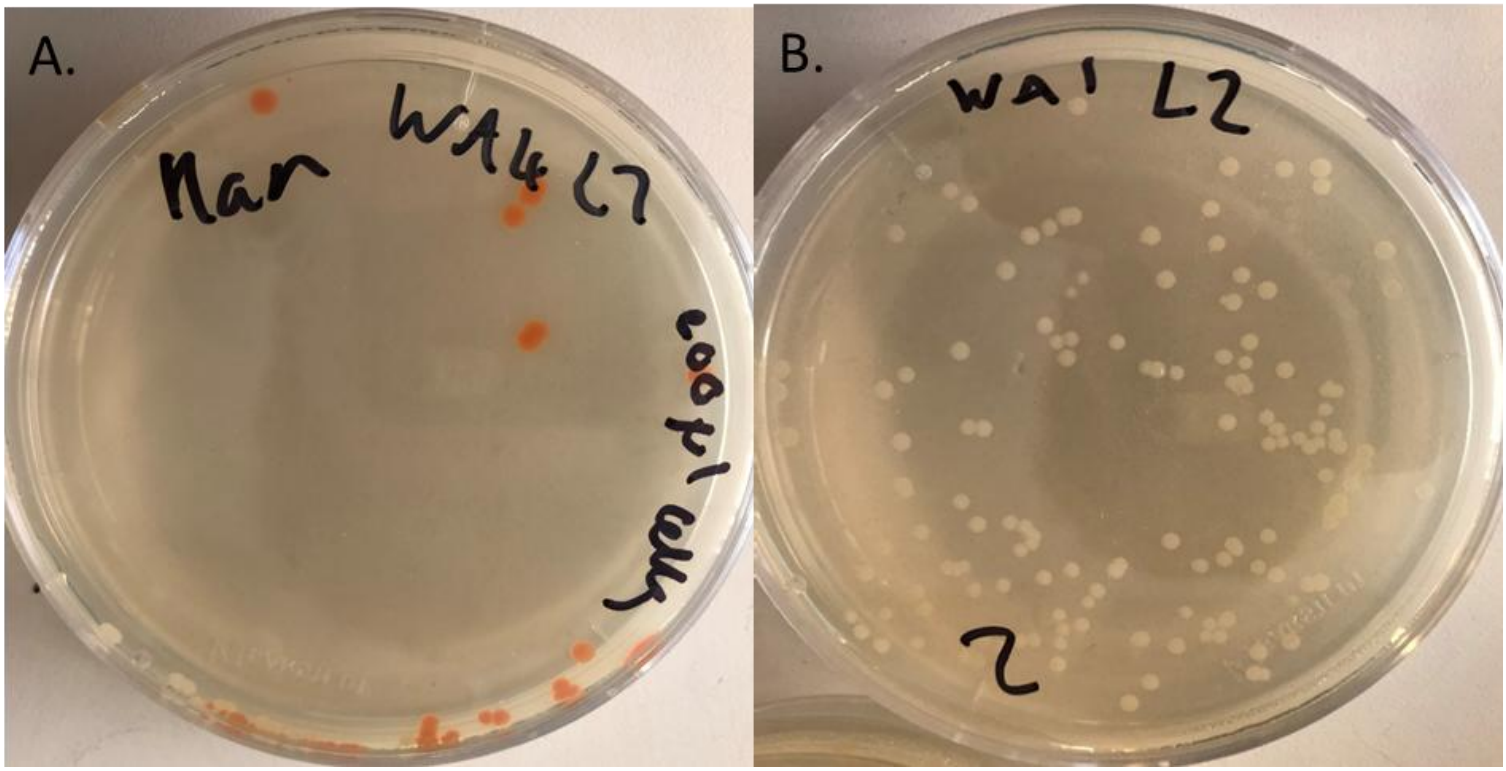

Figure 2.4. Red/white selection of transformed E. coli cells containing a Level 2 Golden Gate final vector. A) Negative control, red colonies contain only the Level 2 destination vector. B) Successfully transformed E. coli, white colonies contain the Level 2 destination vector with the inserted Level 1 modules.

Plasmids were then prepared for sequencing, accompanied by the primers outlined in Figures 2.5-2.8. Primers were designed so that the junctions between the different

components (Level 0 modules) in the Level 1 modules and between the Level 1 modules themselves are sequenced.

Level 2 construct sequences were verified via sequencing using the primers indicated in purple in Figures 2.5-2.8. Correctly assembled Level 2 plasmids were taken forward for plant transformation.

Primers for plasmid construct sequencing were designed using the NCBI Primer-Blast tool (NIH, USA), using the designed plasmid sequence as the template.

Table 2.1. PCR Primers used for construct verification during plasmid cloning.

Name	**Query**	**Direction**	**Sequence**
STO F1	Stomagen	Forward	tagttcaagcctcaagacctcg
HXK F1	Hexokinase	Forward	acggatgcagagctcagggaagtgg
HXK F2	Hexokinase	Forward	ataccgttggaacactagccggtgg
HXK F3	Hexokinase	Forward	atcggttatagccatggatggtgg
Kan vF1	Kanamyicn	Forward	aagatggattgcacgcaggttctcc
Kan vR1	Kanamyicn	Reverse	aacgctatgtcctgatagcggtcc
AHA F1	AHA2	Forward	caagtggagcgaacaagagg
AHA F2	AHA2	Forward	agacaaaggagtccccaggt
AHA F3	AHA2	Forward	gcagatcatggagttttgttga
L0-F(0015)	Level 0 Vector	Forward	cgttatcccctgattctgtggataac
L0-R(K)	Level 0 Vector	Reverse	tcgtatgttgtgtggaattgtgagc
L1M-R-RP	Level 1 Vector	Reverse	gtactggggtggatgcagtg
L1M-R-FP	Level 1 Vector	Forward	cggataaacctttcacgccc
L2-F	Level 2 Vector	Forward	tggcacatacaaatggacgaacgg
L2-R	Level 2 Vector	Reverse	atgggctgcctgtatcgagtgg
L1-R-KAN1	Level 1 Module (60)	Forward	aactgttcgccaggctcaagg

The desired Level 1 module encoding the overexpression cassette of the gene/s of interest (Figure 2.1) and the kanamycin resistance Level 1 module (60) as a selectable marker (Figures 2.5 and 2.6). Constructs shown in Figure 2.1A and D were assembled to form construct 60(WA1) as shown in Figure 2.5. Constructs in Figure 2.1B and D were combined to form construct 60(WA2) as shown in Figure 2.6.

Figure 2.5. The plasmid map of the final Level 2 construct 60(WA1), assembled from constructs A and D in Fig. 2.1. The construct assembly was verified via sequencing using primers indicated by the purple labels. This construct is primarily comprised of the STOMAGEN overexpression cassette and kanamycin resistance. The DNA situated between the Right border (RB) and Left border (LB) T-DNA repeat will be randomly inserted into the plant genome. Plasmid maps were created using SnapGene (SnapGene, United States).

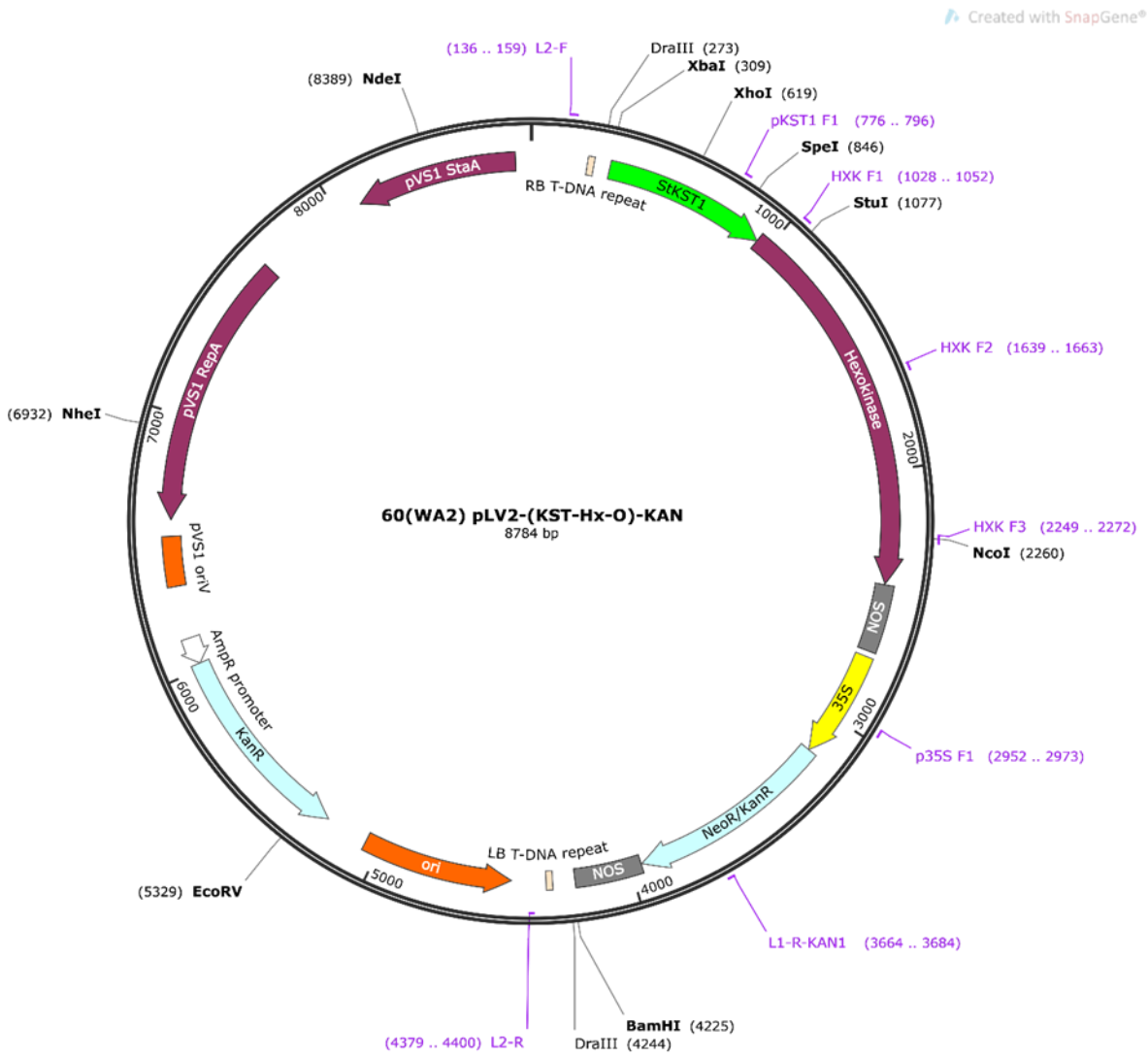

Figure 2.6. The plasmid map of the final Level 2 construct 60(WA2), assembled from constructs B and D in Fig. 2.1. The construct assembly was verified via sequencing using primers indicated by the purple labels. This construct is primarily comprised of Guard cell-specific overexpression of Hexokinase and kanamycin resistance. The DNA situated between the Right border (RB) and Left border (LB) T-DNA repeat will be randomly inserted into the plant genome. Plasmid maps were created using SnapGene (SnapGene, United States).

Multigene constructs (Figures 2.7-2.8) were assembled using the Level 1 modules shown in Figure 2.1. Level 2 construct 60(WA1-6) (Figure 2.6) is comprised of the combination of Level 1 modules for STOMAGEN overexpression (Fig. 2.1A), Guard cell-specific Hexokinase overexpression (Fig. 2.1B) with kanamycin resistance (Fig.

2.1D). Level 2 construct 60(WA2-7) is comprised of the combination of Level 1 modules for Guard cell-specific Hexokinase overexpression (Fig. 2.1B), Guard cell-specific AHA2 overexpression (Fig. 2.1C) and kanamycin resistance (Fig. 2.1D).

Figure 2.7. The plasmid map of the final Level 2 construct 60(WA1-6), assembled from constructs A, B and D in Fig. 2.1. The construct assembly was verified via sequencing using primers indicated by the purple labels. This construct is primarily comprised of STOMAGEN overexpression cassette, Guard cell-specific overexpression of Hexokinase and kanamycin resistance. The DNA situated between the Right border (RB) and Left border (LB) T-DNA repeat will be randomly inserted into the plant genome. Plasmid maps were created using SnapGene (SnapGene, United States).

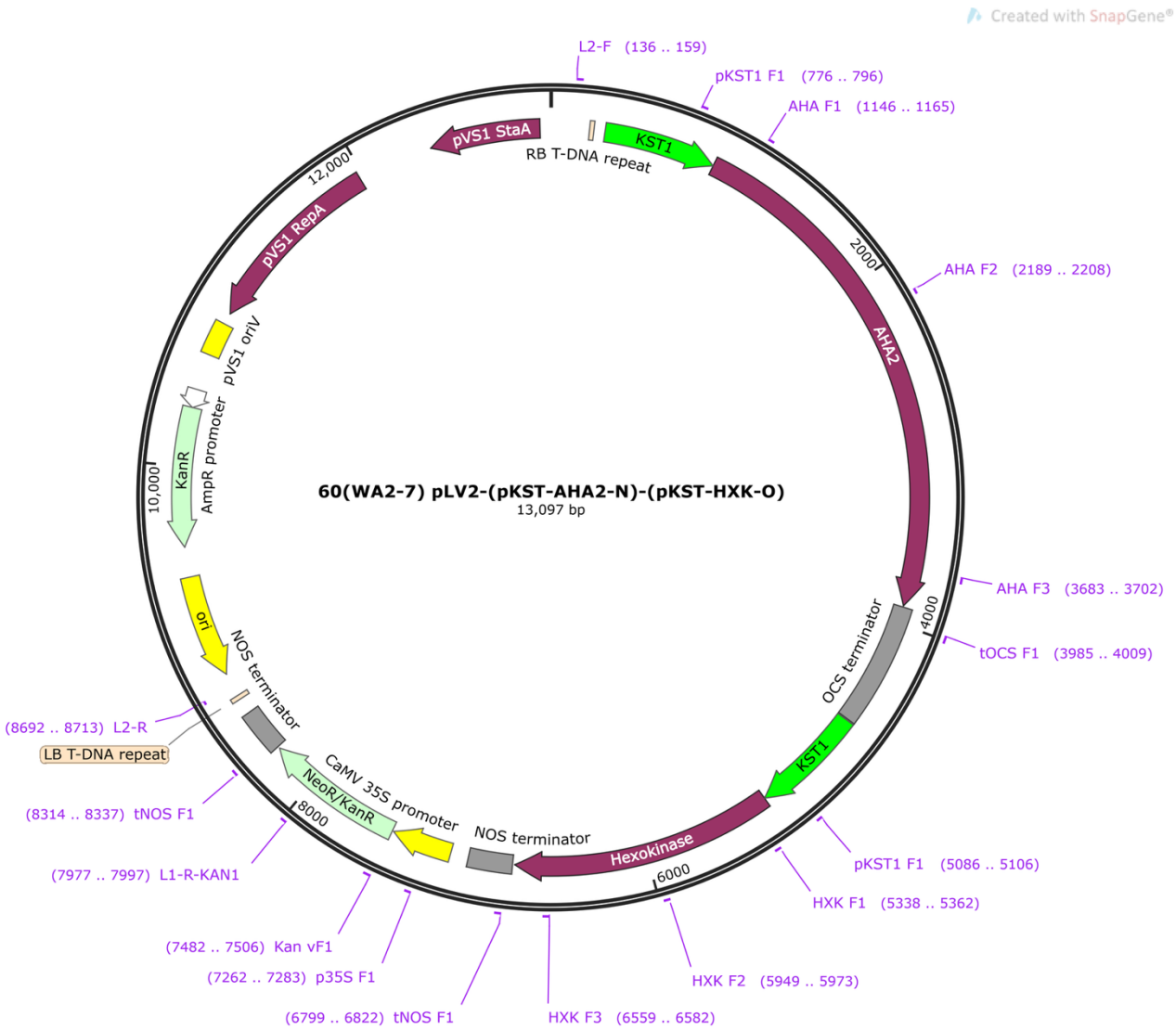

Figure 2.8. The plasmid map of the final Level 2 construct 60(WA2-7), assembled from constructs B, C and D in Fig. 2.1. The construct assembly was verified via sequencing using primers indicated by the purple labels. This construct is primarily comprised of Guard cell-specific overexpression of Hexokinase, Guard cell-specific overexpression of AHA2 and kanamycin resistance. The DNA situated between the Right border (RB) and Left border (LB) T-DNA repeat will be randomly inserted into the plant genome. Plasmid maps were created using SnapGene (SnapGene, United States).

2.2. Plant Material And Growth Conditions

2.2.1. Nicotiana tabacum

Seed stocks of wild-type *Nicotiana tabacum* cv. Samsun (WT), ictB independent line (TB6, from here on referred to as I) and previously transformed T1 transgenic STOMAGEN overexpressing lines (here on referred to as S) and double overexpressing lines (referred to as SI) were obtained from Prof. T. Lawson's laboratory, University of Essex. All tobacco plants were grown on soil (Levington F2, Fisons, Ipswich, UK) for two weeks in a controlled environment at an irradiance of 250 µmol photons m^{-2} s^{-1}, temperature of 25°C, relative humidity of 60%, under a 16-h photoperiod. After which, 12 randomly selected plants per line, including WT and azygous (AZ) controls, were re-potted into 3-inch individual pots and grown under the same conditions for two weeks. Plants were then transferred to 3 L pots and grown in a controlled greenhouse for the duration of the experiment. Tobacco plants were grown in two distinct glasshouse compartments: Low light (100-250 µmol photons m^{-2} s^{-1}) (ictB/STO T1 and T2, and HXK/AHA T2) or high light (600-800 µmol photons m^{-2} s^{-1}) (HXK/AHA T1) at pot height. The low-light condition was supplemented with high-powered LED lamps (LightDNA 8-channel, Vayola, Finland), but had a fixed glasshouse blind that greatly restricted natural sunlight. The high-light condition had unimpaired and natural light supplemented with high-pressure sodium light bulbs. Both high-light and low-light glasshouse conditions had similar environmental conditions, with 25–30°C daytime and 20°C nighttime temperatures, a relative humidity of ~ 60%, and a 16-h photoperiod.

Positions of the plants were changed weekly and watered with a nutrient medium (Hoagland and Arnon, 1950).

2.2.2. Fragaria X Ananassa

Strawberry plant material was provided as *in vitro* stock cultures by Niab (Niab, UK). *In-vitro* shoot cultures of *F. x annanassa* 'Calypso' were maintained in a growth room at 21 °C with a 16/8 h light/dark photoperiod, provided by fluorescent lamps (colour reference 835, colour temperature 3500K). Crowns were subcultured at 4-week intervals, 5-7 per honey jar containing 50 mL medium. Basal culture medium was Murashige and Skoog (MS) macro and microelements and vitamins (Murashige and Skoog, 1962) (4.4 g L^{-1}), supplemented with sucrose (30 g L^{-1}), 6-benzylaminopurine (BAP) 0.1 mg L^{-1} and indole-3-butyric acid (IBA) 0.1 mg L^{-1}, as described by Schaart (2014). The medium was solidified with Daishin agar (Duchefa D1004, 9 g L^{-1}). The pH was adjusted to 5.8 before autoclaving.

Figure 2.9. In vitro culture of untransformed Fragaria x annanassa 'Calypso' on strawberry propagation media.

Post regeneration, Strawberry plants were hardened by transfer to a vermiculite medium (Dupre Minerals, Staffordshire, UK) with very high humidity in six-cell propagation chambers (Artcome Ltd., UK). Plants were grown in these conditions for four weeks, with the humidity gradually decreasing by opening the lid vents and then removing the lid, allowing them to acclimate to the external environment.

Figure 2.10. Regenerated strawberry plants undergoing the hardening process in high high-humidity environment growing in vermiculite mineral substrate.

Strawberry plants were then transferred to soil (Levington F2, Fisons, Ipswich, UK). Plants were grown under two distinct environments: Controlled environment (CT Room) and Glasshouse conditions. The CT Room had a temperature of 23°C during the day and 18˚C at night, with a relative humidity of 65% and illumination of 300 µmol photons m^{-2} s^{-1}. The Glasshouse environment was the same as the high-light environment outlined for the tobacco, but the experiment ran during the summer, meaning that the daytime temperature ranged from 25-60 °C due to GM containment preventing ventilation.

Figure 2.11. Hardened strawberries growing in a controlled environment (day/night temperature 23/ 18 °C, 65% relative humidity and illumination of 300 µmol photons m^{-2} s^{-1}).

2.3. Strawberry Transformation

2.3.1. Transformation Of *Agrobacterium Tumefaciens*

A. tumefaciens strain EHA105 (Hood *et al.*, 1993), stored in 25% glycerol, was thawed on ice. The plasmid of interest (Figures 2.5-2.7) was added to thawed bacteria (1 µL, 100 ng mL^{-1}). The tube was flash-frozen in liquid nitrogen for 5 minutes and flash-thawed in a water bath at 37 °C for 5 minutes. The bacterial mix was added to low salt LB broth (700 µL) and shaken at 28 °C for 2 hours. Cells were pelleted by centrifugation at 8000 g for 2 minutes, 600 µL of the low salt LB broth was decanted and discarded, and cells were re-suspended in the remaining 100 µL of media. Cells were plated on

low salt agar plates with rifampicin (100 µg mL^{-1}) and the selectable marker (kanamycin 50 µg mL^{-1}) and left to grow at 28 °C for a minimum of 48 hours.

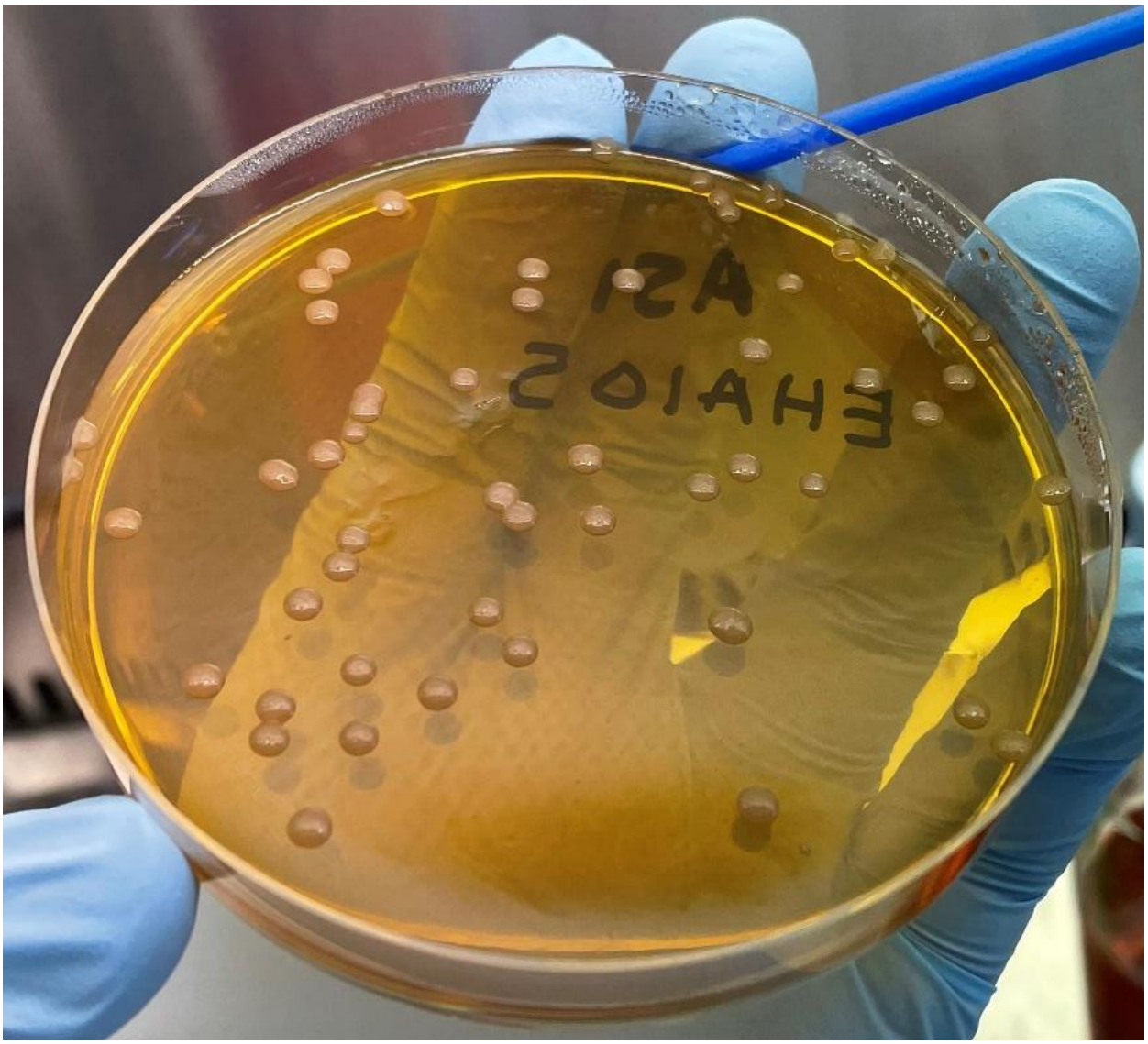

Figure 2.12. Successfully transformed A. tumefaciens strain EHA105.

2.3.2. Transformation Of The Octoploid Strawberry

Transformation of *F. x annanassa* 'Calypso' was performed following (Schaart, 2014), with minor amendments. *Agrobacterium tumefaciens* strain EHA105 (Hood *et al.*, 1993) harbouring the binary vector was grown overnight in a shaker at 28 °C and 180

rpm as a preculture in low salt LB broth with markers (10 mL, rifampicin 100 µg mL^{-1}, kanamycin 50 µg mL^{-1} and streptomycin 50 µg mL^{-1}). The preculture was then added to 80 mL of low salt LB broth, with the same selectable markers and concentrations as the preculture, and was grown overnight in a shaker at 28 °C and 180 rpm. The culture was pelleted at 2,000 g for 10 minutes. An MS-based medium (4.4 g L^{-1}) supplemented with glucose (30 g L^{-1}) and acetosyringone (100 µM) was prepared, pH adjusted to 5.2, and filter sterilised. The bacterial pellet was re-suspended in this medium to give an OD 600 nm 0.2 – 0.3.

Young expanding leaves of *F.* x *ananassa* 'Calypso' were harvested from shoots four weeks after subculture and submerged in the inoculum for approximately 10-15 minutes. Leaflets were separated from each leaf before scoring transversely, leaving one leaf edge intact. Explants were transferred to a filter paper on strawberry regeneration medium (SRM), adaxial face down. SRM is comprised of Murashige and Skoog (MS) macro and microelements and vitamins (Murashige and Skoog, 1962) (4.4 g L^{-1}), supplemented with 1-Naphthaleneacetic acid (NAA) 0.2 mg L^{-1}, thidiazuron (TDZ) 1 mg L^{-1} and filter sterilised glucose (300 g L^{-1}). The medium was solidified with Agargel (Sigma, 5 g L^{-1}) and the pH was adjusted to 5.8 before autoclaving.

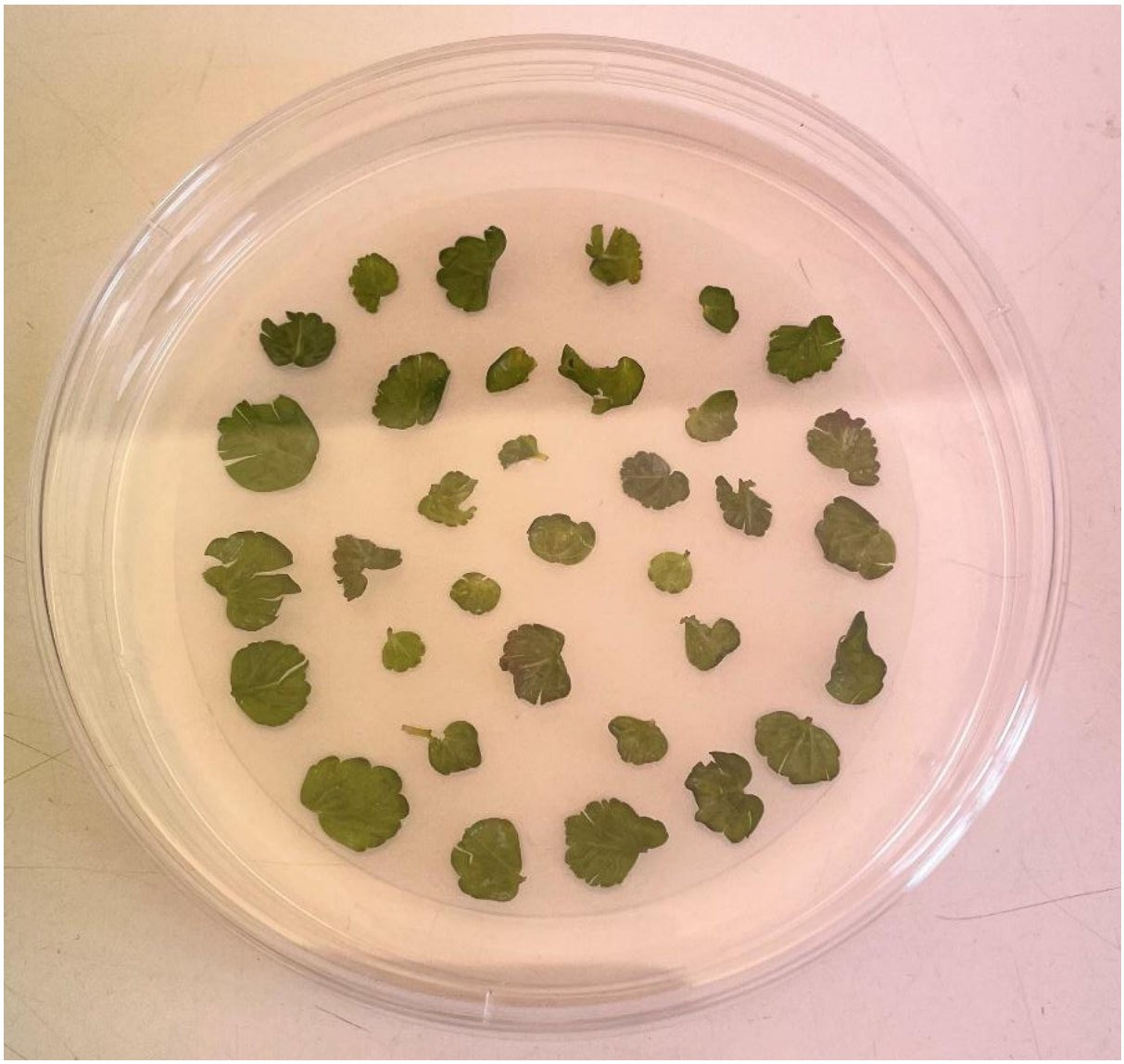

Figure 2.13. Strawberry leaf explants collected from untransformed material were infected with Agrobacterium. Explants are stored in the dark for 4 days on regeneration media without selectable markers. Explants are then subcultured onto regeneration media containing ticarcillin disodium/clavulanate potassium (TCA) for selection against Agrobacterium and kanamycin for selection for transformed tissue.

After four days of dark incubation at 21 °C, explants were transferred to SRM with selectable markers ticarcillin disodium/clavulanate potassium (Duchefa T0190) (400 µg mL^{-1}) and kanamycin (50 µg mL^{-1}). Sterilised filter paper was used to prevent direct contact between the explants and the media. Dishes were sealed with Parafilm® and incubated in the growth room under the same conditions previously

described. Explants were subcultured every 10 days. Leaves were divided between additional dishes as expansion occurred to separate regenerating calli.

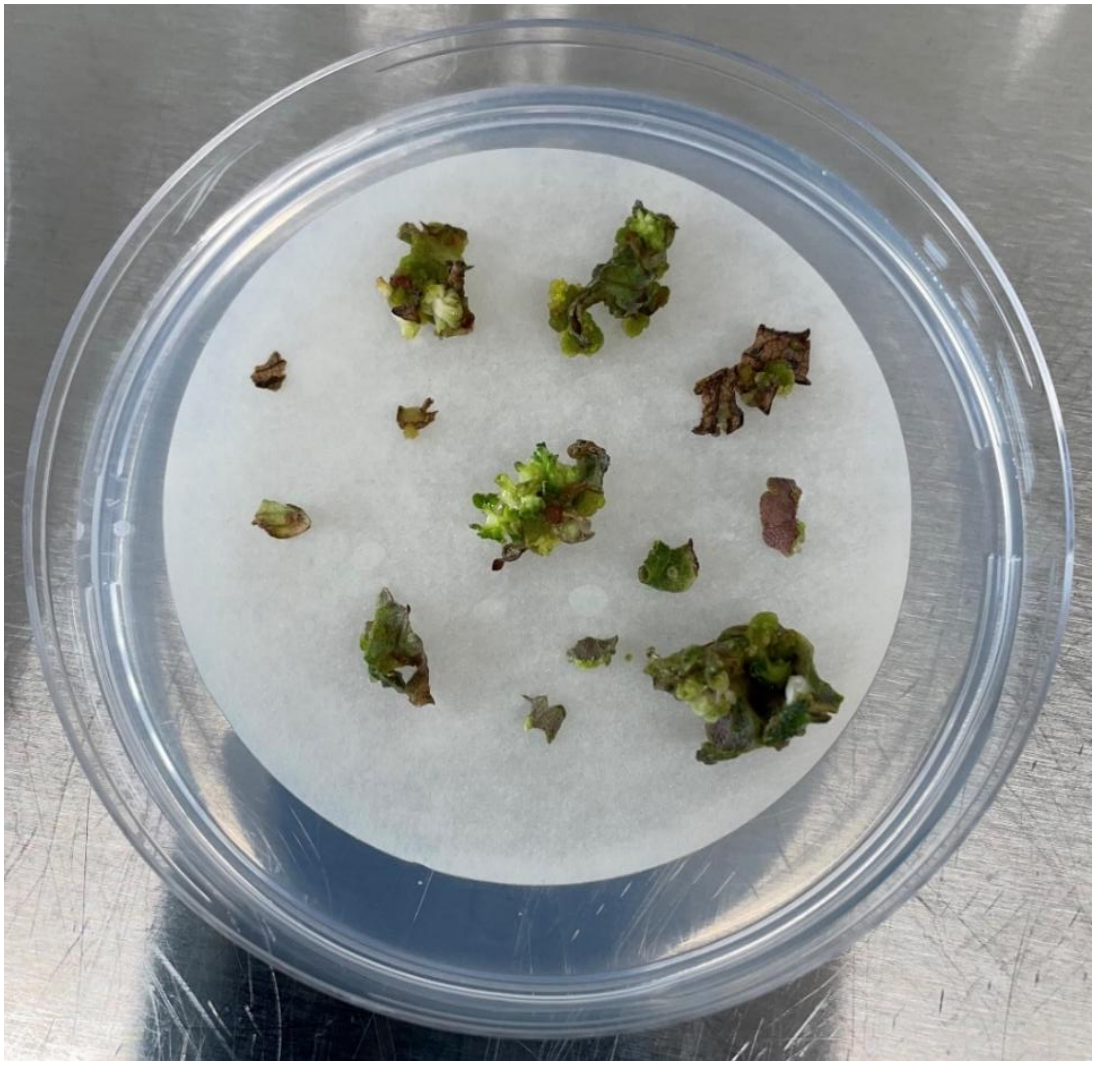

Figure 2.14. Excised calli from transformed strawberry leaf explants. Shoot formation can be seen on the central callus.

Callus formation and shoot emergence were seen at approximately 2 months post-infection (Figure 2.14). Regenerating calli were excised and spread over additional plates to allow space for expansion. Emerging shoots were then transferred to the rooting medium once large enough.

Regenerating shoots were transferred to rooting media (FragR) once greater than approximately 2 mm in size and displaying at least 1-2 leaves. FragR is comprised of Murashige and Skoog (MS) macro and microelements and vitamins (Murashige and Skoog, 1962) (2.2 g L^{-1}), supplemented with sucrose (20 g L^{-1}), 6-benzylaminopurine (BAP) 0.1 mg L^{-1} and indole-3-butyric acid (IBA) 0.1 mg L^{-1}. The medium was solidified with Daishin agar (Duchefa D1004, 9 g L^{-1}). The pH was adjusted to 5.8 before autoclaving. Post autoclaving, the medium was additionally supplemented with ticarcillin disodium/clavulanate potassium (Duchefa T0190) (400 µg mL^{-1}) and kanamycin (50 µg mL^{-1}).

Figure 2.15. A regenerated shoot of 60(WA1) in rooting media (FragR). Small roots have begun to emerge from the shoot and through the remaining callus underneath.

Plants with large root systems are then transferred to strawberry multiplication media (SMM) for crown expansion. SMM FragR is comprised of Murashige and Skoog (MS) macro and microelements and vitamins (Murashige and Skoog, 1962) (4.4 g L^{-1}), supplemented with sucrose (30 g L^{-1}), 6-benzylaminopurine (BAP) 0.5 mg L^{-1}. The

medium was solidified with Daishin agar (Duchefa D1004, 9 g L^{-1}). The pH was adjusted to 5.8 before autoclaving. Post autoclaving, the media was additionally supplemented with ticarcillin disodium/clavulanate potassium (Duchefa T0190) (400 µg mL^{-1}) and kanamycin (50 µg mL^{-1}) to select for putative transgenic plants only.

Roots typically begin to emerge after approximately 2 weeks on rooting media nut with a highly variable rate of emergence and development. Once a large root system has been established, then plants are transferred to multiplication media for crown expansion to create an *in-vitro* stock of that event (Figure 2.16). Upon transfer from FragR to SMM, leaf samples are taken for DNA extraction.

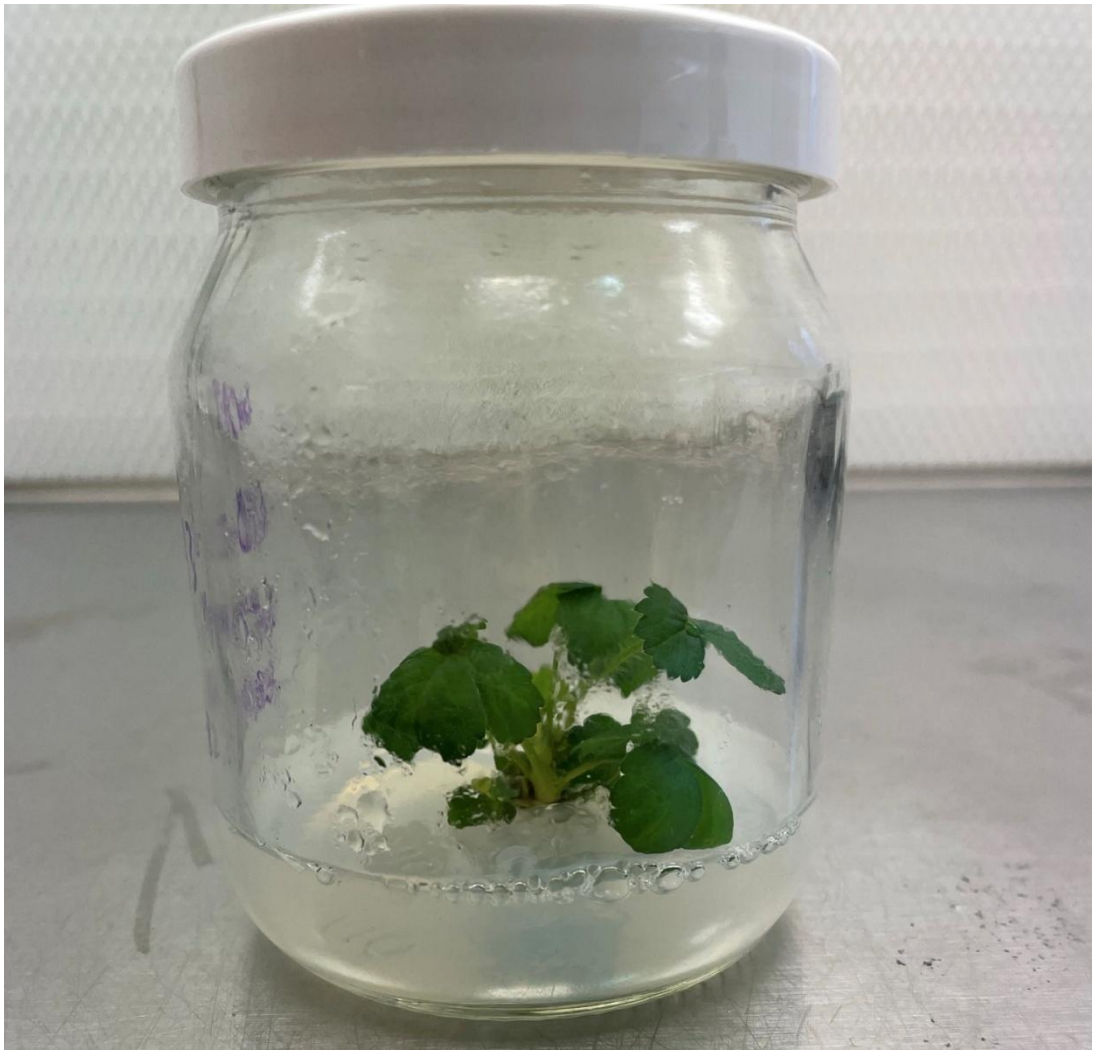

Figure 2.16. A regenerated plant of 60(WA2) in SMM for crown expansion. A large root system has developed (not visible).

2.4. Tobacco Transformation

2.4.1. Transformation Of Agrobacterium Tumefaciens

A. tumefaciens strain LBA4404 (Ooms *et al.*, 1982), stored in 25% glycerol, was thawed on ice. The plasmid of interest (Figures 2.6 and 2.8) was added to thawed bacteria (1 µL, 100 ng mL^{-1}). The tube was flash-frozen in liquid nitrogen for 5 minutes and flash-thawed in a water bath at 37 °C for 5 minutes. The bacteria mix was added to low salt LB broth (700 µL) and shaken at 28 °C for 2 hours. Cells were pelleted by

centrifugation at 8000 g for 2 minutes, 600 µL of the low salt LB broth was decanted and discarded, and cells were re-suspended in the remaining 100 µL of media. Cells were plated on low salt agar plates with rifampicin (100 µg mL^{-1}) and the selectable marker (kanamycin 50 µg mL^{-1}) and left to grow at 28 °C for a minimum of 48 hours.

2.4.2. Tobacco Seed Sterilisation

Wild-type seeds of *Nicotiana tabacum* were provided by the University of Essex (University of Essex, UK). Tobacco seeds were surface-sterilised by immersion in 70% ethanol for 2 minutes with gentle agitation. Ethanol was discarded, and seeds were then treated with 50% commercial bleach (sodium hypochlorite) for 5–10 minutes, with intermittent mixing to ensure uniform exposure. Following bleach treatment, seeds were rinsed thoroughly with sterile distilled water. This washing step was repeated at least four times to ensure complete removal of residual bleach. All steps were carried out in a laminar flow hood under sterile conditions using sterile pipette tips and reagents. Sterilised seeds were sown on MS medium. MS medium was prepared using Murashige and Skoog Basal Salt Mixture (Sigma M5524) at 4.3 g L^{-1}, supplemented with sucrose (30 g L^{-1}). The medium was solidified with agar (8 g L^{-1}), and pH was adjusted to 5.9 using KOH before autoclaving. This medium was used without vitamins and dispensed into Magenta vessels (approximately 1 L per 12 pots).

2.4.3. Transformation Of Tobacco

Agrobacterium tumefaciens strain LBA4404 (Hood *et al.*, 1993) harbouring the binary vector was grown overnight in a shaker at 28 °C and 180 rpm as a preculture in

low salt LB broth with markers (10 mL, rifampicin 100 µg mL^{-1}, kanamycin 50 µg mL^{-1} and streptomycin 50 µg mL^{-1}). The preculture was then added to 80 mL of low salt LB broth, with the same selectable markers and concentrations as the preculture, and was grown overnight in a shaker at 28 °C and 180 rpm. The culture was pelleted at 2,000 g for 10 minutes. An MS-based medium (4.4 g L^{-1}) supplemented with glucose (30 g L^{-1}) and acetosyringone (100 µM) was prepared, pH adjusted to 5.2, and was filter sterilised. The bacterial pellet was re-suspended in this medium to give OD 600 nm 0.5 – 0.6.

Agrobacterium cultures were divided into 50 mL sterile Falcon tubes. Leaf discs (~10 mm) were excised from 6–8 week-old *in vitro* Nicotiana plantlets and submerged in the resuspended Agrobacterium culture for ~10 minutes. Discs were then blotted and placed abaxial side up on NBM (no-antibiotic) plates. NBM consisted of Murashige and Skoog (MS) macro and microelements and vitamins (Murashige and Skoog, 1962) (4.4 g L^{-1}), supplemented with 6-benzylaminopurine (BAP) at 1.0 mg L^{-1} and 1-Naphthaleneacetic acid (NAA) at 0.1 mg L^{-1}. Plates were incubated at 22 °C in the dark (wrapped in foil) for 48 hours.

After the two-day dark co-cultivation with Agrobacterium, explants were transferred to NBM plates containing 50 µg mL^{-1} kanamycin and 400 µg mL^{-1} cefotaxime. Plates were incubated at 24 °C with a 16 h light / 8 h dark photoperiod. Explants were transferred to fresh NBM + antibiotic plates after 7 days. Explants were then moved to EM medium with the same antibiotic concentrations. EM consisted of Murashige and Skoog (MS) macro and microelements and vitamins (Murashige and Skoog, 1962) (4.4 g L^{-1}), supplemented with BAP at 2.5 mg L^{-1} and indole-3-acetic acid (IAA) at 0.2 mg L^{-1}.

Subculturing onto fresh EM medium was performed every 7–10 days. Shoots >1 cm were transferred to MS medium (no hormones) supplemented with antibiotics for rooting. Cefotaxime concentration was reduced to 200 µg mL^{-1} at this stage. After approximately 4 weeks, plants with large root systems (4+ individual roots and 2+ cm length) were then transferred to soil and placed in a controlled environment (250 µmol photons m^{-2} s^{-1}, temperature of 25°C, relative humidity of 60% and 16-h photoperiod) to await flowering.

2.5. Confirmation Of Transgene Insertion

2.5.1. Leaf DNA Extraction

Single strawberry leaves were taken from regenerated plants during the transfer from FragR to SMM. Tobacco leaf discs were taken from young glasshouse-grown plants. Leaf samples were stored in 1.5 mL Eppendorf tubes and frozen in liquid nitrogen for 5 minutes. DNA extraction buffer, comprised of 10% sodium dodecyl sulfate (SDS), 1 M Tris-HCl (pH 8), 0.5 M ethylenediaminetetraacetic acid (EDTA) and polyvinylpyrrolidone (PVP) (0.5 g L^{-1}), was heated to 65 °C pre-extraction. One Qiagen tungsten carbide bead (Qiagen, Manchester, UK) was placed into each sample tube, which was subsequently placed in a Geno/Grinder 2010 (SPEX SamplePrep, Cambridge, UK), which ran at 1500 rpm for 1.5 minutes. 250 µL of preheated extraction buffer was added to each sample, which was then vortexed for 3 seconds. Samples were placed in a water bath at 65 °C for 30 mins, with samples being vortexed every 5 mins. Samples were then centrifuged for 1 min at 4000 rpm. Samples were cooled at -

20 °C for 15 minutes before 250 µL of chilled (4 °C) 5 M NaCl was added to each sample. Samples were mixed and incubated at -20 °C for 15 mins. Samples were centrifuged at 4000 rpm for 20 mins, followed by the transfer of the supernatant to 1.5 mL Eppendorf tubes containing 200 µL of isopropanol, which were mixed at stored at -20 °C overnight for DNA precipitation. After overnight storage, samples were centrifuged at 4000 rpm for 20 minutes, and the supernatant was poured out. The pellet was washed by the addition of 500 µL of 70% ethanol and centrifuged at 4000 rpm for 20 mins, then the supernatant was poured away, with all steps being repeated once. The DNA pellet was air-dried for 4 hours, then rehydrated with 125 µL 1 mM Tris-HCl (pH 8). The quality of the extracted DNA was assessed using a Nanodrop 1000 (ThermoFisher Scientific, US) the following day.

2.5.2. PCR Verification Of Transgene Insertion

PCR reactions using forward (KanF1-aagatggattgcacgcaggttctcc) and reverse (KanR1-aacgctatgtcctgatagcggtcc) primers for the kanamycin resistance gene present in all Level 2 constructs were done to confirm transgene insertion. The reagents per reaction were as follows: 12.5 µL Quick-Load® Taq® 2X Master mix (New England Biolabs, Hertfordshire, UK), 0.5 µL 10 µM KanF1, 0.5 µL 10 µM KanR1, 1 µL DNA sample and 10.5 µL dH_2O. The PCR reaction was as follows: 1x(96 °C for 2 mins), 35x(96 °C for 15 secs, 60 °C for 15 secs, 72 °C for 90 secs) and 1x(72 °C for 5 mins). PCR products were run on a 1% agarose gel for 30 minutes at 145 volts. The banding patterns were compared to the 1 Kb ladder to assess the size, with an expected banding pattern of 657 bp for positive results. The level 1 vector encoding the kanamycin resistance gene

and DNA extracted from leaf tissue of untransformed strawberry Calypso stock or WT tobacco plants, for their respective reactions, were used as the positive and negative controls, respectively.

2.5.3. Copy Number Analysis

To assist with line selection and as a secondary confirmation of transgene insertion, tobacco leaf material was collected from the WT and transgenic lines of HXK/AHA (T0 and T1), and ictB/STO (T1) (T0 material was not available). 10 mm leaf disks were placed in a 2.0 ml microfuge tube and sent for molecular genetic screening. This professional service is used to determine the copy number of the transgene present in the plants' chromosomes based upon the selection marker transgene use, Kanamycin for HXK/AHA and BASTA for ictB/STO. The technology is proprietary intellectual property of Anglia DNA Services (Anglia DNA Services, Norwich, UK).

2.5.4. BASTA Selection Of T2 Transgenic Lines

T2 ictB/STO seeds were sown on agar plates consisting of Murashige and Skoog (MS) macro and microelements and vitamins (Murashige and Skoog, 1962) (4.4 g L^{-1}) containing BASTA (5 mg L^{-1}) to select for heterozygous lines harbouring the BASTA resistance gene and STO. Seedlings that survived positive selection were used in the T2 experiments.

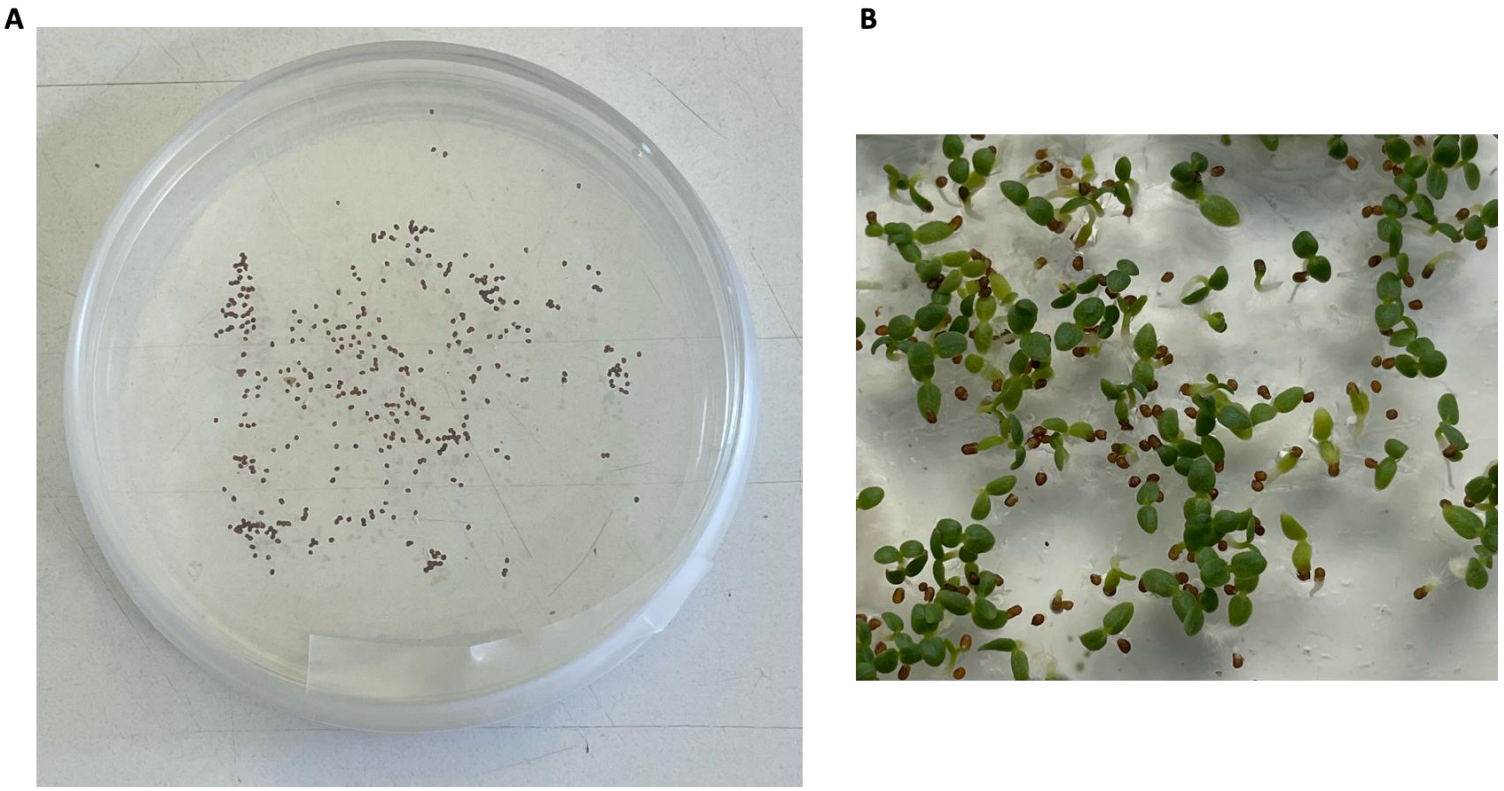

Figure 2.17. Germination and selection of T2 transgenic tobacco for BASTA. A) T2 segregating lines of STO and ictB::STO were sown on BASTA-containing medium to select for the STO transgene. B) Successfully germinated seedlings were used for T2 experiments.

2.6. Analysis Of Transgene Expression

2.6.1. Plant Leaf RNA Extraction

Leaf samples (100 mg) were harvested from growth conditions, in 1.5µl Eppendorf tubes and immediately frozen in liquid nitrogen. The leaves were then ground using a pestle and mortar in liquid nitrogen to prevent the rapid degradation of the RNA. RNA was extracted using the Nucleospin RNA Plant and Fungi Kit (Macherey-Nagel) according to the manufacturer's instructions. A DNase treatment was applied to the extracted RNA to minimise DNA contamination (Nucleospin rDNase kit, Macherey-Nagel). Concentration and quality of extracted RNA were determined using a Nanodrop

1000 spectrophotometer (Thermo Scientific) to confirm sufficient purity for cDNA synthesis.

2.6.2. cDNA Generation

cDNA was generated using the UltraScript™ 2.0 cDNA Synthesis Kit (PCR Biosystems) according to the kit instructions. RNA samples of various concentrations were diluted to 100 ng μL^{-1}. In each instance, 15 µL of RNA was processed (1500 ng total RNA).

2.6.3. qPCR Analysis of Transgene Expression

Primers for qPCR were designed using NCBI Primer-Blast for *Arabidopsis thaliana*, *Nicotiana tabacum* and *Fragaria x ananassa*. *(Duch)*. The *A. thaliana* sequence was derived from plasmid sequences for the transgenes. *F x ananassa* sequences were derived from the *Fragaria x ananassa* Camarosa Genome v1.0.a2 (Liu *et al.*, 2021).

F x ananassa specific housekeeping gene primers were taken from Lin et al., 2021(Lin *et al.*, 2021). The guard cell-specific primers for *Fragaria x ananassa* were designed based on the gene sequence for the strawberry homologue of AKT1, based on protein BLAST (maker-Fvb1-4-augustus-gene-10.65-mRNA-1). ictB transgene primers as well as PP2A housekeeping gene primers were used by Ruiz-Vera *et al.* 2022 (Ruiz-Vera *et al.*, 2022). The tobacco guard cell-specific primers for GORK1 were those used by Almari (2021). Primer sequences were as follows:

Table 2.2. qPCR primers

Gene	Orientation	Sequence	Role
ictB	Forward	gttggtttttgccctagcgg	Transgene
ictB	Reverse	ttggttgaggccgtagacac	Transgene
PP2A	Forward	gtgaagctgtagggcctgagc	*N. tabacum* Housekeeping gene
PP2A	Reverse	cataggcaggcaccaaatcc	*N. tabacum* Housekeeping gene
STOMAGEN	Forward	agttcaagcctcaagacctcg	Transgene
STOMAGEN	Reverse	gggtcatttccttcgactgg	Transgene
HXK	Forward	cgatccctaaatggcatggtctg	Transgene
HXK	Reverse	gaatccaggcgaacagattcttgag	Transgene
26srRNA	Forward	accgttgattcgcacaattggtcatcg	*F.x ananassa* housekeeping gene
26srRNA	Reverse	tactgcgggtcggcaaacgggcg	*F.x ananassa* housekeeping gene
GORK1	Forward	tccgtgtttgtgaactctgc	*N. tabacum* Guard cell-specific housekeeping gene
GORK1	Reverse	actccacttgcttcacacga	*N. tabacum* Guard cell-specific housekeeping gene
AHA2	Forward	tgccgagtcgccttccagtt	Transgene
AHA2	Reverse	ttcgacccaccaaggcacga	Transgene
AKT1	Forward	tttgcaatggcgttcagtgg	*F.x ananassa* Guard cell-specific housekeeping gene
AKT1	Reverse	agagagggcagtattccggt	*F.x ananassa* Guard cell-specific housekeeping gene

Primers were diluted to 10 µmol. A master mix using the 2x qPCRBIO SyGreen Mix Lo-ROX (PCR Biosystems) was made as follows for a total reaction volume of 20 µL:

Table 2.1. PCR reaction recipe for qPCR.

Reagent	Volume (µL)
2x qPCRBIO SyGreen Mix	10
Forward Primer	0.8
Reverse Primer	0.8
cDNA	1
dH2O	6.9

Samples were pipetted into a white rectangular 96-well plate (ThermoFisher Scientific) covered with transparent plastic (ThermoFisher Scientific). Plates were

loaded into the CFX Opus 96 Real-Time PCR System (Bio-Rad) for analysis. Each reaction contained three technical replicates and three biological replicates per cDNA sample (WT reaction included on every plate), three control reactions (no template cDNA) and three null controls (water only). The qPCR programme was as follows:

Cycles	Temperature
1x	95 °C for 10 minutes
40x	95 °C for 15 s followed by 60 °C for 25 seconds

Relative expression levels of the transgene were calculated using the 2(-Delta C(T)) method (Livak and Schmittgen, 2001). Briefly:

1. ΔCt was calculated as the difference between the Ct value of the target gene and the reference gene (Housekeeping gene):

$$\Delta\mathrm{Ct} = Ct_{Target} - Ct_{Reference}$$

2. Fold change in expression was calculated as:

$$Relative\ expression = 2^{-\Delta Ct}$$

Results were expressed as fold change relative to the reference gene.

2.7. Phenotypic Analysis Of Transgenic Plants

2.7.1. Chlorophyll Fluorescence Measurements

Chlorophyll fluorescence measurements were performed using a HEXAGON-Imaging-PAM system (Heinz Walz GmbH, Germany). Chlorophyll fluorescence imaging was performed on the youngest fully expanded leaves of 3-week-old tobacco seedlings that were grown in a controlled environment at an irradiance of 250 µmol mol^{-2} s^{-1}, 65% relative humidity and ambient CO_2 (400µmol mol^{-2} s^{-1}). Plants were dark-adapted for 30 minutes before imaging.

Under actinic illumination, steady-state fluorescence (F') was recorded, followed by application of the same saturating pulse to obtain maximum fluorescence in the light (Fm').

The following parameters were calculated by the imager:

- The maximum fluorescence yield of Photosystem II (Fv/Fm):

$$\frac{F_v}{F_m} = \frac{F_m - F_0}{F_m}$$

- Effective quantum yield of PSII photochemistry (Y(II)) (Genty, Briantais and Baker, 1989):

$$Y(II) = (Fm' - F') / Fm'$$

- Quantum yield of regulated non-photochemical energy dissipation (Y(NPQ)) (Kramer *et al.*, 2004):

$$Y(NPQ) = 1 - Y(II) - (1 / (NPQ + 1 + qL(Fm/Fo' - 1)))$$

- Apparent electron transport rate (ETR):

$$ETR = 0.5 \times Y(II) \times PAR \times 0.84$$

Where PAR is the incident photosynthetically active radiation (µmol m^{-2} s^{-1}), 0.5

assumes equal distribution of energy between PSI and PSII, and 0.84 is the assumed leaf absorptance for a standard green leaf.

Measurements were recorded across a range of actinic light intensities using three distinct protocols, each specific to the experiment:

- ictB/STO T1 (induction and light response curve):

0 → 215 → 215 → 215 → 215 → 215 → 215 → 215 → 215 →

0 → 89 → 100 → 215 → 294 → 400 → 500 → 601 → 700 → 800 → 1000 → 1200.

- ictB/STO T2 (induction and light response curve):

0 → 400 → 400 → 400 → 400 → 400 → 400 → 400 → 400 → 400 → 400 →

0 → 100 → 215 → 294 → 400 → 500 → 601 → 700 → 800 → 1000 → 1200 → 1416.

- HXAH (induction and relaxation): 0 → 400 → 400 → 400 → 400 → 0 → 0 → 0 → 0 → 0 → 0

Each step was maintained until steady-state fluorescence (F') was reached, at which point a saturating pulse (800 ms, 6200 µmol m^{-2} s^{-1}) was applied to determine Fm'. The resulting data were used to calculate Y(II), Y(NPQ) and ETR as described above.

2.7.2. Microscopy Of Leaf Epidermal Peels

Leaf epidermal peels were produced by applying a thin layer of nail polish directly to the abaxial and adaxial leaf surfaces of a recently harvested leaf. Once dried, clear tape was used to gently remove the nail polish, which was then adhered to a microscope slide (ThermoFisher Scientific, US).

Microscopy analysis of epidermal peels was done using a Swift Imaging 5MP camera and its associated SWIFT imaging software (SWIFT, US) attached to a Leica ATC 2000 light microscope (Leica Microsystems, Germany) using 20x magnification for Strawberry and 10x magnification for Tobacco. Stomatal density was calculated by counting the total number of guard cells within a defined area (0.18104843 mm). Counts were done on eight unique proximal areas on the epidermal peel. SD counts were first adjusted to 1 mm by dividing by the surveyed area (0.18104843 mm). Adjusted SD values were then averaged to give the SD of that replicate, with a total of 3 biological replicates per line.

Stomatal clustering was measured in plants overexpressing STOMAGEN. Plants with a stomatal clustering phenotype were counted twice: 1. Each guard cell was counted as unique, and 2. Guard cells within a cluster act as a group and thus count as one. The number of clustered stomata was calculated as follows:

$$SD_{(\text{Clustered stomata})} = SD_{(\text{Unique stomata})} - SD_{(\text{Clustered stomata act as one})}.$$

2.7.3. Gas Exchange Measurements

Leaf CO_2 was measured on the youngest fully expanded leaves using portable open gas exchange systems incorporating CO_2 and water vapour infra-red gas analysers (LI-6800, LI-COR Biosciences, Lincoln, NE, USA). Plants were subject to three gas exchange programmes: *A/C*$_i$, *A/Q* and Step-change, the specifics of which are as follows.

1. *A/C$_i$* Response Curves:

The response of net CO_2 assimilation rate (A) to intercellular CO_2 concentration (C_i) was measured using a portable open gas exchange system (LI-6800, LI-COR Biosciences, Lincoln, NE, USA) equipped with a 6 cm^2 fluorometer chamber (LI-6800-01A). Measurements were performed on the youngest fully expanded leaves under saturating irradiance (1500 µmol m^{-2} s^{-1} PPFD) supplied by the integrated red/blue LED light source. Chamber conditions were maintained at 25 °C leaf temperature and 65% relative humidity. Flow rate was set to 500 µmol s^{-1}, and reference CO_2 concentration (C_a) was initially held at 400 µmol mol^{-1} until steady-state gas exchange was achieved.

Following equilibration, C_a was decreased stepwise to 250, 150, 100, and 50 µmol mol^{-1}, then returned to 400 µmol mol^{-1} before being increased to 550, 700, 900, 1100, 1300, and 1500 µmol mol^{-1}. At each step, *A* was allowed to stabilise before recording (minimum wait of 90 seconds and maximum wait of 300 seconds).

The maximum carboxylation rate of Rubisco (V_{cmax}) and the maximum electron transport rate supporting RuBP regeneration (J_{max}) were estimated from the *A/C$_i$* response curves using the Farquhar-von Caemmerer-Berry model (von Caemmerer and Farquhar, 1981) as implemented in the plantecophys package in R (Duursma, 2015). The maximum rate of CO_2 assimilation (A_{max}) was taken as the rate at 1500 µmol mol^{-1} CO_2 under saturating light.

2. Light-response (*A/Q)* Response Curves:

Photosynthetic light-response curves were measured using a portable open gas exchange system (LI-6800, LI-COR Biosciences, Lincoln, NE, USA) fitted with a 6 cm^2

fluorometer chamber (LI-6800-01A). Measurements were made on the youngest fully expanded leaves under ambient CO_2 concentration (~400 µmol mol^{-1})supplied by the reference channel. Chamber conditions were maintained at 25 °C leaf temperature and 65% relative humidity. Flow rate was set to 500 µmol s^{-1}.

Actinic light intensity was applied in the following sequence (µmol m^{-2} s^{-1} PPFD): 1500, 1300, 1100, 900, 700, 550, 400, 250, 100, 0. At each step, leaves were allowed to reach steady-state photosynthesis before data were recorded.

Light-response parameters were estimated by fitting the non-rectangular hyperbola model:

$$A = \frac{\alpha Q + A_{sat} - \sqrt[2]{(\alpha Q + A_{sat})^2 - 4\alpha Q\theta A_{sat}}}{2\theta} - R_d$$

Where A is the net CO_2 assimilation rate (µmol m^{-2} s^{-1}), Q is the incident photon flux density (µmol m^{-2} s^{-1}), α is the apparent quantum yield, A_{sat} is the light-saturated assimilation rate, θ is the curvature factor, and R_d is the dark respiration rate.

Model fitting was performed in R using nonlinear least squares regression, and parameter estimates for A_{sat}, α, and R_d were derived directly from the fitted model.

3. Step-change measurements and modelling of stomatal kinetics

Stomatal conductance (g_{sw}) and net CO_2 assimilation (A) responses to step changes in photosynthetic photon flux density (PPFD) were measured using a portable open gas exchange system (LI-6800, LI-COR Biosciences, Lincoln, NE, USA) with an integrated LED light source (LI-6800-01A). The youngest fully expanded leaf was clamped in the chamber (6 cm^2) and equilibrated at low light (50 or 100 µmol m^{-2} s^{-1} PPFD), 400 µmol mol^{-1} CO_2, 25 °C, and a vapour pressure deficit of 1.0 ± 0.2 kPa until steady state was

reached. A single rapid increase in PPFD to 1000 µmol m^{-2} s^{-1} was applied, followed by a return to low light (50 or 100 µmol m^{-2} s^{-1})to characterise stomatal opening and closing kinetics, respectively.

Step-change programmes were as follows:

- 100 µmol m^{-2} s^{-1} for 900 s, 1000 µmol m^{-2} s^{-1} for 2700 s, then 100 µmol m^{-2} s^{-1} for 1800 s (Strawberry).
- 100 µmol m^{-2} s^{-1} for 600 s, 1000 µmol m^{-2} s^{-1} for 2400 s, then 100 µmol m^{-2} s^{-1} for 1400 s (HXK/AHA T1 and ictB/STO T2).
- 50 µmol m^{-2} s^{-1} for 900 s, 1000 µmol m^{-2} s^{-1} $^{-1}$ for 2700 s, then 50 µmol m^{-2} s^{-1} for 1800 s (HXK/AHA T2).

Measurements were logged every 10 seconds for all experiments except HXK/AHA T2, which were logged every 3 seconds.

Stomatal kinetics were quantified by fitting separate sigmoidal models to the opening (step-increase) and closing (step-decrease) phases, adapted from Vialet-Chabrand et al. (2017). The step-increase model was:

$$g_{sw}(t) = (G_{max} - G_{min})e^{-e^{\left(\frac{\lambda - t}{k_i} + 1\right)}} + G_{min}$$

and the step-decrease model was:

$$g_{sw}(t) = (G_{min} - G_{max})e^{-e^{\left(\frac{\lambda - t}{k_d} + 1\right)}} + G_{max}$$

where t is time (s), λ is the inflexion point of the response, k is a time constant describing the rate of change, and G_{min} and G_{max} are the asymptotic minimum and maximum conductance values, respectively.

All model fitting was conducted in R (version 4.5.1), with parameter estimates extracted for subsequent statistical analysis.

2.8. Statistical Analyses

All statistical analyses were conducted in R (version 4.5.1; R Core Team, 2025) using RStudio (Posit Software, PBC). Data were inspected for normality and homogeneity of variance before hypothesis testing. Where assumptions of normality were met, comparisons between groups were performed using one-way or two-way analysis of variance (ANOVA) followed by Tukey's honestly significant difference (HSD) post-hoc test. Where assumptions were violated, non-parametric equivalents were applied. Model fitting for stomatal kinetics was performed using non-linear least squares (nls) with separate fits for the step-increase and step-decrease phases. Coefficients of determination (R^2) and 95% confidence intervals were calculated for each fitted model. Data visualisation was performed using the ggplot2 and ggpubr packages, with figures generated directly from processed data to ensure reproducibility. Statistical significance was accepted at $p < 0.05$ unless otherwise stated.

3. Genetic Manipulation of Stomatal Patterning and Behaviour to Optimise Gas Exchange in the Cultivated Strawberry

3.1. Introduction

Crop productivity can be improved through increasing photosynthetic carbon assimilation. Photosynthetic carbon assimilation gains can be achieved through the manipulation of stomatal density. Stomata are pores in the epidermal layer of the aerial parts of plants (Kirkham, 2014). The pore of a singular stoma is formed between a pair of specialised epidermal cells called guard cells (Kirkham, 2005). Stomata function to control the movement of gases between the external atmosphere and the internal leaf air spaces (Lawson and Morison, 2004). This is measured at the leaf level as stomatal conductance (g_{sw}), which is determined by the number of stomata and how open the pores are (Lawson, Weyers and Brook, 1998). The resistance of gas diffusion from the atmosphere to the chloroplast is one of the major limitations to CO_2 assimilation (Farquhar and Sharkey, 1982), and therefore, g_{sw} is strongly correlated with CO_2 assimilation (Wong, Cowan and Farquhar, 1979). One possible mechanism for increasing photosynthetic carbon assimilation would be manipulating stomatal density (SD) of the leaf, defined as the number of stomata per unit leaf area, as increasing SD effectively increases stomatal conductance due to the greater number of pores to allow for greater gas exchange. Using the constitutive overexpression of STOMAGEN, an epidermal patterning factor gene that promotes stomatal development, Tanaka et al. (2013) produced *Arabidopsis* plants with a 200-300% increase in SD. The CO_2

assimilation of these plants was increased by 30% due to greater CO_2 diffusion into the leaf (Tanaka et al., 2013). However, the consequent increase in SD has one major consequence: the increase in transpiration and thus the reduction in water-use efficiency (WUE).

As global water usage is set to double by 2030, attempts to increase photosynthetic carbon assimilation by increasing SD cannot be compromised by the resultant increased transpiration and decreased WUE (Tanaka et al., 2013; Lawson and Blatt, 2014; Lawson and Vialet-Chabrand, 2019; Sakoda et al., 2020). Guard cells alter in turgor pressure to control stomatal aperture in order to maintain an optimal balance of CO_2 intake necessary for photosynthesis and water loss, the ratio of which is known as iWUE (Lawson et al., 2014; Hatfield and Dold, 2019). Thus, manipulations of stomatal function could be used to offset the reduction in iWUE caused by increased SD. The overexpression of Hexokinase, a sugar-sensing enzyme that induced stomatal closure, in guard cells, has been shown to result in accelerated stomatal closure, and reduced stomatal conductance without compromising photosynthesis, improving iWUE and enhanced growth in some cases (Kelly *et al.*, 2013; Lugassi *et al.*, 2015). Guard cell-specific overexpression of Hexokinase could therefore work in tandem with STOMAGEN overexpression to aid in mitigating water loss.

The cultivated strawberry (*Fragaria x ananassa*) is an economically important fruit crop in the UK, with annual production in 2019 valued at £394 million, accounting for 45% of total fresh fruit production value and only exceeded in single crop production value by cereals, oilseed rape and potatoes (DEFRA, 2019). A recent quantitative limitation study in greenhouse-grown strawberries demonstrated that stomatal limitation (SL) is the dominant constraint on photosynthesis, primarily due to reduced

stomatal conductance, even when water is non-limiting during mid-day periods (Yokoyama *et al.*, 2023). These data suggest that strawberries grown in glasshouses, a common production system in the UK accounting for 6-10% of total strawberry production between 2021 and 2023 (Crane *et al.*, 2023), may benefit from the mitigation of the stomatal constraint on photosynthetic carbon assimilation. The overexpression of STOMAGEN in strawberry plants may benefit greenhouse-grown plants due to an increase in maximum potential g_{sw}, through increasing SD (Drake, Froend and Franks, 2013; Tanaka et al., 2013). An increase in maximum potential g_{sw} may help to alleviate the constraint on photosynthetic carbon assimilation during and following the midday depression and may result in greater CO_2 assimilation over the diurnal period (Yokoyama *et al.*, 2023).

This chapter covers the molecular and physiological characterisation of transgenic strawberry lines (*Fragaria x ananassa, cv.* Calypso*)* overexpressing: 1. STOMAGEN under the control of the constitutive 35S CMV promoter, 2. Guard cell-specific overexpression of Hexokinase and 3. Concomitant overexpression of both constructs. These three genotypes were created to ascertain the effects of altered stomatal patterning and environmental response in a readily transformable strawberry cultivar.

3.2. Results

3.2.1. Molecular Validation Of Transgenic Lines

3.2.1.1. PCR Confirmation Of NPTII Insertion In Transformed Lines

To confirm the insertion of the transgene into the genome of the putative transgenic strawberry lines, a PCR was used to confirm the presence of the positive selection marker NPII and thus, by proxy, the presence of the transgene/s (Fig. 3.1). Plants transformed with STOMAGEN (S), Hexokinase (H) and the double construct (SH) display bands at 658 bp, in concordance with the positive control (Band 2, Figure 3.1). Lines with no bands at the expected position were classified as escapes and thus grouped into an azygous line. Following the PCR analysis, only plants that exhibited an appropriate band were selected for vegetative stolon propagation and further analysis.

Table 3.1 Table of plants used in this chapter. Lines that did not survive until stomatal density quantification are not included.

Codename	Background	Transgene	Promoter	Terminator	Source
AZ_1	Wild Type	N/a	N/A	N/A	This study
H_14	Wild Type	Hexokinase	KST1	NOS	This study
H_242	Wild Type	Hexokinase	KST1	NOS	This study
H_251	Wild Type	Hexokinase	KST1	NOS	This study
H_254	Wild Type	Hexokinase	KST1	NOS	This study
H_272	Wild Type	Hexokinase	KST1	NOS	This study
H_352	Wild Type	Hexokinase	KST1	NOS	This study
H_353	Wild Type	Hexokinase	KST1	NOS	This study
H_354	Wild Type	Hexokinase	KST1	NOS	This study
H_62	Wild Type	Hexokinase	KST1	NOS	This study
H_93	Wild Type	Hexokinase	KST1	NOS	This study
H_95	Wild Type	Hexokinase	KST1	NOS	This study
S_152	Wild Type	STOMAGEN	35S	HSP	This study
S_261	Wild Type	STOMAGEN	35S	HSP	This study
S_271	Wild Type	STOMAGEN	35S	HSP	This study
S_32	Wild Type	STOMAGEN	35S	HSP	This study
S_63	Wild Type	STOMAGEN	35S	HSP	This study
S_71	Wild Type	STOMAGEN	35S	HSP	This study
S_91	Wild Type	STOMAGEN	35S	HSP	This study
SH_112	Wild Type	STOMAGEN and Hexokinase	35S and KST1	HSP and NOS	This study
SH_12	Wild Type	STOMAGEN and Hexokinase	35S and KST1	HSP and NOS	This study
SH_15	Wild Type	STOMAGEN and Hexokinase	35S and KST1	HSP and NOS	This study
SH_20	Wild Type	STOMAGEN and Hexokinase	35S and KST1	HSP and NOS	This study
SH_28	Wild Type	STOMAGEN and Hexokinase	35S and KST1	HSP and NOS	This study
SH_32	Wild Type	STOMAGEN and Hexokinase	35S and KST1	HSP and NOS	This study
SH_51	Wild Type	STOMAGEN and Hexokinase	35S and KST1	HSP and NOS	This study
SH_52	Wild Type	STOMAGEN and Hexokinase	35S and KST1	HSP and NOS	This study
SH_71	Wild Type	STOMAGEN and Hexokinase	35S and KST1	HSP and NOS	This study

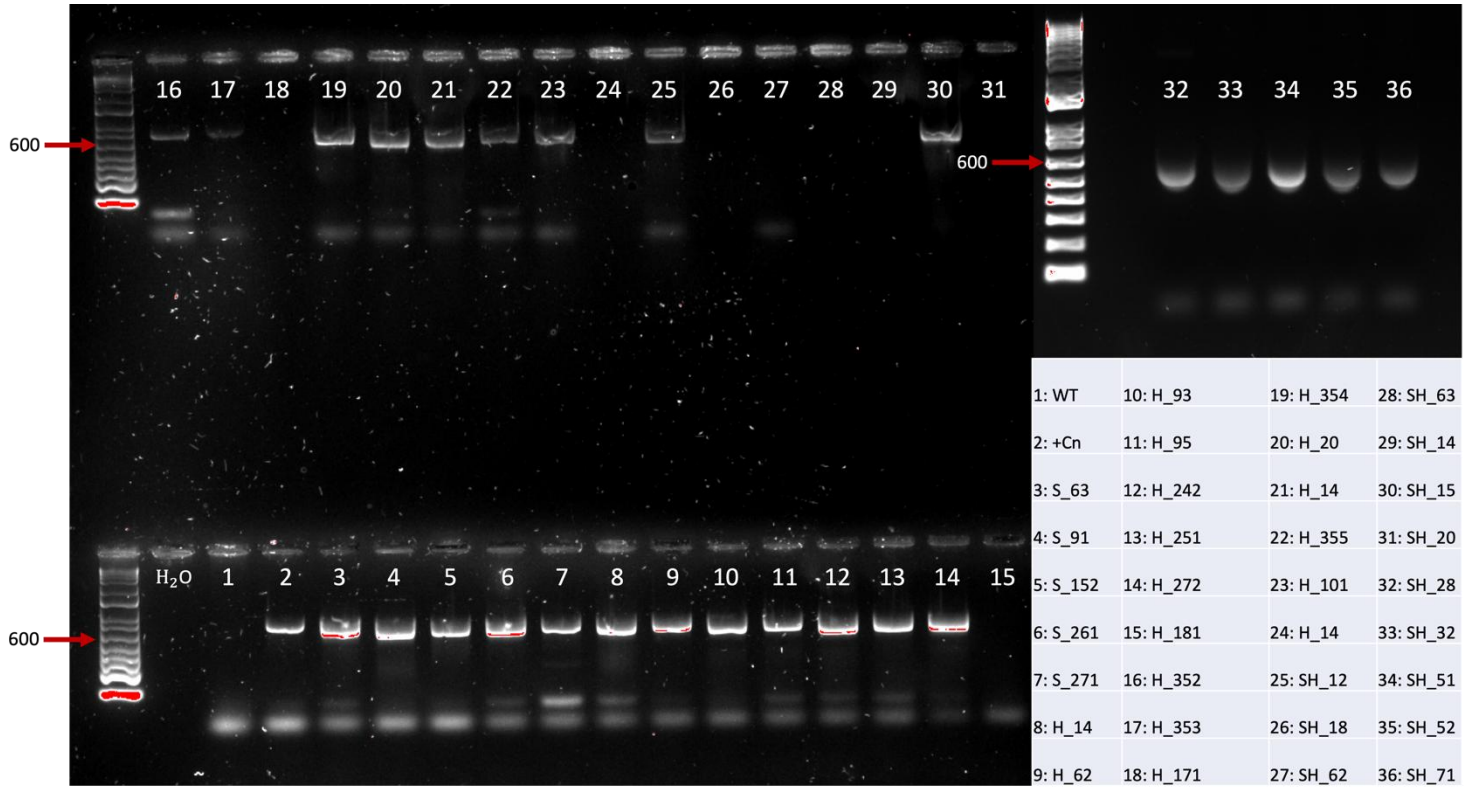

Figure 3.1. Agarose gel showing the banding patterns of DNA fragments produced from a PCR using the forward and reverse primers for the kanamycin resistance gene (NPII) and DNA from putatively transformed T0 strawberry plants. Positive results display a banding pattern of 658 bp. The Level 1 module 60 encoding kanamycin resistance was used as a positive control (+ Cn) and DNA extracted from the untransformed stock of F. x annanassa 'Calypso' was used as a negative control (WT). Transgenic line labels are as follows: STOMAGEN (S), Hexokinase (H) and the STOMAGEN + Hexokinase double construct (SH). CT Room: 23°C day and 18°C night, 65% RH, and a 16-h photoperiod of 300 µmol photons m^{-2} s^{-1}.

3.2.1.2. Qualitative Detection of Transgene Expression Via PCR with cDNA

As a secondary qualitative screen to transgene insertion, PCR analysis of cDNA synthesised from total leaf RNA was used to visualise the expression of both the transgene(s) and resistance gene *NPII* (Figure 3.2). Bands of a size 658 bp indicate a positive reaction and the expression of the resistance gene for kanamycin *NPII* (Figure 3.2A and B), bands of a size 183 bp (Figure 3.2A) and 181 bp (Figure 3.2B) indicate a positive reaction and the transgenic expression of STOMAGEN (STO) and Hexokinase

(HXK), respectively. No bands are observed for the WT negative controls wells 1 upper, lower and well 1(S) (*NPII*, HXK and STO, respectively) (Figure 3.2B). Lines with no presence of either resistance gene or transgene expression, later quantitatively confirmed via qPCR (Figure 3.3), were considered Azygous.

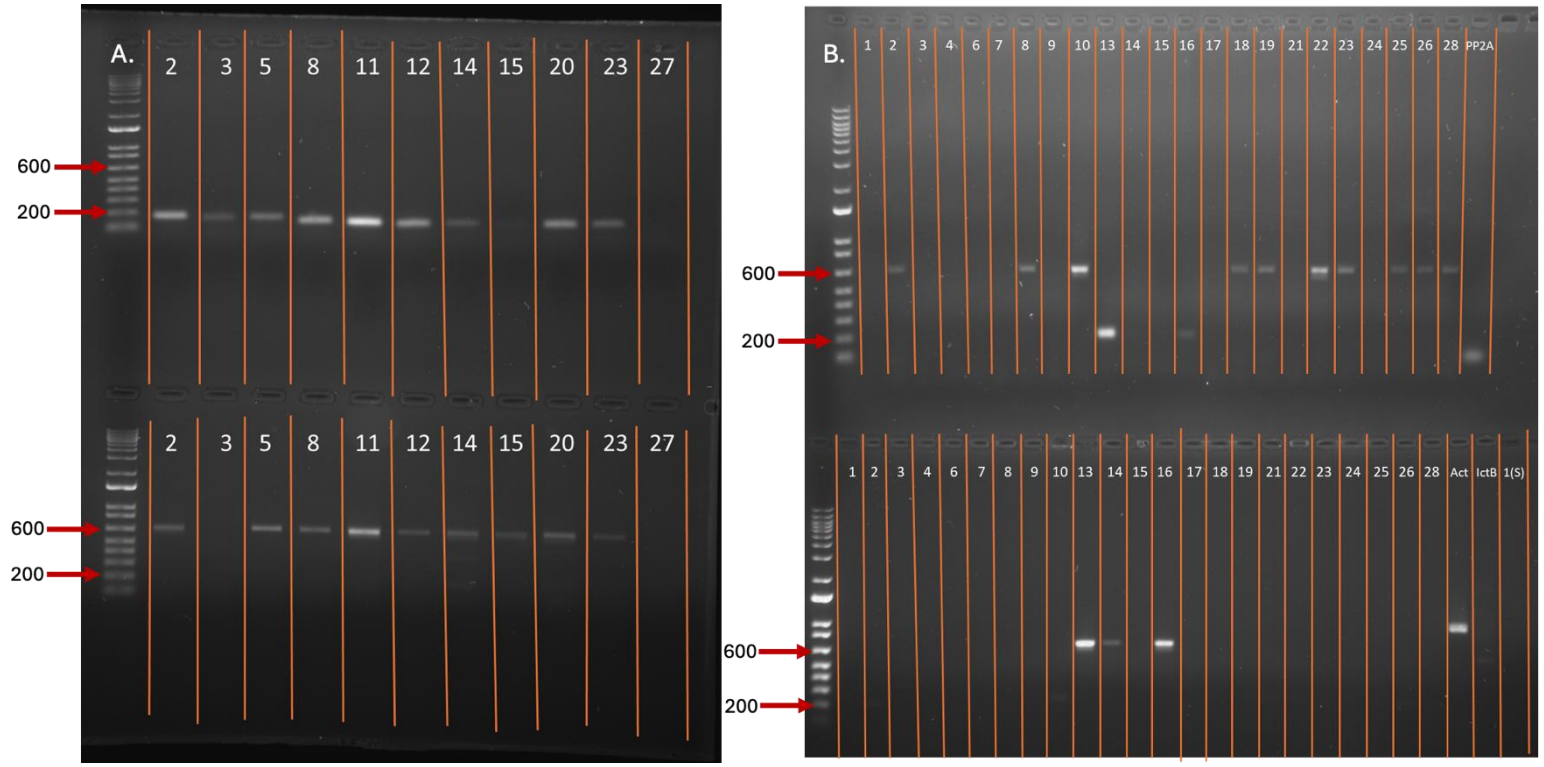

Figure 3.2. Agarose gel shows the banding patterns of DNA fragments produced from a PCR reaction using the forward and reverse primers for transgenes on cDNA synthesised from RNA from T0 strawberry leaf samples. A) STO (upper) and NPII (lower) reactions producing banding patterns of 183 and 685 bp, respectively. B) HXK and NPII reactions (mixed) produce banding patterns of 181 and 685 bp, respectively. The numbers at the top of the wells correspond to the cDNA label of the transgenic line in Table 2.1. CT Room: 23°C day and 18°C night, 65% RH, and a 16-h photoperiod of 300 µmol photons m^{-2} s^{-1}.

3.2.1.3. Quantitative Expression Analysis Of STOMAGEN And Hexokinase

To select transgenic lines of interest, quantitative PCR was used to compare relative transgene expression between lines of interest (Fig. 3.3). Transgenic plants had a wide range of expression levels for STO and HXK, relative to 26S rRNA and the

strawberry orthologue of the guard-cell-specific ion channel GORK. For STO and HXK (Fig. 3.3A and B), statistical group A had little to no detectable expression levels, equivalent to the azygous, and thus were considered azygous. STO lines (Fig. 3.3A) formed six distinct expression groups (including the azygous) (ANOVA, Tukey HSD, $p < 0.05$), with a range of expression from 0.00064 to 0.004x relative to 26S rRNA. Double overexpressing lines, SH_32 and SH_71, had the highest levels of expression (Groups D and E, ANOVA, Tukey HSD, $p < 0.05$). HXK lines fell into five statistical groups (Fig. 3.3B) (ANOVA, Tukey HSD, $p < 0.05$). HXK lines had a range of expression from 0.6 to 6x that of the strawberry orthologue of GORK. One single line, H_354, and two double lines, SH_15 and SH_71, had the highest levels of relative expression (ANOVA, Tukey HSD, $p < 0.05$).

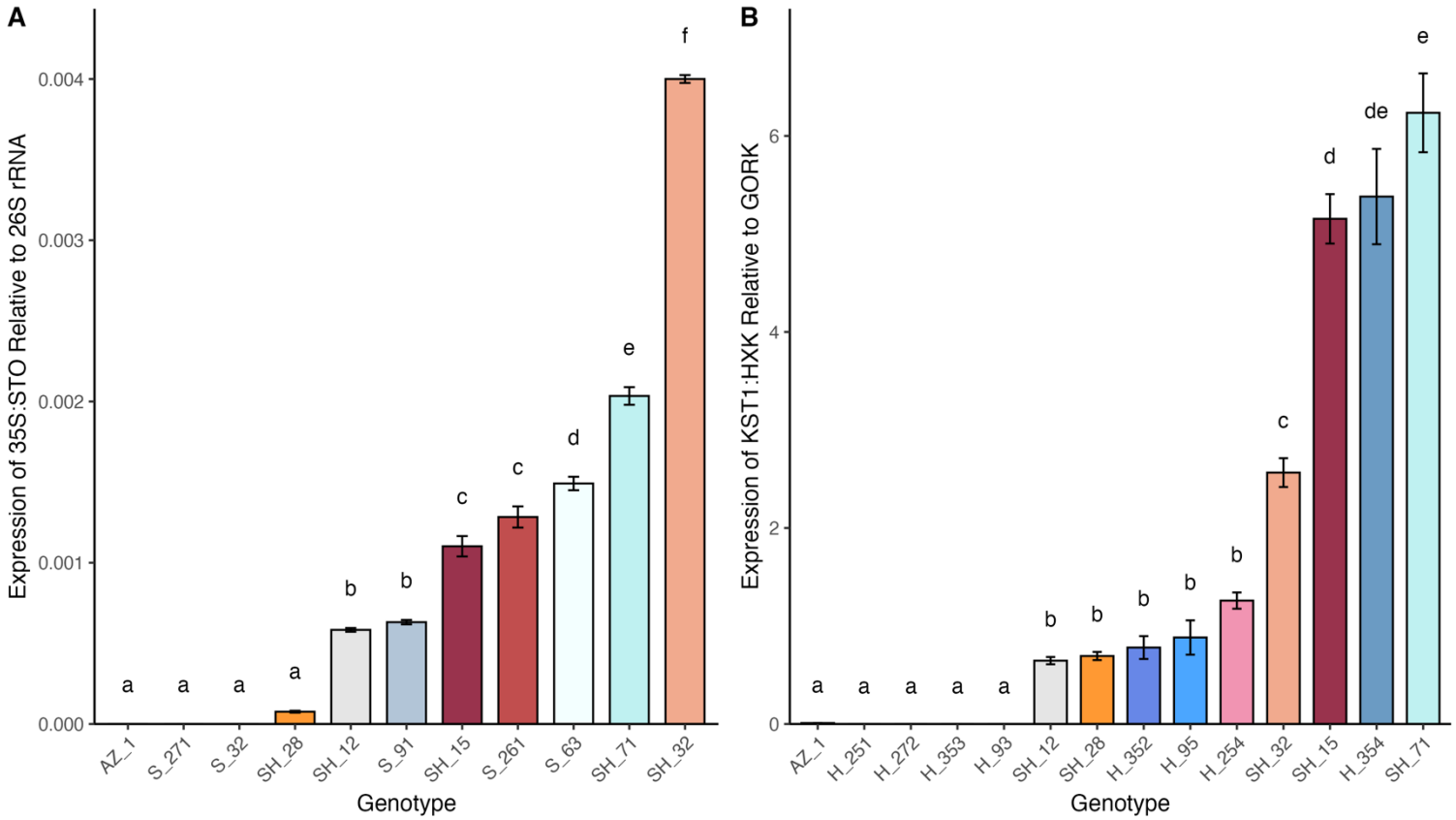

Figure 3.3. Quantitative PCR (qPCR) analysis of relative expression of the transgenes 35S STO and KST1 HXK in transgenic T0 strawberry lines. A) STO transgene expression normalised to the expression of 26S rRNA. B) HXK transgene expression normalised to the expression of AKT1 ortholog in Strawberry (Fvb1-4_1088267..1088726 (- strand)). Relative gene expression was calculated by normalising to the respective WT housekeeping gene. Bars show means ± SE (n = 3 biological replicates). Statistical groupings (CLD) are displayed by the letters above each respective genotype (ANOVA, Tukey HSD, $p < 0.05$). CT Room: 23°C day and 18˚C night, 65% RH, and a 16-h photoperiod of 300 µmol photons m^{-2} s^{-1}.

3.2.2. Microscopic Characterisation Of Stomatal Development

3.2.2.1. Changes In Epidermal Patterning In Transgenic Lines

To assess the epidermal changes resulting from the overexpression of the transgenes, SD in epidermal peels was quantified using brightfield microscopy. Transgenic strawberry plants overexpressing STO not only displayed greater stomatal

densities, but also frequent incidences of stomatal clustering (a violation of the one-cell spacing rule) (Fig. 3.4). Stomata formed clusters accounting for 7.2-23.1% of total stomata of all surveyed areas and were present in all surveyed areas of STO overexpressing lines. Stomatal clusters ranged from groups of 2 to 10 (possibly even higher) stomata per cluster. Stomatal clusters were produced in a variety of orientations, but typically, high clusters of higher numbers formed a chain of stomata 'top to tail'. Stomatal clustering occurred seldom in Azygous and HXK overexpressing lines.

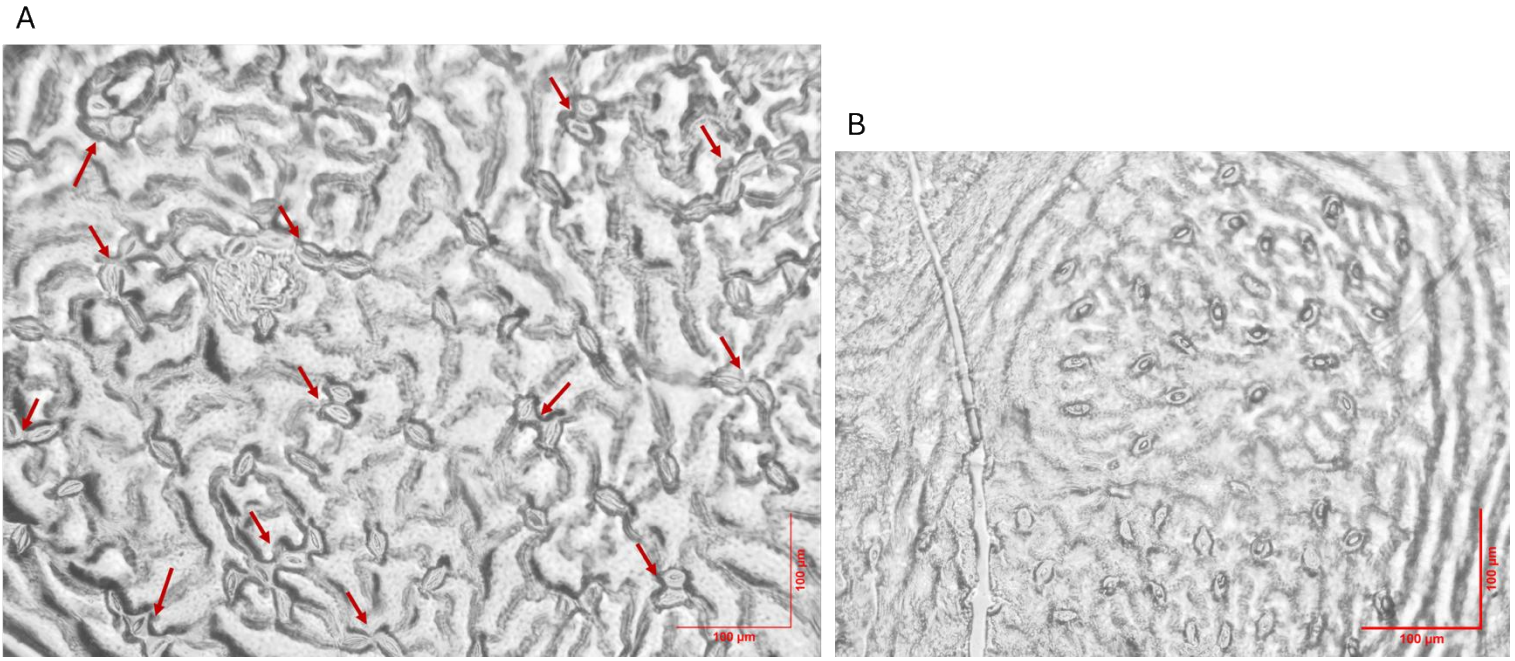

Figure 3.4. Brightfield microscopy images of strawberry leaf epidermal peels under 20x magnification. A) The epidermis of an exemplar T0 STO overexpressing line shows the stomatal clustering phenotype typically observed in these lines. B) The epidermis of an Azygous control with typical unclustered stomata. The red arrows indicate stomatal clusters. These impressions were taken from strawberries grown in a CT Room: 23°C day and 18˚C night, 65% RH, and a 16-h photoperiod of 300 µmol photons m^{-2} s^{-1}. Stomatal clustering seldom occurred in non-STO overexpressing lines.

3.2.2.2. Quantification Of Stomatal Density Across Transgenic Genotypes

The transgenic strawberry lines produced had significantly different stomatal densities when grown in the CT Room environment. Strawberry is a hypostomatous species, having stomata only on the abaxial leaf surface. Azygous lines had an average abaxial SD of 210 (±2.68) stomata mm^{-2}. STO overexpressing line S_32 and double lines SH_51 and SH_52 showed no significant difference in abaxial SD (Fig. 3.5, Statistical group A), which reflects the lack of transgene expression for S_32, as outlined in Figure

3.3 (Lines SH_51 and SH_52 were lost to disease before expression analysis was done). STO overexpressing lines in statistical groups C, D, E and F had significantly higher SD than the Azygous, with an SD average ranging from 240 to 400 stomata mm^{-2}. HXK lines either showed no significant difference in SD from the Azygous (Statistical group A: H_251, H_352, H_353, H_354, H_93) or significantly reduced SD with an average SD range of 175 to 188 stomata mm^{-2} (Group B: H_14, H_242, H_254, H_62, H_95). All lines were hypostomatous, with stomata only present on the abaxial surface. STO overexpressing lines did not have additional stomata present on the adaxial leaf surface. These data suggest that transgenic overexpression of STO increases abaxial stomatal density but is unable to induce stomatal development on the astomatous adaxial surface, and that guard-cell-specific HXK can decrease stomatal density in ~50% of lines produced.

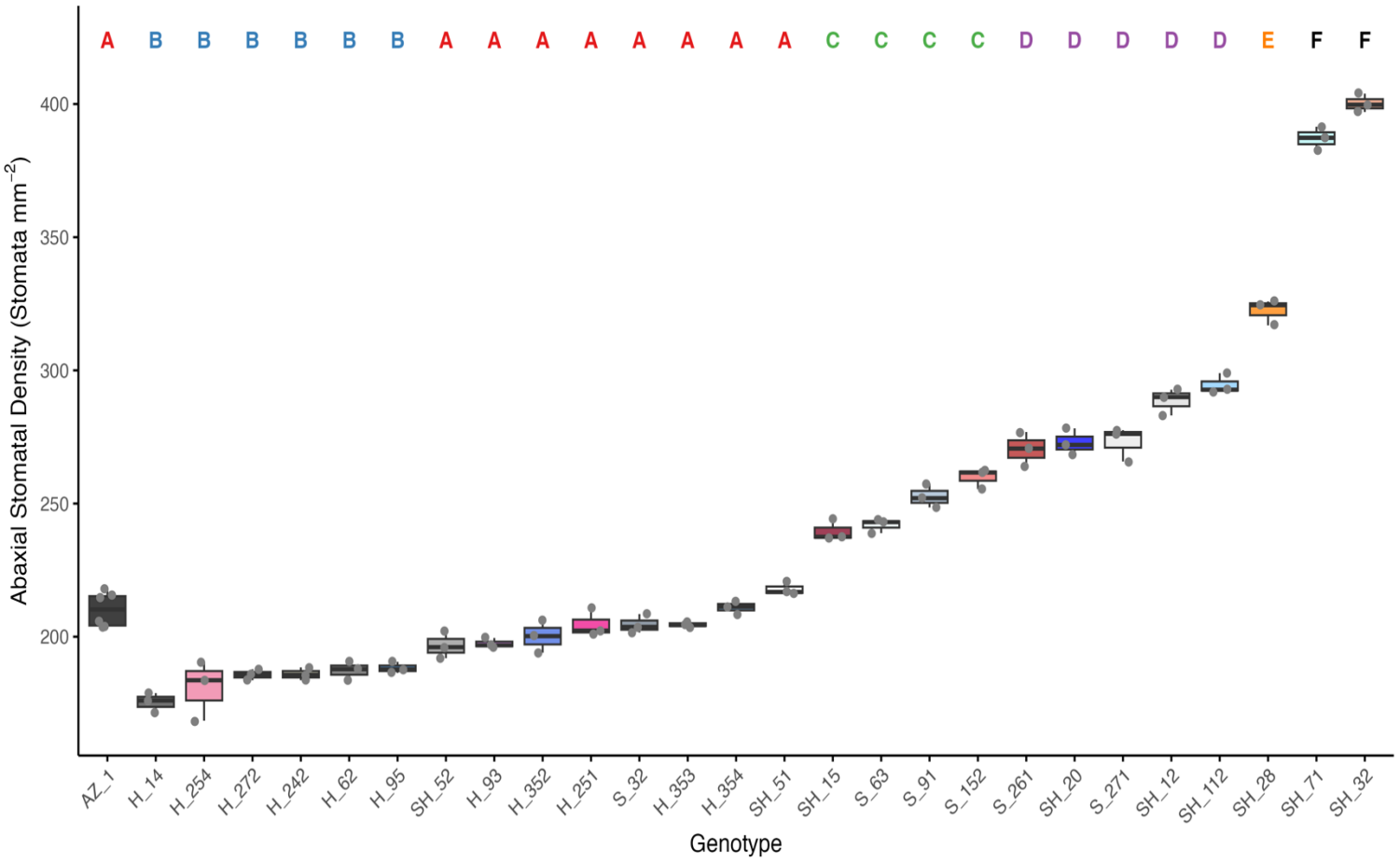

Figure 3.5. Stomatal density comparison between transgenicnT0 Strawberry lines grown in the CT room environment (23 ℃, 65% RH and 350 mol m^{-2} s^{-1} white light). Stomatal density counts were done on 8 areas of an epidermal peel to form a sample average. Statistical groupings (CLD) are displayed by the letters above each respective genotype (ANOVA, Tukey test, $p < 0.05$). For transgenic lines, $n = 3$, and for AZ_1, $n = 6$. Each biological replicate is the average SD of 8 unique stomata counts. Environmental conditions: CT Room, day 23℃, night 18˚C, 65% RH and 300 µmol photons m^{-2} s^{-1}.

To better understand the effect of transgenic STO expression on stomatal density, relative STO expression was correlated against SD and clustered SD (number of stomata in clusters mm^{-1}). A strong positive statistically significant correlation was detected between STO expression and the number of clustered stomata per mm^2 (R^2 = 0.793, $p < 0.001$) (Fig. 3.6B), and a statistically significant moderate positive association was found between 35S::STO expression and total stomatal density (R^2 = 0.491, p =

0.035) (Fig. 3.6A). This data suggests that 35S::STO expression has a stronger association with stomatal clustering under these growth conditions, rather than a uniform increase across the epidermis.

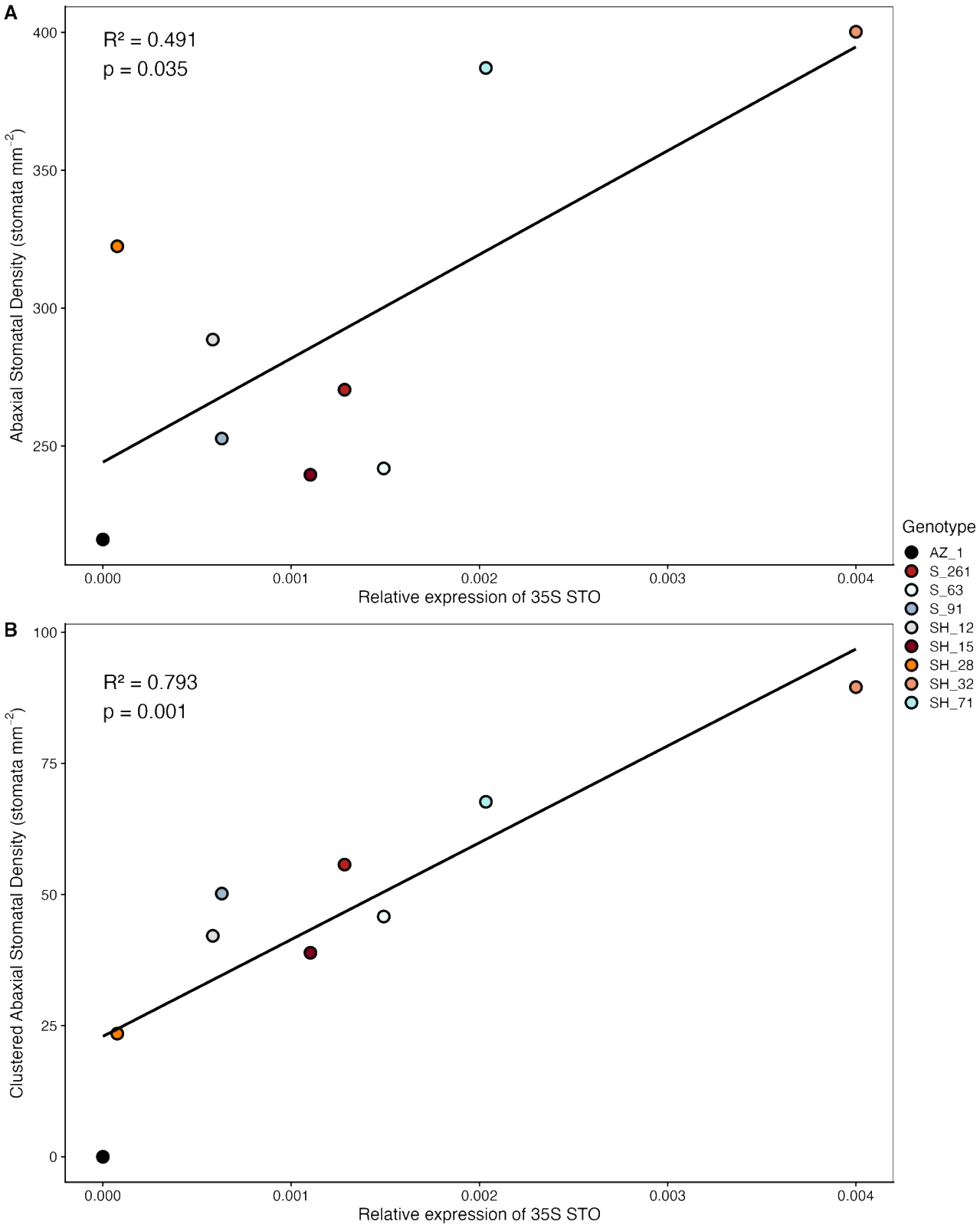

Figure 3.6. Correlation between 35S::STO expression and stomatal patterning traits in transgenic T0 strawberry lines. Each point represents a genotype, coloured by genotype identity. A) Abaxial stomatal density (stomata mm $^{-2}$) plotted against relative 35S::STO expression. B) Abaxial clustered stomatal density (clustered stomata mm $^{-2}$) for the same genotypes. Linear regression lines are shown in black, with associated coefficients of determination (R^2) and p-values reported in each panel.

3.2.2.3. Comparison Of Stomatal Patterning Across Growth Environments

To assess how extreme greenhouse temperatures influenced epidermal development, additional stomatal patterning measurements were collected from transgenic strawberry plants grown under these conditions (Fig. 3.7). No statistically significant differences in abaxial SD were detected between genotypes ($p > 0.05$). While visual differences in median stomatal density were observed, for example, higher values in S_71 and lower values in H_95 (313 and 232 stomata mm^{-2}, respectively), these differences were not statistically significant. These findings suggest that, within the surviving genotypes, stomatal density is similar across all transgenic lines and is not significantly influenced by the transgenes under the tested conditions, contrary to what was previously observed on the same plants grown under the CT Room conditions (Fig. 3.5).

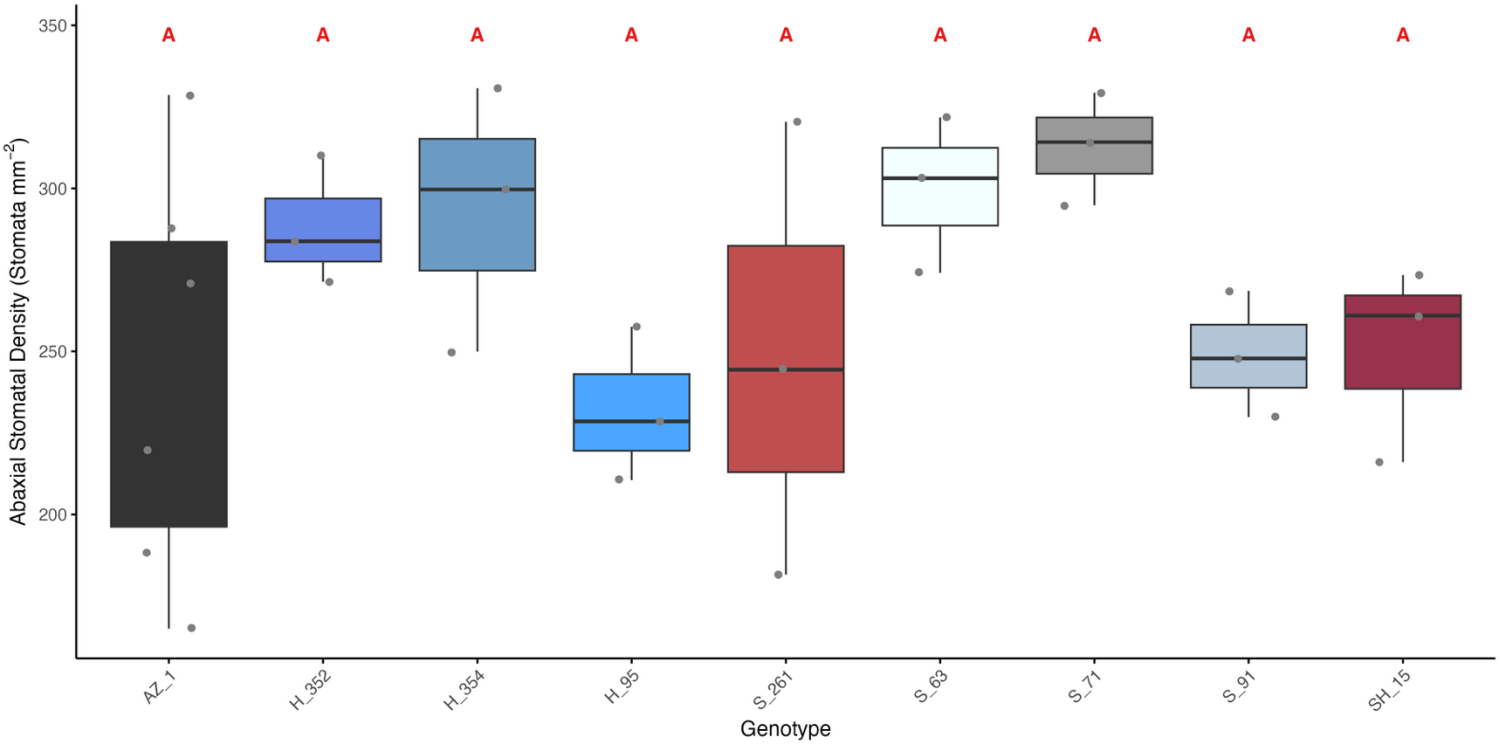

Figure 3.7. Stomatal density (stomata mm^{-2}) on the abaxial surface of nine T0 transgenic strawberry genotypes in the Glasshouse environment. Boxplots show the distribution of stomatal density measurements per genotype, with individual data points overlaid. Different shades represent different genotypes. Compact letter display (CLD) annotations above each box indicate statistical groupings based on ANOVA, followed by Tukey's HSD test ($p < 0.05$); genotypes sharing the same letter are not significantly different from one another. For transgenic lines, n = 3, and for AZ_1, n = 6. Each biological replicate is the average SD of 8 unique stomata counts. Glasshouse: 25-60 °C day, 20°C night, 60% RH and a 16-h photoperiod of 600-800 µmol photons m^{-2} s^{-1}.

To determine whether the stomatal density of individual lines differed between growth environments, two-sided t-tests were conducted for each genotype, comparing plants grown in the CT Room and the Glasshouse (Fig. 3.8). A significant effect of environment on stomatal density was identified for genotype H_352 (p = 0.0107), with higher SD values observed in the glasshouse. Trends toward significance were detected for H_354, S_63, and H_95 (p = 0.0722, 0.0515, and 0.0836, respectively), where increased stomatal densities were observed on plants grown under glasshouse conditions. For the remaining genotypes (AZ_1, S_261, S_91, and SH_15), no significant

differences were detected in SD irrespective of the growth environments, indicating that the effect of environmental conditions on stomatal development varied among genotypes and the effects of the transgenes on stomatal density were reduced for the same plants grown in a stressful environment.

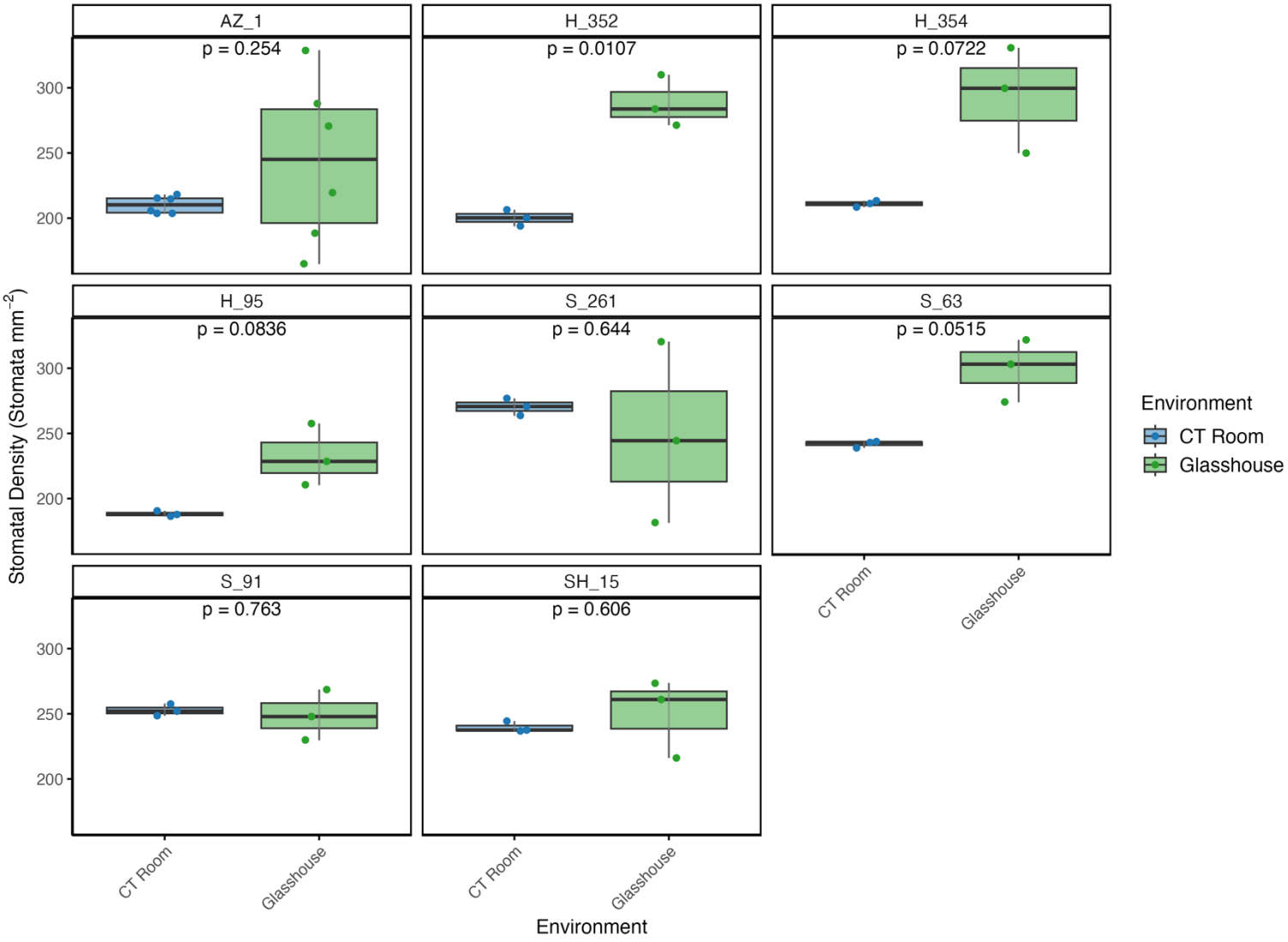

Figure 3.8. Stomatal density (stomata mm $^{-2}$) across two growth environments, CT Room and Glasshouse, for nine transgenic T0 strawberry genotypes. Each panel represents a different genotype, with the genotype displayed as the title for each plot. Boxplots show the distribution of stomatal density per environment, with individual data points overlaid. P values from two-sided t-tests are displayed above each panel, comparing the environments for each genotype. Colours indicate environment: blue for the CT Room and green for the Glasshouse. Environmental conditions: CT Room, day 23°C, night 18˚C, 65% RH and 300 µmol photons m^{-2} s^{-1}. The Glasshouse day 25 to 60 °C, night 18- 20°C, 60% RH, and a 16-h photoperiod with 600-800 µmol photons m^{-2} s^{-1}.

3.2.3. Plant Disease And Management

3.2.3.1. Disease Symptoms And Plant Survival Under Controlled Conditions

During the course of the project, transgenic strawberry plants were severely affected by pests, diseases, and environmental stress. In the CT room, the first challenge was a Whitefly infestation (Fig. 3.9A). Although this did not kill plants, it necessitated quarantine and intensive pesticide treatments, which prevented measurements at a stage when many lines still had sufficient replicates. The major loss of material occurred later due to widespread Strawberry Crown Rot (Fig. 3.9B), which eliminated numerous unique lines. Surviving plants were then weakened by a severe outbreak of Powdery Mildew (Fig. 3.9C). While this disease caused limited direct mortality, it greatly reduced plant vigour and completely halted stolon production, preventing the generation of new replicates by vegetative propagation. A subsequent infestation of Spider Mites (Fig. 3.9D) added further stress and compounded the overall decline in plant health. Powdery mildew and mite infestations were managed with pesticide applications, soapy water washes, and removal of infected tissue, allowing a few plants to recover. All of the disease outbreaks and pest pressure occurred in the CT room and once remedied, plants were transferred from the CT room to glasshouse conditions, where vigorous new growth was observed. However, exposure to high light and temperatures of up to 55 °C in the glasshouse led to further losses (Fig. 3.9E).

Altogether, 22 of the 27 transgenic lines were lost, either directly through disease or effectively through a reduction in replicate numbers below three.

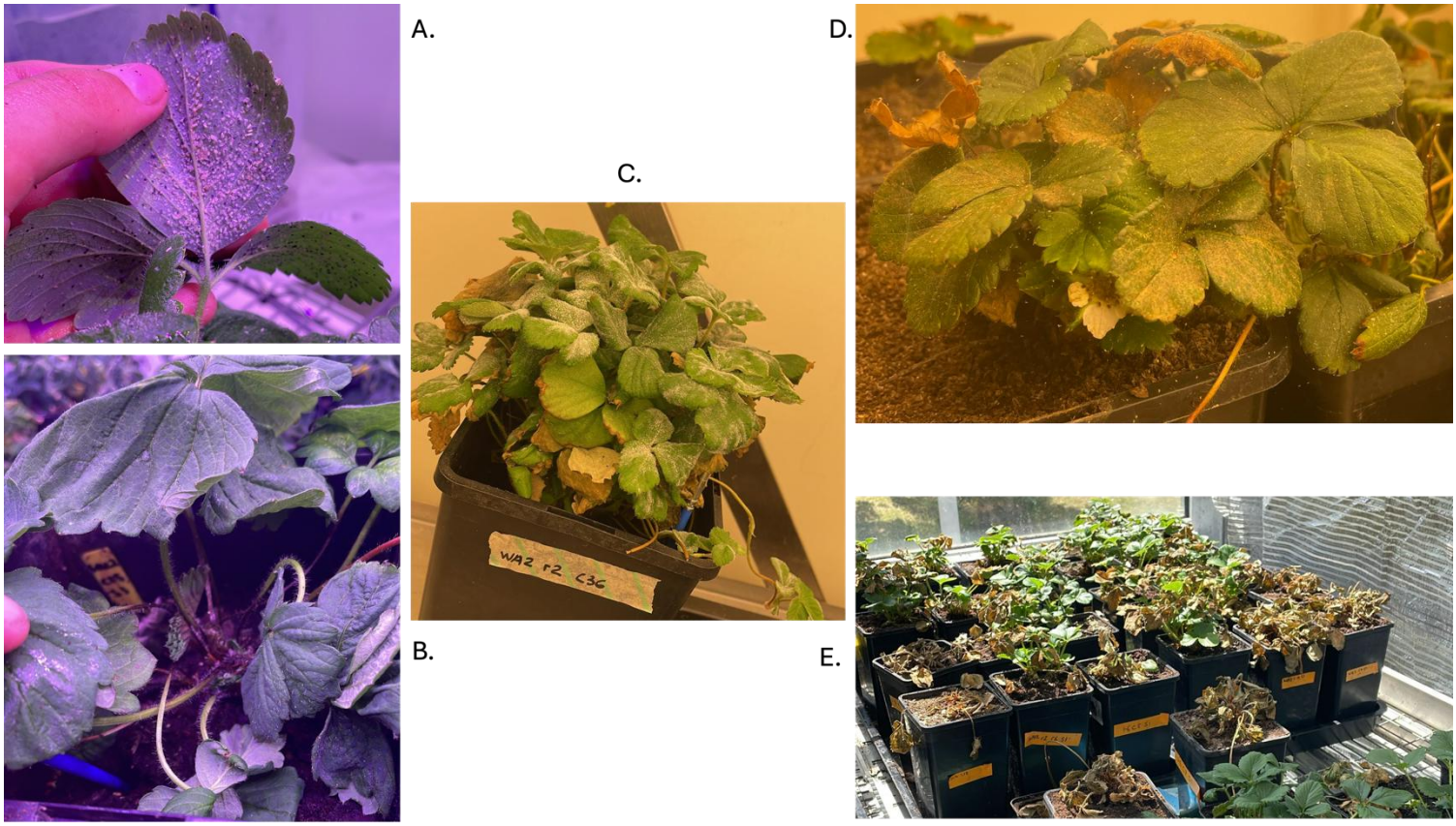

Figure 3.9. Pictures of transgenic T0 strawberry plants afflicted with a variety of plant diseases and stresses throughout experimentation. A) Plants were afflicted with Whitefly (Trialeurodes vaporariorum). B) Plants affected by water stress/ Crown and Root rot (Phytophthora cactorum, Rhizoctonia spp.). C) Plants affected by powdery mildew (Podosphaera aphanis). D) Plants affected by Spider mites (family Tetranychidae). E) Plants affected by sun/ heat stress. Diseases shown in A, B, C and D occurred in the CT Room: 23°C day and 18˚C night, 65% RH, and a 16-h photoperiod of 300 µmol photons m^{-2} s^{-1}. Heat stress occurred in the Glasshouse: 25-60 °C day, 20°C night, 60% RH and a 16-h photoperiod of 600-800 µmol photons m^{-2} s^{-1}.

3.2.4. Determining Photosynthetic Capacity Via Photosynthetic Response To Intracellular CO_2 Concentrations

A/C$_i$ response curves were used to determine if transgenic expression of STO and/or HXK affected photosynthetic capacity. All genotypes exhibited a typical *A/C$_i$* response curve, with the assimilation rate (A) displaying a rapid linear increase at low intercellular CO_2 concentrations (*C$_i$*) before plateauing when approaching saturation at higher *C$_i$* levels (Fig. 3.10).

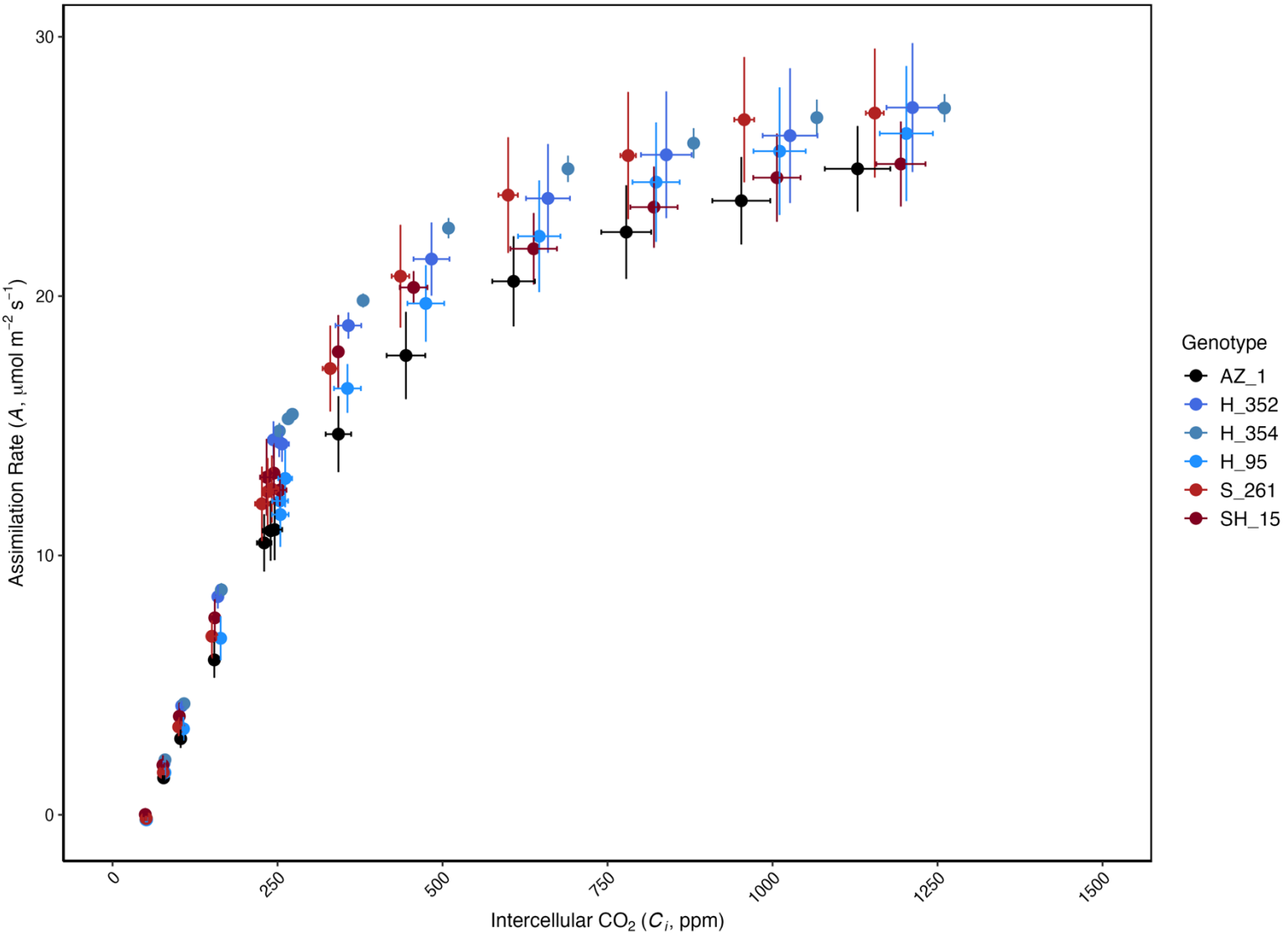

Figure 3.10. Photosynthetic response of T0 transgenic strawberry plants under different intracellular CO_2 concentrations (C_i). The net CO_2 assimilation rate (A, µmol m^{-2} s^{-1}) is plotted as a function of intercellular CO_2 concentration (C_i, µmol mol^{-1}). Each point represents the mean (n = 3, n = 5 for AZ_1) for a given genotype, with the error bars indicating standard error (SE), for A and C_i (vertical and horizontal, respectively). Glasshouse conditions: 25-60 °C day, 20°C night, 60% RH and a 16-h photoperiod of 600-800 µmol photons m^{-2} s^{-1}. Measurements were performed on the youngest fully expanded leaf.

While some genotypes, such as H_352 and H_354, tended to exhibit higher *A* values at elevated C_i, these trends were not statistically supported by modelled photosynthetic parameters (Fig. 3.11). Due to only one line surviving for both S and SH

genotypes, definite conclusions cannot be made about either of these genotypes. Derived values of A_{max}, Vc_{max}, and J_{max} did not differ significantly between genotypes (ANOVA, Tukey's test, $p < 0.05$), suggesting that the transgenic expression of STO and/or HXK did not affect the maximum rate of photosynthesis, maximum rate of carboxylation, or the maximum rate of electron transport.

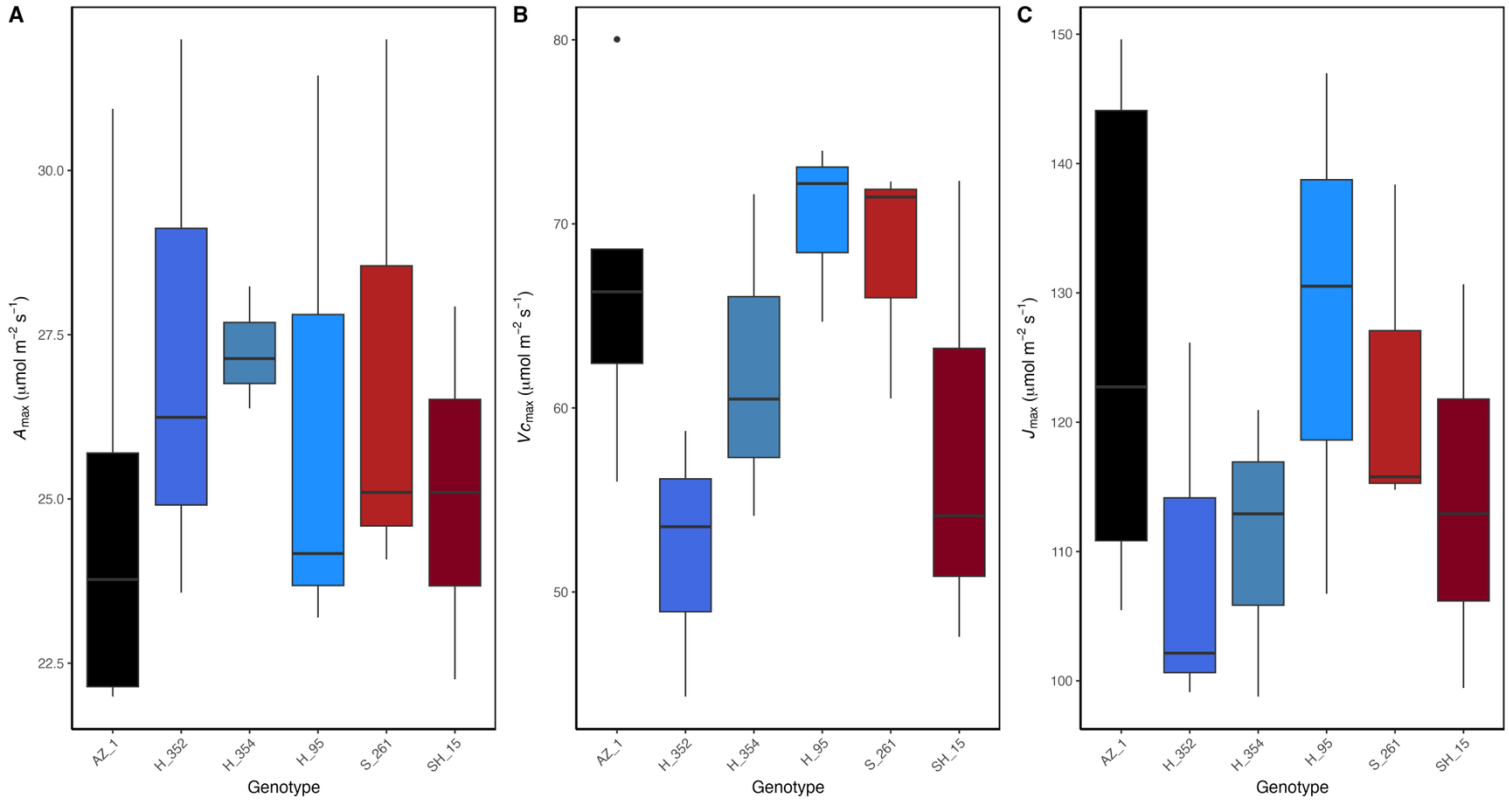

Figure 3.11. Photosynthetic parameters modelled from A/C_i curves across T0 genotypes. (A) CO_2 and Light-saturated assimilation rate (A_{max}), (B) maximum Rubisco carboxylation capacity (Vc_{max}) and (C) maximum electron-transport rate (J_{max}). Boxplots display the median (horizontal line), interquartile range (box), and whiskers extending to 1.5 × the interquartile range, with black dots marking observations beyond this range (outliers). No statistical differences were found between genotypes for A_{max}, Vc_{max}, or J_{max} ANOVA, p >0.05 (n = 3, n = 5 for AZ_1). Glasshouse conditions: 25-60 °C day, 20°C night, 60% RH and a 16-h photoperiod of 600-800 µmol photons m^{-2} s^{-1}. Measurements were performed on the youngest fully expanded leaf.

3.2.5. Stomatal Conductance, Photosynthesis And Intrinsic Water Use Efficiency Dynamics In Response To Dynamic Light

To assess genotypic differences in stomatal responses to induced opening and closure, transgenic strawberry plants were subjected to step-changes in light intensity. Following a step-increase in light intensity (100 to 1000 µmol m^{-2} s^{-2}), all genotypes exhibited a rapid rise in net photosynthesis (*A*) and stomatal conductance to water vapour (g_{sw}), with peak values occurring just before the step-decrease in light intensity (Fig. 3.12). After the return to low light (shaded region), both *A* and g_{sw} declined across genotypes. Intrinsic water-use efficiency (iWUE) increased in most genotypes following a step-increase in light intensity, before declining sharply after a step decrease in light intensity.

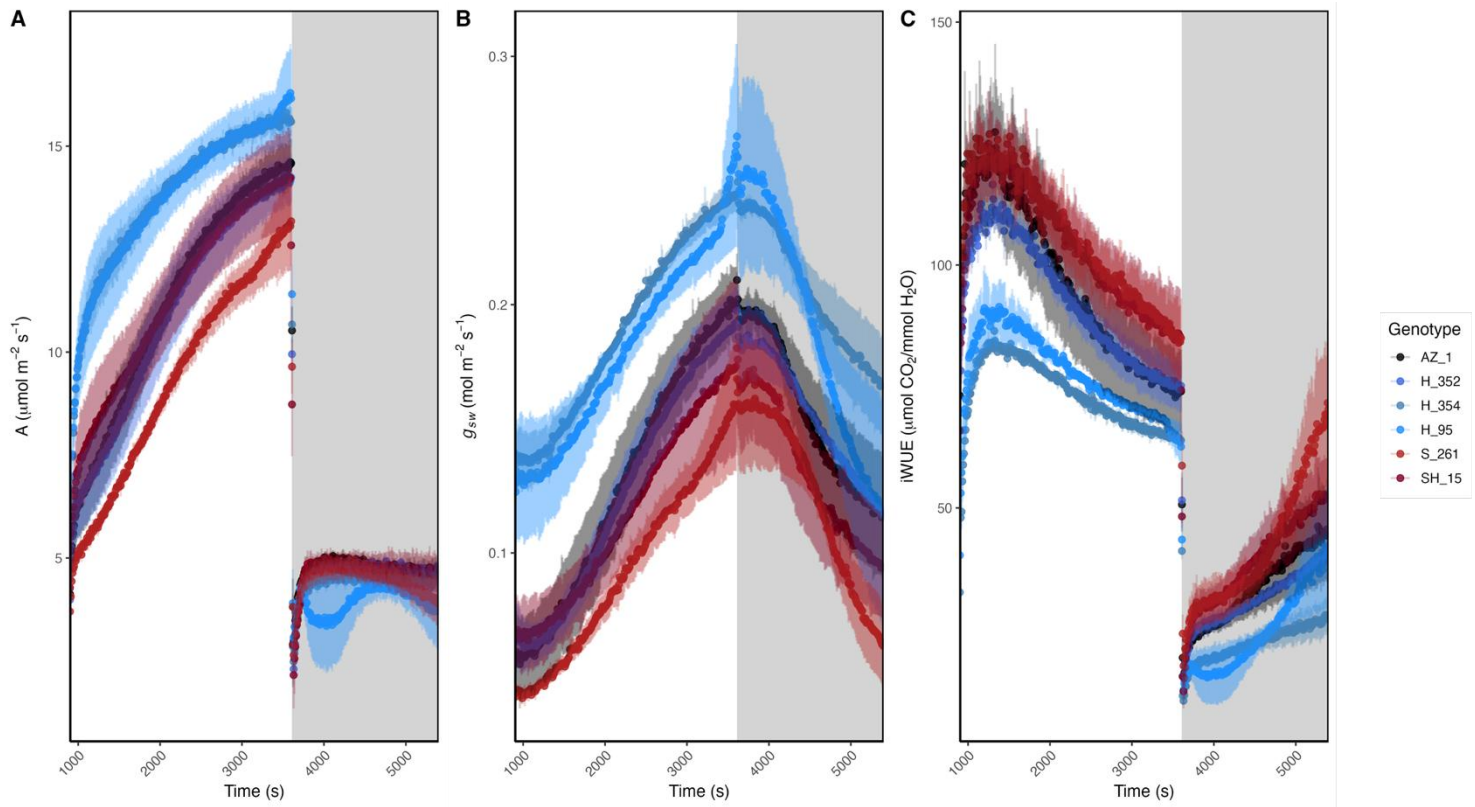

Figure 3.12. Time-course responses of (A) net photosynthesis (A), (B) stomatal conductance to water vapour (g_{sw}), and (C) intrinsic water-use efficiency (iWUE) in T0 transgenic strawberry lines during step changes in light intensity. Light intensity increased from 100 to 1000 µmol m^{-2} s^{-1} at 900 s and returned to 100 µmol m^{-2} s^{-1} at 3600 s, as indicated by the shaded region. Lines represent genotype means; ribbons show ± standard error (n = 3 and for H_352 n = 4). Glasshouse conditions: 25-60 °C day, 20°C night, 60% RH and a 16-h photoperiod of 600-800 µmol photons m^{-2} s^{-1}. Measurements were performed on the youngest fully expanded leaf.

To determine genotypic differences in the stomatal responses, three distinct time points were chosen to analyse genotypic differences during the step increase and decrease in light intensity: steady-state pre-induction (100 µmol m^{-2} s^{-1}, 900 s), High-Low transition (1000 µmol m^{-2} s^{-1}, 3600 s) and steady-state post-induction (100 µmol m^{-2} s^{-1}, 5400 s). Significant differences were found between genotypes for g_{sw} and iWUE at the steady-state pre-induction time point (100 µmol m^{-2} s^{-1}, 900 s). The HXK overexpressing line H_354 had significantly higher g_{sw} than the azygous control, fellow HXK line H_352 and STO line S_261 (ANOVA, Tukey HSD, p = 0.025, 0.027 and 0.007,

respectively). The HXK line H_95 also trended towards having higher g_{sw} than the azygous control, but was not significant at the 5% threshold (ANOVA, Tukey HSD, p = 0.067); however, this line had significantly higher g_{sw} than the STO line S_261 (ANOVA, Tukey HSD, p = 0.019). The inverse relationship was seen for iWUE, with H_354 having significantly lower iWUE than the azygous control and S_261 (ANOVA, Tukey HSD, p = 0.038 and 0.006, respectively). The HXK line H_95 also had significantly lower iWUE than the STO line S_261, but did not differ statistically from the control (ANOVA, Tukey HSD, p = 0.02 and 0.12, respectively). These data suggest that guard-cell-specific overexpression of HXK can lead to higher low-light steady-state g_{sw} and, as a result, reduced iWUE.

Normalising *A* and g_{sw} to the initial and final values of each step change enables visualisation of induction rates and the genotypic differences therein (Fig. 3.13). While apparent genotypic differences can be seen in relative *A* during the step increase in light intensity (Fig. 3.13A), no statistical differences were found between genotypes for the time taken to reach 33, 50, 66 and 90% of the relative *A* (ANOVA, Tukey HSD, all p > 0.05). These data suggest that the expression of the transgenes did not alter the rate of photosynthetic induction during a step increase in light intensity.

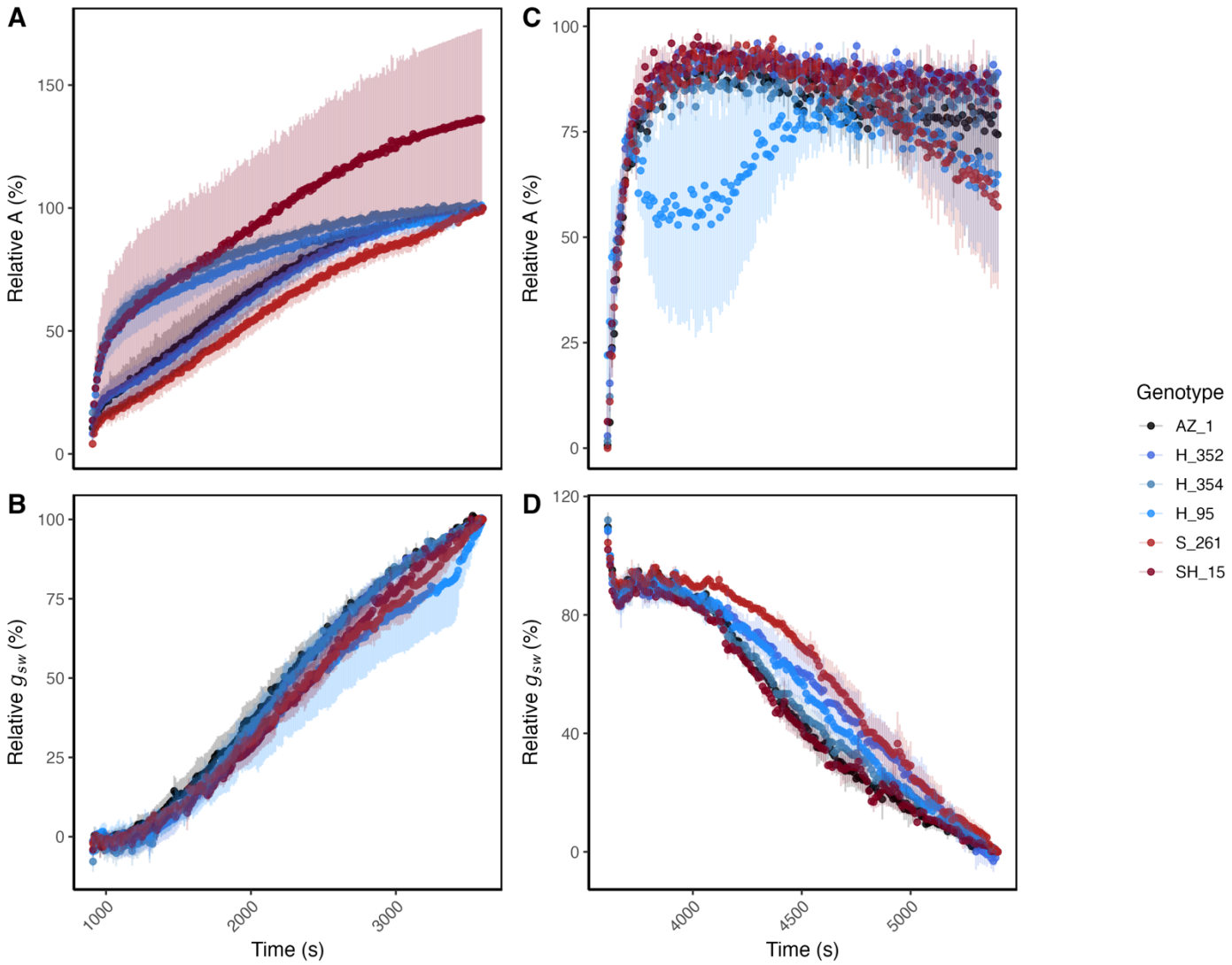

Figure 3.13. Relative CO_2 assimilation (A, %) and stomatal conductance (g_{sw}, %) response to a step change in light intensity over time in T0 transgenic strawberry mutant genotypes. The x-axis represents time (seconds), and the y-axis represents relative A and g_{sw} (%), normalised to initial values (outlined in Chapter 2). The left panels show the response of A (A) and g_{sw} (B) to a step-increase in light intensity, where light intensity increased at Time = 900 s, while the right panel show the response of A (C) and g_{sw} (D) to a step-decrease in light intensity, where light intensity decreased at Time = 3600 s. Each coloured line represents the mean response for a specific genotype, with shaded areas indicating standard error (SE). (n = 3 and for H_352 n = 4). Glasshouse conditions: 25-60 °C day, 20°C night, 60% RH and a 16-h photoperiod of 600-800 µmol photons m^{-2} s^{-1}. Measurements were performed on the youngest fully expanded leaf.

To identify if constitutive overexpression of STO and/or the guard-cell-specific overexpression of HXK altered stomatal behaviour during the step changes in light

intensity, stomatal kinetics (*k*, the time constant describing the speed of stomatal movement) and lag time (*l*, time before a significant stomatal response) were modelled according to Vialet-Chabrand et al. (2017). No significant differences were found between genotypes for stomatal kinetics (*k)* in either the step-increase in light intensity (Kruskal-Wallis, $p = 0.5774$) or step-decrease in light intensity (ANOVA, $p = 0.752$), nor for stomatal lag time (*l*) of the step-increase or decrease in light intensity (ANOVA, $p = 0.934$ and $p = 0.242$, respectively) (Fig. 3.14).

When comparing genotypic responses to a step-increase versus step-decrease in light intensity, STO overexpressing lines S_261 and SH_15 had a trend towards greater stomatal kinetics in response to a step-increase than to a step-decrease in light intensity (Two Sample t-test, $p = 0.062$ and $p = 0.060$, respectively), but no significant differences in stomatal kinetics (*k*) were found. Significantly lower lag time (*l*) in response to a step-decrease in light intensity was found for H_354 and SH_15 (Two Sample t-tests, $p < 0.01$), with no significant differences found for the other genotypes. The other HXK overexpressing lines H_352 and H_95 displayed a trend towards a lower stomatal lag time (*l*) in response to a step-decrease in light intensity (Two Sample t-test, $p = 0.064$ and $p = 0.058$), as well as the Azygous (Two Sample t-test, $p = 0.083$). The trend of having a shorter delay in stomatal response to closure (*l* in response to a step-decrease in light intensity) in all lines except the STO single line S_261 suggest STO expression may interfere with an innate rapid response to closure signals. These data suggest that the transgenic expression of HXK did not result in any changes in stomatal response to changes in light intensity, but STO expression alone may interfere with an apparent innate rapid response to closure signals.

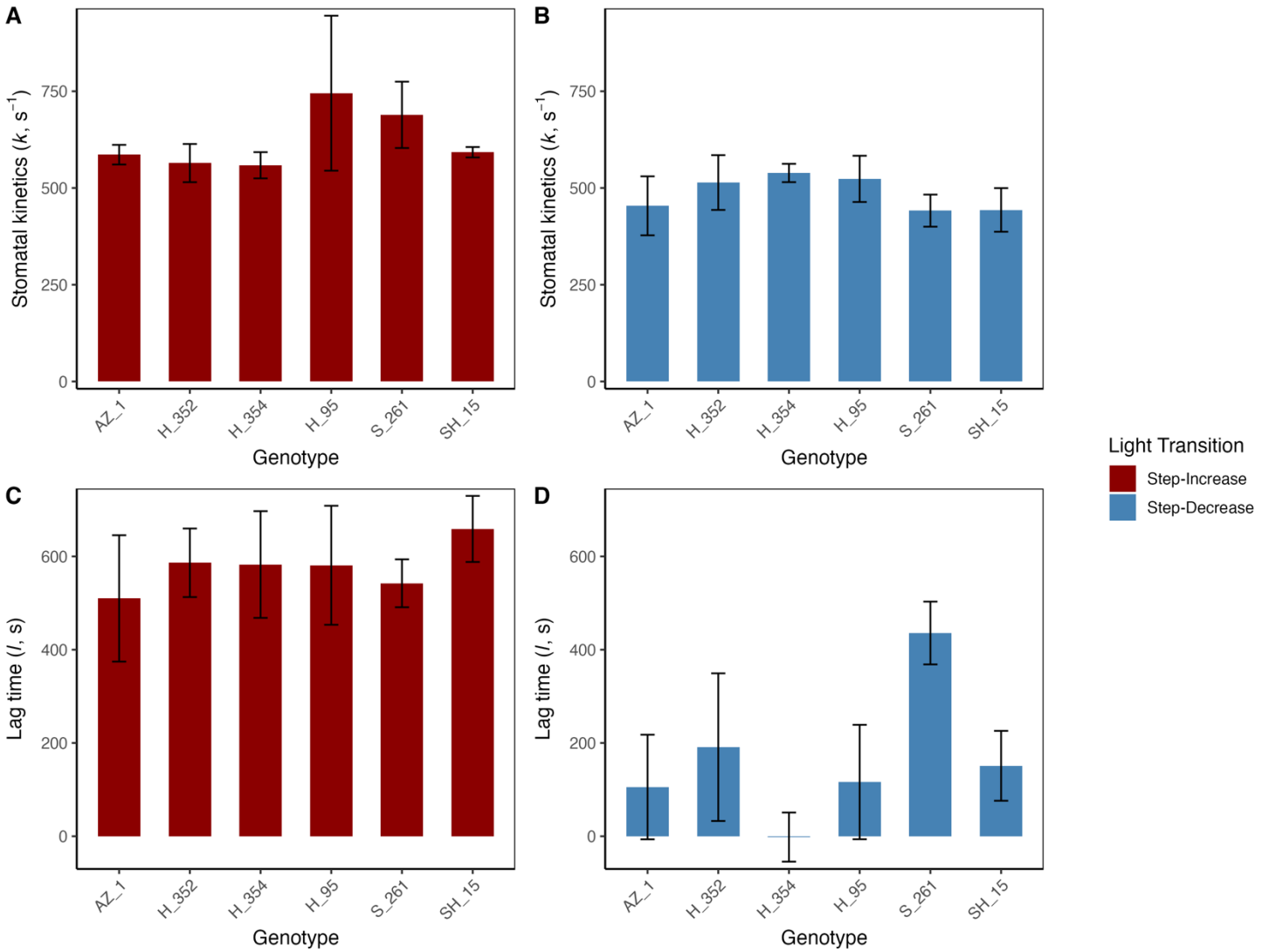

*Figure 3.14. Stomatal response kinetics across transgenic strawberry genotypes during light step transitions. (A) Stomatal kinetics parameter (k) and (B) lag time (l) for transgenic strawberry genotypes during a step-increase and step-decrease in light intensity. Bars represent genotype means (± standard error) for each phase, with red bars indicating responses during light induction (Step-Increase) and blue bars during light reduction (Step-Decrease). Stomatal kinetics (k) reflects the rate of the g_{sw} response to a light step change, while lag time (l) represents the temporal delay before the onset of response. Statistical differences are denoted by asterisks and brackets between comparisons (ANOVA with Tukey HSD, * p < 0.05, ** p < 0.01, *** p < 0.001) above the bar charts (n = 3 and for H_352 n = 4). Glasshouse conditions: 25-60 ºC day, 20ºC night, 60% RH and a 16-h photoperiod of 600-800 µmol photons m^{-2} s^{-1}. Measurements were performed on the youngest fully expanded leaf.*

3.3. Discussion

Improving stomatal traits has the potential to enhance both photosynthetic performance and water-use efficiency. In particular, manipulating stomatal density (SD) and guard cell function provides complementary routes to influence leaf gas-exchange dynamics. Increased SD will raise the anatomical maximum for stomatal conductance (g_{smax}) and improve CO_2 uptake under high light (Tanaka et al., 2013; Sakoda et al., 2020), while altered guard cell metabolism can directly modify the responsiveness of stomata to environmental and internal signals (Kelly *et al.*, 2013; Lugassi *et al.*, 2015). The cultivated strawberry (*Fragaria* × *ananassa*) has previously been shown to have a significant stomatal limitation on photosynthetic carbon assimilation, particularly after midday (Yokoyama *et al.*, 2023). Enhancing SD through overexpression of STO could therefore alleviate these constraints by increasing maximum diffusive capacity, while simultaneous expression of HXK in guard cells offers a strategy to improve water-use efficiency and prevent excessive transpiration, providing a complementary balance between carbon gain and water conservation.

In this study, STO was constitutively overexpressed to enhance stomatal development, while HXK was expressed specifically in guard cells using the KST1 promoter, to assess their individual and combined effects on gas exchange dynamics and plant productivity. The overexpression of STO successfully increased stomatal density but also led to frequent clustering, which may impair function by slowing the lag time to closure in response to environmental signals. However, due to the survival of only one line of both STO and the double, definitive conclusions cannot be made about the effect of STO overexpression on strawberry physiology, particularly regarding its

effects on photosynthesis or stomatal dynamics. By contrast, HXK expression did not alter stomatal kinetics but often increased steady-state g_{sw} under low light. Interestingly, in double transgenic lines, HXK partially rescued the impaired closure response associated with clustering, reducing lag times and restoring more functional stomatal behaviour. Although the experimental timeline was complicated by repeated biotic stresses that reduced overall plant vigour, these results demonstrate that different genetic routes to modify stomatal traits in strawberry have contrasting outcomes: STO increases density, but may compromise function when clustering occurs, whereas HXK may improve baseline conductance without negatively impacting responsiveness, and may even compensate for defects introduced by clustering.

3.3.1. Effect Of Transgenes On Epidermal Patterning

The transgenes overexpressed in strawberry had varying impacts on epidermal patterning (Fig. 3.4-3.5). Under low-stress conditions in the CT room environment, KST1::HXK lines (H) showed stomatal densities consistent with those of the Azygous (AZ) plants or slightly reduced (22-35 stomata mm^{-2} less). Previous work with KST1::HXK tomato and citrus plants also showed no differences in stomatal density between WT and transgenic plants (Kelly *et al.*, 2013; Lugassi *et al.*, 2015). Moreover, since stomatal density is determined during epidermal development, well before the mature guard cells are functional, it seems biologically implausible that expression of HXK within guard cells would directly alter the number of stomata (Geisler, Nadeau and Sack, 2000; Nadeau and Sack, 2002; Shpak et al., 2005; Bergmann and Sack, 2007; Hara et

al., 2007, 2009; Nadeau, 2009). Therefore, while some of our lines show lower SD, this is more likely to be due to natural line-to-line variation, positional effects of transgene insertion, subtle developmental differences or subtle microclimatic differences, rather than a causal effect of HXK expression (Bhat and Srinivasan, 2002; Casson and Gray, 2008; Casson and Hetherington, 2010; Schnell *et al.*, 2014; Nunes *et al.*, 2022). Differences in environmental conditions, such as water stress, as well as disease stress from Crown and Root rot (*Phytophthora cactorum* and *Rhizoctonia spp*.) and strawberry powdery mildew (*Podosphaera aphanis*), are likely strong contributors to the lowering of SD. These plants may have decreased stomatal density as a defence mechanism to limit pathogen entry, as bacterial infections can systemically suppress SD, resulting in lower SD on leaves developing post-infection (Dutton *et al.*, 2019). Black root rot in strawberries has previously been shown to result in a loss of root function and root mass, which could produce a physiological stress response akin to drought stress (LaMondia, 2004). Leaves developing under severe drought conditions have shown reduced stomatal development (lower stomatal index (SI) or SD) across multiple species, which may explain the reduction in SD seen in KST1::HXK strawberries, previously unseen in other species (Xu and Zhou, 2008; Hamanishi, Thomas and Campbell, 2012; Ouyang et al., 2017; Mano, Madore and Mickelbart, 2023).

STO overexpressing lines (S and SH) had increased SD alongside stomatal clustering. Figure 3.6 illustrates the relationship between the relative expression of 35S::STO and two key stomatal traits: total stomatal density (SD) and the density of clustered stomata. The positive moderate significant relationship between 35S::STO expression and SD suggests that while STO overexpression may promote stomatal

initiation, its effect is modulated by additional regulatory inputs. Stomatal density is influenced by a combination of environmental factors (such as light, humidity, and CO_2 concentration) and endogenous signals, including phytohormones and developmental cues (Lake, Woodward and Quick, 2002; Casson and Hetherington, 2010). Additionally, downstream EPF-family peptides and receptors such as EPF1/EPF2 and ERECTA-family kinases interact to buffer stomatal density within a physiologically optimal range (Hara et al., 2007, 2009; Hunt and Gray, 2009). The positive moderate correlation observed here likely reflects this developmental complexity and the system's capacity to maintain SD homeostasis even with constitutive STO overexpression. In contrast, the highly significant positive correlation between STO expression and the number of clustered stomata indicated that increased STO expression directly compromises spacing fidelity. This aligns with findings in *Arabidopsis*, where excess STO has been shown to override EPF1-mediated spacing inhibition, resulting in the breakdown of the one-cell spacing rule (Sugano et al., 2009; Tanaka et al., 2013; Dow, Bergmann and Berry, 2014; Sakoda et al., 2020). The disproportionately strong effect on clustering suggests that high STO expression does not merely increase stomatal number, but also disrupts spatial patterning, potentially impairing coordinated guard cell function and gas exchange regulation (Dow, Berry and Bergmann, 2014). These results imply that cluster formation is a more direct and sensitive developmental output of STO overexpression, whereas SD is shaped by a broader, environmentally buffered signalling network.

Conversely, in the glasshouse-grown plants, the influence of transgene expression on stomatal density appeared markedly diminished. Notably, previously

high-SD STO genotypes, such as S_71, exhibited a significant reduction in stomatal density, suggesting that environmental factors (most notably sustained and sometimes extreme heat stress) may have overridden or suppressed transgene-driven effects on stomatal development. Elevated temperatures can influence stomatal development by suppressing key transcription factors involved in stomatal lineage initiation. For example, elevated temperatures in *Arabidopsis* downregulate *SPEECHLESS*, causing reduced stomatal production on leaves, which has been linked to lower stomatal densities in plants grown under warmer conditions (Lau et al., 2018). The glasshouse temperatures ranged from 25-60 °C, exceeding the optimum growth temperature of 18–24 °C for cultivated Strawberry (Gonzalez-Fuentes *et al.*, 2016), creating a thermal environment likely to elicit stress responses. This suggests that environmental stress may have overridden transgene-driven stomatal initiation, possibly through suppression of meristemoid proliferation or enhanced activity of inhibitory signals such as EPF2 or abscisic acid (ABA) (Pillitteri and Torii, 2012; Lau et al., 2018). Moreover, such heat stress likely induced secondary drought stress via increased soil water evaporation, especially in the well-ventilated glasshouse, further modulating stomatal development. Drought and high VPD are known to repress stomatal formation in developing leaves through systemic ABA signalling (Yoo *et al.*, 2012; Yoko Tanaka *et al.*, 2013), and may explain why some transgenic lines failed to maintain elevated SD despite high STO expression. In hypostomatous species like strawberry, this may interact with inherent epidermal limits, leading to a developmental ceiling in stomatal number, particularly under combined heat and drought-like conditions caused by increased evapotranspirative demand and soil drying (Franks and Farquhar, 2007; Tanaka et al., 2013).

While relative expression data for 35S::STO were available only from plants grown in the CT room, due to tissue loss from stress and mortality in the glasshouse, the significant correlation observed between STO expression and stomatal clustering in the CT environment remains biologically meaningful. Importantly, stomatal clustering remained evident in the glasshouse SD measurements (Fig. 3.4), even where total density stagnated, indicating that clustering defects persist under environmental stress. This suggests that the disruption of the one-cell spacing rule, mediated by STO overexpression and likely saturation of the EPF1/TMM regulatory module, is a robust and less environmentally labile developmental outcome (Hara et al., 2007; Dow, Bergmann and Berry, 2014). The results presented here are consistent with the well-established plasticity of stomatal development in response to environmental conditions, as stomatal density was found to be sensitive to stress, suggesting that environmental suppression can override genetically driven increases in stomatal density (Farquhar and Sharkey, 1982; Grassi and Magnani, 2005; Xu and Zhou, 2008). In contrast, clustering represents a more stable phenotype of STO transgene activity. This has critical implications for genetic manipulation strategies: density gains may be limited by stress-induced suppression, but patterning disruptions may persist and impair gas exchange responsiveness, even when transgene expression is dampened by environmental override.

3.3.2. Effect Of Transgenes On Photosynthetic Capacity

Changes in stomatal density and function have been shown to impact photosynthetic rates (Franks and Beerling, 2009; Wang et al., 2013; Tanaka et al., 2013; Dow, Berry and Bergmann, 2014; Lawson and Blatt, 2014; Antunes et al., 2017; Caine et al., 2019). Despite clear differences in stomatal development and patterning among transgenic lines, no significant differences were observed in photosynthetic capacity, including A_{max}, Vc_{max} *and* J_{max}. This was consistent across both KST1::HXK and 35S::STO overexpressing lines. These findings align with previous studies showing that genetic manipulation of stomatal traits alone is often insufficient to alter the biochemical parameters that limit photosynthesis (Kelly et al., 2013; Tanaka et al., 2013; Lugassi et al., 2015). Owing to the limited number of STO-expressing lines recovered, no strong conclusions can be drawn regarding the effect of STO overexpression on photosynthetic capacity in strawberry.

Theoretically, increasing stomatal conductance (g_{sw}) may enhance CO_2 delivery and raise A_{max}, particularly under ambient CO_2 concentrations. However, in the present study, no lines displayed consistent increases in g_{sw}, and those with increased stomatal density (SD) often exhibited greater stomatal clustering, a condition previously shown to impair gas exchange efficiency and limit functional gains in photosynthesis (Dow, Berry and Bergmann, 2014). When accounting for the clustering, STO lines S_261 and SH_15 have an effective SD equivalent to the AZ (when counting stomata in a cluster as one functional unit), which may account for the lack of expected increase in g_{sw} and potential increase in A_{max}. Additionally, Vc_{max} *and* J_{max} are biochemical traits, reflecting

Rubisco content and activity, and electron transport capacity, respectively, and are not typically influenced by stomatal traits unless sustained increases in carbon availability drive biochemical acclimation, a phenomenon not expected in the absence of enhanced sink demand or altered carbohydrate turnover (Lawson & Blatt, 2014).

Furthermore, the guard cell-specific overexpression of HXK, which promotes closure initiation in response to sugar accumulation, may indirectly reinforce carbon balance homeostasis and prevent overstimulation of photosynthetic enzymes (Kelly *et al.*, 2013; Lugassi *et al.*, 2015). Similarly, Tanaka et al. (2013) reported that changes in stomatal density mediated by STO overexpression were not accompanied by shifts in photosynthetic capacity, supporting the idea that stomatal development and mesophyll biochemistry are often uncoupled, particularly in the absence of environmental drivers such as CO_2 enrichment or increased sink strength (Tanaka et al., 2013). These results highlight the importance of considering source-sink coordination when interpreting or engineering photosynthetic traits and reinforce the notion that modifying stomatal traits alone does not necessarily lead to increased photosynthetic capacity.

3.3.3. Effect Of Transgenes On Stomatal Behaviour

Stomatal density is one of the primary determinants of stomatal conductance, particularly the maximum stomatal conductance (g_{max}) (Lawson and Morison, 2004; Lawson, Caemmerer and Baroli, 2010; Drake, Froend and Franks, 2013). Genotypic differences in g_{sw} were most pronounced under low-light conditions preceding a step-

increase in light intensity, with HXK line H_354 exhibiting significantly higher g_{sw} than the azygous control and STO lines. As measurements were conducted *ex-situ* in the early morning, before the onset of acute heat stress, the pretreatment differences likely reflect physiological carryover from the preceding day's conditions. Previous studies have shown that plants can exhibit “stomatal memory”, maintaining partial closure or altered stimuli sensitivity following stress exposure, and exposure to stress events can have persisting effects, even on newly developing leaves (Atkinson, Davies and Mansfield, 1989; Pospíšilová, 1996; Galmés *et al.*, 2007; Fanourakis *et al.*, 2011). Low g_{sw} under initial low light conditions in this context may, therefore, represent a conservative response to residual drought or thermal stress, potentially mediated by ABA accumulation or limited hydraulic recovery overnight (Skelton *et al.*, 2017; Li *et al.*, 2021). The observed differences between HXK and STO lines are consistent with their respective transgenic identities. Guard cell-specific overexpression of HXK has previously shown enhanced drought tolerance and improved stomatal regulation under stress conditions in both controlled environments and field trials (Kelly *et al.*, 2019; Lugassi *et al.*, 2019; Acevedo-Siaca *et al.*, 2022). In contrast, STO overexpression, which increases stomatal density but often results in clustering and reduced stomatal functionality, impairing aperture dynamics and increasing susceptibility to abiotic stress (Tanaka et al., 2013; Dow, Berry and Bergmann, 2014; Sakoda et al., 2020). The significantly lower g_{sw} in the STO line S_261 than the HXK line H_354 may therefore reflect dysfunctional stomatal behaviour under glasshouse conditions, compounded by residual stress effects from the previous photoperiod. Due to the small number of STO-expressing lines generated, the data are insufficient to draw robust conclusions

about the role of STO in regulating stomatal development in strawberry and how that may affect stomatal behaviour.

Stomatal clustering may impair stomatal function through disruptions of cell turgor, mechanical interference, impaired signalling coordination, and hydraulic limitations (Dow, Berry and Bergmann, 2014). While the glasshouse-grown strawberries showed no differences in SD, the gas exchange dynamics of the STO overexpressing lines S_261 and SH_15 consistently trended towards lower g_{sw} throughout the step-changes in light intensity, particularly the STO single line S_261 (Fig. 3.12). While not statistically significant, this trend may corroborate the notion that clustered stomata may also suffer from reductions in the effective g_{sw} of the individuals present within the cluster due to boundary layer alterations (Dow, Berry and Bergmann, 2014). This finding supports previous observations that stomata within clusters often fail to operate independently, with impaired pore responsiveness and reduced contribution to effective conductance (Dow, Berry and Bergmann, 2014; Papanatsiou *et al.*, 2019). Clustering has been shown to disrupt the one-cell spacing rule**,** which is essential for the correct propagation of signalling gradients (such as CO_2, light, and ABA) that mediate coordinated stomatal behaviour (Hara et al., 2007, 2009; Zoulias et al., 2018). These results highlight the importance of stomatal patterning, not just total density, in determining the physiological capacity for gas exchange, especially during dynamic environmental transitions and in genotypes with known spacing defects.

Stomatal behaviour and pore function regulate the real-time dynamics of stomatal conductance (Lawson et al., 1998; Dow, Berry and Bergmann, 2014; Takahashi et al., 2015). Both the speed and rate of stomatal response can limit

CO_2 assimilation rate and reduce iWUE during opening and closure, respectively (Lawson and Blatt, 2014; Qu *et al.*, 2016, 2020; Lawson and Vialet-Chabrand, 2019; Long *et al.*, 2022). To further explore the effects of the transgenes on stomatal dynamics, stomatal conductance response curves were fit using the Vialet-Chabrand model, allowing derivation of key kinetic parameters: stomatal kinetics constant (k) and lag time (l) for stomatal opening and closure (Vialet-Chabrand *et al.*, 2017). In this framework, the lag time (*l*) represents the delay between an environmental change and the initiation of a measurable stomatal response, while the kinetics constant (*k*) describes the rate at which stomatal conductance approaches its new steady state once the response has begun (with smaller values indicating a faster kinetics) (Vialet-Chabrand *et al.*, 2017). No genotypic differences in *k* or *l* were found across stomatal opening or closure, suggesting that the transgenes had little to no effect on stomatal behaviour. A trend toward shorter lag time (*l*) during light stomatal closure, relative to stomatal opening, was observed across most genotypes, except for the STO-only line S_261. While not always statistically significant, this pattern was apparent even in the Azygous line (510s delay before significant stomatal opening vs ~106s delay before significant stomatal closure), suggesting that an asymmetric stomatal response to light transitions may represent an inherent physiological trait in strawberry. This interpretation is supported by observations from Yokoyama *et al.* (2023), in which strawberry stomata were shown to close under relatively mild midday water stress, indicating a conservatively biased stomatal behaviour that may favour early closure to minimise water loss under fluctuating environmental conditions (Yokoyama *et al.*, 2023).

Notably, the double-expressing line, SH_15, exhibited a significantly reduced lag time before stomatal closure compared to opening, in contrast to the STO-only line. This divergence in response may reflect partial restoration of stomatal functionality by HXK, potentially through its role in sugar sensing and regulation of guard cell turgor. This interpretation is consistent with prior studies demonstrating that guard cell-specific expression of HXK can enhance closure dynamics and water-use efficiency without impairing photosynthesis, particularly under conditions of environmental stress (Kelly *et al.*, 2013, 2019; Lugassi *et al.*, 2015). Mechanistically, higher HXK activity in guard cells could reduce closure lag by amplifying ABA- and sugar-mediated signalling, effectively lowering the threshold for initiating ion efflux and turgor loss. In clustered stomata, where mechanical and spatial constraints can delay closure, this stronger signalling input may help overcome the sluggish onset of the response, allowing closure to begin more promptly even if the subsequent kinetics remain constrained (Kelly *et al.*, 2013, 2019; Lugassi *et al.*, 2015, 2019). However, this rescue of lag under clustered conditions does not equate to an enhancement of the innate rapid closure response in HXK single lines lacking clustering, where lag times remain similar to the control or are not significantly improved.

In addition, the double-expressing line was found to have fewer clustered stomata per mm^2 compared to the STO-only line (39 and 56, respectively). The reduced incidence of clustering may also have contributed to the reduced lag time, as stomatal clustering has been previously associated with impaired responsiveness, reduced conductance, and aberrant pore behaviour (Dow, Berry and Bergmann, 2014). The findings presented here suggest that the impaired responsiveness observed in the STO-

only line may result from both clustering-induced dysfunction and the absence of HXK-mediated regulatory control, whereas the double line may benefit from HXK-mediated compensation and reduced local interference among neighbouring stomata. However, again due to the lack of STO overexpressing lines, it is difficult to draw conclusions about the role of STO overexpression in either the single or double lines, or how STO and HXK may interact in the double transgenic line.

Together, these results point to a complex interaction between stomatal patterning and behaviour, in which HXK expression may rescue clustering-induced limitations in stomatal dynamics and support faster closure in response to declining light. The combination of a conserved kinetic response with a trend toward faster closure further supports the view that strawberry may employ an intrinsically conservative stomatal strategy**,** likely evolved to prioritise water conservation under variable field conditions.

4. Stacking Photosynthetic and Stomatal Traits to Improve Productivity in Tobacco

4.1. Introduction

Crop productivity can be improved by increasing photosynthetic carbon assimilation. Overexpressing multiple genes from the CBC, as well as in multigene combinations, has reliably been used to improve photosynthetic carbon assimilation through enhanced regeneration of Ribulose bisphosphate (Lefebvre *et al.*, 2005; Feng, Han, *et al.*, 2007; Simkin *et al.*, 2015, 2017; Ding *et al.*, 2016; Driever *et al.*, 2017), in combination with the putative inorganic carbon transporter B gene (ictB) in tobacco (Simkin *et al.*, 2015) and CBC enzymes alongside photorespiratory glycine decarboxylase-H protein (GDC-H) in Arabidopsis (Simkin *et al.*, 2017) have been shown to result in additive benefits by increasing photosynthetic parameters and thus plant productivity. Combining the effects of enhancing photosynthesis with alterations in stomatal density (SD) presents an exciting opportunity to further enhance photosynthetic traits or to improve water use efficiency (WUE) while maintaining enhanced photosynthesis by altering SD.

The inorganic carbon transporter B gene (ictB) has been widely shown to improve photosynthetic efficiency in C3 plants, despite its exact function remaining unclear (Simkin, López-Calcagno and Raines, 2019). Several studies have demonstrated the effects of overexpressing ictB in a variety of different species, with plants grown in conditions from greenhouse-grown plants to field trials (Lieman-Hurwitz *et al.*, 2003; Yu Gong *et al.*, 2015; Hay *et al.*, 2017; Koester *et al.*, 2021). Focusing on tobacco, plants overexpressing ictB grown in a controlled environment had a significantly lower

photosynthetic compensation point (Γ*) than the wild type (WT) (Lieman-Hurwitz *et al.*, 2003), suggesting that ictB expression led to increased carboxylation via increased [CO_2] at Rubisco, while simultaneously inhibiting the oxygenation reaction through the same mechanism. In greenhouse-grown tobacco, ictB expression led to an increase in the maximum rate of carboxylation (Vc_{max}), the maximum rate of electron transport (J_{max}), leaf CO_2 uptake rate (A), and stomatal conductance (g_{sw}) (Simkin *et al.*, 2015). These same plants, grown in greenhouse conditions, showed a 71% increase in biomass. Combining the overexpression of ictB with a stomatal trait that not only has an impact on photosynthesis, but also water loss, evaporative cooling, and water use, has the potential to have additive productivity benefits. Importantly, such combinations may also help ensure that the gains from enhanced photosynthetic traits can be realised under stressful environments, where water limitation, heat, or fluctuating light would otherwise constrain their effectiveness.

The resistance of gas diffusion from the atmosphere to the chloroplast is one of the major limitations to CO_2 assimilation (Farquhar and Sharkey, 1982). Therefore, one of the major determining factors of CO_2 assimilation is stomatal conductance (g_{sw}) (Wong, Cowan and Farquhar, 1979). One possible mechanism for increasing photosynthetic carbon assimilation would be manipulating the stomatal density (SD) of the leaf, defined as the number of stomata per unit leaf area, as increasing SD effectively increases stomatal conductance due to the greater number of pores to allow for gas exchange. Using the constitutive overexpression of STOMAGEN/EPFL9, an epidermal patterning factor gene that promotes stomatal development, Tanaka et al. (2013) produced *Arabidopsis* plants with a 200-300% increase in SD. CO_2 assimilation of these

plants was increased by 30% due to greater CO_2 diffusion into the leaf (Tanaka et al., 2013). However, the consequent increase in SD has one major consequence: the increase in transpiration and thus the reduction in water use efficiency (WUE). Increased stomatal density may enhance the potential for CO_2 diffusion into the leaf, which under some conditions could influence the CO_2 environment experienced by Rubisco. However, photorespiration is regulated primarily at the chloroplast level, and therefore stomatal modifications alone are unlikely to directly replicate the effects of targeted photorespiratory engineering strategies, such as overexpression of the GCS H-protein (Simkin *et al.*, 2017). Nonetheless, these approaches act at distinct points within the photosynthetic pathway, and future work could explore whether combining stomatal and metabolic engineering strategies provides complementary benefits.

This chapter covers the molecular and physiological characterisation of transgenic tobacco lines (*Nicotiana tabacum cv. Samsun)* overexpressing: 1. STOMAGEN (STO) under the control of the constitutive 35S CMV promoter, 2. ictB under the control of the constitutive 35S CMV promoter and 3. Concomitant overexpression of both constructs. These three genotypes were created to ascertain the effects of Ictb on photosynthetic capacity and altered stomatal patterning on stomatal behaviour and gaseous exchange, photosynthesis and water use efficiency.

4.2. Results

4.2.1. Selection Of T1 Transgenic Lines

Previously generated *Nicotiana tabacum* cv. Samsung transformants were subject to different experiments to select lines of interest. Background lines of WT and ictB6 (I) previously transformed with constitutive overexpression (35S) of STO (S) to produce an altered stomatal density phenotype. Here, 4 genotypes were grown: WT, I, S and IS, to select the T1 lines of S and IS. T1 seeds from 4 unique lines of S (S_8, S_110, S_113, S_4, S_14) and 5 unique lines of IS (IS_2, IS_3, IS_4, IS_6, IS_7) were tested with 10 replicates of each to account for T1 segregation.

Table 4.1 Table of plants used in this chapter. T0 lines that did not pass selection are not included.

Codename	Background	Transgene	Promoter	Terminator	Source	Generation
AZ_1	Wild Type	N/A	N/A	N/A	This study	T1
I_1	Wild Type	ictB	35S	NOS	Simkin et al. 2015	T1
IS_2	ictB TB6	ictB and STOMAGEN	35S both	NOS both	Oyemike 2018 (Thesis)	T1
IS_3	ictB TB6	ictB and STOMAGEN	35S both	NOS both	Oyemike 2018 (Thesis)	T1
IS_4	ictB TB6	ictB and STOMAGEN	35S both	NOS both	Oyemike 2018 (Thesis)	T1
IS_6	ictB TB6	ictB and STOMAGEN	35S both	NOS both	Oyemike 2018 (Thesis)	T1
IS_7	ictB TB6	ictB and STOMAGEN	35S both	NOS both	Oyemike 2018 (Thesis)	T1
S_110	Wild Type	STOMAGEN	35S	NOS	Oyemike 2018 (Thesis)	T1
S_113	Wild Type	STOMAGEN	35S	NOS	Oyemike 2018 (Thesis)	T1
S_14	Wild Type	STOMAGEN	35S	NOS	Oyemike 2018 (Thesis)	T1
S_4	Wild Type	STOMAGEN	35S	NOS	Oyemike 2018 (Thesis)	T1
WT_1	Wild Type	N/A	N/A	N/A	N/A	N/A
S_1105	S_110	STOMAGEN	35S	NOS	Oyemike 2018 (Thesis)	T2
S_11312	S_113	STOMAGEN	35S	NOS	Oyemike 2018 (Thesis)	T2
S_142	S_14	STOMAGEN	35S	NOS	Oyemike 2018 (Thesis)	T2
IS_316	IS_3	ictB and STOMAGEN	35S both	NOS both	Oyemike 2018 (Thesis)	T2
IS_67	IS_6	ictB and STOMAGEN	35S both	NOS both	Oyemike 2018 (Thesis)	T2
IS_718	IS_7	ictB and STOMAGEN	35S both	NOS both	Oyemike 2018 (Thesis)	T2

4.2.1.1. Copy Number Analysis Of T1 Transgenic Lines

Analysis of transgene copy number for the Basta resistance gene BAR, the positive selection marker for transformation and regeneration, was used to confirm transgene insertion and heterozygosity in the stomatal patterning mutants (Figure 4.1) and copy number. Copy number analysis provides the equivalent information as a traditional PCR screen using primers for the transgene. Plants containing at least 1 insertion of the Basta resistance transgene (BAR) were selected for further analysis.

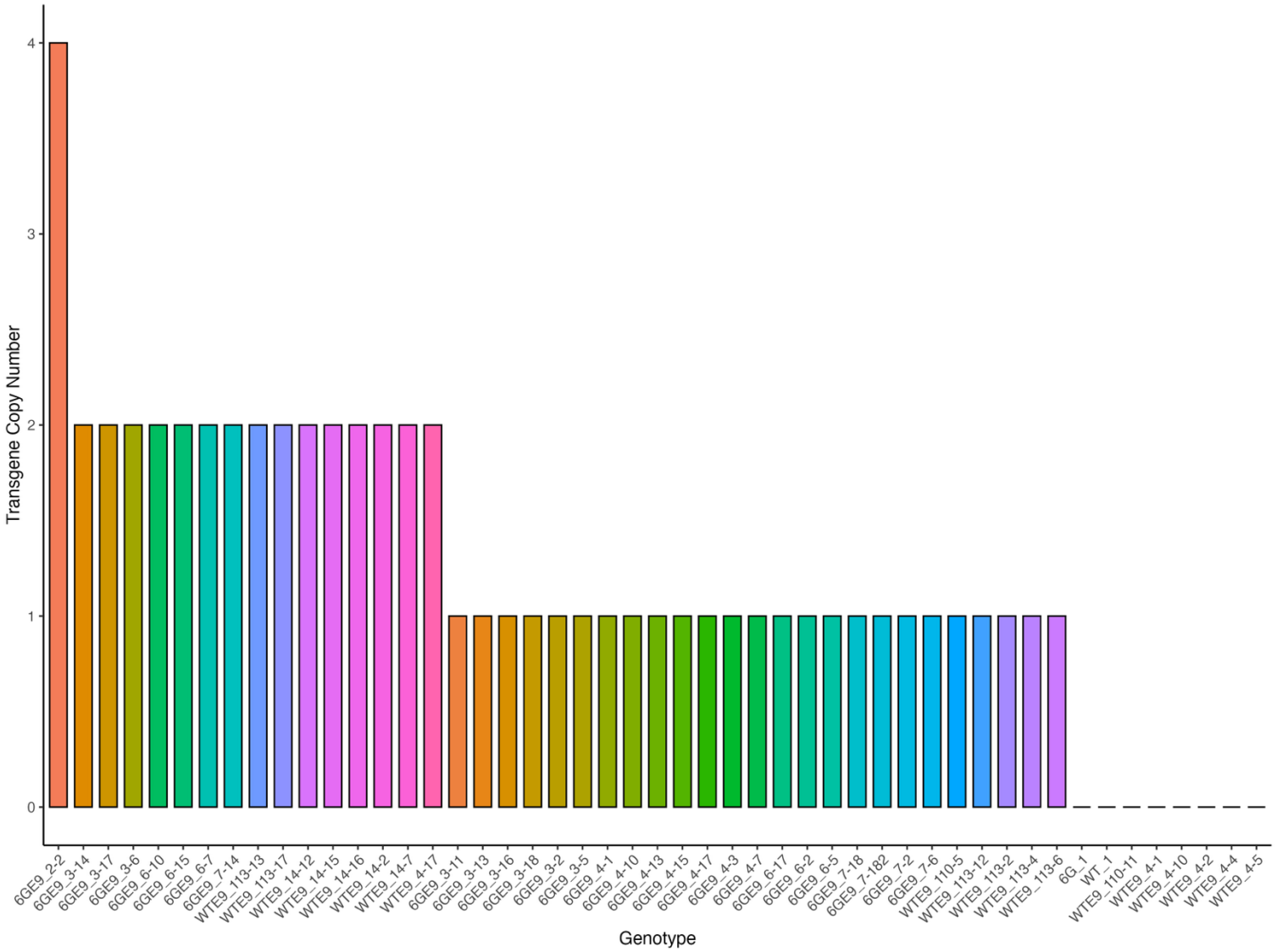

Figure 4.1. Copy number analysis shows the number of copies of the transgene inserted into the genome by Agrobacterium tumefaciens. T1 copy number analysis is used to discriminate between azygous plants (0 copies) and select for transformed plants (1 + copies). No data is available for T0 copy number analysis; thus, conclusions about homozygosity cannot be made. Copy number analysis was performed by Anglia DNA Services using their proprietary technology (Anglia DNA Services, Norwich, UK). Environmental conditions: 25–30°C day and 20°C night, 60% RH and a 16-h photoperiod of 100-250 µmol photons m^{-2} s^{-1}.

Copy number analysis revealed that 48 of the 68 samples were at least heterozygous (Figure 4.1). 30 lines contained 1 copy (heterozygous) of the Basta resistance gene, and 17 lines had 2+ copies and were potentially homozygous. No data

is available for the T0 copy number; thus, conclusive statements about homozygosity cannot be made. The presence of a range of copy numbers indicated that T1 individuals are segregating. 1 copy lines are heterozygous, and 2 copy lines may be homozygous for a single insertion or heterozygous for a double insertion.

4.2.1.2. Stomatal Density Screening Of T1 Transgenic Lines

Transgenic lines with altered SD showed stomatal ratios (AD: AB) consistent with those of the controls (between 0.5-0.6, Figure 4.10C), making counting one surface a useful proxy for quick screening of many transgenic lines with the same genetic background. Lines were determined to have an altered SD phenotype if the measured value was outside of the range of the WT SD values, accounting for natural variation (Fig. 4.2). Six transgenic lines (IS_3, IS_4, IS_6, IS_7, S_113 and S_14) had significantly higher SD than the controls (Kruskal-Wallis, Dunn test, $p < 0.05$). Six transgenic individuals (S_1105-1 copy, S_11312- 1 copy, S_142- 2 copies, IS_67- 2 copies, IS_316- 1 copy and IS_718- 1 copy), which had greater SD than WT (1.5-2.25 fold higher), were selected for further analysis in T2. Three plants overexpressing STO from both the WT and ictB TB6 (I) background overexpressing STO (S) were also taken forward.

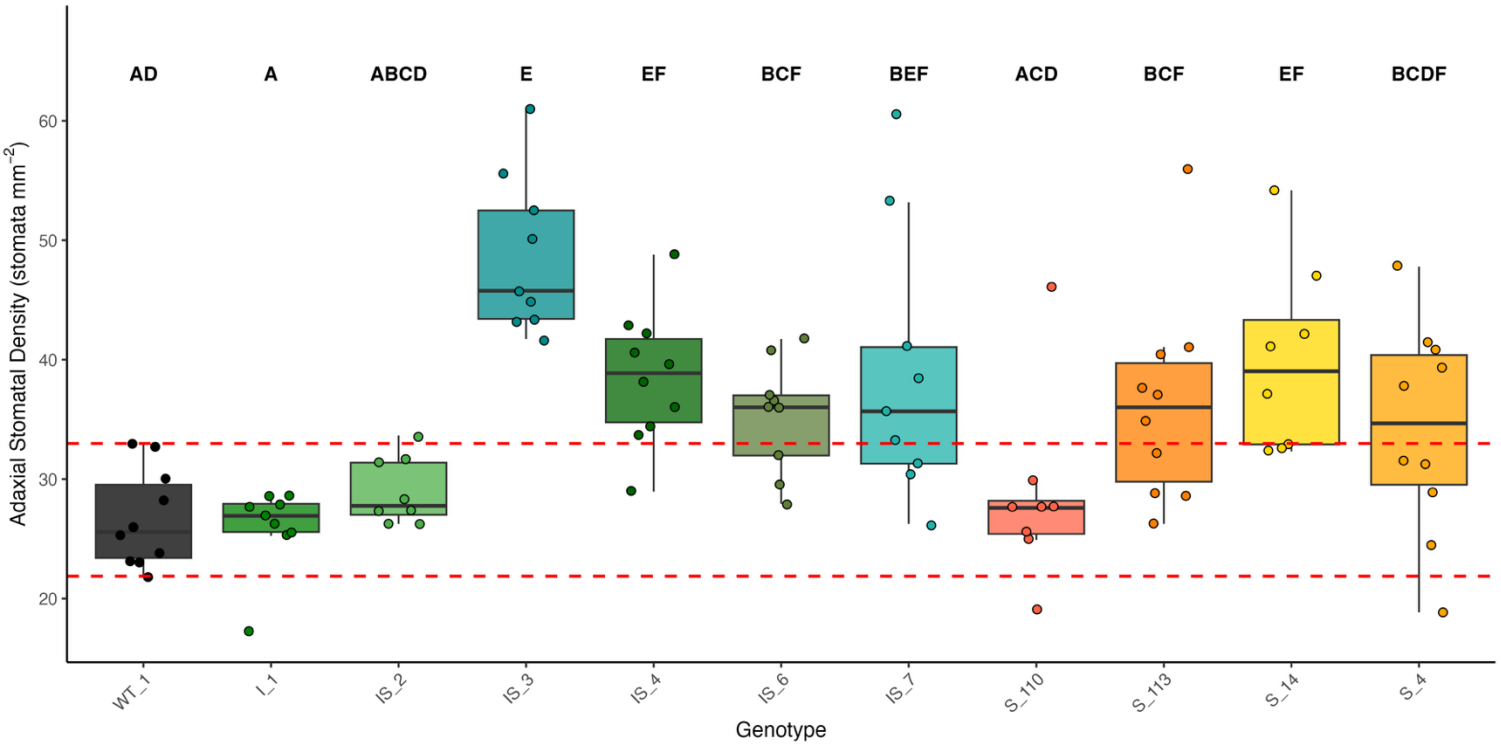

Figure 4.2. Stomatal density of T1 Tobacco transformants. Stomata were counted in 8 unique locations within the abaxial leaf surface on the epidermal peel. Adaxial stomatal density (SD; stomata mm $^{-2}$) across wild-type (WT) and transgenic tobacco genotypes. Boxplots display the median (horizontal line), interquartile range (box), and whiskers extending to 1.5 × the interquartile range, with individual biological replicates shown as jitter points (n > 8 per line). Compact letter display (CLD) annotations above each box indicate statistical groupings based on the Kruskal-Wallis test, followed by the Dunn test ($p < 0.05$); genotypes sharing the same letter are not significantly different from one another. Environmental conditions: 25–30°C day and 20°C night, 60% RH and a 16-h photoperiod of 100-250 µmol photons m^{-2} s^{-1}.

4.2.2. Chlorophyll Fluorescence Analysis Of Selected T1 Lines

4.2.2.1. Light Induction

To determine if the transgenes resulted in differences in the operating efficiency of photosystem II (YII), photosynthetic induction on three-week-old T1 lines was performed using chlorophyll fluorescence imaging. All lines exhibited typical F_v/F_m values of 0.83, suggesting that all lines were healthy and there was no photoinhibition of the photosynthetic machinery (Fig. 4.3A). All lines showed a typical response to

application of light and photosynthetic induction: a sharp decrease in YII followed by stabilisation. No differences in the shape of the photosynthetic induction were observed between genotypes.

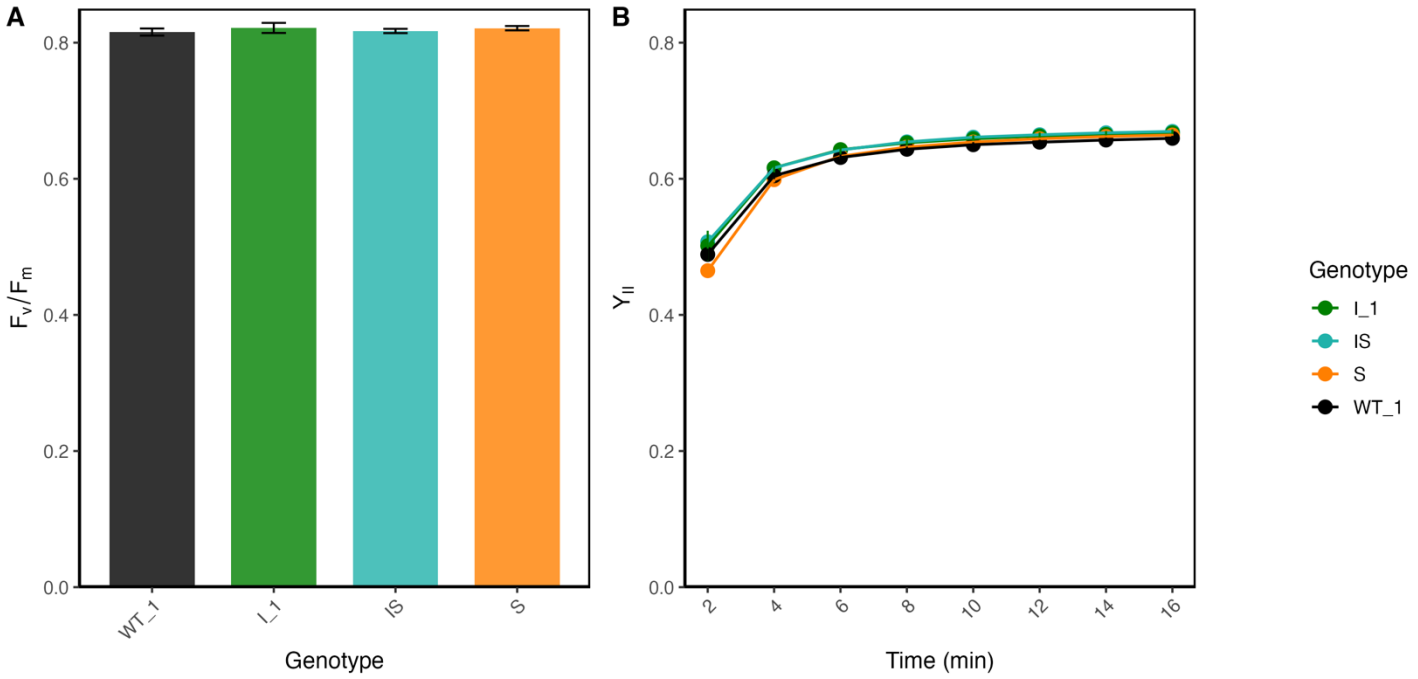

Figure 4.3. Chlorophyll fluorescence response of 3-week-old T1 transgenic tobacco to photosynthetic induction. A) Dark-adapted plants were subject to a saturating pulse to determine Fv/Fm. B) The response over time of the operating efficiency of photosystem II (YII) following addition of actinic light of 215 µmol m^{-2} s^{-1} PAR induced photosynthesis over 16 minutes. No significant differences were seen between genotypes for Fv/Fm (Kruskal-Wallis, p> 0.05) (n = 12). Environmental conditions: 25–30°C day and 20°C night, 60% RH and a 16-h photoperiod of 100-250 µmol photons m^{-2} s^{-1}.

Plants overexpressing ictB in conjunction with STO (IS) had significantly higher operating efficiency of photosystem II (YII) than the wild type at 10 and 16 minutes following a photosynthetic induction at 215 µmol m^{-2} s^{-1} PAR (ANOVA, p = 0.029 and 0.043, respectively) (Figure 4.4B and C). No other genotypes showed differences from the WT. These results suggest that the simultaneous expression of ictB and STO

provides benefits to photosynthetic efficiency during photosynthetic induction in 3-week-old tobacco at low light intensities.

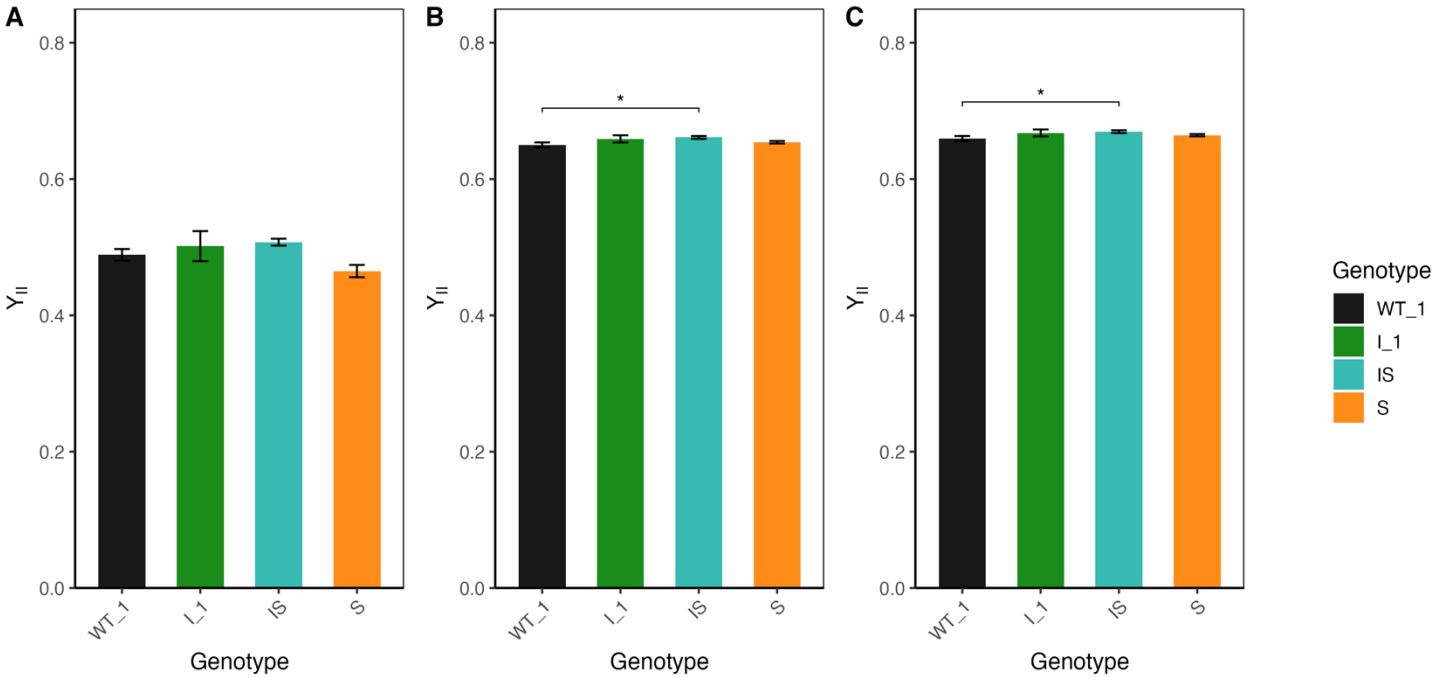

*Figure 4.4. Statistical analysis of photosynthetic response at three time points during induction of 3-week-old T1 transgenic tobacco. Bar charts represent the mean values ± standard error of YII. A) YII at 2 minutes post-induction at 215 µmol m^{-2} s^{-1} PAR. B) YII at 10 minutes post-induction. C) YII at 16 minutes post-induction. Statistical differences are denoted by a * and bracket between comparisons (ANOVA, Tukey-HSD, $p < 0.05$) above the bar charts (n = 12). Environmental conditions: 25–30°C day and 20°C night, 60% RH and a 16-h photoperiod of 100-250 µmol photons m^{-2} s^{-1}.*

4.2.2.2. Light Response Curve

To further investigate the effects of the transgenes on carbon assimilation, photosynthesis was assessed as a function of light intensity (light response curves). All lines again exhibited the typical value of 0.83 for F_v/F_m, indicating no damage to the photosynthetic machinery (Fig. 4.5A). All lines showed a typical decrease in YII as light

intensity increased, and genotypic differences in YII were apparent between 500-700 µmol m^{-2} s^{-1} PAR.

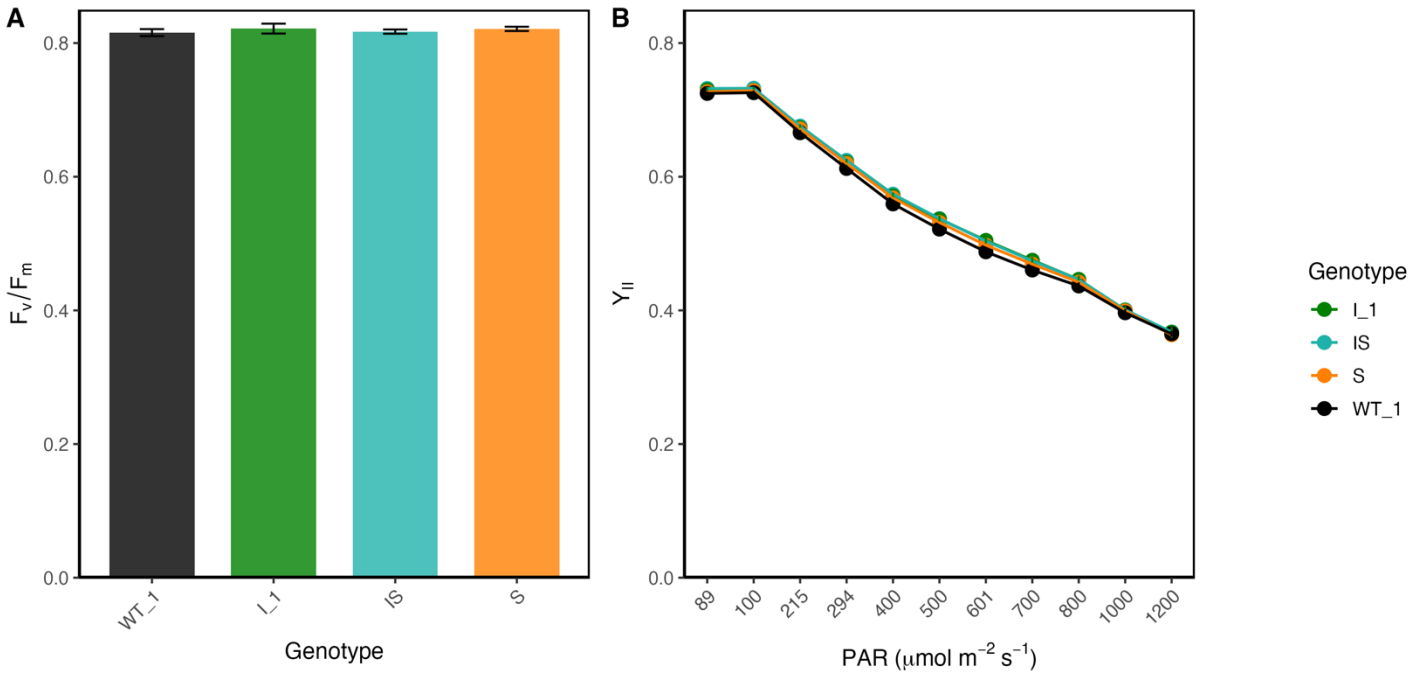

Figure 4.5. Chlorophyll fluorescence response of 3-week-old T1 transgenic tobacco to increasing light intensities. A) Dark-adapted plants were subject to a saturating pulse to determine Fv/Fm. B) The response over time of the operating efficiency of photosystem II (YII) to a step-wise increase in light intensity from 89-1200 µmol m^{-2} s^{-1} PAR, with the light intensity increasing at 2-minute intervals. No significant differences were seen between genotypes for Fv/Fm (Kruskal-Wallis, p> 0.05) (n = 12). Environmental conditions: 25–30°C day and 20°C night, 60% RH and a 16-h photoperiod of 100-250 µmol photons m^{-2} s^{-1}.

Lines overexpressing ictB had significantly higher YII than the wild-type at 600, 800 (6G and IS), and 1200 µmol m^{-2} s^{-1} PAR (IS) (ANOVA, $p < 0.05$). These results indicate that ictB overexpression in combination with STO can provide benefits to the operating efficiency of photosystem II at moderate light intensities in 3-week-old tobacco.

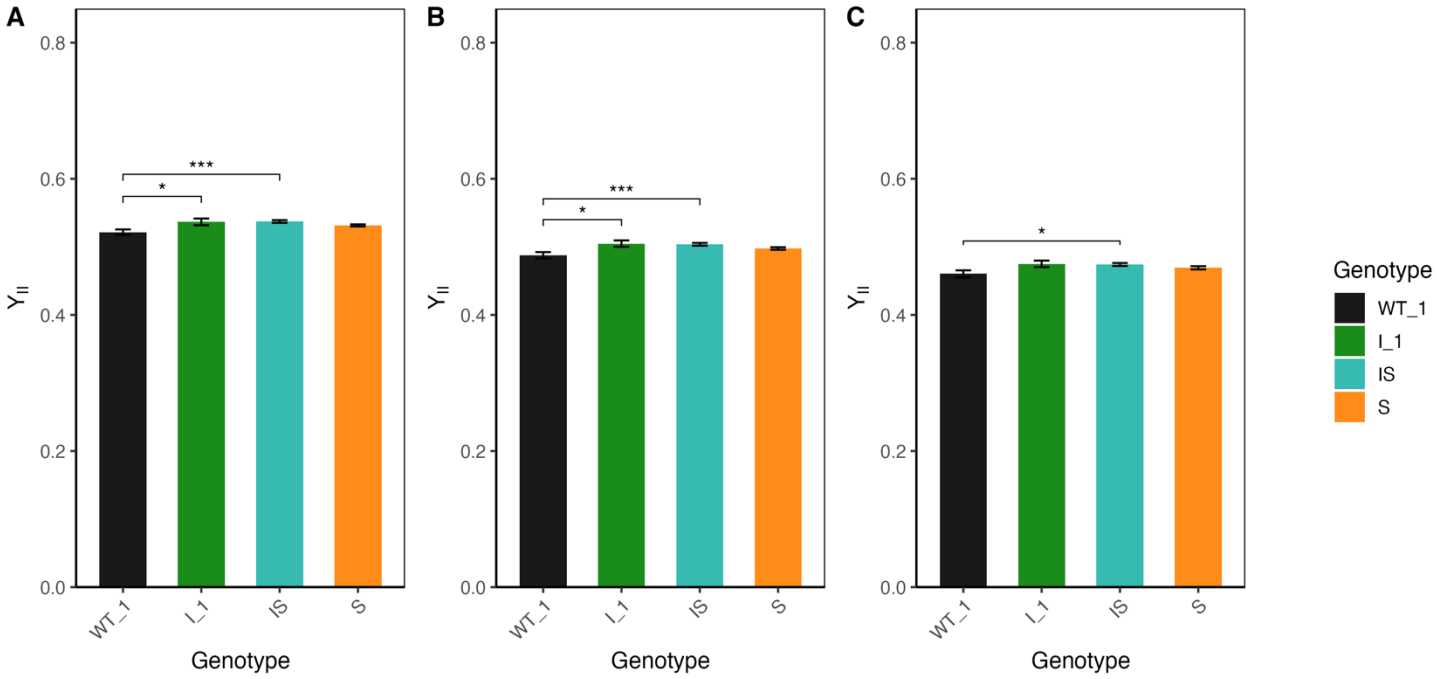

*Figure 4.6. Statistical analysis of photosynthetic response at three light intensities during the light response curve of 3-week-old T1 transgenic tobacco. Bar charts represent the mean values ± standard error of YII. A) YII at 500 µmol m $^{-2}$ s $^{-1}$ PAR. B) YII at 600 µmol m $^{-2}$ s $^{-1}$ PAR. C) YII at 700 µmol m $^{-2}$ s $^{-1}$ PAR. Statistical differences are denoted by asterisks and brackets between comparisons (ANOVA with Tukey HSD, $p < 0.05$, ** $p < 0.01$, *** $p < 0.001$) above the bar charts (n = 12). Environmental conditions: 25–30°C day and 20°C night, 60% RH and a 16-h photoperiod of 100-250 µmol photons m^{-2} s^{-1}.*

4.2.3. Molecular Characterisation Of Transgene Expression

4.2.3.1. PCR Confirmation Of Heterozygosity Of STOMAGEN

To ensure that the T2 lines harboured the STO transgene, given that these lines segregate with 1-2 copies of the transgene (Fig. 4.1), PCR was used to confirm the presence of the positive selection marker BASTA in DNA from plants that survived BASTA germination selection (Section 2.5.4) (Fig. 4.7). All eight individuals from STO single lines S_1105 (wells 2-9), S_11312 (wells 10-17), S_142 (wells 18-25), and STO::ictB double lines IS_316 (wells 26-33), IS_67 (wells 34-41), and IS_718 (wells 42-49) showed the appropriate banding at 655 bp confirming the presence of the BASTA

resistance gene and by proxy STO (Fig. 4.7). No banding was observed in the negative control wells 0 and 50. These data suggest that the BASTA germination selection was effective at selecting for heterozygous individuals in a segregating population.

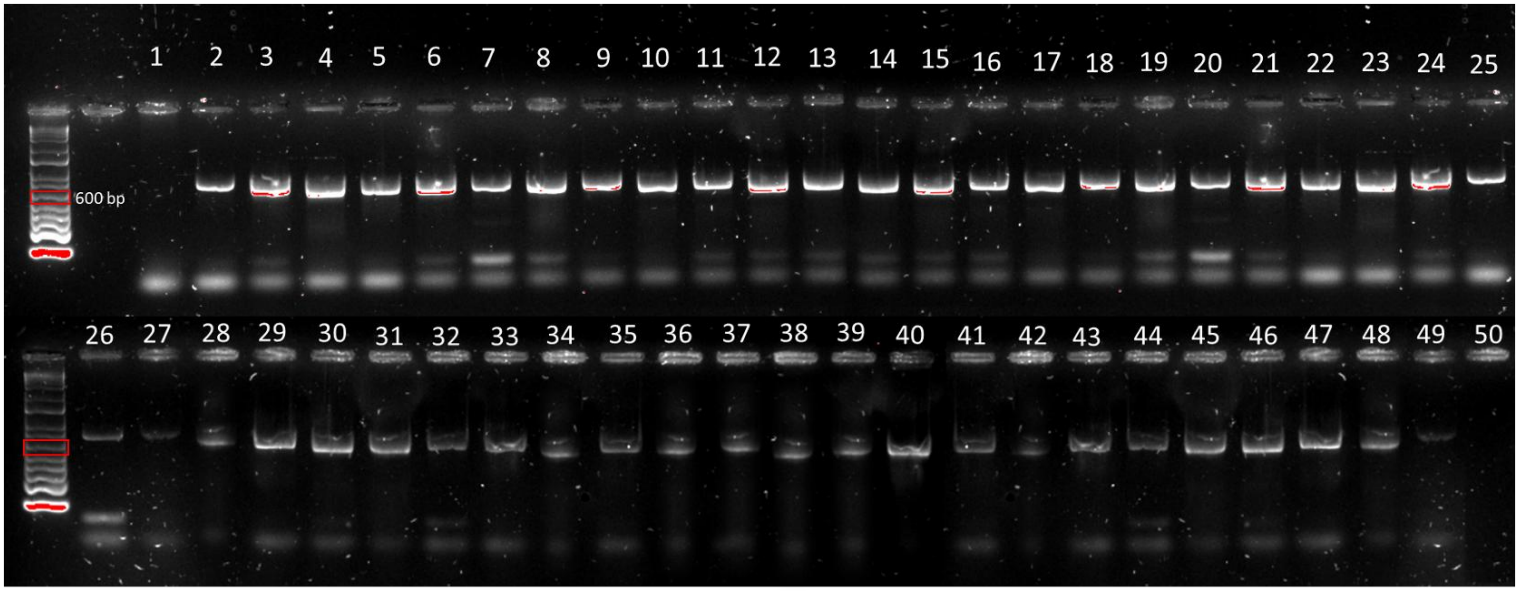

Figure 4.7. Agarose gel showing the banding patterns of DNA fragments produced from a PCR using the forward and reverse primers for the BASTA resistance gene and DNA from four-week-old T2 tobacco plants that survived BASTA germination selection. Positive results display a banding pattern of 655 bp. Red squares on the DNA ladder highlight the band representing 600 bp. Wells 2-9 represent samples from the 8 replicates of S_1105 (individuals 1-8, respectively), wells 10-17 represent S_11312 (individuals 1-8, respectively), wells 18-25 represent S_142 (individuals 1-8, respectively), wells 26-33 represent IS_316 (individuals 1-8, respectively), wells 34-41 represent IS_67 (individuals 1-8, respectively), and wells 42-49 represent IS_718 (individuals 1-8, respectively). Environmental conditions: 25–30°C day and 20°C night, 60% RH and a 16-h photoperiod of 100-250 µmol photons m^{-2} s^{-1}.

4.2.3.2. qPCR

To understand the differences in transgene expression between the T2 lines, quantitative PCR was conducted. Lines overexpressing STO exhibited a wide range of transgene expression relative to the protein phosphatase 2A housekeeping gene (Fig.

4.8A). Two lines, S_1105 and IS_718, exhibited low relative expression, similar to that of the Azygous, suggesting little to no transgene expression in these lines. One double genotype, IS_67, had an average expression of 50x PP2A. The remaining genotypes had very high expression relative to PP2A and formed two distinct significance groups, with an average of 918 and 930 for S_147 and S_11312 in group D, respectively. The highest expression relative to PP2A was the double line IS_316, significantly higher than any other STO-expressing lines.

For lines overexpressing ictB, detectable expression of ictB was found in the double lines IS_67 and IS_316, with average expression levels relative to PP2A of 1 and 3.25x, forming statistical groups b and c, respectively. No detectable levels of expression of the background line ictB (I_1) nor IS_718, despite I_1 being a T4 homozygous transformed line and double lines having the homozygous T2 ictB (I_1) as their genetic background.

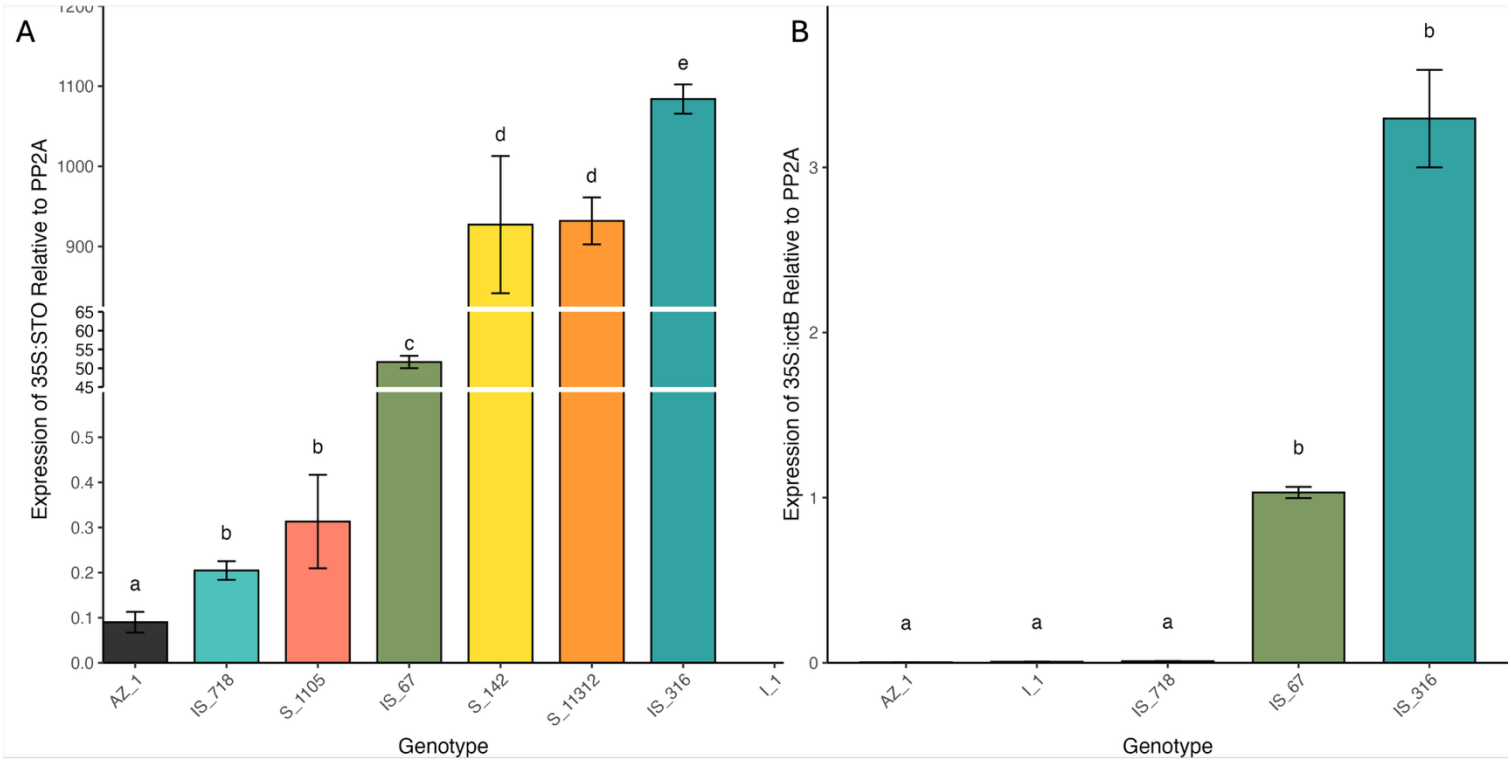

Figure 4.8. Quantitative PCR (qPCR) analysis of relative expression of the transgenes in 4-week-old T2 transgenic Tobacco lines. A) 35S:STO normalised to the expression of protein phosphatase 2A (PP2A). B) 35S:ictB transgene expression was normalised to the expression of protein phosphatase 2A (PP2A). STO and ictB were amplified using their respective qPCR primers (Table 2, Chapter 2). Relative expression of the genes was calculated by normalising expression to the expression of PP2A in the Azygous. Compact letter display (CLD) annotations above each box indicate statistical groupings based on ANOVA, followed by the Tukey-HSD ($p < 0.05$) ($n = 3$); genotypes sharing the same letter are not significantly different from one another. Environmental conditions: 25–30°C day and 20°C night, 60% RH and a 16-h photoperiod of 100-250 µmol photons m^{-2} s^{-1}.

4.2.4. Microscopic Characterisation Of Stomatal Development

4.2.4.1. Changes In Epidermal Patterning In T2 Transgenic Lines

On the selected lines, SD of the T2 plants was determined to confirm the effect of STO overexpression. Transgenic Tobacco plants overexpressing STO exhibited a higher stomatal density than the control. Some lines overexpressing STO had stomata that formed clusters. Stomatal clusters ranged from groups of 2 to 3 stomata per cluster. Stomatal clustering occurred on both abaxial and adaxial sides of the leaf. However, stomatal clustering was not the norm, accounting for <5% of total stomata in a measured area (1-2 stomata formed clusters per area) and thus was not quantified. Stomatal clustering was uncommon in the Azygous and ictB background line, 6G.

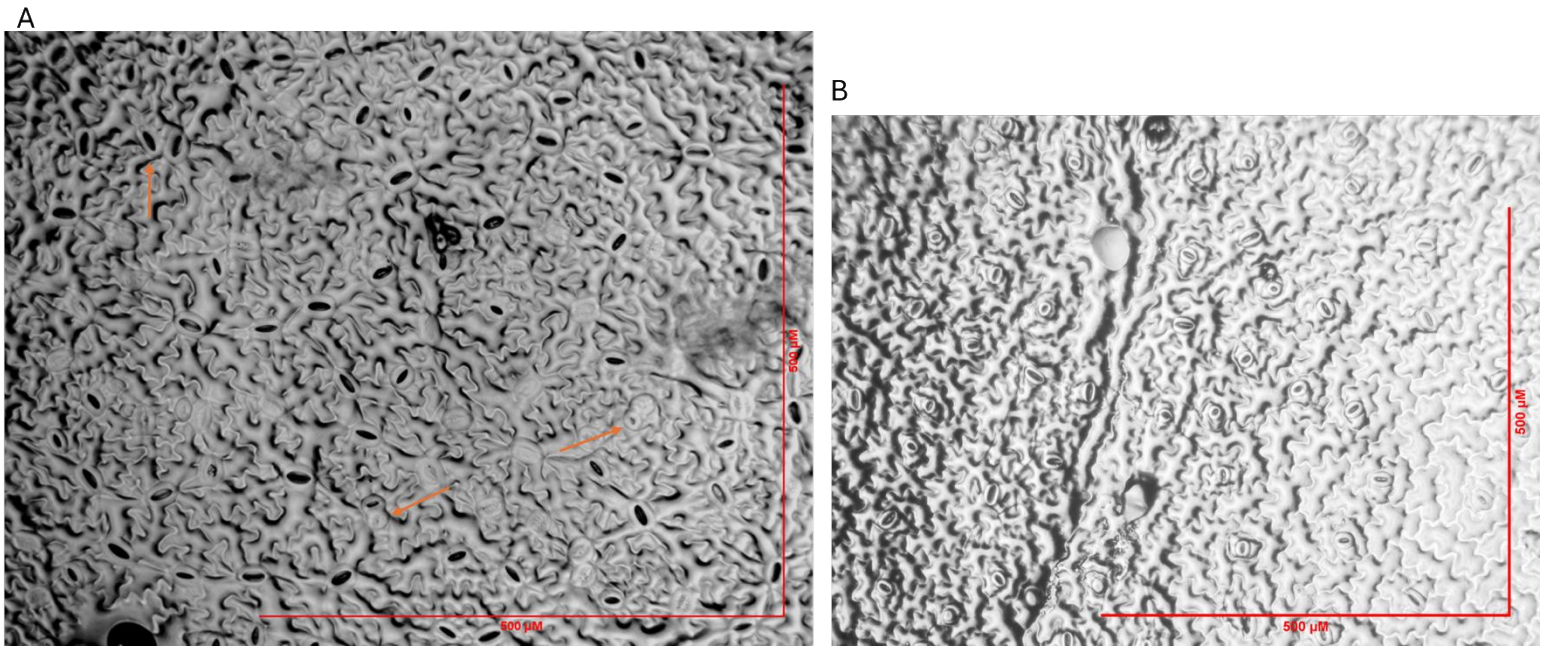

Figure 4.9. Brightfield microscopy images of T2 transgenic tobacco leaf epidermal peels under 10x magnification. A) Stomatal impressions of transgenic tobacco overexpressing STO show stomatal clustering. B) Epidermal impressions of azygous tobacco. Stomatal clusters are indicated by arrows. These impressions were taken from glasshouse tobacco following destructive harvest. Environmental conditions: 25–30°C day and 20°C night, 60% RH and a 16-h photoperiod of 100-250 µmol photons m^{-2} s^{-1}.

4.2.4.2. Quantification Of Stomatal Density Across Transgenic Genotypes

The transgenic tobacco lines overexpressing STO had significantly different stomatal densities than the Azygous controls and the ictB background line, 6G. The azygous control had an adaxial SD of 75.6 ± 4.1 and an abaxial SD of 41 ± 3.2 stomatal mm^{-2}. Three transgenic lines overexpressing STO had significantly higher SD than the azygous control (Fig. 4.10A and B): with IS_67, S_11312 and S_142 having a relative increase in SD of approximately 1.85, 2 and 2 times greater SD than the control. Stomatal ratios (AD:AB) remained consistent across genotypes (0.5-0.57) (Fig. 4.10C), suggesting a uniform increase in SD across both leaf surfaces.

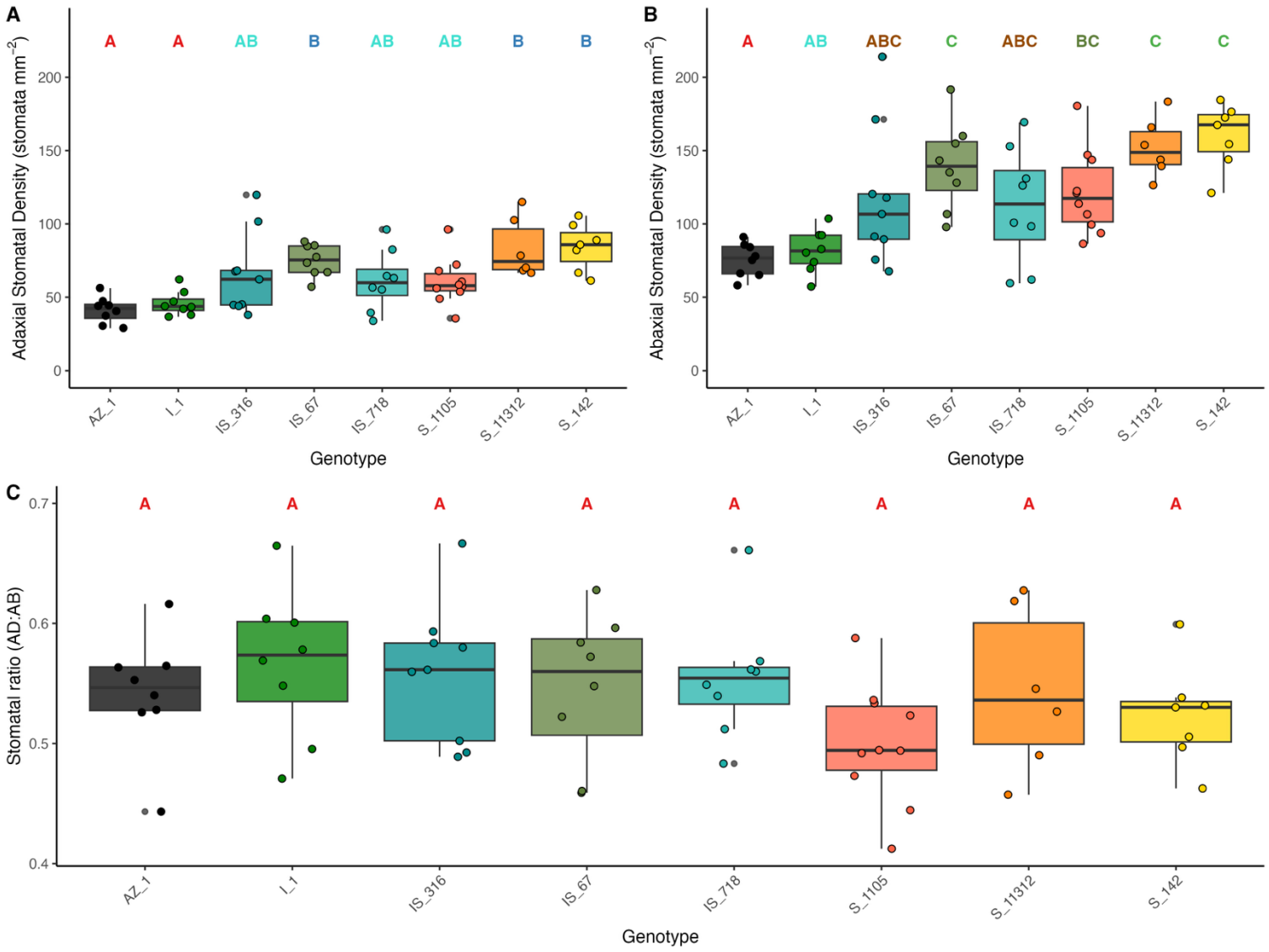

Figure 4.10. Epidermal patterning in T2 transgenic tobacco lines. Adaxial stomatal density (A), Abaxial stomatal density (B) and the stomatal Ratio (C) of genotypes grown in low light conditions. Boxplots show the distribution of stomatal density measurements per genotype, with individual data points overlaid. Different shades represent different genotypes. Compact letter display (CLD) annotations above each box indicate statistical groupings based on ANOVA, followed by Tukey's HSD test ($p < 0.05$) ($n = 8$); genotypes sharing the same letter are not significantly different from one another. Measurements were taken from full expanded leaves post-destructive harvest. Environmental conditions: 25–30°C day and 20°C night, 60% RH and a 16-h photoperiod of 100-250 µmol photons m^{-2} s^{-1}.

4.2.4.3. Relationship Between 35S::STO *Expression And Stomatal Density*

Stomatal density of both the adaxial and abaxial leaf surfaces was correlated with the expression of STO to better understand the relationship between gene expression and stomatal density. Linear regression revealed a non-significant positive relationship between STO expression and stomatal density on the abaxial and adaxial leaf surfaces (r^2 = 0.402, p = 0.126 and r^2 = 0.523, p = 0.066, respectively). These data suggest that 35S::STO expression has a moderate association with both adaxial and abaxial stomatal density under these conditions and that other factors are influencing stomatal development.

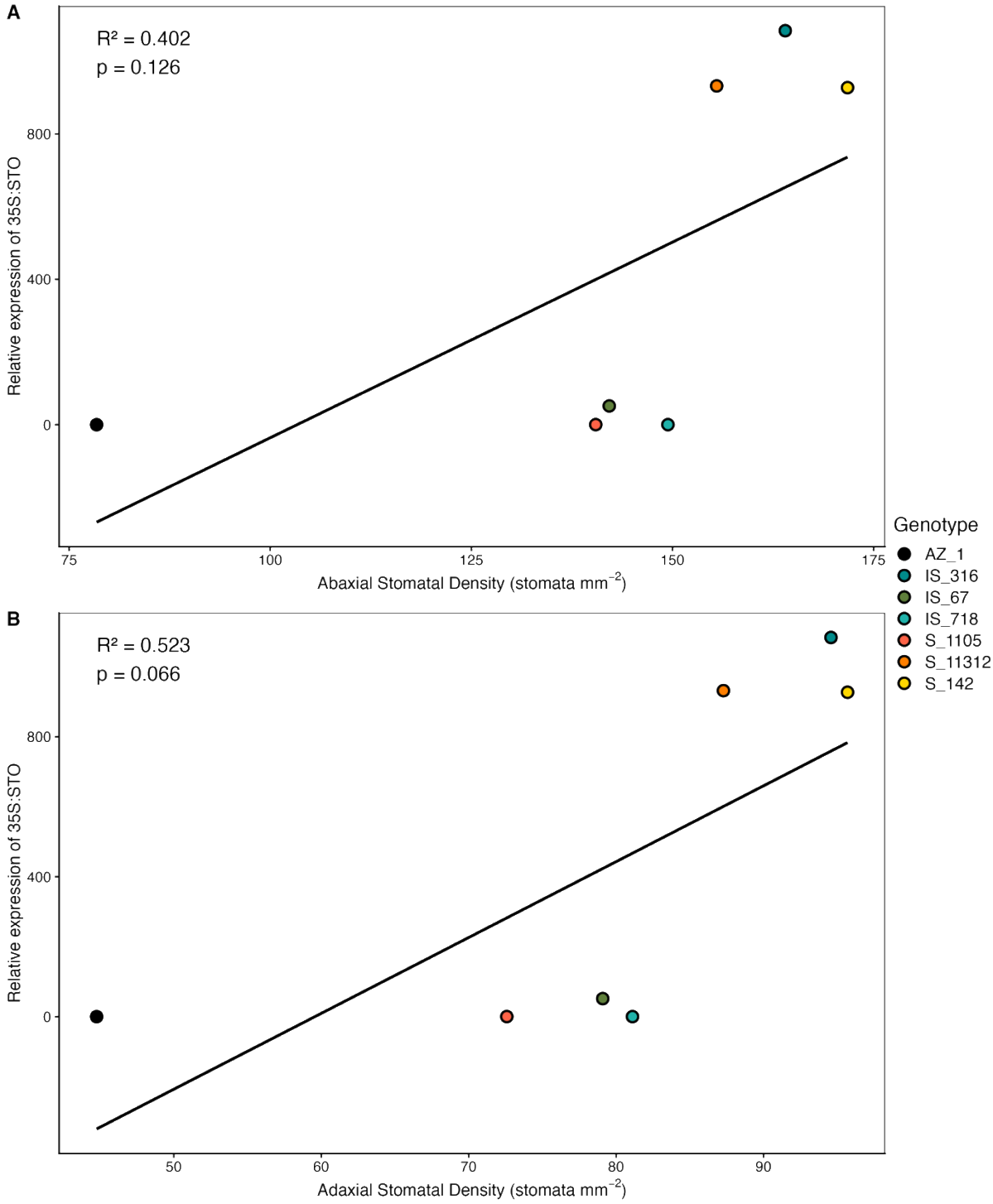

Figure 4.11. Correlation between 35S::STO expression and stomatal patterning traits in T2 transgenic tobacco lines. Each point represents a genotype, coloured by genotype identity. A) Adaxial stomatal density (stomata mm $^{-2}$) plotted against relative 35S::STO expression. B) Abaxial stomatal density (stomata mm $^{-2}$) for the same genotypes. Linear regression lines are shown in black, with associated coefficients of determination (R^2) and p-values reported in each panel. Measurements were taken from full expanded leaves post-destructive harvest. Environmental conditions: 25–30°C day and 20°C night, 60% RH and a 16-h photoperiod of 100-250 µmol photons m^{-2} s^{-1}.

4.2.5. Chlorophyll Fluorescence Analysis Of T2 Lines

4.2.5.1. Photosynthetic Induction

To establish if the transgenes convey any benefit to the photosynthetic efficiency of PSII during photosynthetic induction, T2 selected lines were subject to chlorophyll fluorescence imaging. As expected, all lines exhibited typical values of F_v/F_m (Fig. 4.12A) and similarly shaped photosynthetic induction responses, as observed in the T1 plants. However, genotypic differences were apparent between lines at 400 µmol m^{-2} s^{-1} PAR.

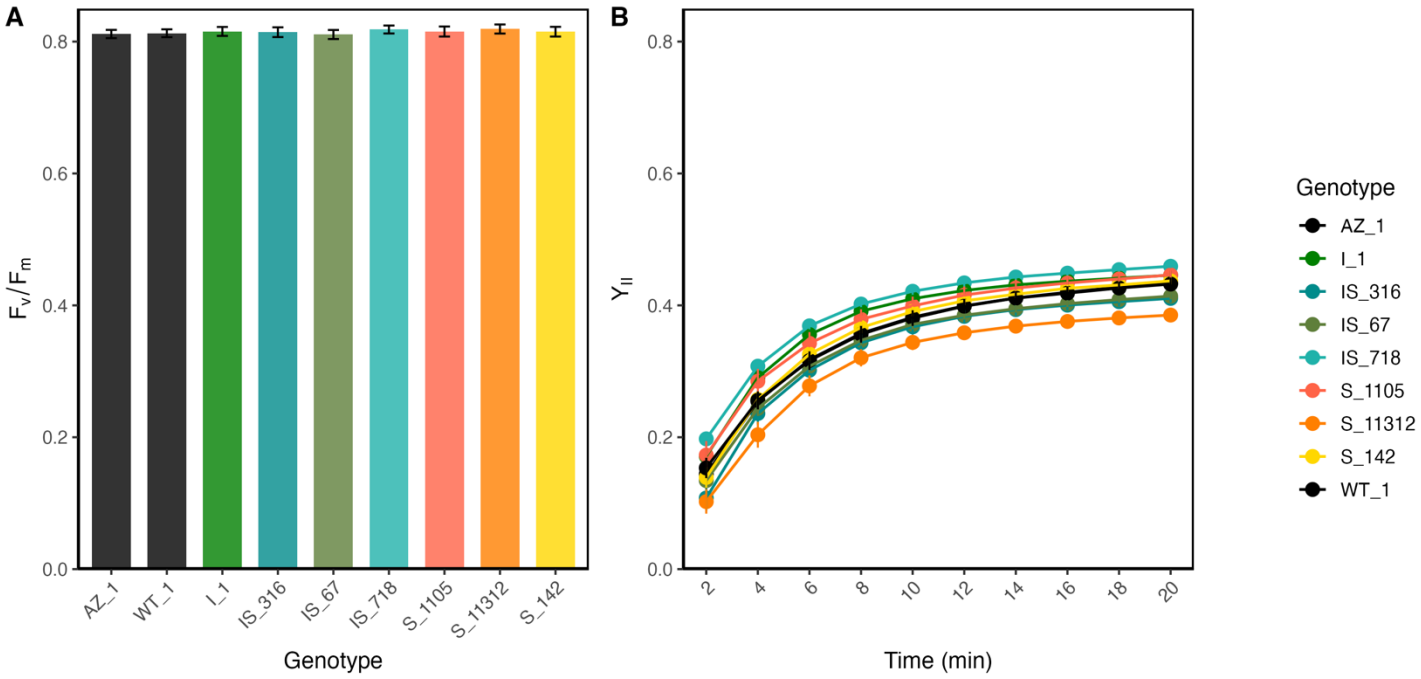

Figure 4.12. Chlorophyll fluorescence response of 3-week-old T2 transgenic tobacco to photosynthetic induction. A) Dark-adapted plants were subject to a saturating pulse to determine Fv/Fm. B) The response over time of the operating efficiency of photosystem II (YII) following addition of actinic light of 400 µmol m^{-2} s^{-1} PAR induced photosynthesis over 20 minutes. No significant differences were seen between genotypes for Fv/Fm (Kruskal-Wallis, p> 0.05) (n=12). Environmental conditions: 25–30°C day and 20°C night, 60% RH and a 16-h photoperiod of 100-250 µmol photons m^{-2} s^{-1}.

One line overexpressing STO (S_11312) had a significantly lower YII than the azygous control at both 12 and 20 minutes into the induction (ANOVA and Tukey HSD, $p = 0.049$ and $p = 0.0036$, respectively). Conversely, one line overexpressing both ictB and STOMAGEN (IS_718) had significantly higher YII 12 minutes into the light induction (ANOVA and Tukey HSD, $p = 0.047$). No differences were observed between the control and STO lines of similar SD (S_142), which may indicate that the observed difference in YII between the STO line 11312 and the control may not be a result of higher SD. As the advantageous double line 718 has negligible expression of either ictB or STO (Fig. 4.7) and a nonsignificant increase in SD than the control (Fig. 4.10), it is unlikely that the observed differences are a result of transgene function.

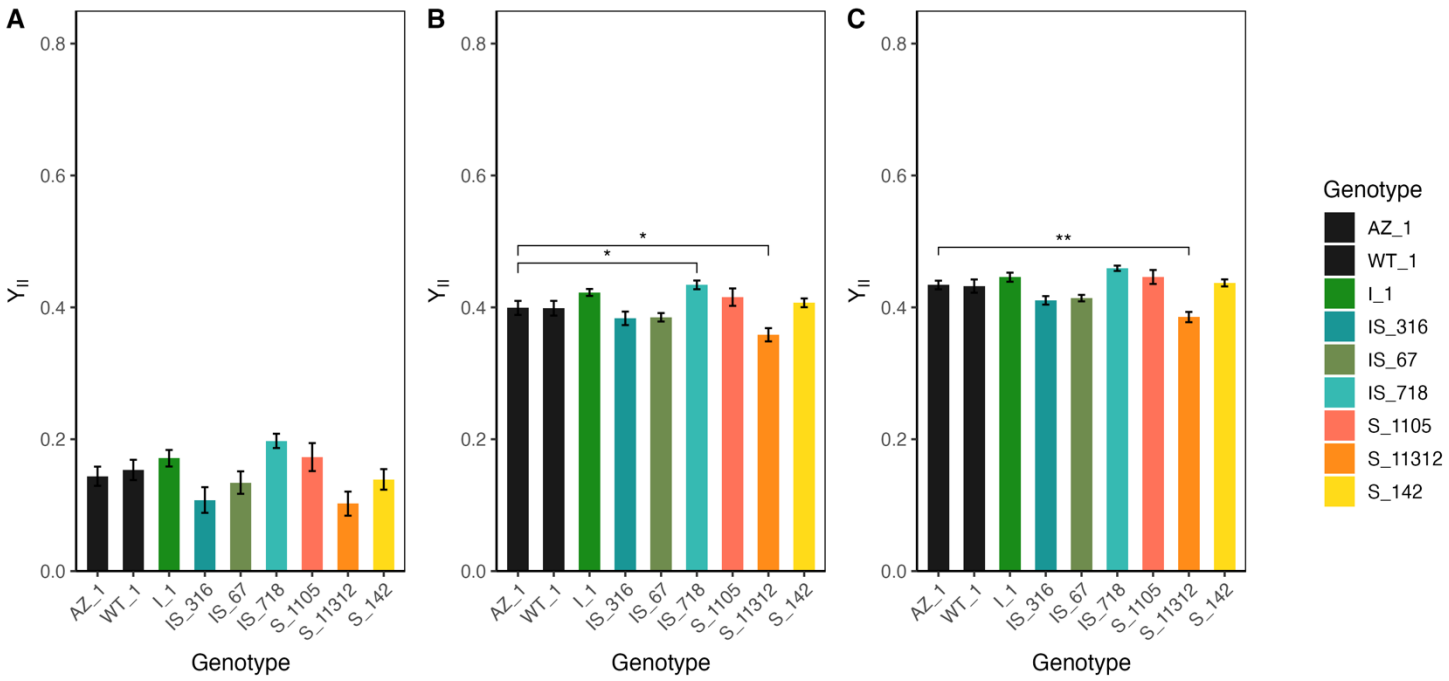

*Figure 4.13. Statistical analysis of photosynthetic response at three time points during photosynthetic induction of 3-week-old T2 transgenic tobacco. Bar charts represent the mean values ± standard error of YII. Panels A-C depict values 2, 12 and 20 minutes post-induction at 400 µmol m^{-2} s^{-1} PAR, respectively. Statistical differences are denoted by asterisks and brackets between comparisons (ANOVA with Tukey HSD, $p < 0.05$, ** $p < 0.01$, *** $p < 0.001$) (n = 12) above the bar charts. Environmental conditions: 25–30°C day and 20°C night, 60% RH and a 16-h photoperiod of 100-250 µmol photons m^{-2} s^{-1}.*

4.2.5.2. Light Response Curve

To further investigate the effects of the transgenes on the photosynthetic response to light, T2 plants were subject to a light response curve to assess the photosynthetic response across a range of increasing light intensities. No difference in F_v/F_m was observed (Fig. 4.14A). Genotypic differences in YII were apparent throughout the light curve, with two lines (S_11312 and IS_316) exhibiting consistently lower YII between 600-1200 µmol m^{-2} s^{-1} PAR.

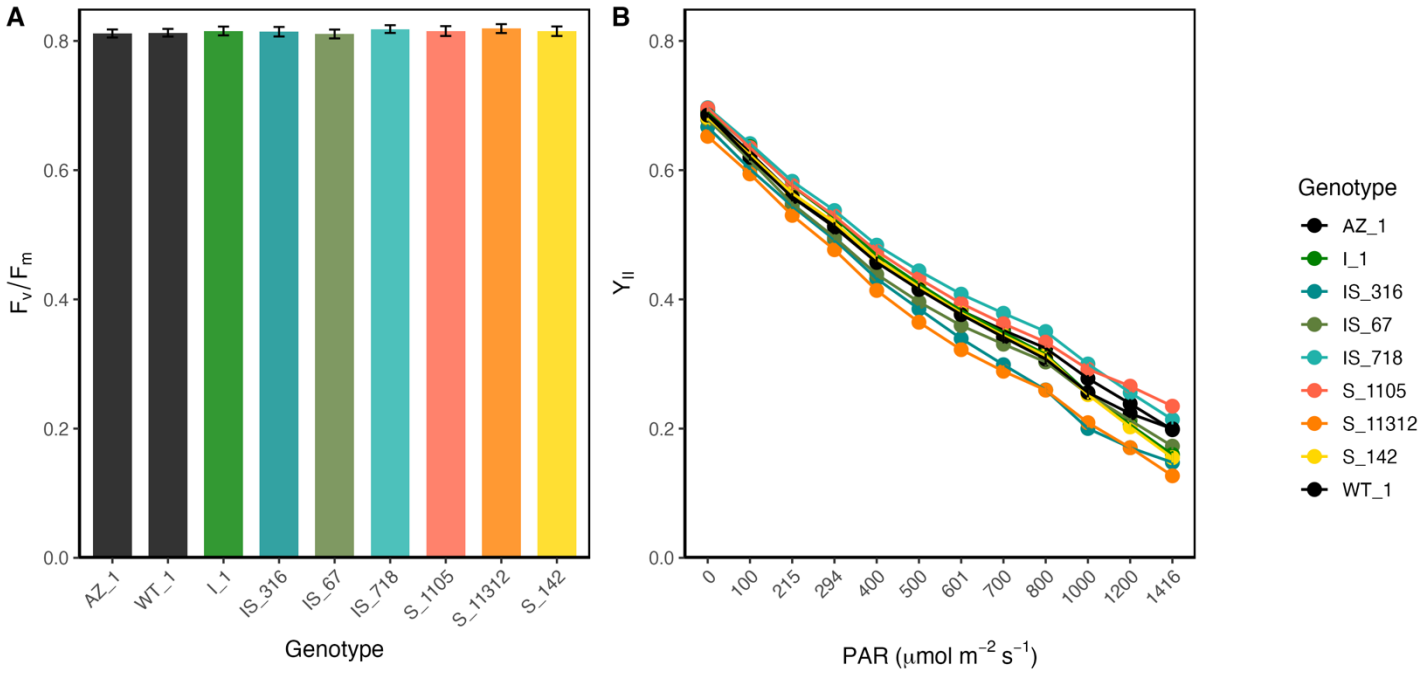

Figure 4.14. Chlorophyll fluorescence response of 3-week-old T2 transgenic tobacco to increasing light intensities. Dark-adapted plants were subject to a saturating pulse to determine Fv/Fm (A). Stepwise increases in light intensity from 0-1200 µmol m^{-2} s^{-1} PAR, with the light intensity increasing at 2-minute intervals. Panel B shows the response of the operating efficiency of photosystem II (YII) to increasing light intensity. No significant differences were seen between genotypes for Fv/Fm (Kruskal-Wallis, p> 0.05) (n = 12). Environmental conditions: 25–30°C day and 20°C night, 60% RH and a 16-h photoperiod of 100-250 µmol photons m^{-2} s^{-1}.

Several lines were significantly different from the azygous control at higher light intensities. At 600 µmol m^{-2} s^{-1} PAR, two lines overexpressing STO with and without ictB (IS_316 and S_11312) had significantly reduced YII (ANOVA and Tukey HSD, $p < 0.01$) compared to the control. Conversely, one line with negligible T2 expression of either ictB or STO (Fig. 4.8) had significantly higher YII ($p = 0.048$). At 1000 µmol m^{-2} s^{-1} PAR, the same reduction in YII was seen with the same lines as at 600 µmol m^{-2} s^{-1} PAR (IS_316 and S_11312) ($p < 0.001$). At 1400 µmol m^{-2} s^{-1} PAR, many lines expressing STO with or without ictB had significantly reduced YII (IS_316, S_11312 and S_142) ($p < 0.001$). These three lines all had significantly higher SD than the controls (Fig. 4.10A and B). Interestingly, the ictB control had significantly reduced YII at the highest light intensity ($p < 0.001$). Lines with low expression of STO, with only slight non-significant increases in SD, either maintained or had increased YII compared to the controls (IS_718 and S_1105, respectively) ($p = 0.011$). These data may suggest, conversely to the T1 data, that ictB expression does not facilitate higher operating efficiencies of Photosystem II and that increased SD may contribute to reducing YII at high light intensities.

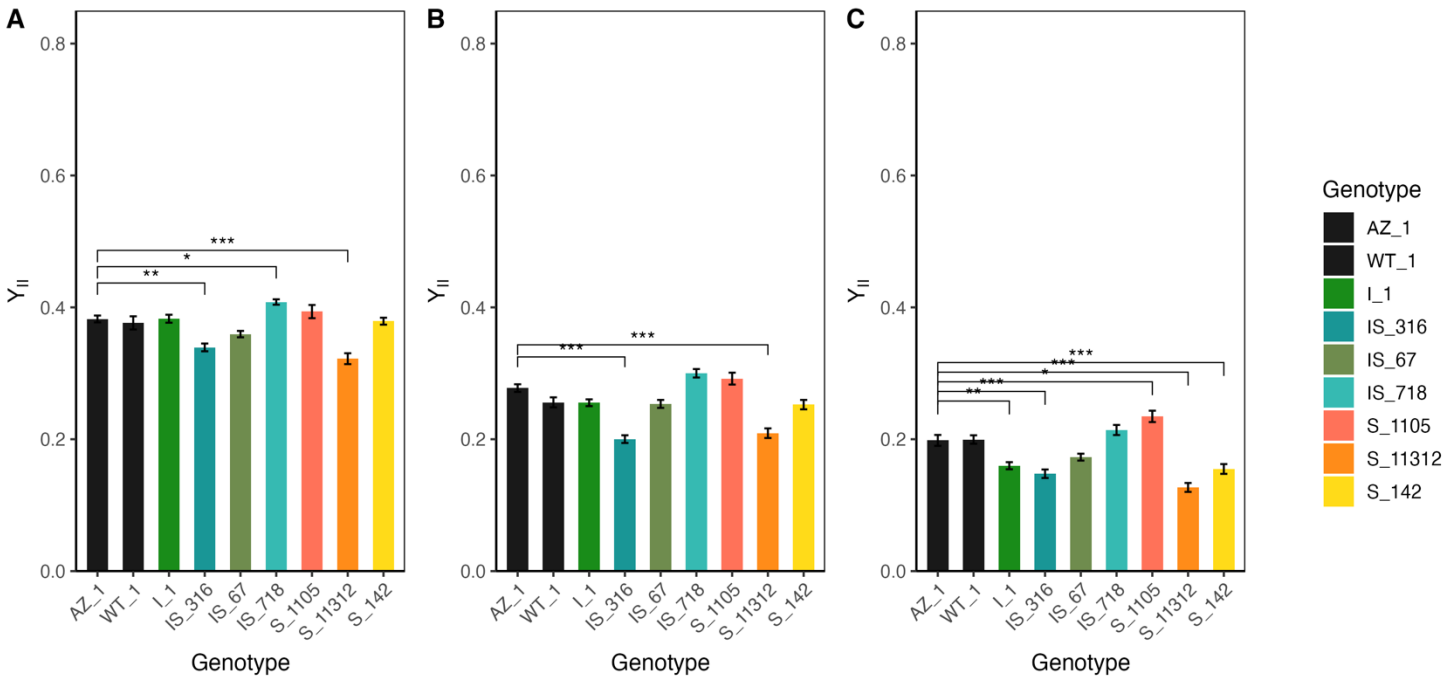

*Figure 4.15. Statistical analysis of photosynthetic response at three light intensities during the light response curve of 3-week-old T2 transgenic tobacco. Bar charts represent the mean values ± standard error of YII. Panels A-C depict values recorded at 600, 1000, 1400 µmol m^{-2} s^{-1} PAR. Statistical differences are denoted by asterisks and brackets between comparisons (ANOVA with Tukey HSD, $p < 0.05$, ** $p < 0.01$, *** $p < 0.001$) ($n = 12$) above the bar charts. Environmental conditions: 25–30°C day and 20°C night, 60% RH and a 16-h photoperiod of 100-250 µmol photons m^{-2} s^{-1}.*

4.2.6. Determining Photosynthetic Capacity

Photosynthesis as a function of internal CO_2 concentration (C_i) was used to determine if transgenic expression of STO and/or ictB affected photosynthetic capacity. All genotypes showed a typical *A/C*$_i$ response curve, with assimilation rate (*A*) increasing steeply at low intercellular CO_2 concentrations (C_i) before approaching saturation at higher C_i levels (Fig. 4.16).

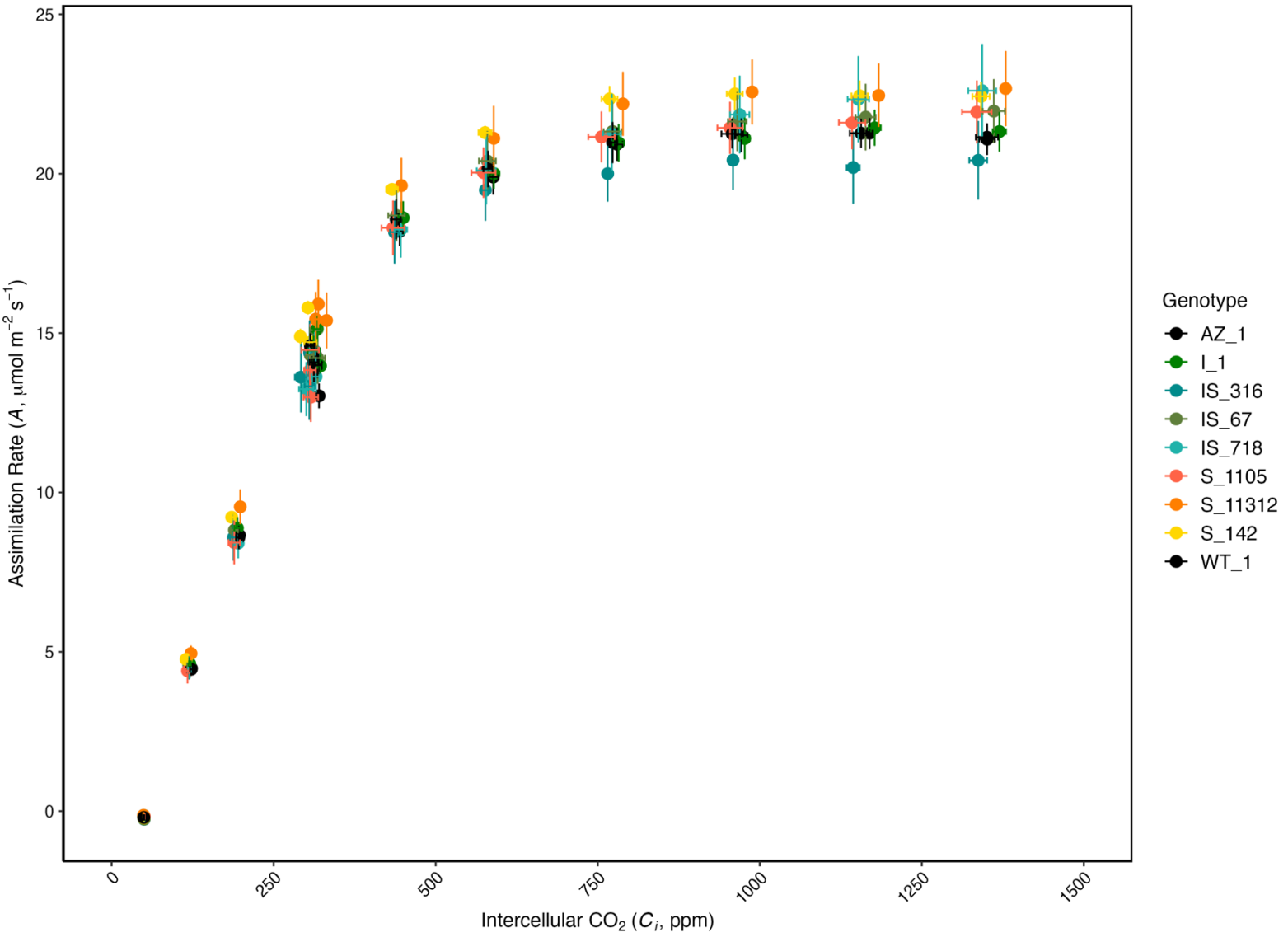

Figure 4.16. Photosynthetic response of T2 transgenic tobacco plants under different intracellular CO2 concentrations (C_i). The net CO_2 assimilation rate (A, µmol m^{-2} s^{-1}) is plotted as a function of intercellular CO_2 concentration (C_i, µmol mol^{-1}). Each point represents the mean (n = 4-7) for a given genotype, with the error bars indicating standard error (SE), for A and C_i (vertical and horizontal, respectively). Environmental conditions: 25–30°C day and 20°C night, 60% RH and a 16-h photoperiod of 100-250 µmol photons m^{-2} s^{-1}. Measurements were performed on the youngest fully expanded leaf.

Derived values of A_{max}, Vc_{max}, and J_{max} did not differ significantly between genotypes (Fig. 4.17) (ANOVA, Tukey HSD, $p < 0.05$), suggesting that the maximum rate of photosynthesis, maximum rate of carboxylation, or the maximum rate of electron

transport were not affected by the function of STO or ictB when grown at low light conditions.

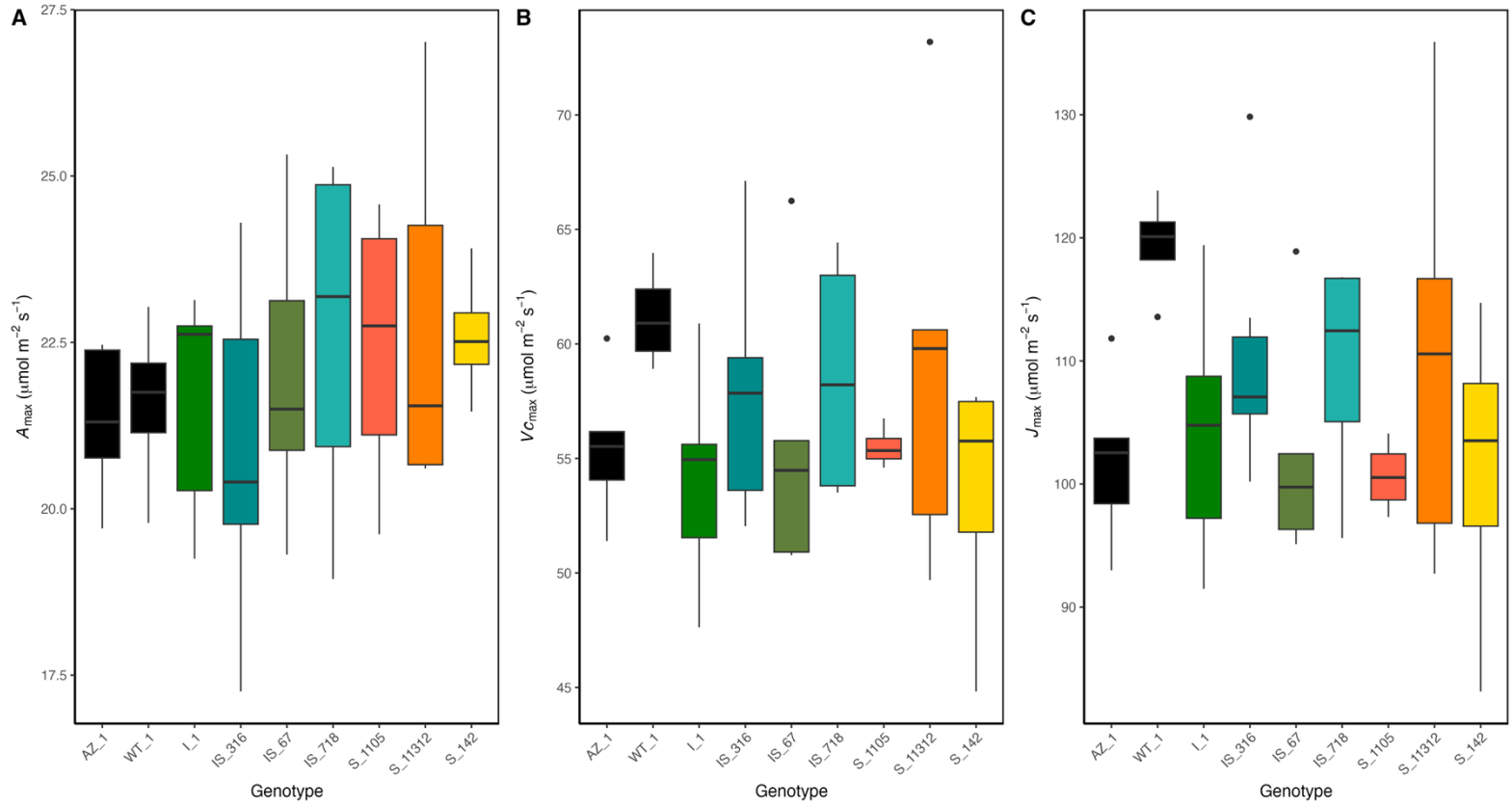

Figure 4.17. Photosynthetic parameters modelled from A/C_i curves across genotypes of T2 transgenic tobacco. A) CO_2 and Light-saturated assimilation rate (A_{max}), (B) maximum Rubisco carboxylation capacity (Vc_{max}) and (C) maximum electron-transport–limited rate (J_{max}). Boxplots display the median (horizontal line), interquartile range (box), and whiskers extending to 1.5 × the interquartile range, with black dots marking observations beyond this range (outliers). No statistical differences were found between genotypes for A_{max}, Vc_{max}, or J_{max} ANOVA, p >0.05 (n = 4-7). Environmental conditions: 25–30°C day and 20°C night, 60% RH and a 16-h photoperiod of 100-250 µmol photons m^{-2} s^{-1}. Measurements were performed on the youngest fully expanded leaf.

4.2.7. Photosynthetic Response To Changes In Light Intensity

To understand the photosynthetic response to changing light intensity between the transgenic tobacco lines and controls, CO_2 assimilation rate (*A*) was measured over a stepwise ramp of irradiance (Q) from 0 to 1500 µmol photons m^{-2} s^{-1} (Fig. 4.18). All

genotypes showed the characteristic linear increase in *A* with increasing light intensity before saturating and plateauing at intensities between 500 µmol m^{-2} s^{-1} and 800 µmol m^{-2} s^{-1}.

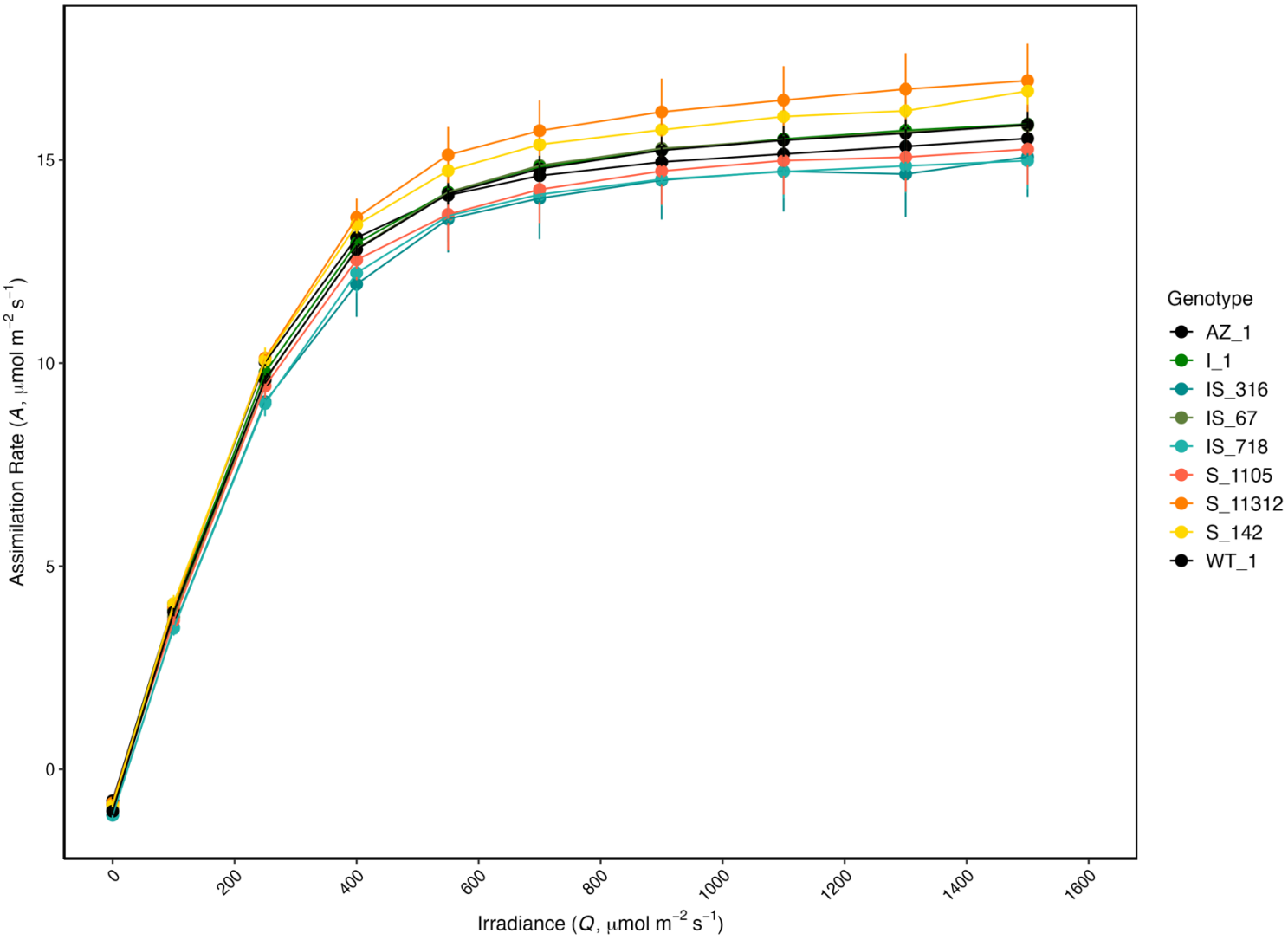

Figure 4.18. Photosynthetic response to increasing light intensity of T2 transgenic tobacco. *CO_2 assimilation rate (A) of transgenic tobacco lines under a range of PPFD irradiance intensities from 0 to 1500 µmol m^{-2} s^{-1}. Dots represent the mean values ± standard error (n = 4-7). Environmental conditions: 25–30°C day and 20°C night, 60% RH and a 16-h photoperiod of 100-250 µmol photons m^{-2} s^{-1}. Measurements were performed on the youngest fully expanded leaf.*

No significant differences were found between genotypes for light-saturated assimilation rates (A_{sat}), with values 19–22 µmol CO_2 m^{-2} s^{-1}, nor the quantum efficiency of CO_2 assimilation (*QE*), with values between 0.09–0.11 µmol CO_2 $µmol^{-1}$ photons (ANOVA and Tukey HSD, $p > 0.05$). These data suggest that neither STO overexpression nor its combination with ictB provides any benefit to light-saturated or light-limited photosynthetic rates.

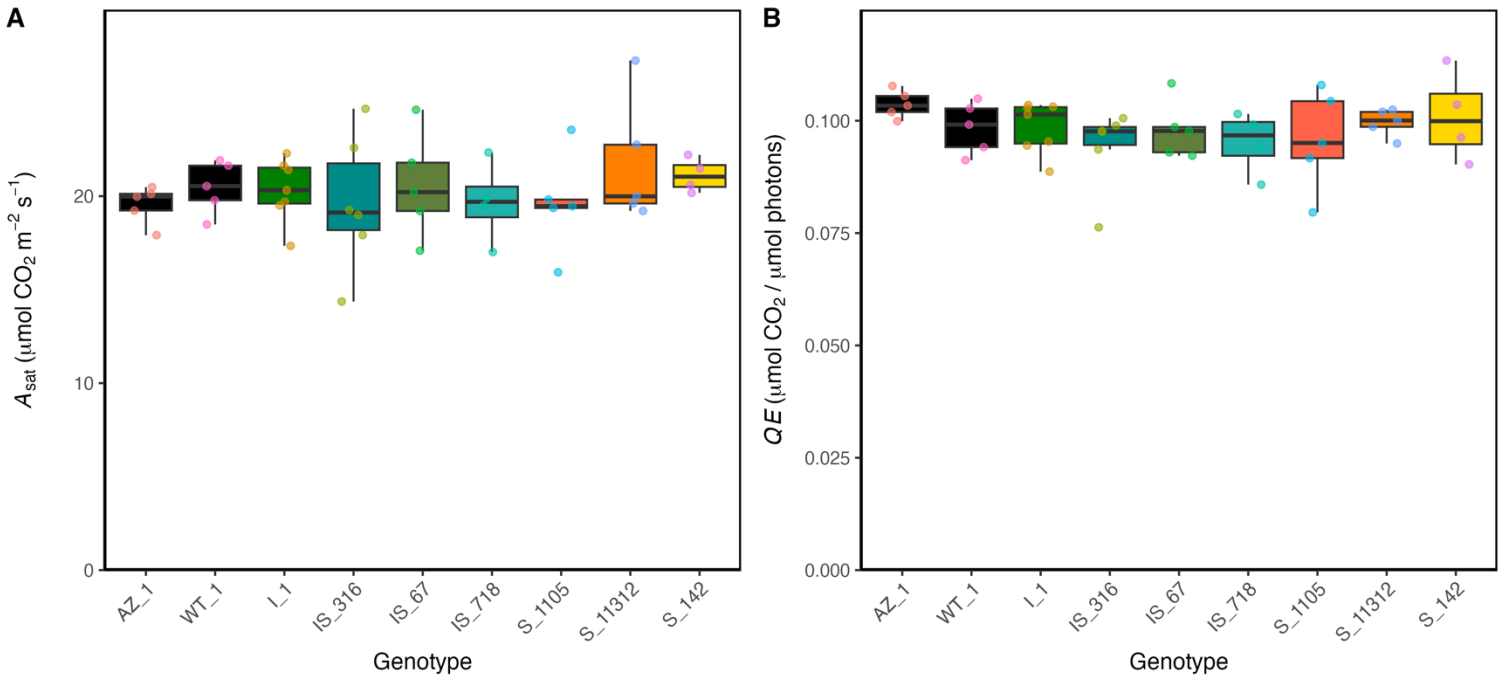

Figure 4.19. Photosynthetic parameters derived from a photosynthetic response to increasing light intensity across T2 transgenic tobacco genotypes. Parameters are derived from the method in Stevens, Jones and Lawson (2021). (A) Light-saturated net CO_2 assimilation (A_{sat}, µmol CO_2 m^{-2} s^{-1}). (B) Quantum efficiency of CO_2 assimilation (QE, µmol CO_2 per µmol photons). For each genotype, boxplots show the median (horizontal line), interquartile range (IQR) (box), and whiskers extending to the most extreme points within 1.5× IQR; points are individual plants/replicates. No significant differences were found between genotypes for A_{sat} or QE (ANOVA and Tukey HSD, $p > 0.05$) (n = 4-7). Environmental conditions: 25–30°C day and 20°C night, 60% RH and a 16-h photoperiod of 100-250 µmol photons m^{-2} s^{-1}. Measurements were performed on the youngest fully expanded leaf.

4.2.8. Stomatal Conductance, Photosynthesis And Intrinsic Water Use Efficiency Dynamics In Response To Dynamic Light

To assess the impact of changes in SD on stomatal function, stomatal responses were assessed following step changes in light intensity. Following a step increase in light intensity (100 to 1000 µmol m^{-2} s^{-2}), all genotypes exhibited a rapid rise in net photosynthesis (*A*) and stomatal conductance (g_{sw}), with values plateauing between 1400-1600 s and 2000-2500 s, respectively (Fig. 4.20). Intrinsic water-use efficiency (iWUE) increased in most genotypes following the step increase in light intensity before declining as g_{sw} increased. The inverse response was seen following a step decrease in light intensity (1000 to 100 µmol m^{-2} s^{-2}), with a rapid decrease, followed by a rise and plateau in *A* and g_{sw}, with values plateauing between 3200-3400 s and 4800-5400 s, respectively. iWUE exhibited a similar decline, then an increase to a plateau.

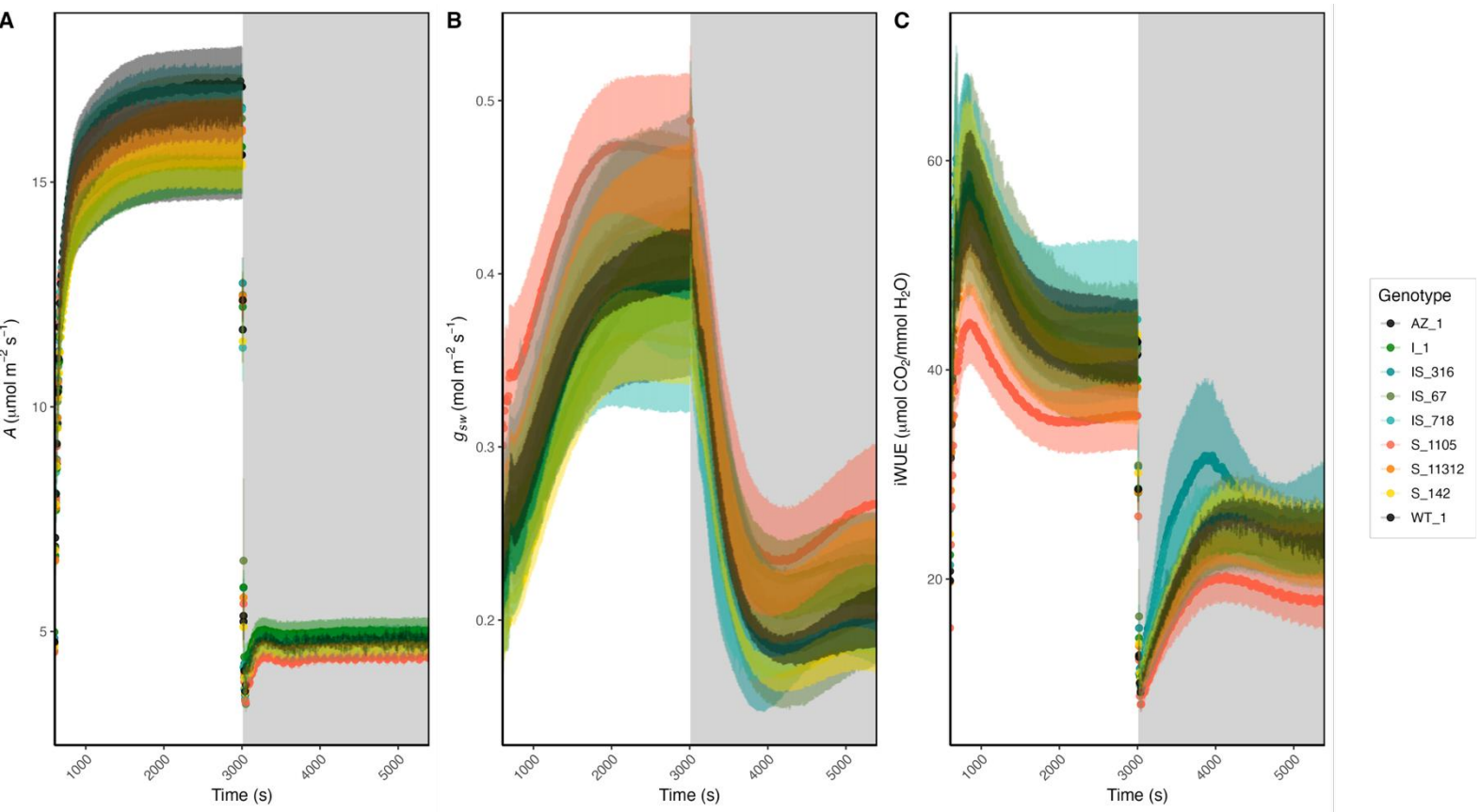

Figure 4.20. Time-course responses of (A) net photosynthesis (A), (B) stomatal conductance to water vapour (g_{sw}), and (C) intrinsic water-use efficiency (iWUE) in T2 transgenic tobacco lines during a step change in light intensity. Light intensity increased from 100 to 1000 µmol m $^{-2}$ s $^{-1}$ at 900 s and returned to 100 µmol m $^{-2}$ s $^{-1}$ at 3000 s, as indicated by the shaded region. Lines represent genotype means; ribbons show ± standard error (n = 3-6). Environmental conditions: 25–30°C day and 20°C night, 60% RH and a 16-h photoperiod of 100-250 µmol photons m^{-2} s^{-1}. Measurements were performed on the youngest fully expanded leaf.

Three distinct time points were chosen to analyse genotypic differences during the step increase and decrease in light intensity: steady-state pre-induction (100 µmol m^{-2} s^{-1}, 600 s), High-Low transition (1000 µmol m^{-2} s^{-1}, 3000 s) and steady-state post-induction (100 µmol m^{-2} s^{-1}, 5400 s). Across all time points, no significant genotype effects were detected for *A*, g_{sw} or iWUE (Kruskal-Wallis/ANOVA; all $p > 0.05$). A lack of genotypic difference in stomatal kinetic responses suggests that neither

overexpression of STO nor ictB conferred any changes in stomatal regulation, stomatal conductance or photosynthetic performance under fluctuating light.

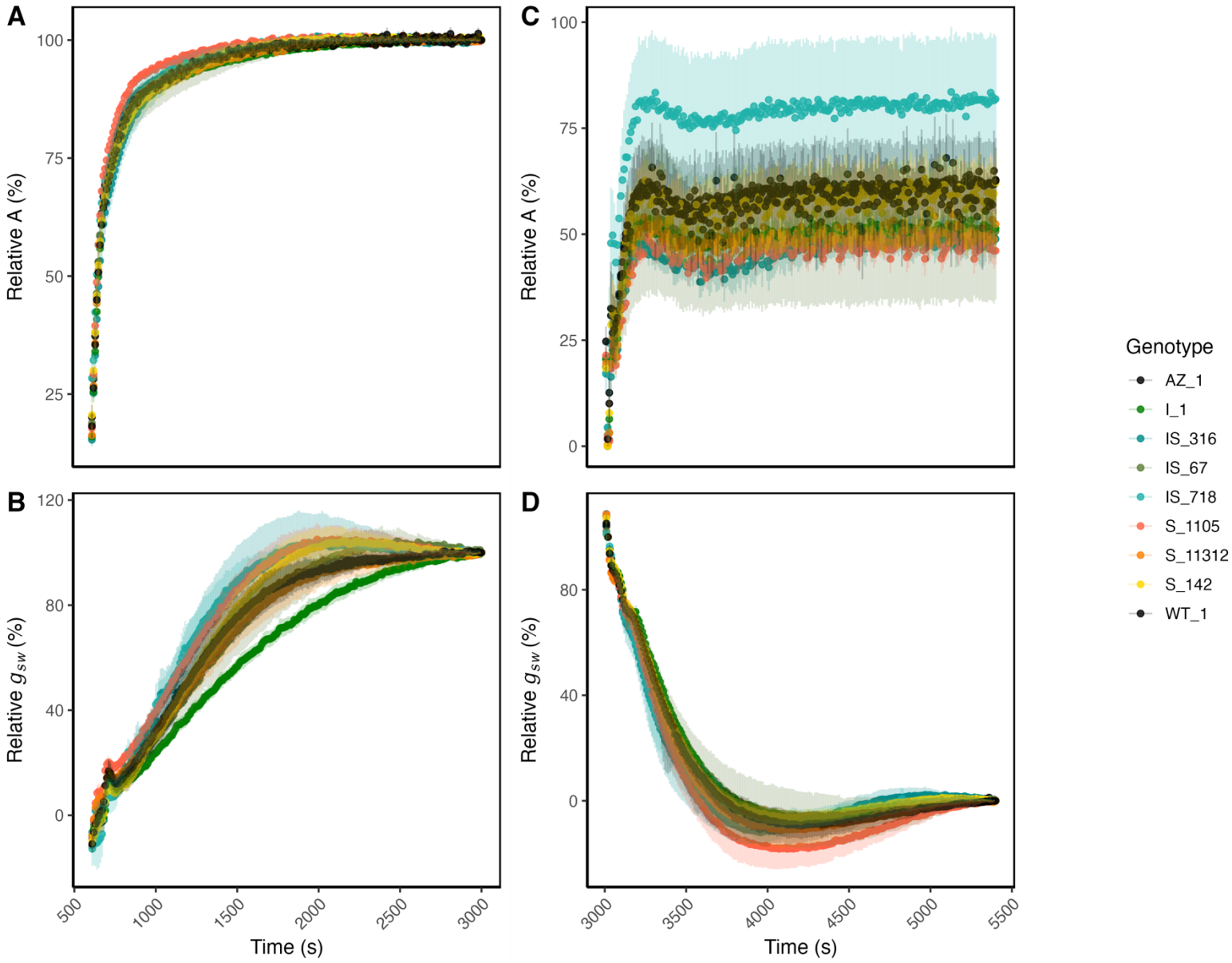

Figure 4.21. Relative CO_2 assimilation (A, %) and stomatal conductance (g_{sw}, %) response to a step change in light intensity over time in different T2 tobacco genotypes. The x-axis represents time (seconds), and the y-axis represents relative A and g_{sw} (%), normalised to initial values. The left panels show the response of A (A) and g_{sw} (B) to a step-increase in light intensity, where light intensity increased at Time = 600 s, while the right panel show the response of A (C) and g_{sw} (D) to a step-decrease in light intensity, where light intensity decreased at Time = 2400 s. Each coloured line represents the mean response for a specific genotype, with shaded areas indicating standard error (SE) (n = 3-6). Environmental conditions: 25–30°C day and 20°C night, 60% RH and a 16-h photoperiod of 100-250 µmol photons m^{-2} s^{-1}. Measurements were performed on the youngest fully expanded leaf.

To quantify genotypic differences in stomatal dynamics, the sigmoidal model proposed by Vialet-Chabrand et al. (2017) was fitted to g_{sw} data following light transitions (Vialet-Chabrand *et al.*, 2017). This model characterises the temporal response of stomatal conductance using biologically meaningful parameters (*k, l*, G_{max}, G_{min}). The two key kinetic parameters: *k*, which describes the time constant (the rate at which g_{sw} changes), and *l*, which denotes the inflection point, the time at which the rate of change is maximal, allow direct comparison of response speed and amplitude between genotypes. Together, these parameters characterise both the speed and timing of stomatal responses during light transitions, and were compared across genotypes to assess differences in dynamic behaviour.

All lines displayed significantly faster stomatal kinetics (lower *K* values) and lower lag time (*l*) when responding to a step decrease in light intensity compared to a step increase in light intensity (Two Sample t-test, $p < 0.05$), except the double overexpressing line IS_67. No differences in stomatal kinetics or lag times were observed between the transgenics and the controls (ANOVA, Tukey HSD, $p > 0.05$). These data would suggest that the overexpression of STO yielded no effect on stomatal responses to dramatic changes in light intensity.

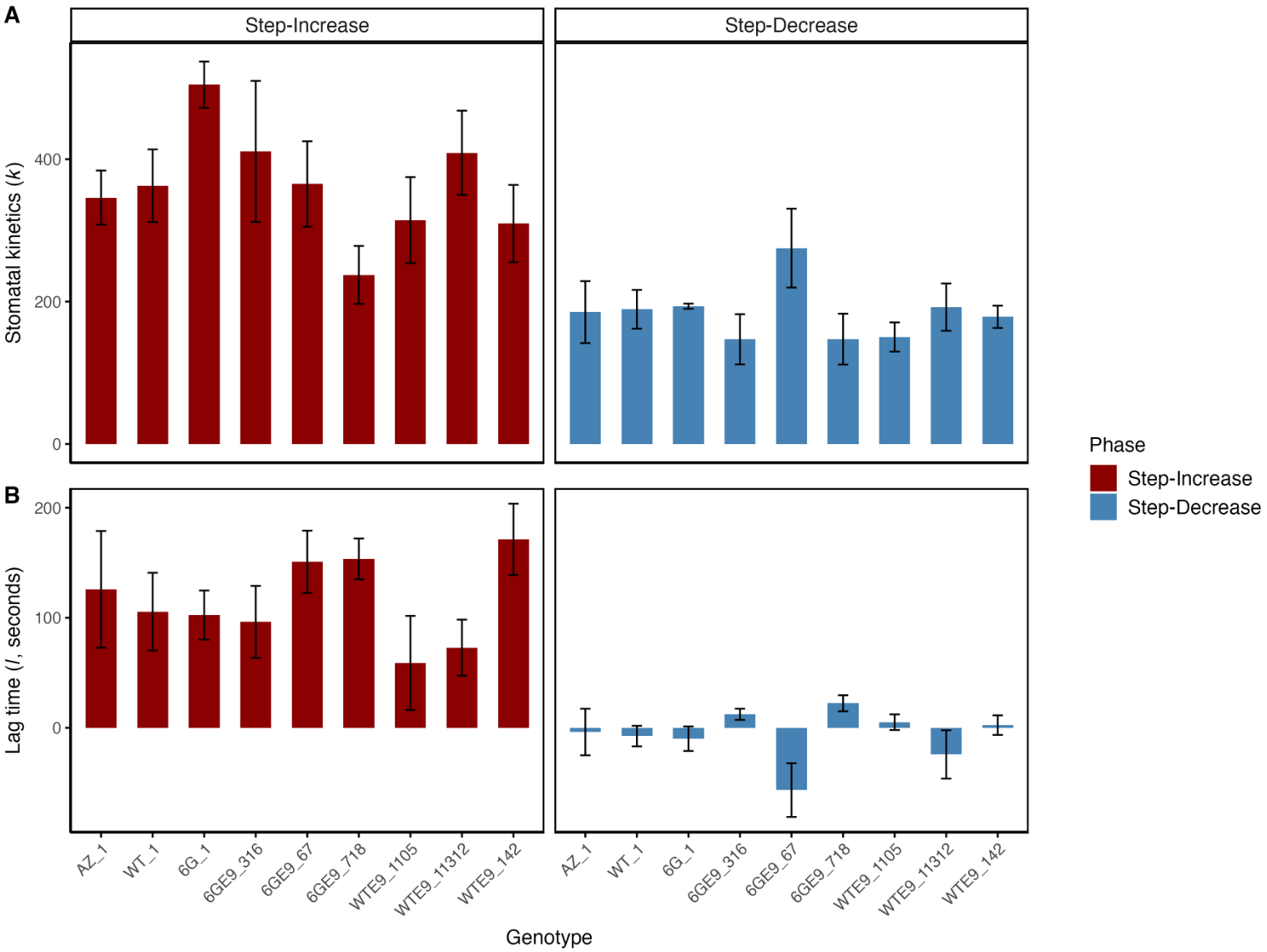

Figure 4.22. Stomatal response kinetics across genotypes during light step transitions. (A) Stomatal kinetics parameter (k) and (B) lag time (l) for transgenic tobacco genotypes during a step-increase and step-decrease in light intensity. Bars represent genotype means (± standard error) for each phase, with red bars indicating responses during light induction (Step-increase) and blue bars during light reduction (Step-Decrease). Stomatal kinetics (k) reflects the rate of g_{sw} response to a light step change, while lag time (l) represents the temporal delay before the onset of response. No significant differences in k or l were found between genotypes (ANOVA, Tukey HSD, $p > 0.05$) (n = 3-6). Environmental conditions: 25–30°C day and 20°C night, 60% RH and a 16-h photoperiod of 100-250 µmol photons m^{-2} s^{-1}. Measurements were performed on the youngest fully expanded leaf.

4.2.9. Transgene Effect On Plant Growth

To assess the impact of transgene expression on plant growth and productivity, a harvest analysis was performed. No significant differences were observed between control genotypes (AZ and WT) and transgenic lines in fresh weight, leaf area, dry weight, or the leaf area-to-fresh weight ratio (ANOVA, Tukey HSD, $p > 0.05$). However, some genotypic differences were detected among the transgenic lines: S_11312 exhibited a significantly larger leaf area than IS_718 (ANOVA, Tukey HSD, $p = 0.049$), and differences in leaf area-to-fresh weight ratio were observed between the ictB::STO lines, with IS_316 having a higher leaf area-to-fresh weight ratio than IS_718 (Kruskal Wallis, Dunn Test, $p = 0.0011$).

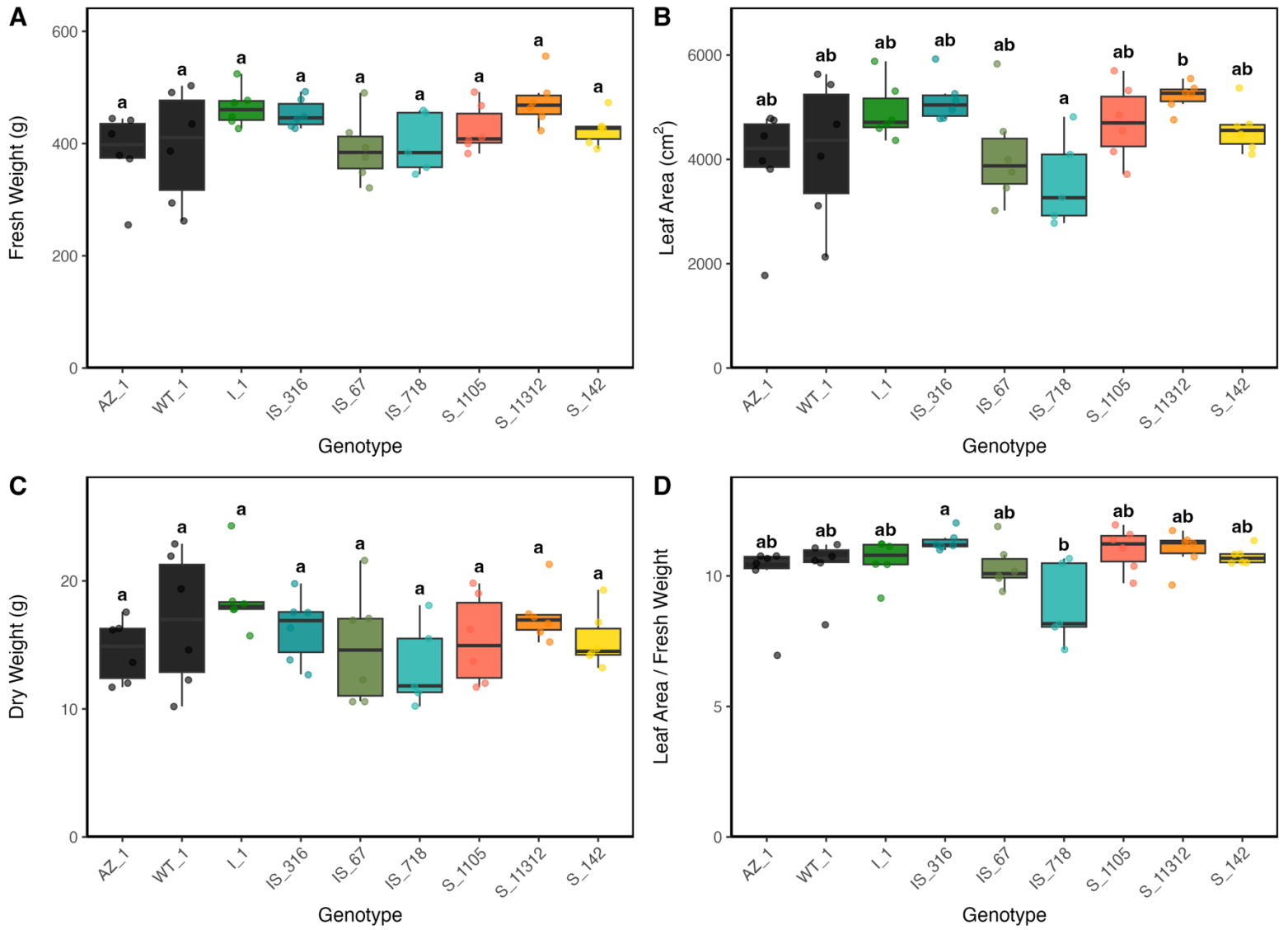

Figure 4.23. Comparison of destructive harvest data among T2 transgenic tobacco lines. (A) Fresh weight, (B) Leaf area and (D) Leaf Area to Fresh Weight ratio measurements were taken during destructive harvest. (C) Dry Weight was collected from oven-dried samples. Boxplots display the median (horizontal line), interquartile range (box), and whiskers extending to 1.5 × the interquartile range, with individual biological replicates shown as jitter points. Compact letter display (CLD) annotations above each box indicate statistical groupings based on ANOVA, Tukey's HSD test ($p < 0.05$)or Kruskal-Wallis, Dunn test ($p < 0.05$) ($n = 6$); genotypes sharing the same letter are not significantly different from one another. Environmental conditions: 25–30°C day and 20°C night, 60% RH and a 16-h photoperiod of 100-250 µmol photons m^{-2} s^{-1}.

4.3. Discussion

Improving photosynthetic efficiency remains a key target in efforts to enhance crop productivity. Stomatal diffusional limitations are widely recognised as key constraints on photosynthesis. For example, under fluctuating light, slow stomatal opening often exerts the greatest restriction on carbon assimilation, while mesophyll diffusion plays a secondary role (McAusland *et al.*, 2016c; Sakoda *et al.*, 2021). Similarly, studies in tree species have shown that both g_{sw} and g_m become limiting under environmental stress (Grassi and Magnani, 2005; Aranda *et al.*, 2012). In this study, the potential of two transgenes: *ictB*, previously associated with enhanced photosynthetic capacity (Simkin *et al.*, 2015), and STO*,* a positive regulator of stomatal development shown to increase CO_2 assimilation by 30% due to greater CO_2 diffusion into the leaf, were explored to determine their capacity to improve photosynthetic performance and growth in *Nicotiana tabacum*. Transgenic lines expressing ictB, STO, or both were evaluated under controlled conditions using gas exchange measurements, stomatal density analysis, and biomass harvest. Lines with strong levels of expression of STO had the greatest increases in SD, with little effect on gas exchange when grown under low light conditions. Overall, neither transgene nor both in combination conferred consistent improvements in photosynthesis, stomatal conductance, or whole-plant growth compared to wild-type and azygous controls.

4.3.1. Effect Of STOMAGEN On Epidermal Patterning And Stomatal Behaviour

The overexpression of 35S::STO in tobacco altered abaxial and adaxial epidermal patterning (Fig. 4.10). STO overexpressing lines (S and IS) had increased SD on both leaf surfaces, with uniform increases in SD to both surfaces maintaining the stomatal ratio, alongside occasional stomatal clustering (<5% of stomata measured). A significant positive correlation between 35S::STO and SD on both abaxial and adaxial surfaces suggests that STO expression is a strong predictor of stomatal density under these experimental conditions.

The increased SD as a result of STO overexpression, however, did not result in differences in stomatal conductance (g_{sw}). The regulation of g_{sw} is a complex trait that integrates both anatomical features, such as stomatal density (SD), and dynamic physiological processes, namely stomatal aperture control. An increased SD theoretically provides a greater number of pores per unit leaf area, thereby increasing the maximum potential for gas diffusion across the epidermis (Franks and Beerling, 2009; Dow, Bergmann and Berry, 2014). Transgenic plants with increased SD have also been shown to have increased g_{sw}, as well as having faster photosynthetic induction following a step increase in light intensity, owing to higher low-light g_{sw} (Tanaka et al., 2013; Sakoda et al., 2020).

Nevertheless, the relationship between SD and g_{sw} is not strictly deterministic. While a higher SD establishes the anatomical potential for increased gas exchange, the realised g_{sw} in any given environment depends strongly on the extent to which individual stomata open. Stomatal aperture can compensate for variations in SD, such

that plants with lower SD achieve comparable g_{sw} to WT counterparts by maintaining wider pore openings (Büssis et al., 2006; Lunn et al., 2024). Conversely, plants with high SD have shown similar ability to maintain g_{sw}. Negative correlations also exist between SD and stomatal size, which have been modelled across multiple species (Hetherington and Woodward, 2003; Wang *et al.*, 2015; Haworth *et al.*, 2018; Yin *et al.*, 2020). This developmental and physiological plasticity highlights the integrated nature of stomatal function, in which both number and aperture jointly contribute to the regulation of leaf conductance.

The consequences of this compensatory relationship are particularly relevant when considering water use efficiency (WUE). A simple increase in SD, while potentially advantageous for maximising carbon gain, also carries the risk of disproportionately elevating transpirational water loss (Drake, Froend and Franks, 2013; Tanaka et al., 2013). However, the observation that higher SD is frequently accompanied by smaller average apertures suggests an adaptive balance, whereby plants avoid a linear trade-off between photosynthetic capacity and water conservation (McElwain, Yiotis and Lawson, 2016). Instead, the interaction between anatomical capacity and aperture regulation ensures that conductance is fine-tuned to environmental conditions. This dual mechanism enables plants to maintain photosynthetic productivity while mitigating excessive water loss, a strategy particularly advantageous under fluctuating light or drought-prone environments. Engineering or breeding plants with higher SD may give plants the potential for higher photosynthetic rates, owing to higher g_{max}, which may thus potentially lead to unrealised benefits to carbon assimilation due to this compensation mechanism. The compensatory dynamics between stomatal number

and aperture must be accounted for to ensure improvements in carbon gain are not offset by deleterious effects on WUE.

Despite the known role of STO as a positive regulator of stomatal development, the magnitude of its effect on stomatal density may be attenuated under low light conditions. Light intensity is a well-established environmental regulator of stomatal development, with low irradiance leading to larger epidermal cell size, reduced stomatal index, and ultimately lower stomatal density (Casson and Gray, 2008). Although STO overexpression can elevate stomatal density even under shade (Sugano et al., 2009), its effect is superimposed on this environmentally determined baseline, potentially dampening the absolute increase. Native STO expression has been shown to increase under high light but not under low light conditions (Hronková *et al.*, 2015). Moreover, the absence of abiotic stresses such as heat or drought, which are known to suppress stomatal development through hormonal and epigenetic signalling, likely removed conflicting cues that might otherwise override the transgene's effect (Dow, Bergmann and Berry, 2014). As a result, under the low-light, non-stressful conditions used here, STO expression may have altered stomatal patterning less strongly than it would under more dynamic or challenging environments, but the changes in epidermal patterning can be more confidently attributed to the function of the transgene.

4.3.2. Effect Of Transgenes On Photosynthetic Capacity

The chlorophyll-fluorescence measurements demonstrated that the effective quantum yield of photosystem II (YII) varied between genotypes. In the T1 generation, plants expressing ictB had greater YII under moderate to high light intensities (500–700

μmol m^{-2} s^{-1} PAR). This finding is novel, as ictB tobacco reported in Simkin et al. (2015) showed no benefit to YII from ictB expression at either 400 or 800 μmol m^{-2} s^{-1} PAR (Simkin *et al.*, 2015). Additionally, when photosynthesis was induced at growth light levels, the combination of ictB and STO produced higher YII. Higher g_{sw}, provided by increased SD, in combination with the unknown role of ictB, may have produced additive benefits resulting in higher YII at growth conditions. In contrast, T2 plants no longer showed benefits to YII from ictB, but also showed a negative relationship between increased SD and YII.

One explanation for the contrasting T1 and T2 results lies in the physiological consequences of increased SD. While high SD enhances the maximum potential stomatal conductance (Franks and Beerling, 2009), this does not always translate into higher realised gas exchange or improved photosynthetic efficiency. When plants are grown under low irradiance, the carbon assimilation capacity is limited. Under these conditions, increased SD may elevate the metabolic cost of maintaining additional stomata and lead to smaller average apertures, constraining CO_2 diffusion to the mesophyll (Drake, Froend and Franks, 2013; Tanaka et al., 2013). Consequently, higher SD can reduce YII by increasing excitation pressure on PSII, particularly when downstream carbon metabolism cannot match the electron transport capacity (Lawson and Blatt, 2014). The negative association between SD and YII observed in T2 plants may therefore reflect a trade-off between anatomical capacity for diffusion and the biochemical and energetic limitations imposed by low-light acclimation.

A second factor is methodological. Simkin et al. (2015) measured chlorophyll fluorescence only at the respective growth irradiances (400 and 800 μmol m^{-2} s^{-1} PAR). By contrast, the use of a full fluorescence light-response curve in this study revealed

ictB-associated improvements at intermediate irradiances (500–700), which were not previously tested. This suggests that ictB benefits may be most pronounced under partially light-saturating conditions, where PSII efficiency is particularly sensitive to improvements in CO_2 availability. The discrepancy between studies, therefore, reflects differences in measurement design, with the present approach uncovering functional effects that earlier discrete sampling overlooked.

The most important factor, however, was the loss of ictB expression in T2, consistent with transgene silencing. The absence of transcripts in the homozygous ictB background (line 6G) and negligible expression of ictB and STO in the double line (IS_718) indicate that gene silencing, rather than segregation, underlies the observed phenotypes. Although homozygous transgenic lines are generally considered stable from the T2 generation onwards (Kohli *et al.*, 2006; Choi *et al.*, 2009; Tizaoui and Kchouk, 2012; Prohens *et al.*, 2022), silencing of transgenes in *Nicotiana tabacum* has been reported in multiple instances (Elmayan and Vaucheret, 1996; Thierry and Vaucheret, 1996; Velten *et al.*, 2012). Both transcriptional gene silencing, via DNA methylation, and post-transcriptional silencing, via small RNA pathways, can persist across generations, and the likelihood of silencing increases with higher copy number, greater expression, and the use of repetitive regulatory sequences such as the CaMV 35S promoter (Elmayan and Vaucheret, 1996; Thierry and Vaucheret, 1996; Kohli *et al.*, 2006). The retransformation of the stable T2 ictB line (6G) with 35S::STO introduced additional 35S-driven elements, which may have triggered homology-dependent silencing across both constructs in IS_718. Thus, the loss of ictB benefits to YII in T2 is best explained by silencing events that occurred between the T3 and T4 generations.

These findings underscore three key points. First, while increased SD can in principle support higher CO_2 uptake, under low-light acclimation, it may reduce YII due to energetic and diffusional trade-offs. Second, the detection of ictB benefits depends on the methodological resolution of fluorescence measurements, with intermediate irradiances providing insight into conditions where CO_2 diffusion constrains PSII efficiency. Third, the stability of transgene expression remains a major obstacle to long-term evaluation of stacked traits. The use of highly repetitive viral promoters such as CaMV 35S may be effective in short-term physiological studies, but is less suitable for multigenerational analyses. Future work should therefore employ strong endogenous promoters or synthetic alternatives to ensure stable expression across generations and to allow reliable interpretation of engineered trait combinations.

4.3.3. The Effect Of The Transgenes On Photosynthetic Gas Exchange

Transgenic expression of ictB and STO have been shown to positively impact photosynthetic rates (Lieman-Hurwitz et al., 2003; Tanaka et al., 2013; Yu Gong et al., 2015; Hay et al., 2017; Sakoda et al., 2020; Koester et al., 2021). Gas exchange analysis revealed no significant differences between genotypes for A/C_i parameters (A_{max}, Vc_{max}, J_{max}) or A/Q parameters (A_{sat}, QE). The absence of any ictB-associated enhancement in photosynthetic parameters contrasts with previous findings in tobacco (Simkin *et al.*, 2015), where expression of ictB was associated with increased A_{max}, Vc_{max}, and J_{max} when plants were grown under higher irradiance. STO has previously shown photosynthetic benefits at high light intensities at atmospheric [CO_2], which was not replicated in this study (Tanaka et al., 2013). STO has also not shown photosynthetic

benefits under elevated [CO_2], as diffusional limitations are largely alleviated at higher CO_2 concentrations, thus no benefit is derived from higher SD (Tanaka et al., 2013).

The lack of transgenic benefit to photosynthesis in the present study can be explained by several factors. First, all plants were grown under low irradiance, which strongly constrains the acclimation of the photosynthetic apparatus. Under such shaded conditions, plants typically exhibit reduced Rubisco content, downregulated electron transport capacity, and lower maximum rates of carboxylation and electron transport (Boardman, 1977; Walters and Horton, 1994; Evans and Poorter, 2001). Consequently, even if ictB function enhanced the delivery or utilisation of inorganic carbon, the photosynthetic machinery may have lacked the biochemical capacity to exploit this advantage. This interpretation is consistent with the findings of Simkin et al. (2015), where ictB lines showed clear benefits under high light, but, while not tested on its own, under shaded conditions provided no additional benefits to A_{max}, A_{sat}, Vc_{max} *and* J_{max} outside of that provided by SBPase, suggesting that ictB effects are contingent on light regime and the associated photosynthetic acclimation state (Simkin *et al.*, 2015). Importantly, field-based evidence aligns with our findings. Ruiz-Vera et al. (2022) conducted a comprehensive field experiment evaluating ictB tobacco transformants for photosynthetic efficiency and biomass (Ruiz-Vera *et al.*, 2022). They observed no significant improvements in Vc_{max}, J_{max}, PSII quantum yield, mesophyll conductance, or biomass relative to wild type. This reinforces the notion that ictB benefits are highly conditional, likely limited to controlled environments where both light and biochemical resources support enhanced carbon assimilation processes.

A second explanation lies in ictB gene expression stability. As previously discussed, evidence of reduced or absent ictB transcript accumulation in several T2 lines suggests that transgene silencing may have compromised function. The absence of enhanced *A/Ci* parameters in these lines therefore reflects not only low-light acclimation but also the possibility that ictB was not expressed at sufficient levels to influence carbon assimilation.

In the case of STO lines, there was no expectation that photosynthetic capacity would be influenced as stomata play a role limiting realised through diffusional constraints and not the biochemical capacity for photosynthesis, which is what *A*/*Ci* analysis assesses. (Tanaka et al., 2013). However, stomatal modifications may play a role during the *AQ* response, where photosynthesis is CO_2-limited. In principle, higher SD could enhance CO_2 diffusion into the leaf, leading to greater assimilation at sub-saturating external CO_2 (Lawson and Weyers, 1999; Woodward, Lake and Quick, 2002; Tanaka et al., 2013; Sakoda et al., 2020). Yet, in the present study, no significant advantage was observed. This likely reflects the same low-light acclimation constraints: the reduced biochemical demand for CO_2 in shaded plants means that even if higher stomatal conductance increased internal CO_2 availability, assimilation was capped by the limited activity of Rubisco and electron transport capacity.

Taken together, these findings emphasise that both ictB and STO-associated modifications are strongly context-dependent. Under high light, ictB has previously been shown to increase photosynthetic capacity by enhancing Vc_{max} and J_{max}, but under low-light acclimation, such as in this study, the downregulation of photosynthetic machinery appears to mask any potential benefits. Similarly, increased SD through STO

does not translate into improved photosynthesis when CO_2 diffusion is not limiting relative to biochemical demand. These results underscore the importance of considering growth irradiance and acclimation state when evaluating the functional impact of photosynthetic transgenes.

Together, these results highlight the importance of environmental context when aiming to genetically enhance photosynthesis. Under low-light growth, biochemical acclimation downregulated Rubisco and electron transport capacity, constraining the ability of plants to utilise additional CO_2 made available through either enhanced diffusion (STO) or putative transport (ictB). Moreover, evidence of transgene silencing in later generations further diminished the potential for ictB to enhance photosynthesis. These findings, together with the lack of ictB-associated improvements in field trials (Ruiz-Vera et al., 2022), emphasise that both anatomical and metabolic modifications are highly context-dependent, with their benefits only realised when the photosynthetic machinery is sufficiently expressed to exploit them.

4.3.4. Potential influence of selection regime on transgenic performance

It is also important to consider the potential impact of the selection regime on the growth and performance of the transgenic lines used in this study. All STO tobacco lines (S and IS) were selected at germination using a herbicide resistance marker, meaning that seedlings were exposed to herbicide during early development. Although herbicide-based selection is standard practice in plant transformation, early exposure to herbicides has been shown to impose physiological stress, affecting seedling establishment, growth rate and subsequent biomass accumulation (Orcaray *et al.*,

2012; Black, 2018; Hess, 2018). Such stress responses can persist beyond the initial selection phase and influence carbon allocation, photosynthetic capacity and overall plant vigour (Rutherford and Krieger-Liszkay, 2001; Takayama *et al.*, 2003; Black, 2018).

These effects are particularly relevant for traits such as enhanced carbon assimilation or stomatal function, where expected gains are often modest and highly sensitive to early developmental conditions. Consequently, the absence of strong growth or photosynthetic phenotypes in the ictB and STO tobacco lines may reflect, at least in part, constraints imposed by the selection process rather than a lack of functional impact of the transgenes themselves.

5. Manipulating Guard cell behaviour to optimise gas exchange in Tobacco

5.1. Introduction

Stomata, formed by a pair of guard cells surrounding a central pore, regulate the exchange of CO_2 and water vapour between the leaf mesophyll and the atmosphere (Hetherington and Woodward, 2003; Kirkham, 2005). While mesophyll photosynthetic responses to changing irradiance can occur within seconds, stomatal adjustments are comparatively sluggish**,** often lagging by several minutes (Lawson and Blatt, 2014; McAusland et al., 2016). This temporal mismatch under fluctuating light has two major negative consequences: first, a loss of carbon gain during light increases, when mesophyll demand for CO_2 rises rapidly but stomatal conductance cannot keep pace; and second, excess water loss during light decreases, as stomata remain open after mesophyll demand has already declined (McAusland et al., 2016; Lawson and Vialet-Chabrand, 2019). Improving the speed and sensitivity of stomatal responses is therefore a promising target for engineering crops with enhanced photosynthetic efficiency and water-use efficiency (Lawson and Matthews, 2020). Guard cell movements are controlled by dynamic solute fluxes and are tightly regulated by their sensitivity to environmental and hormonal signals, including CO_2, light, and abscisic acid (Heath, 1938; Fujino, 1967; Weyers, 1990; Willmer and Fricker, 1996; Blatt, 2000; Outlaw, 2010; Chen *et al.*, 2012; Hills *et al.*, 2012). Advances in molecular tools, particularly the use of guard cell-specific promoters, such as the *Solanum tuberosum* KST1 partial promoter, now allow the targeted manipulation of transporters, signalling

enzymes, and regulatory factors that control both the mechanics of stomatal movement and their responsiveness to signals (Müller-Röber *et al.*, 1995; Zimmerli *et al.*, 2012; Kelly *et al.*, 2013, 2019; Lu *et al.*, 2013; Tsuzuki *et al.*, 2013; Wang *et al.*, 2013; Lugassi *et al.*, 2015, 2019; Daloso *et al.*, 2016; Antunes *et al.*, 2017; Gilor Kelly *et al.*, 2017; Na and Metzger, 2017; Riu *et al.*, 2021; Acevedo-Siaca *et al.*, 2022; Huang *et al.*, 2023). Such strategies hold promise for creating plants with faster and more finely tuned stomatal kinetics, enabling greater CO_2 uptake under dynamic light while minimising unnecessary water loss, thereby optimising gas exchange in future crop systems.

Plasma membrane H^+-ATPases are a family of P-type proton pumps that extrude protons from the cytosol, generating the electrochemical proton gradient that drives guard cell turgor and stomatal opening (Assmann and Jegla, 2016; Jezek and Blatt, 2017). In leaves, the isoforms AHA1 and AHA2 provide the majority of proton-pumping capacity in the epidermis (Haruta *et al.*, 2010; Wang *et al.*, 2013; Haruta, Gray and Sussman, 2015; Falhof *et al.*, 2016). Their activity is strongly regulated by light, particularly blue light, which induces phosphorylation of a conserved penultimate threonine and subsequent binding of 14-3-3 proteins, stabilising the pump in its active conformation (Kinoshita and Shimazaki, 1999; Ueno et al., 2005). Proton extrusion hyperpolarises the guard cell plasma membrane, providing the driving force for K^+ influx through inward-rectifying channels, anion uptake, and the accumulation of organic osmolytes (Schroeder *et al.*, 2001). These osmotic changes promote water entry and guard cell swelling, thereby enabling stomatal opening (Lawson and Blatt, 2014). Guard-cell-specific overexpression of AHA2 in Arabidopsis resulted in enhanced light-induced stomatal opening, higher stomatal conductance, and increased rates of CO_2

assimilation and biomass production, while retaining sensitivity to ABA-induced closure (Wang *et al.*, 2013). These findings demonstrated that stimulating guard cell H^+-ATPase activity can accelerate the kinetics of stomatal opening, improving photosynthetic performance without compromising the ability of stomata to respond to drought signals.

Hexokinase (HXK) is a conserved enzyme of primary metabolism that catalyses the phosphorylation of hexose sugars, such as glucose and fructose, to their corresponding hexose-6-phosphates, thereby committing them to glycolysis and other central metabolic pathways (Rolland, Baena-González & Sheen, 2006). In addition to this catalytic role, plant HXKs also function as sugar sensors, integrating carbohydrate status with developmental and stress-response signalling. In guard cells, HXK modulates stomatal behaviour by linking elevated sugar levels to the activation of abscisic acid (ABA) signalling pathways, thereby promoting stomatal closure (Kelly *et al.*, 2013; Lugassi *et al.*, 2015). Apoplastic sucrose is metabolised into glucose and fructose, which are phosphorylated by HXK to generate a sugar-derived signal that stimulates ABA responses in guard cells, thereby promoting stomatal closure (Kelly *et al.*, 2013). Guard cell-targeted expression of AtHXK1 in Arabidopsis, tomato, tobacco, and citrus consistently reduced stomatal conductance and transpiration without negatively affecting photosynthetic rates, leading to enhanced intrinsic water-use efficiency (Kelly *et al.*, 2013, 2019; Lugassi *et al.*, 2015, 2019; Acevedo-Siaca *et al.*, 2022). These plants also exhibited improved tolerance to drought and salinity, maintaining growth and photosynthesis under water-limited conditions (Lugassi *et al.*, 2019). In perennial citrus, HXK expression reinforced stomatal closure in both leaves and fruit, confirming the conservation of this sugar–ABA regulatory mechanism beyond

annual model species (Lugassi *et al.*, 2015). Together, these studies establish HXK as a robust regulator of guard cell function, enhancing WUE by restricting unnecessary water loss while sustaining carbon gain.

The complementary actions of the H^+-ATPase and HXK suggest that a dual approach may provide synergistic benefits: accelerating stomatal opening to maximise CO_2 uptake under increasing irradiance, while reinforcing closure via HXK–ABA signalling to minimise water loss under declining light or drought. By integrating mechanisms that act on opposing ends of stomatal dynamics, it may be possible to create plants with stomata that have both faster movement kinetics and speed of response, aligning guard cell behaviour more closely with mesophyll demand and thereby optimising photosynthesis and water-use efficiency under fluctuating environmental conditions.

This chapter describes the molecular and physiological characterisation of transgenic tobacco lines overexpressing: 1. Guard cell-targeted plasma membrane H^+-ATPase, 2. Guard cell-targeted Hexokinase, and 3. A combination of both constructs. These lines were generated to determine whether simultaneously enhancing stomatal opening and reinforcing closure could synergistically optimise the balance between CO_2 assimilation and water loss.

5.2. Results

5.2.1. Selection Of T1 Transgenic Lines

5.2.1.1. Copy Number Analysis Of T1 Transgenic Lines

Analysis of transgene copy number for the Kanamycin resistance gene NPII, the positive selection marker during transformation and regeneration, was used as a tool for line selection to find T1 homozygous lines of stomatal kinetics mutants with guard cell specific expression of HXK (H) and HXK plus overexpression of AHA2 (HA) (Figure 5.1), discerning plants that have a copy of a stomatal kinetics transgene and the number of copies each plant holds. Four T0 HXK single lines, H_10, H_7, H_B and H_N, and three HXK::AHA2 double lines, HA_8, HA_9 and HA_12, were selected for further analysis (Fig. 5.1A). The copy number information of the T1 plants (Fig. 5.1B) was used in combination with T1 line selection data (Figs. 5.2-5.6) to select lines of interest for the T2 generation experiments.

Table 5.1 Table of plants used in this chapter. Plants that did not pass the selection process are not included.

Codename	Background	Transgene	Promoter	Terminator	Source	Generation	Copy numbe
AZ_1	Wild Type	N/A	N/A	N/A	This study	T1	0
HA_12	Wild Type	Hexokinase and AHA2	KST1 both	NOS and OCS	This study	T1	1
H_N	Wild Type	Hexokinase	KST1	NOS	This study	T1	1
HA_8	Wild Type	Hexokinase and AHA2	KST1 both	NOS and OCS	This study	T1	1
HA_9	Wild Type	Hexokinase and AHA2	KST1 both	NOS and OCS	This study	T1	1
H_10	Wild Type	Hexokinase	KST1	NOS	This study	T1	1
H_B	Wild Type	Hexokinase	KST1	NOS	This study	T1	1
HA_121	HA_12	Hexokinase and AHA2	KST1 both	NOS and OCS	This study	T2	2
A_31	Wild Type	AHA2	KST1	OCS	Fan 2025 (Th	T2	2
H_N4	H_N4	Hexokinase	KST1	NOS	This study	T2	2
HA_83	HA_8	Hexokinase and AHA2	KST1 both	NOS and OCS	This study	T2	2
A_1	Wild Type	AHA2	KST1	OCS	Fan 2025 (Th	T2	2
HA_96	HA_9	Hexokinase and AHA2	KST1 both	NOS and OCS	This study	T2	2
H_108	H_10	Hexokinase	KST1	NOS	This study	T2	2
A_19	Wild Type	AHA2	KST1	OCS	Fan 2025 (Th	T2	2
H_B4	H_B	Hexokinase	KST1	NOS	This study	T2	2

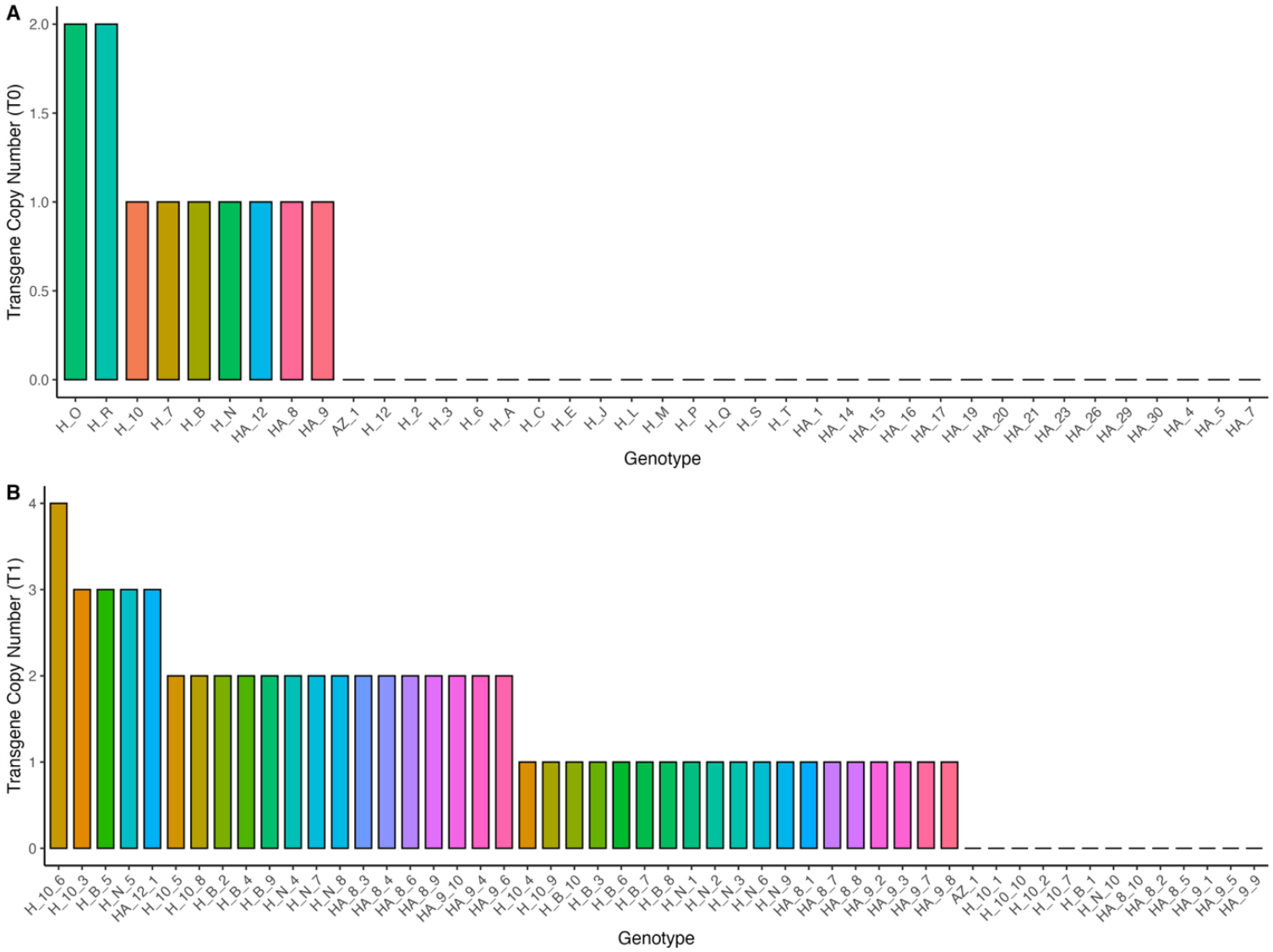

Figure 5.1. Copy number analysis shows the number of copies of the transgene inserted into the genome by Agrobacterium tumefaciens across generations. A) T0 copy number analysis was used to discriminate between false positive plants (0 copies) and select for transformed plants (1 + copies). B) T1 copy number analysis was used to identify homozygous lines to be used in T2 experimentation. Lines that had one copy at T0 and two copies at T2 were assumed homozygous.

Copy number analysis revealed that 7 of the 39 regenerated T0 lines had a single insertion (Fig. 5.1A). These lines were taken forward to the next generation (T1) to select and achieve homozygosity. Of the T1 lines, 15 individuals were identified as

homozygous (Fig. 5.1B), having two copies of NPII, and thus were selected as lines of interest for further experimentation at the T2 generation.

5.2.2. Determining The Photosynthetic Capacity Of T1 Transformants

To assess photosynthetic capacity of the T1 selected lines, plants were evaluated for photosynthesis as a function of changing [CO_2]. Selected plants grouped by genotype all showed a typical A/C_i response curve, with assimilation rate (A) increasing steeply at low intercellular CO_2 concentrations (C_i) before approaching saturation at higher C_i levels (Fig. 5.2).

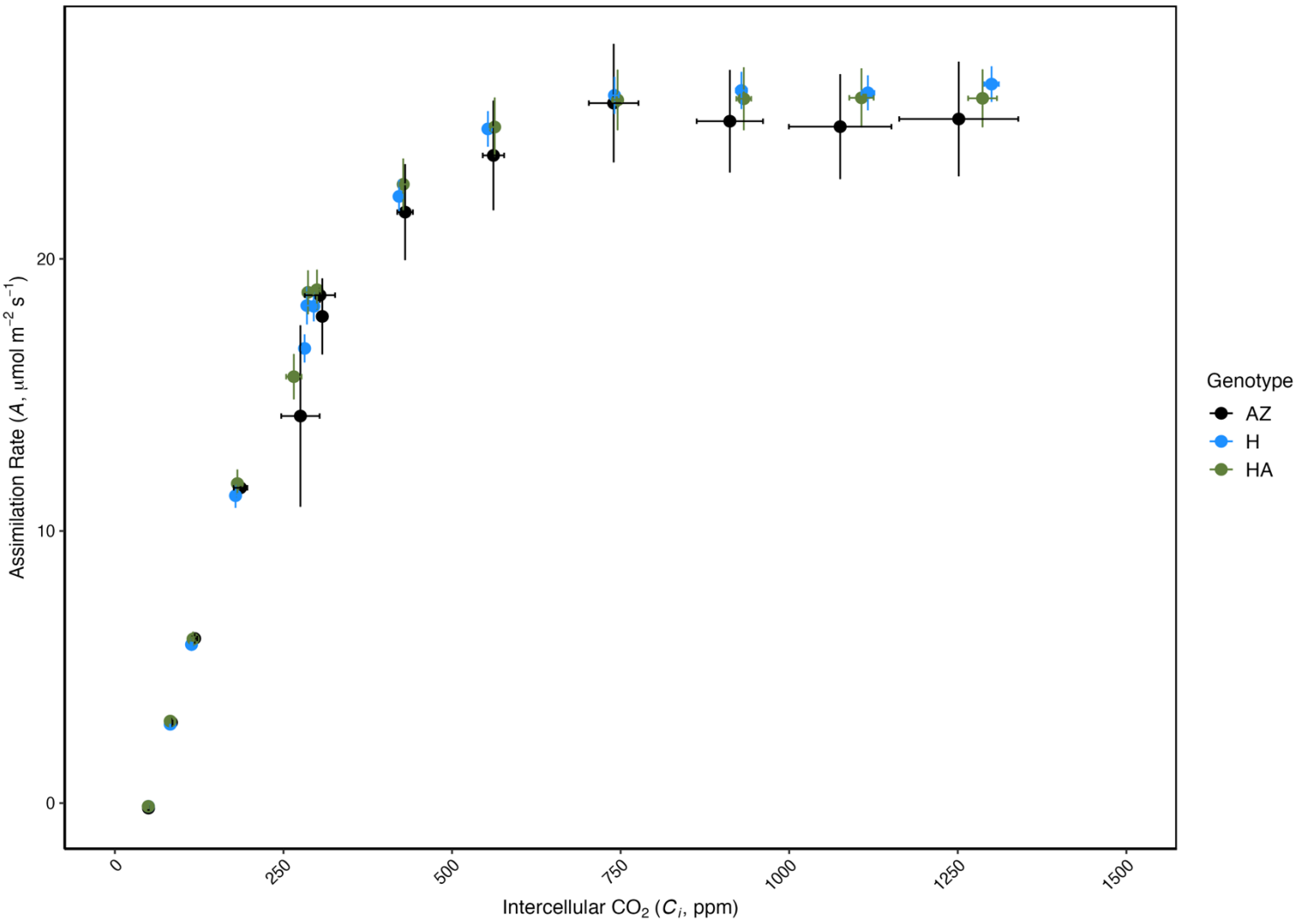

Figure 5.2. Photosynthetic response of T1-segregating transgenic tobacco plants under different intracellular CO2 concentrations (C_i). The net CO_2 assimilation rate (A, µmol m $^{-2}$ s $^{-1}$) is plotted as a function of intercellular CO_2 concentration (C_i, µmol mol $^{-1}$). Each point represents the mean (n = 8 for AZ, 31 for H and 14 for HA) for a given genotype, with the error bars indicating standard error (SE), for A and C_i (vertical and horizontal, respectively). Environmental conditions: 25–30°C day and 20°C night, 60% RH and a 16-h photoperiod of 600-800 µmol photons m^{-2} s^{-1}. Measurements were performed on the youngest fully expanded leaf.

Modelled parameters A_{max}, Vc_{max}, and J_{max} did not differ significantly between genotypes (Fig. 5.3) (ANOVA, Tukey HSD, $p < 0.05$), suggesting that the maximum rate of photosynthesis, maximum rate of carboxylation, or the maximum rate of electron transport were not affected by the function of HXK or HXK in combination with AHA2.

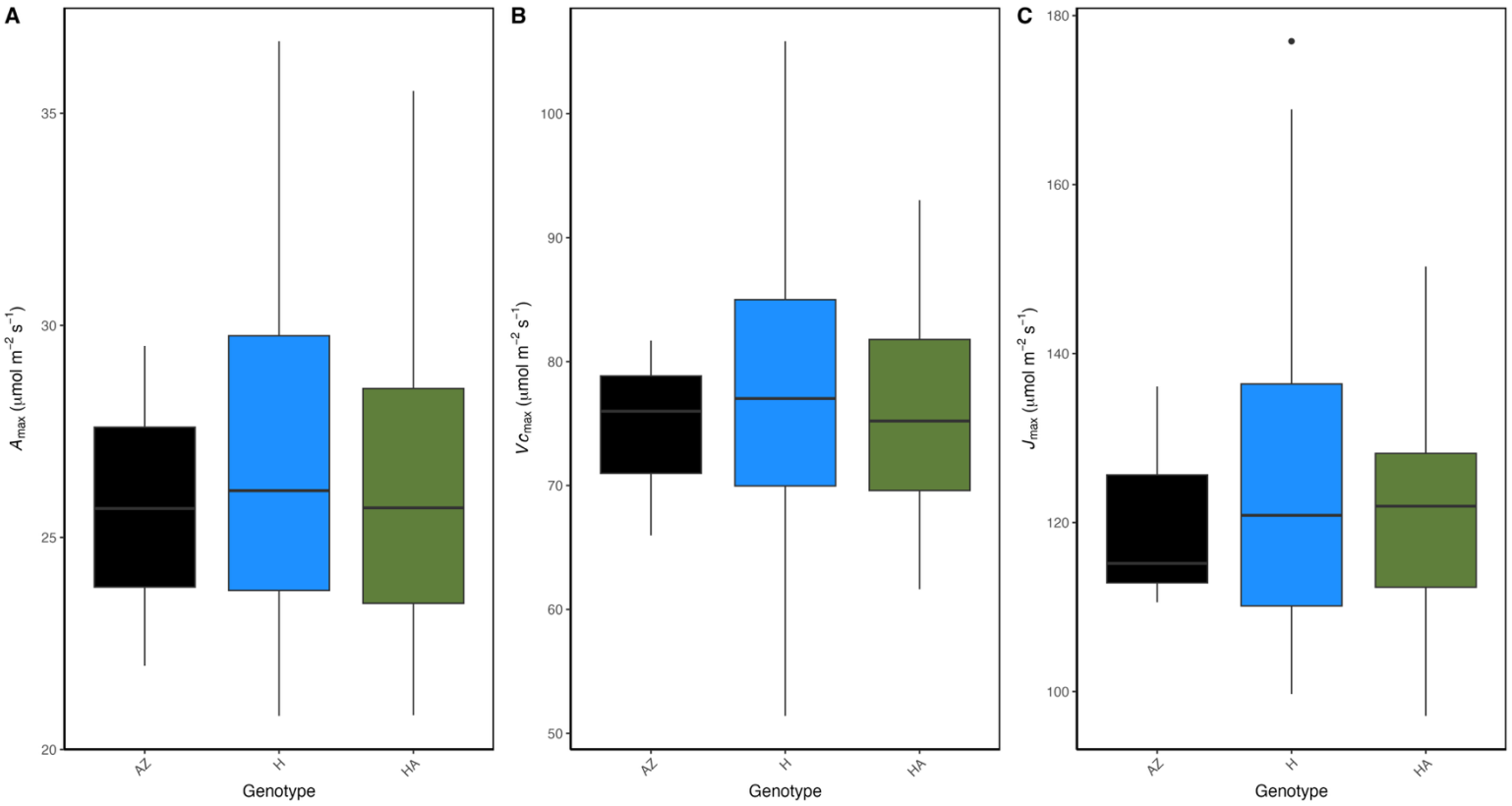

Figure 5.3. Photosynthetic parameters modelled from A/C_i curves across T1 transgenic tobacco genotypes. (A) CO_2 and Light-saturated assimilation rate (A_{max}), (B) maximum Rubisco carboxylation capacity (Vc_{max}) and (C) maximum electron-transport rate (J_{max}). Boxplots display the median (horizontal line), interquartile range (box), and whiskers extending to 1.5x the interquartile range, with black dots marking observations beyond this range (outliers). No significant differences were found between genotypes for A_{max}, Vc_{max}, and J_{max} (ANOVA, Tukey HSD, $p < 0.05$) (n = 8 for AZ, 31 for H and 14 for HA). Environmental conditions: 25–30°C day and 20°C night, 60% RH and a 16-h photoperiod of 600-800 µmol photons m^{-2} s^{-1}. Measurements were performed on the youngest fully expanded leaf.

5.2.3. Stomatal Conductance, Photosynthesis And Intrinsic Water Use Efficiency Dynamics In Response To Dynamic Light Of T1 Transformants

To assess the impact of guard-cell-specific expression of HXK and HXK in combination with AHA2 on stomatal function, stomatal responses were assessed following step changes in light intensity. Following a step increase in light intensity (100 to 1000 µmol m^{-2} s^{-2}), all genotypes exhibited a rapid rise in net photosynthesis (*A*) and stomatal conductance (g_{sw}), with values plateauing between 1400-1600 s and 2000-2500 s, respectively (Fig. 5.4). Intrinsic water-use efficiency (iWUE) increased in most genotypes following the step increase in light intensity before declining as g_{sw} increased. The inverse response was seen following a step decrease in light intensity (1000 to 100 µmol m^{-2} s^{-2}), with a rapid decrease, followed by a rise and plateau in *A* and g_{sw}, with values plateauing between 3200-3400 s and 4800-5400 s, respectively. iWUE exhibited a similar decline, then an increase to a plateau. Clear genotypic differences were seen throughout the step increase and decrease in light intensity, with the HXK single lines

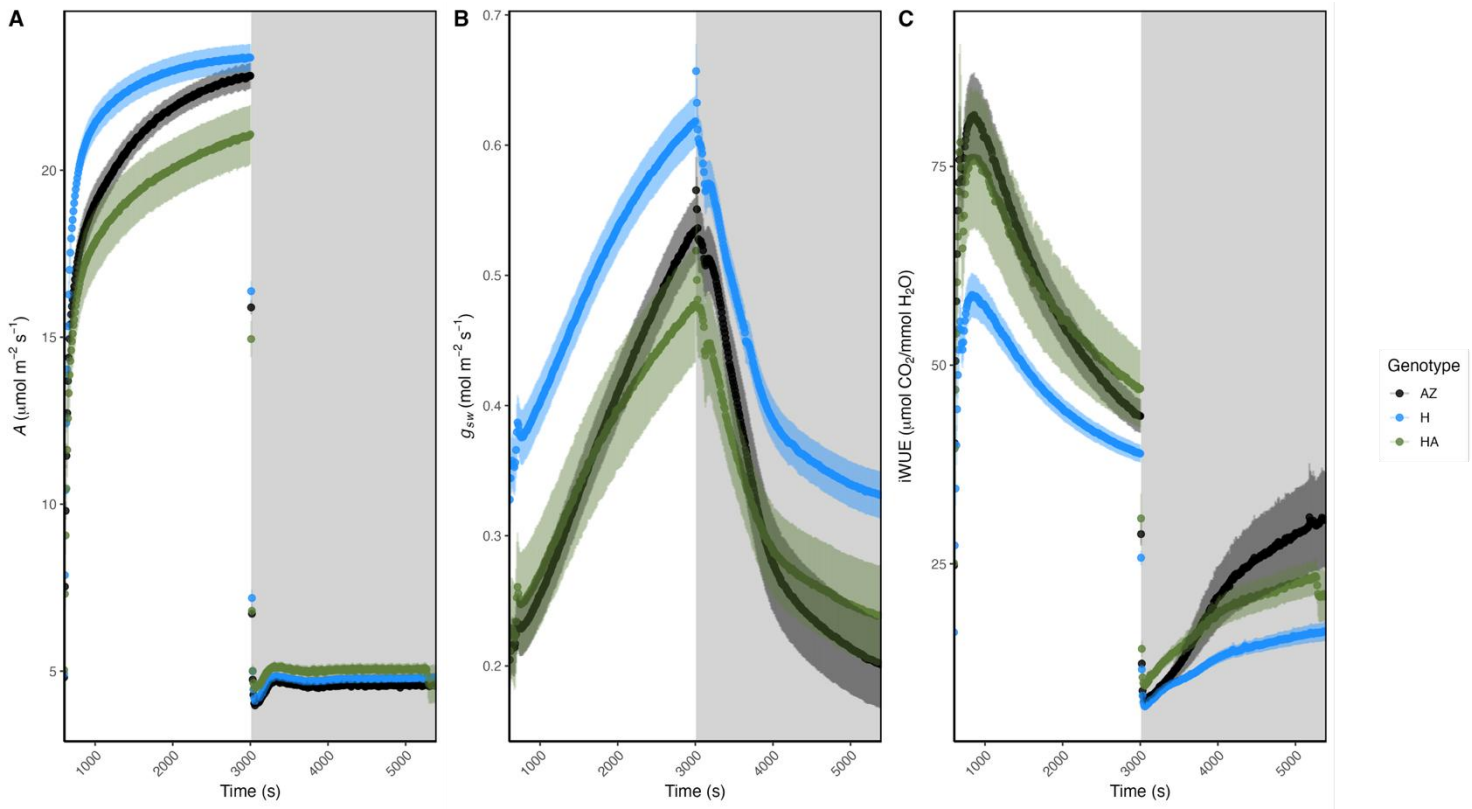

*Figure 5.4. Time-course responses of (A) net photosynthesis (A), (B) stomatal conductance to water vapour (g_{sw}), and (C) intrinsic water-use efficiency (*iWUE*) in T1 tobacco stomatal kinetics mutant lines during step changes in light intensity. Light intensity increased from 100 to 1000 µmol m^{-2} s^{-1} at 600 s and returned to 100 µmol m^{-2} s^{-1} at 3000 s, as indicated by the shaded region. Lines represent genotype means; ribbons show ± standard error (n = 8 for AZ, 31 for H and 14 for HA). Environmental conditions: 25–30°C day and 20°C night, 60% RH and a 16-h photoperiod of 600-800 µmol photons m^{-2} s^{-1}. Measurements were performed on the youngest fully expanded leaf.*

Three distinct time points were chosen to analyse genotypic differences during the step increase and decrease in light intensity: steady-state pre-induction (100 µmol m^{-2} s^{-1}, 600 s), High-Low transition (1000 µmol m^{-2} s^{-1}, 3000 s) and steady-state post-induction (100 µmol m^{-2} s^{-1}, 5400 s). HXK single lines (H) had significantly higher g_{sw} than the azygous control at 600 and 5400 seconds, but no differences in *A* across the step changes in light intensity, resulting in significantly lower iWUE at those time points (ANOVA, Tukey HSD, all $p < 0.05$). These data would suggest that guard-cell-specific

expression of HXK alone and not in combination with AHA2 increased stomatal conductance with no effect on carbon assimilation, reducing intrinsic water use efficiency.

When normalised to the beginning and end values of each respective step change, differences in the induction rates of A and g_{sw} can be visualised (Fig. 5.5). Clear genotypic differences can be seen in relative A during the step increase in light intensity (Fig. 5.5A) and relative g_{sw} across the step increase and decrease in light intensity (Fig. 5.5B and D). During the step increase, HXK lines were significantly faster at reaching 33, 50, 66 and 90% of the relative A compared to the azygous control (Kruskal-Wallis, Dunn Test, all $p < 0.05$). No differences were found between the HXK::AHA2 double lines and the azygous control (Kruskal-Wallis, Dunn Test, all $p > 0.05$).

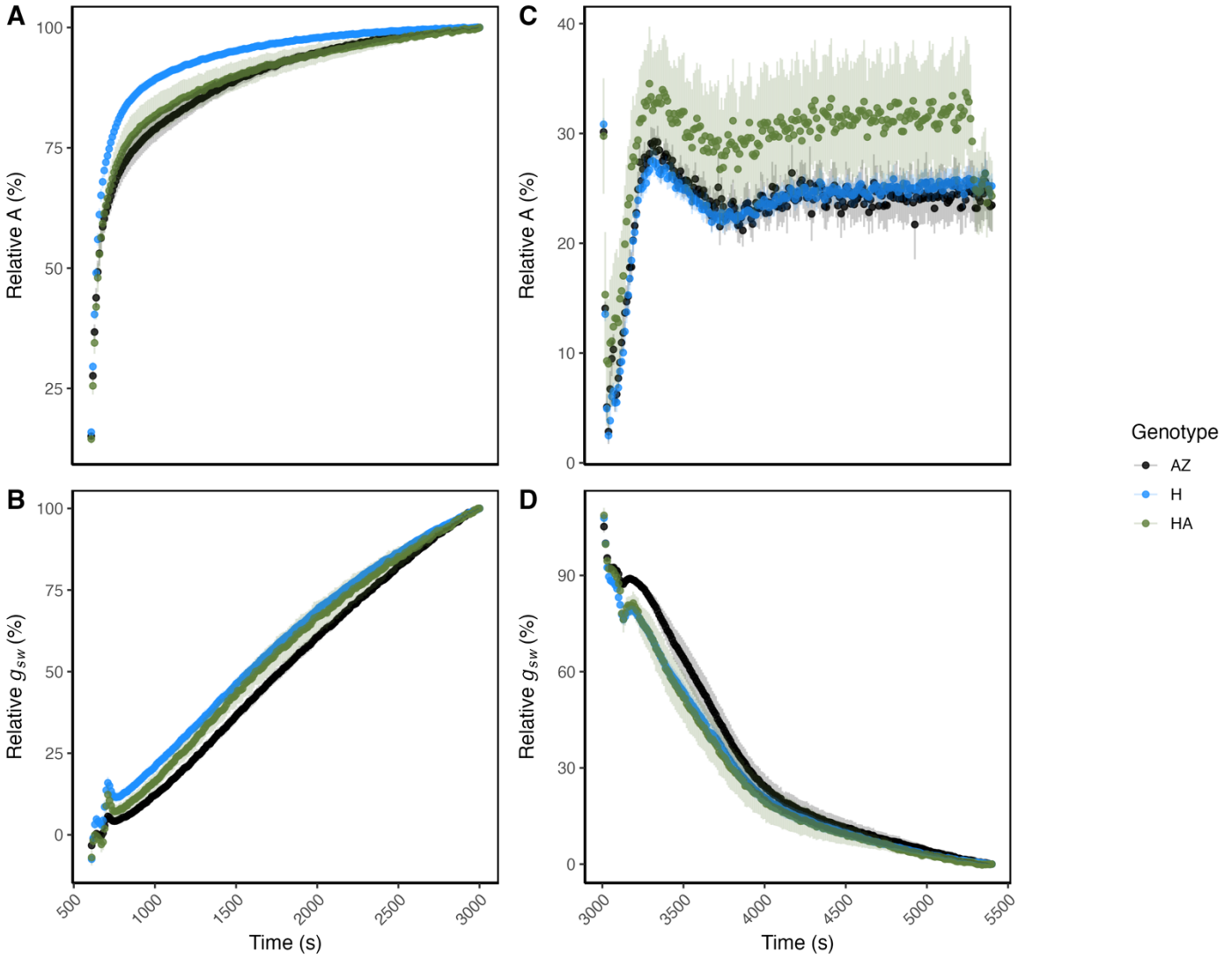

Figure 5.5. Relative CO_2 assimilation (A, %) and stomatal conductance (g_{sw}, %) response to a step change in light intensity over time in T1 tobacco stomatal kinetics mutant genotypes. The x-axis represents time (seconds), and the y-axis represents relative A and g_{sw} (%), normalised to initial values. The left panels show the response of A (A) and g_{sw} (B) to a step-increase in light intensity, where light intensity increased at Time = 600 s, while the right panel show the response of A (C) and g_{sw} (D) to a step-decrease in light intensity, where light intensity decreased at Time = 2400 s. Each coloured line represents the mean response for a specific genotype, with shaded areas indicating standard error (SE) (n = 8 for AZ, 31 for H and 14 for HA). Environmental conditions: 25–30°C day and 20°C night, 60% RH and a 16-h photoperiod of 600-800 µmol photons m^{-2} s^{-1}. Measurements were performed on the youngest fully expanded leaf.

All lines displayed significantly faster stomatal kinetics (lower *K* values) and lower lag time (*l*) when responding to a step decrease in light intensity compared to a step

increase in light intensity (Two Sample t-test, all $p < 0.05$) (Fig. 5.6). HXK single lines had significantly lower stomatal lag times than the azygous for both step increase and step decrease in light intensity (Kruskal-Wallis, Dunn Test, p = 0.003 and 0.024, respectively) (Fig. 5.6C and D). These data would suggest that the overexpression of HXK in the guard cells allows for faster photosynthetic induction through a faster response to changes in light intensity, but the simultaneous expression of HXK with AHA2 removes any advantages provided by HXK alone.

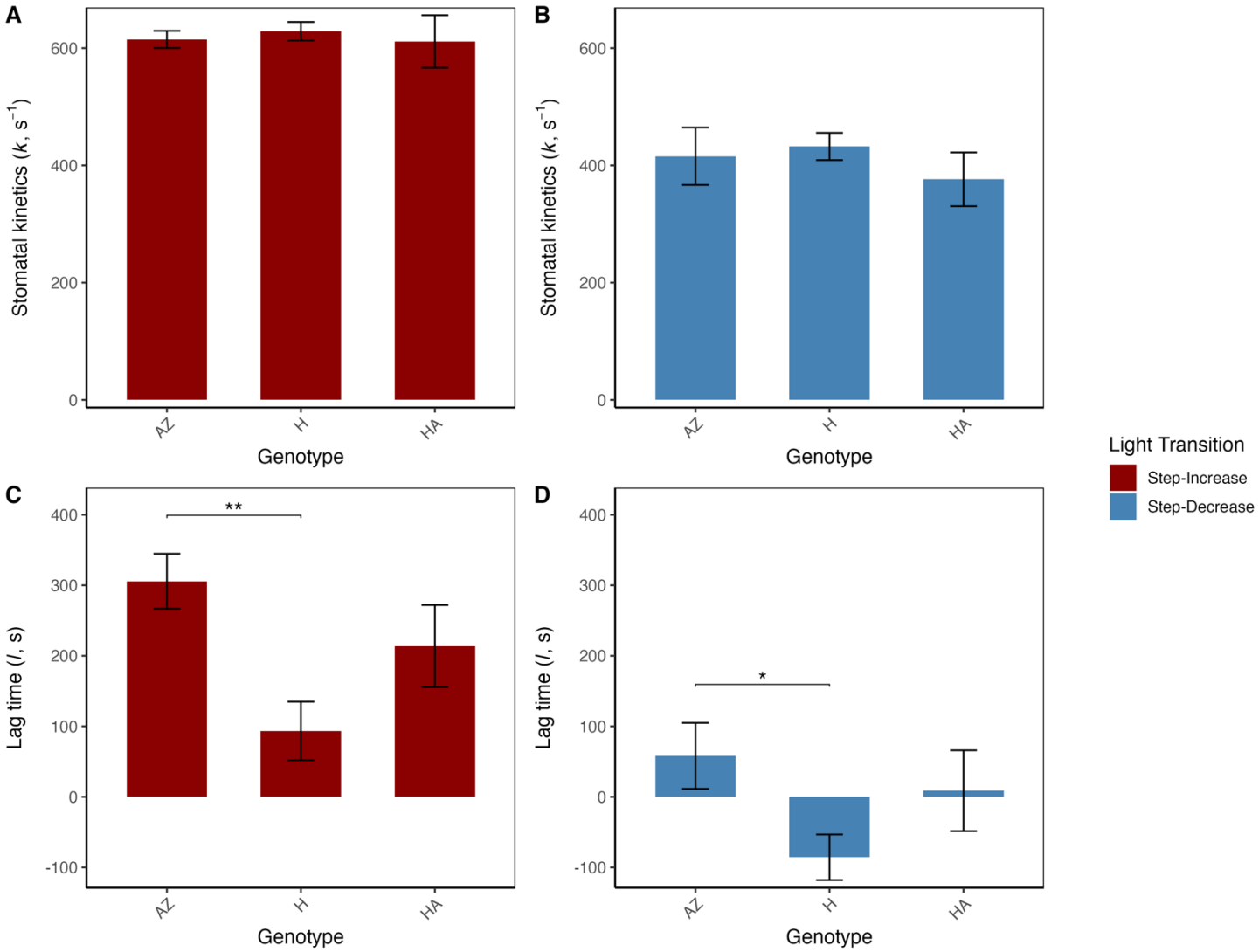

*Figure 5.6. Stomatal response kinetics across T1 genotypes during light step transitions. (A) Stomatal kinetics parameter (k) and (B) lag time (l) for transgenic tobacco genotypes during a step-increase and step-decrease in light intensity. Bars represent genotype means (± standard error) for each phase, with red bars indicating responses during light induction (Step-Increase) and blue bars during light reduction (Step-Decrease). Stomatal kinetics (k) reflects the rate of g_{sw} response to a light step change, while lag time (l) represents the temporal delay before the onset of response. Statistical differences are denoted by asterisks and brackets between comparisons (ANOVA with Tukey HSD, * p < 0.05, ** p < 0.01, *** p < 0.001) above the bar charts (n = 8 for AZ, 31 for H and 14 for HA). Environmental conditions: 25–30°C day and 20°C night, 60% RH and a 16-h photoperiod of 600-800 µmol photons m^{-2} s^{-1}. Measurements were performed on the youngest fully expanded leaf.*

Following T1 experimentation, three lines of both the HXK single and HXK::AHA2 double lines that were homozygous at T1 and showed accelerated stomatal response

were selected for T2 experiments. The selected lines are as follows: H_N4, H_B4 and H_108 for the HXK single and HA_83, HA_96 and HA_121 for the HXK::AHA2 double.

5.2.4. Molecular Characterisation Of Transgene Expression In T2 Transformants

Following the T1 line selection, selected lines were taken to the T2 generation and were tested alongside the T2 homozygous KST1::AHA2 single lines provided by Mengjie Fan (Lawson Lab, University of Essex) to compare the effect of both genes alone and together.

To understand the differences in transgene expression between the T2 lines, quantitative PCR was used to compare relative transgene expression between transgenic lines. Lines overexpressing HXK and AHA2 in the guard cells exhibited varied levels of transgene expression relative to the guard-cell-specific GORK housekeeping gene (Fig. 5.7). Distinct statistical groups were present among lines expressing both genes. Lines expressing HXK had average expression levels between 1.4 and 7.5x that of GORK (Fig. 5.7A). HXK lines formed two distinct statistical groups, with three lines, H_N4, H_B4 and HA_83 (Group C), had the highest levels of expression, with all lines having significantly higher expression than the azygous and WT controls (ANOVA, Tukey HSD, $p < 0.05$). Lines expressing AHA2 had considerably lower expression compared to GORK, ranging from 0.13 to 0.5x that of GORK (Fig. 5.7B). Three distinct groups of AHA2-expressing lines were formed, with the double lines having the lowest expression (Groups B and C) and the single lines (Group D) having the highest level of expression.

One single AHA2 line, A_19, had no difference in expression from the controls and thus can be considered azygous.

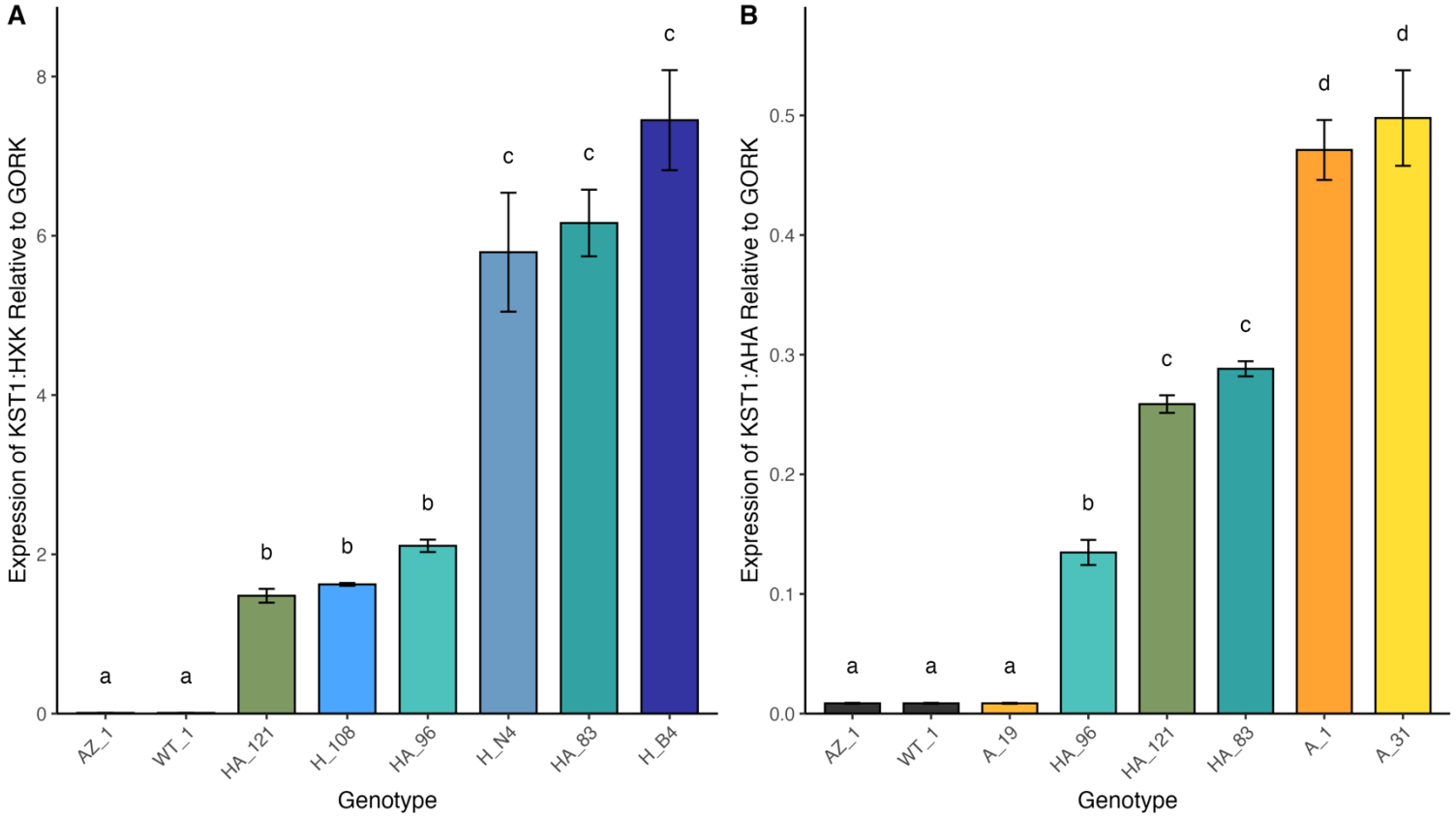

Figure 5.7. Quantitative PCR (qPCR) analysis of relative expression of the transgenes KST1:Hexokinase, KST1:AHA2 and KST1:Hexokinase:: KST1:AHA2 transgenic tobacco lines. A) Hexokinase expressionand normalised to the expression of Guard Cell Outward Rectifying K+ channel (GORK). B) AHA2 normalised to the expression of Guard Cell Outward Rectifying K+ channel (GORK). Transgenes were amplified using their respective qPCR primers (Table 2, Chapter 2). Relative expression of the genes was calculated by normalising expression to the expression of GORK in the Azygous. Bars show means ± SE (n = 3 biological replicates). Statistical groupings (CLD) are displayed by the letters above each respective genotype (ANOVA, Tukey HSD, $p < 0.05$). Environmental conditions: 25–30°C day and 20°C night, 60% RH and a 16-h photoperiod of 100-250 µmol photons m^{-2} s^{-1}.

5.2.5. Microscopic Characterisation Of Stomatal Development

To assess whether the guard-cell-specific overexpression of HXK and/or AHA2 had any effect on epidermal patterning, SD in epidermal peels was quantified using brightfield microscopy (Fig. 5.8). No significant differences were observed between transgenic genotypes in adaxial SD (Fig. 5.8A), abaxial SD (Fig. 5.8B) or stomatal ratio (Fig. 5.8C) (ANOVA, Tukey HSD, all $p > 0.05$). These data suggest that the transgene expression within the guard cells does not affect guard cell development or epidermal patterning.

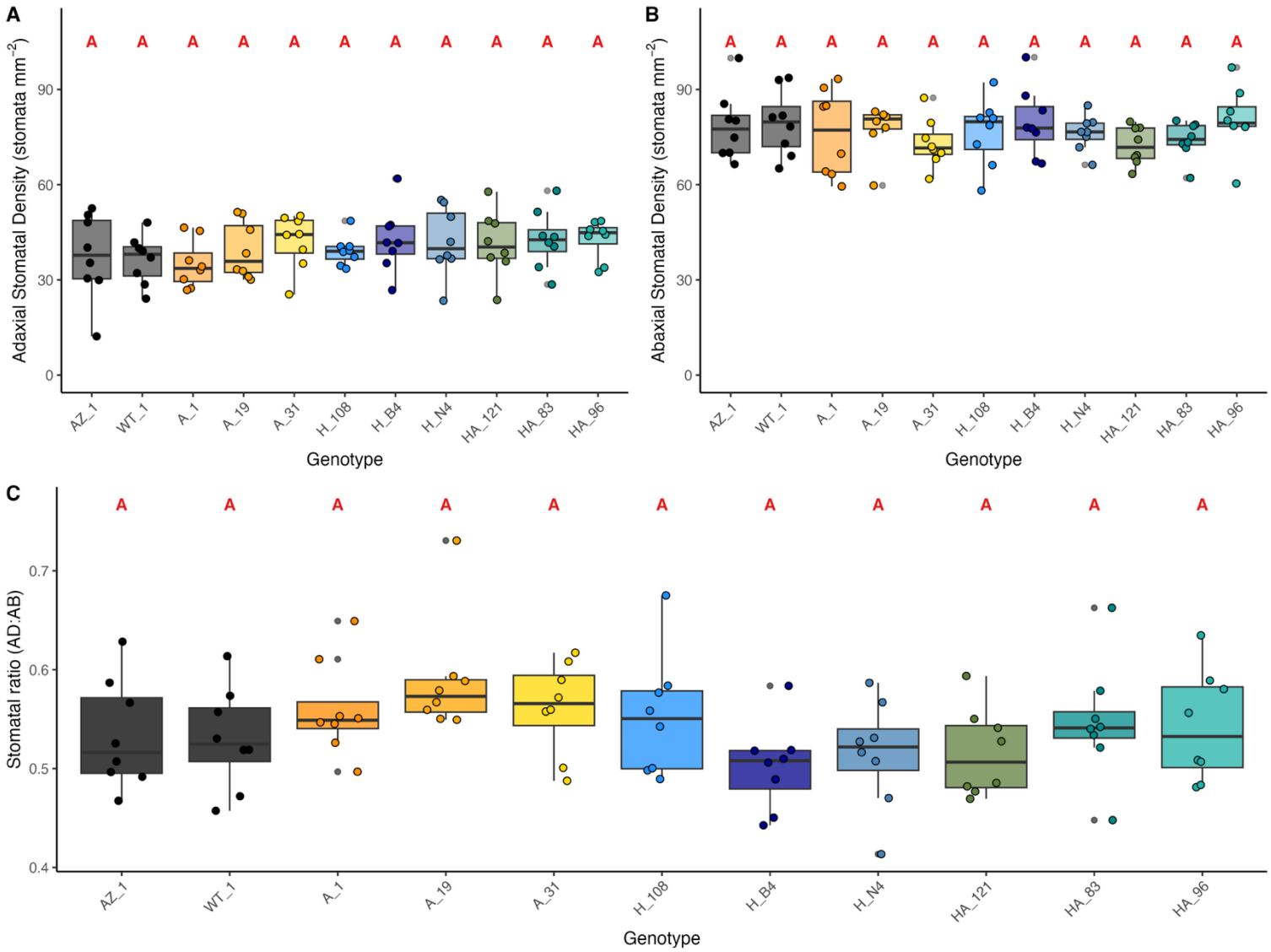

Figure 5.8. Epidermal patterning in T2 stomatal kinetics mutant transgenic tobacco lines. A) Adaxial stomatal density. B) Abaxial stomatal density. C) Stomatal Ratio of genotypes grown in low light conditions. Boxplots show the distribution of stomatal density measurements per genotype, with individual data points overlaid. Different shades represent different genotypes. Compact letter display (CLD) annotations above each box indicate statistical groupings based on ANOVA, followed by Tukey's HSD test ($p < 0.05$); genotypes sharing the same letter are not significantly different from one another. Environmental conditions: 25–30°C day and 20°C night, 60% RH and a 16-h photoperiod of 100-250 µmol photons m^{-2} s^{-1}. Epidermal impressions were taken from fully expanded leaves post-destructive harvest.

5.2.6. Chlorophyll Fluorescence Analysis Of T2 Lines

5.2.6.1. Photosynthetic Induction

To establish if the transgenes convey any benefit to the photosynthetic efficiency of PSII during photosynthetic induction, T2 selected lines were subject to chlorophyll fluorescence imaging (Fig. 5.9). All HXK single lines and one double line, HA_83, exhibited significantly reduced F_v/F_m, suggesting chronic photoinhibition of PSII. (Fig. 5.9A). All lines showed a typical response to photosynthetic induction: a sharp decrease in YII followed by stabilisation as plants acclimate to the light. Genotypic differences were apparent throughout induction at 400 µmol m^{-2} s^{-1} PAR.

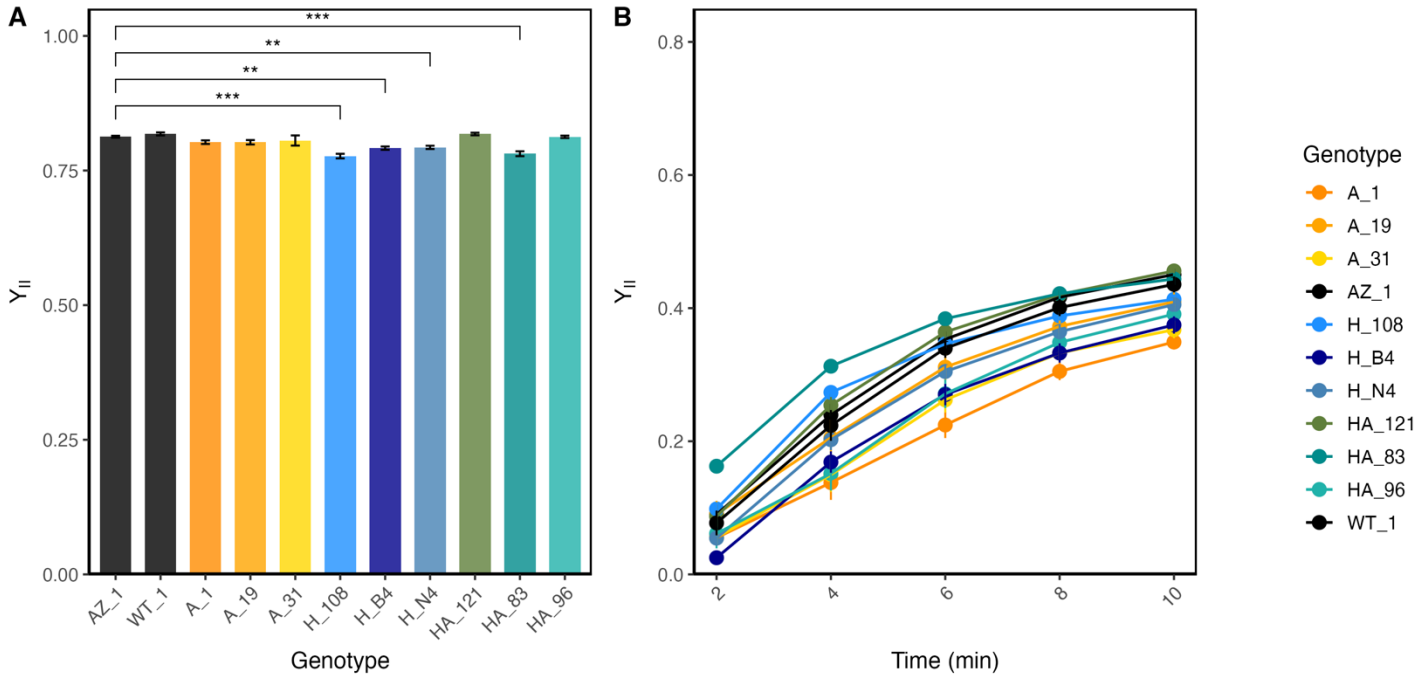

*Figure 5.9. Chlorophyll fluorescence response of 3-week-old T2 transgenic tobacco to photosynthetic induction. A) Dark-adapted plants were subject to a saturating pulse to determine Fv/Fm. B) The response over time of the operating efficiency of photosystem II (YII) to the addition of Actinic light of 400 µmol m^{-2} s^{-1} PAR induced photosynthesis over 10 minutes. Statistical differences are denoted by asterisks and brackets between comparisons (ANOVA with Tukey HSD, or Kruskal-Wallis with Dunn test * $p < 0.05$, ** $p < 0.01$, *** $p < 0.001$) above the bar charts (n = 12). Environmental conditions: 25–30°C day and 20°C night, 60% RH and a 16-h photoperiod of 100-250 µmol photons m^{-2} s^{-1}.*

Many statistical differences were observed in YII across all three time points during photosynthetic induction (Fig. 5.10). At two minutes post-induction (Fig. 5.10A), the double line HA_83 had significantly higher YII than the controls (ANOVA, Tukey HSD, $p = 0.0018$), despite having significantly reduced F_v/F_m (Fig. 5.9A). At six and ten minutes post-induction (Fig. 5.10B), AHA2 single-expressing lines, A_1 and A_31, HXK single line H_B4 and double line HA_96 all had significantly reduced YII during photosynthetic induction (ANOVA, Tukey HSD, all $p < 0.01$). These data would suggest that stomatal

kinetics mutants may have a detrimental effect on the maximum quantum efficiency and the operating efficiency of photosystem II during photosynthetic induction.

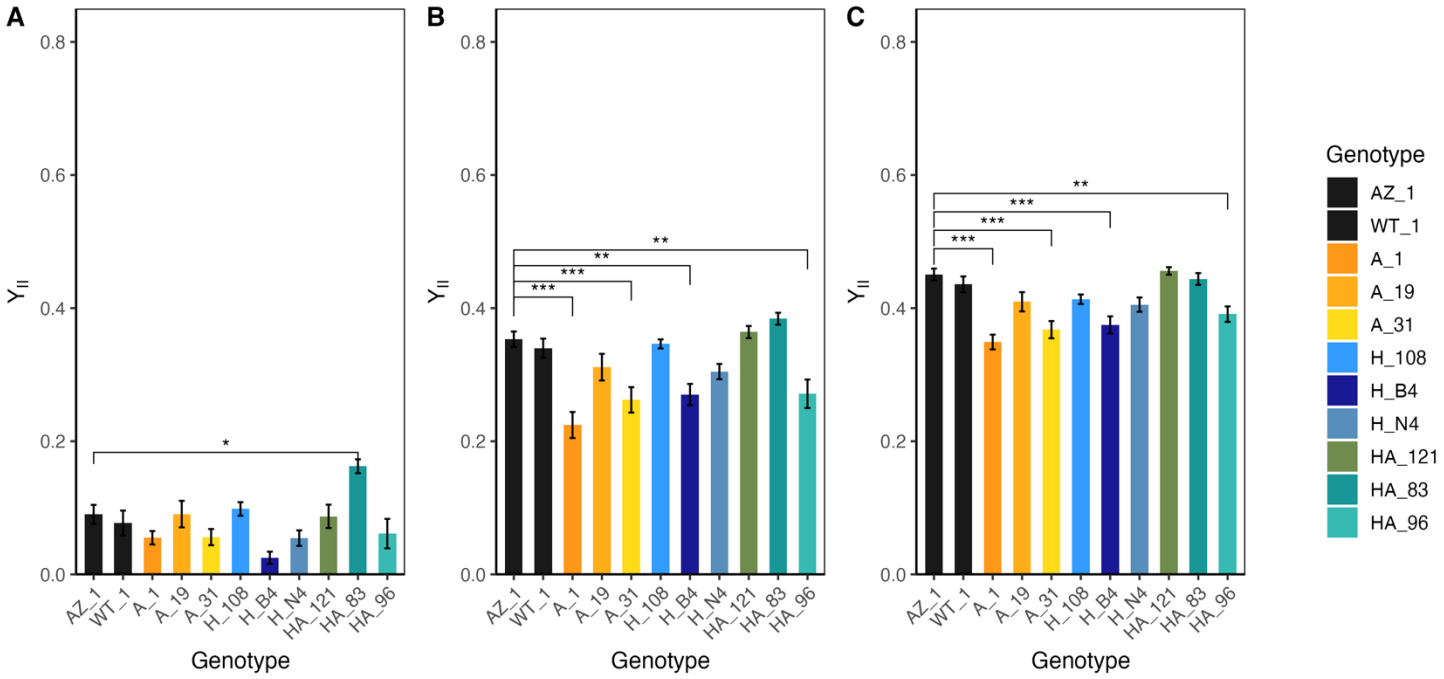

*Figure 5.10. Statistical analysis of photosynthetic response at three time points during photosynthetic induction of 3-week-old T2 transgenic tobacco genotypes. Bar charts represent the mean values ± standard error of YII. A) YII at 2 minutes post-induction at 400 µmol m^{-2} s^{-1} PAR. B) YII at 6 minutes post-induction. C) YII at 10 minutes post-induction. Statistical differences are denoted by asterisks and brackets between comparisons (ANOVA with Tukey HSD, or Kruskal-Wallis with Dunn test * $p < 0.05$, ** $p < 0.01$, *** $p < 0.001$) above the bar charts (n = 12). Environmental conditions: 25–30°C day and 20°C night, 60% RH and a 16-h photoperiod of 100-250 µmol photons m^{-2} s^{-1}.*

5.2.6.2. Photosynthetic Relaxation

To further investigate the effects of the transgenes on PSII operating efficiency, T2 plants were subjected to dark relaxation following induction to assess the recovery dynamics of YII over time (Fig. 5.11). All lines showed a rapid recovery of YII towards the maximum operating efficiency of PSII, with genotypic differences observed throughout relaxation (Fig. 5.11B).

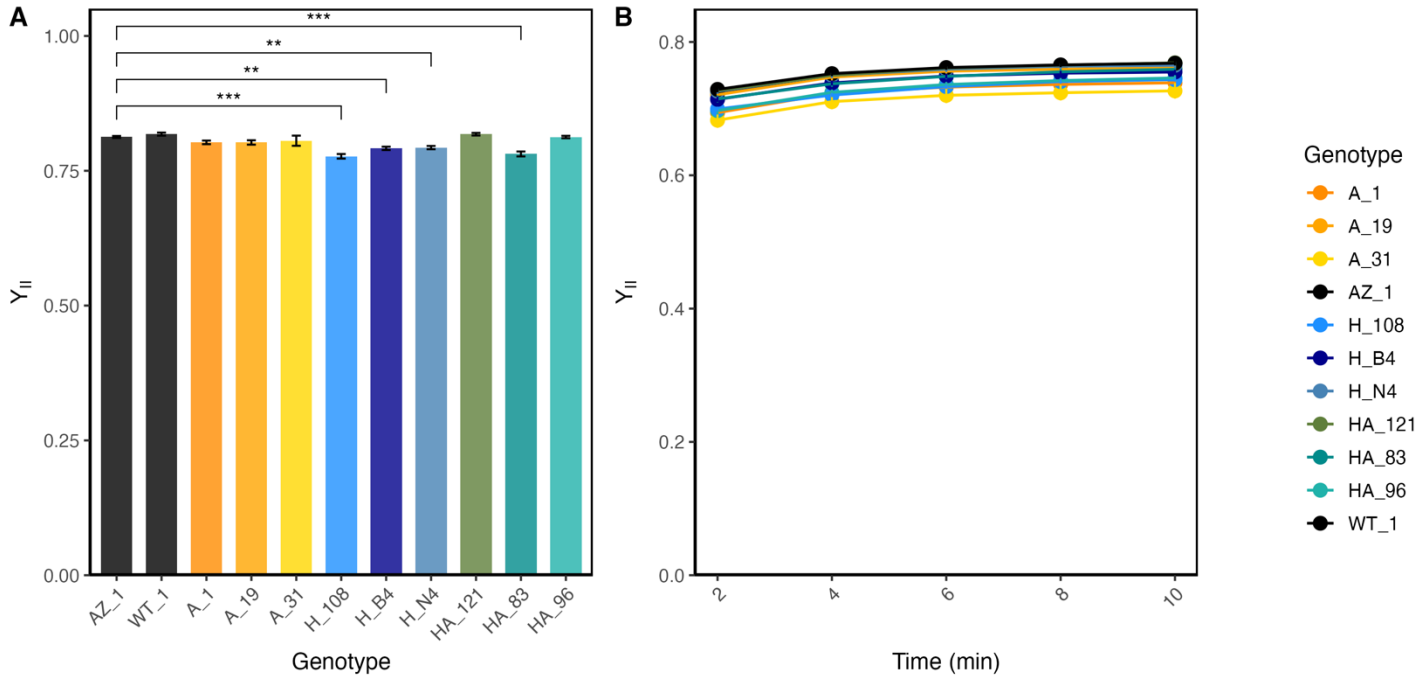

*Figure 5.11. Chlorophyll fluorescence relaxation of 3-week-old T2 transgenic tobacco following illumination. A) Dark-adapted plants were subject to a saturating pulse to determine Fv/Fm. B) The recovery response over time of the operating efficiency of photosystem II (YII) to the removal of Actinic light of 400 µmol m^{-2} s^{-1} PAR induced photosynthesis over 10 minutes returning the plants to darkness. Statistical differences are denoted by asterisks and brackets between comparisons (ANOVA with Tukey HSD, or Kruskal-Wallis with Dunn test * $p < 0.05$, ** $p < 0.01$, *** $p < 0.001$) above the bar charts (n = 12). Environmental conditions: 25–30°C day and 20°C night, 60% RH and a 16-h photoperiod of 100-250 µmol photons m^{-2} s^{-1}.*

Similar to photosynthetic induction, many statistical differences were observed in YII during photosynthetic relaxation (Fig. 5.12). After two, six and ten minutes of relaxation, AHA2 expressing lines, A_1 and A_31, HXK single line H_108, and the double

line HA_96 had significantly lower YII than the controls (ANOVA, Tukey HSD, all $p < 0.01$). These data, alongside the photosynthetic induction data (Figs. 5.9 and 5.10), suggest that guard-cell-specific overexpression of both HXK and AHA2 can be detrimental to the maximum quantum efficiency and the operating efficiency of photosystem II during photosynthetic induction and relaxation.

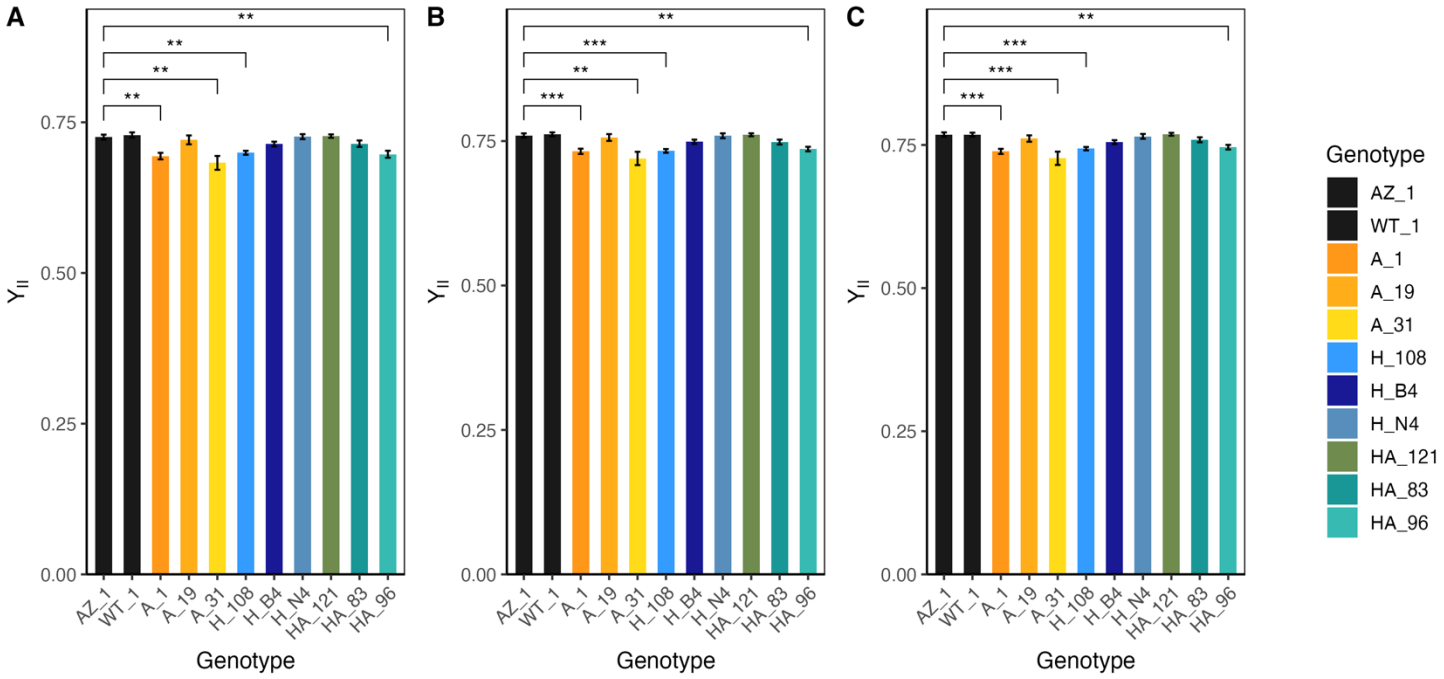

*Figure 5.12. Statistical analysis of photosynthetic response at three time points during photosynthetic relaxation of three-week-old T2 transgenic tobacco genotypes. Bar charts represent the mean values ± standard error of YII. A) YII at 2 minutes post-relaxation. B) YII at 6 minutes post-relaxation. C) YII at 10 minutes post-relaxation. Statistical differences are denoted by asterisks and brackets between comparisons (ANOVA with Tukey HSD, $p < 0.05$, ** $p < 0.01$, *** $p < 0.001$) above the bar charts ($n = 12$). Environmental conditions: 25–30°C day and 20°C night, 60% RH and a 16-h photoperiod of 100-250 µmol photons m^{-2} s^{-1}.*

5.2.7. Determining Photosynthetic Capacity Via Photosynthetic Response To Intracellular CO_2 Concentrations

Photosynthetic response to CO_2 curves were used to establish the effect of guard-cell-specific overexpression of HXK and/or AHA2 on maximum photosynthetic capacity. All genotypes showed a typical A/C_i response curve, with assimilation rate (A) increasing steeply at low intercellular CO_2 concentrations (C_i) before approaching saturation at higher C_i levels (Fig. 5.13). Most lines show very similar groupings during the increasing [CO_2]; however, two lines are distinct from the rest. The azygous control shows elevated A from 400-1500 ppm C_i. Conversely, one AHA2 single line (A_1) displayed reduced A from 400-1500 ppm C_i.

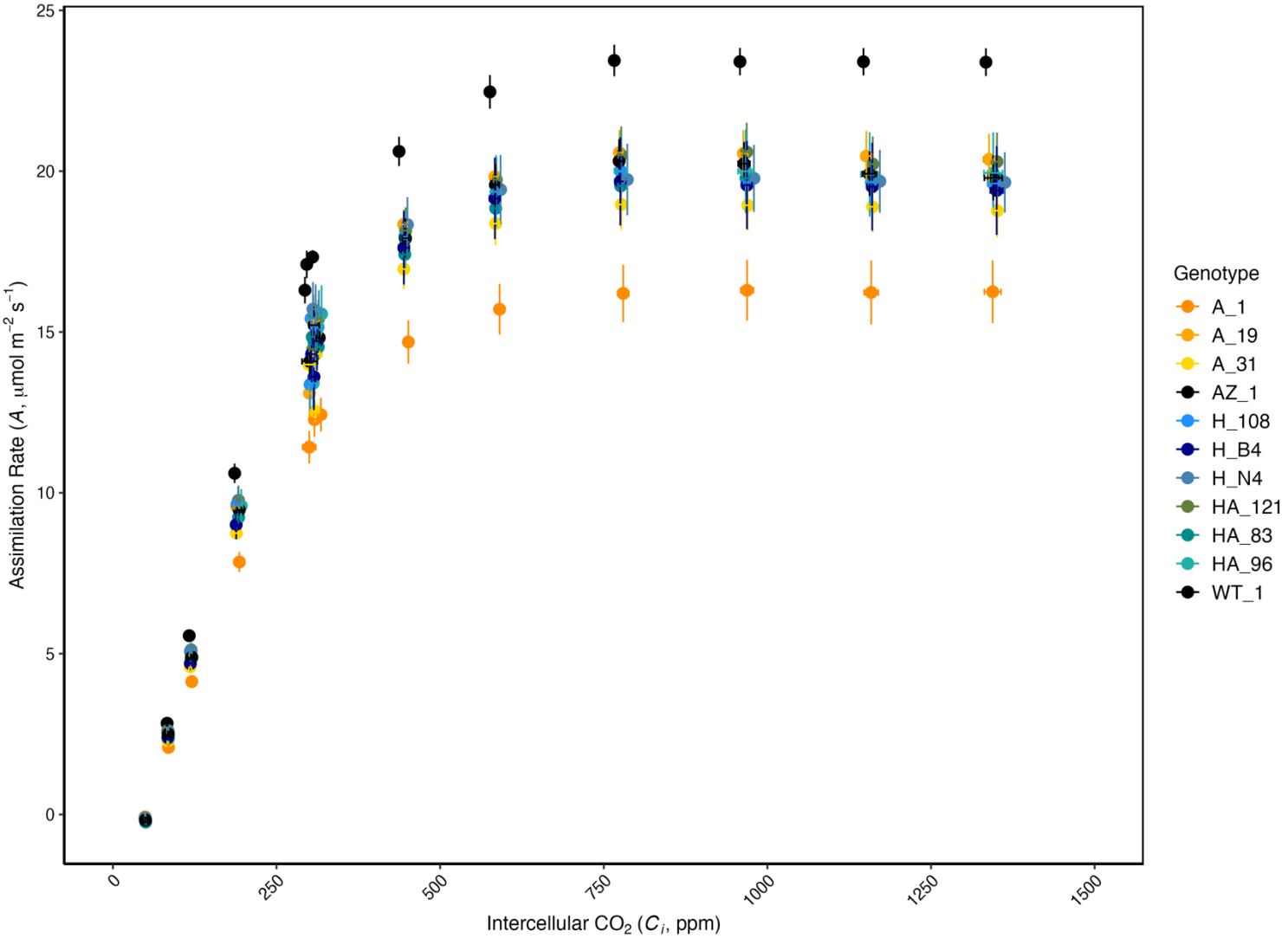

Figure 5.13. Photosynthetic response of T2 transgenic tobacco plants under different intracellular CO2 concentrations (C_i). The net CO_2 assimilation rate (A, µmol m^{-2} s^{-1}) is plotted as a function of intercellular CO_2 concentration (C_i, µmol mol^{-1}). Each point represents the mean (n = 5-8) for a given genotype, with the error bars indicating standard error (SE), for A and C_i (vertical and horizontal, respectively). Environmental conditions: 25–30°C day and 20°C night, 60% RH and a 16-h photoperiod of 100-250 µmol photons m^{-2} s^{-1}. Measurements were performed on the youngest fully expanded leaf.

Modelled values of Vc_{max} and J_{max} using the Farquhar–von Caemmerer–Berry model (von Caemmerer and Farquhar, 1981) did not differ significantly between genotypes (Fig. 5.14B and C) (ANOVA, Tukey HSD, $p < 0.05$). However, AHA2-expressing lines A_1 and A_31 had significantly lower A_{max} than the controls (ANOVA, Tukey HSD, $p < 0.001$ and $p = 0.023$, respectively). Guard-cell-specific expression of AHA2 significantly reduces light and CO_2-saturated photosynthesis rates, when stomata should not be limiting photosynthesis.

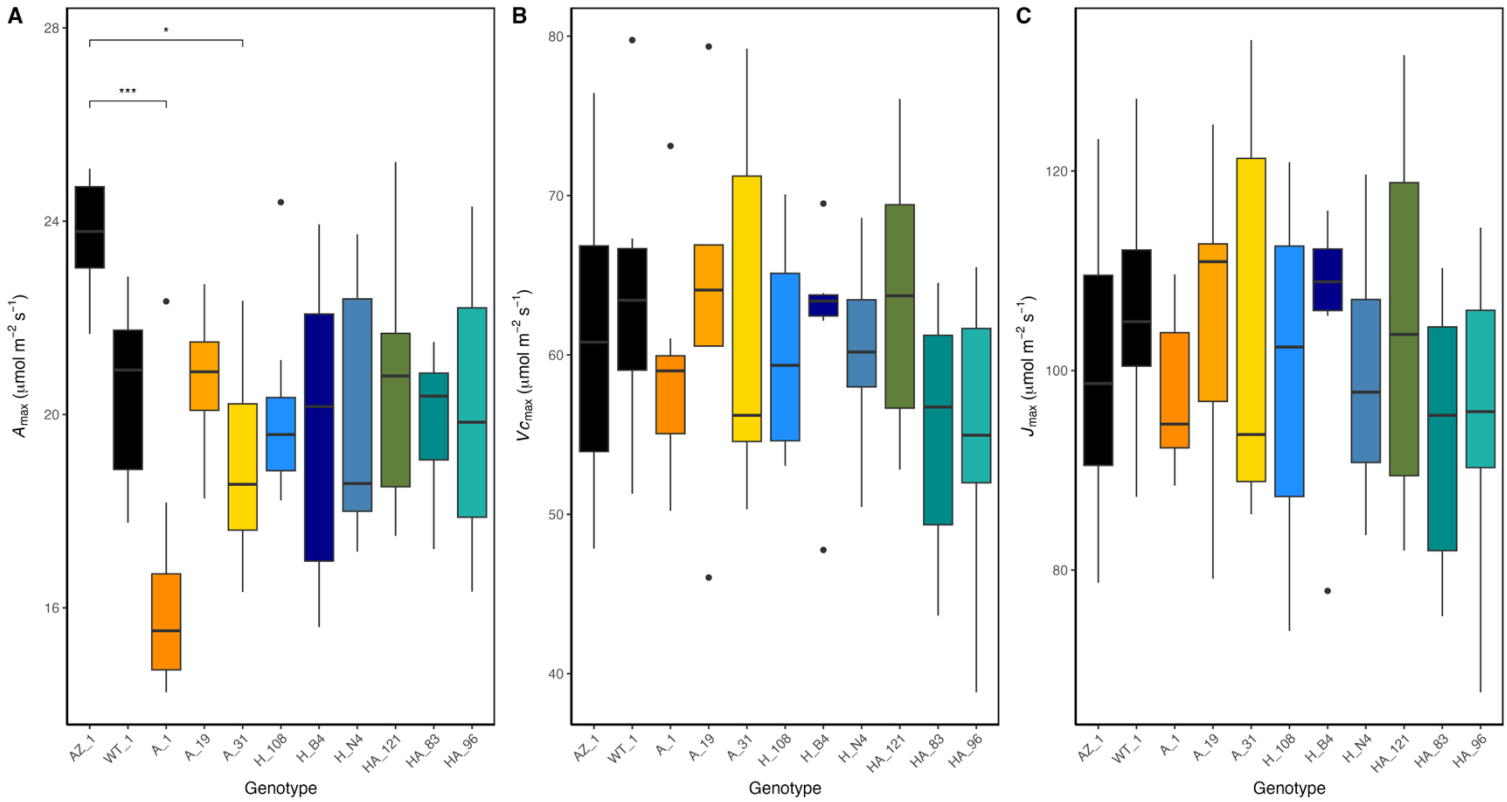

*Figure 5.14. Photosynthetic parameters modelled from A/C_i curves across T2 transgenic tobacco genotypes. (A) CO_2 and Light-saturated assimilation rate (A_{max}), (B) maximum Rubisco carboxylation capacity (Vc_{max}) and (C) maximum electron-transport rate (J_{max}). Boxplots display the median (horizontal line), interquartile range (box), and whiskers extending to 1.5 × the interquartile range, with black dots marking observations beyond this range (outliers) (n = 5-8). Statistical differences are denoted by asterisks and brackets between comparisons (ANOVA with Tukey HSD, p < 0.05, ** p < 0.01, *** p < 0.001) above the bar charts. Environmental conditions: 25–30°C day and 20°C night, 60% RH and a 16-h photoperiod of 100-250 µmol photons m^{-2} s^{-1}. Measurements were performed on the youngest fully expanded leaf.*

5.2.8. Stomatal Conductance, Photosynthesis And Intrinsic Water Use Efficiency Dynamics In Response To Dynamic Light

To assess the impact of guard-cell-specific overexpression of HXK and AHA2 on stomatal function, stomatal responses were assessed following step changes in light intensity. Following a step increase in light intensity (50 to 1000 µmol m^{-2} s^{-2}), all

genotypes exhibited a rapid rise in net photosynthesis (*A*) and stomatal conductance (g_{sw}), with values plateauing between 1400-1600 s and 2500-3000 s, respectively (Fig. 5.15A and B, respectively). Intrinsic water-use efficiency (iWUE) increased in most genotypes following the step increase in light intensity before declining as g_{sw} increased. The inverse response was seen following a step decrease in light intensity (1000 to 50 µmol m^{-2} s^{-2}), with a rapid decrease, followed by a rise and plateau in *A* and g_{sw}, with values plateauing between 3900-4100 s and 5000-5400 s, respectively. iWUE exhibited a similar decline, then an increase to a plateau.

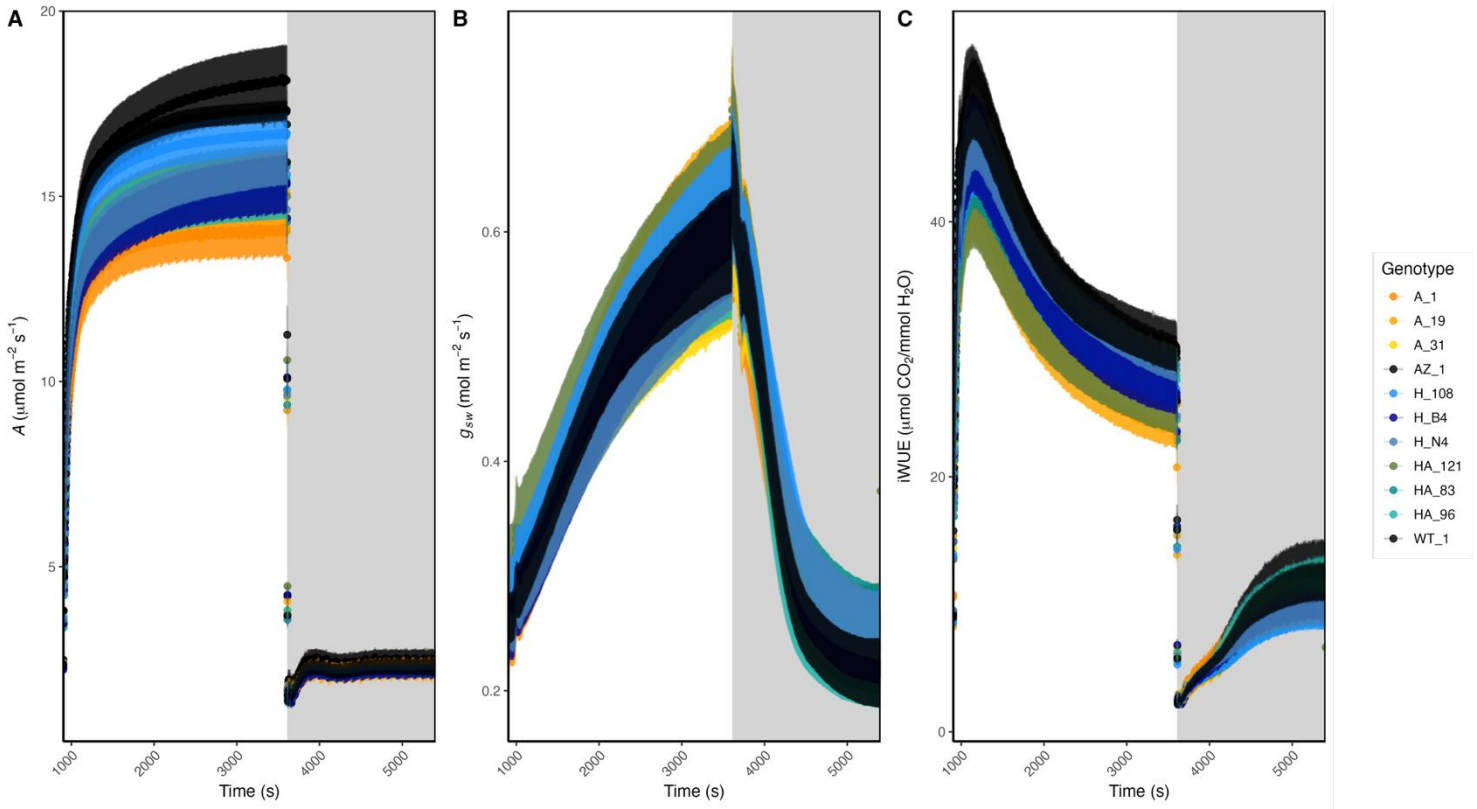

*Figure 5.15. Time-course responses of (A) net photosynthesis (A), (B) stomatal conductance to water vapour (g_{sw}), and (C) intrinsic water-use efficiency (*iWUE*) in stomatal kinetics T2 transgenic tobacco lines during a step change in light intensity. Light intensity increased from 50 to 1000 µmol m^{-2} s^{-1} at 900 s and returned to 50 µmol m^{-2} s^{-1} at 3600 s, as indicated by the shaded region. Lines represent genotype means; ribbons show ± standard error (n = 7-8). Environmental conditions: 25–30°C day and 20°C night, 60% RH and a 16-h photoperiod of 100-250 µmol photons m^{-2} s^{-1}. Measurements were performed on the youngest fully expanded leaf.*

Three distinct time points were chosen to analyse genotypic differences during the step increase and decrease in light intensity: steady-state pre-induction (50 µmol m^{-2} s^{-1}, 900 s), High-Low transition (1000 µmol m^{-2} s^{-1}, 3600 s) and steady-state post-induction (50 µmol m^{-2} s^{-1}, 5400 s). No significant differences in *A,* g_{sw}, or iWUE were identified at 900 or 3600 seconds (ANOVA, Tukey HSD, all $p > 0.05$). However, AHA2 single line A_1 had significantly lower *A* than both controls (ANOVA, Tukey HSD, both $p < 0.05$). Guard-cell-specific overexpression of AHA2 resulted in lower steady-state photosynthetic rates at low light intensity following a step decrease in light intensity, again demonstrating a reduced photosynthetic capacity.

During the step increase, no significant differences were found between genotypes for time taken to reach 33, 50, 66 and 90% of the relative *A* (Kruskal-Wallis, Dunn Test, all $p > 0.05$). These data suggest that the expression of the transgenes did not facilitate any benefit to the rate of photosynthetic induction during a step increase in light intensity.

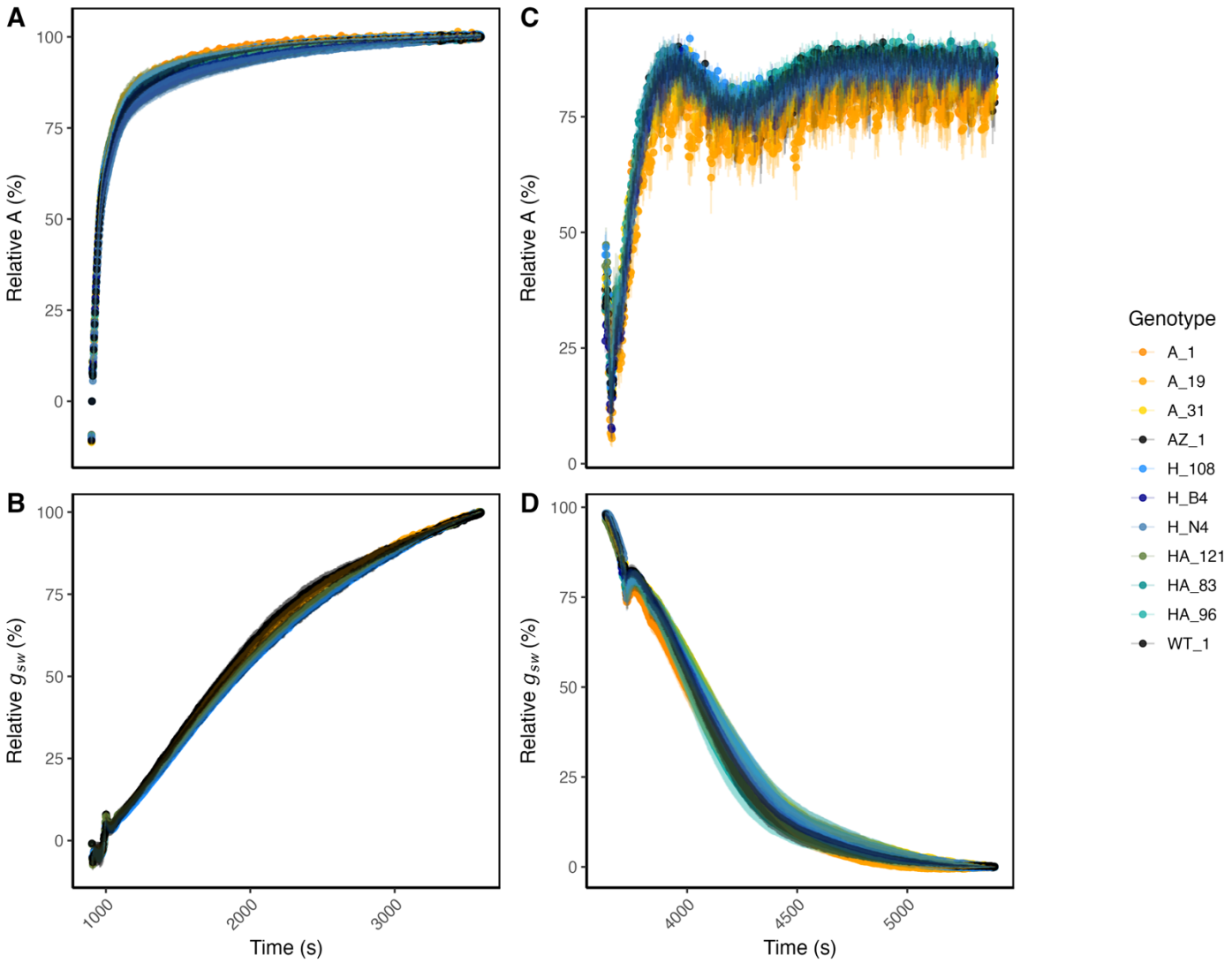

Figure 5.16. Relative CO_2 assimilation (A, %) and stomatal conductance (g_{sw}, %) response to a step change in light intensity over time in T2 tobacco stomatal kinetics mutant genotypes. The x-axis represents time (seconds), and the y-axis represents relative A and g_{sw} (%), normalised to initial values. The left panels show the response of A (A) and g_{sw} (B) to a step-increase in light intensity, where light intensity increased at Time = 600 s, while the right panel show the response of A (C) and g_{sw} (D) to a step-decrease in light intensity, where light intensity decreased at Time = 2400 s. Each coloured line represents the mean response for a specific genotype, with shaded areas indicating standard error (SE) (n= 7-8). Environmental conditions: 25–30°C day and 20°C night, 60% RH and a 16-h photoperiod of 100-250 µmol photons m^{-2} s^{-1}. Measurements were performed on the youngest fully expanded leaf.

To identify if guard-cell-specific overexpression of HXK and/or AHA2 altered stomatal behaviour during the step changes in light intensity, stomatal kinetics (k) and lag time (l, time before a significant stomatal response) were modelled according to

Vialet-Chabrand et al. (2017). All lines displayed significantly faster stomatal kinetics (lower *K* values) when responding to a step decrease in light intensity compared to a step increase in light intensity (Two Sample t-test, all $p < 0.05$) (Fig. 5.17A and B). All genotypes except double lines HA_121and HA_96 and AHA2 single line A_31 (Two Sample t-test, all $p > 0.05$) had lower lag time (*l*) when responding to a step decrease in light intensity compared to a step increase in light intensity (Two Sample t-test, all $p < 0.05$) (Fig. 5.17C and D). Conversely to the T1 generation, no differences were seen between genotypes for *k* or *l* (ANOVA, $p > 0.05$). These data would suggest that neither HXK nor AHA2 expression in the guard cells conveys any benefit to stomatal kinetics or response time when grown in low light conditions.

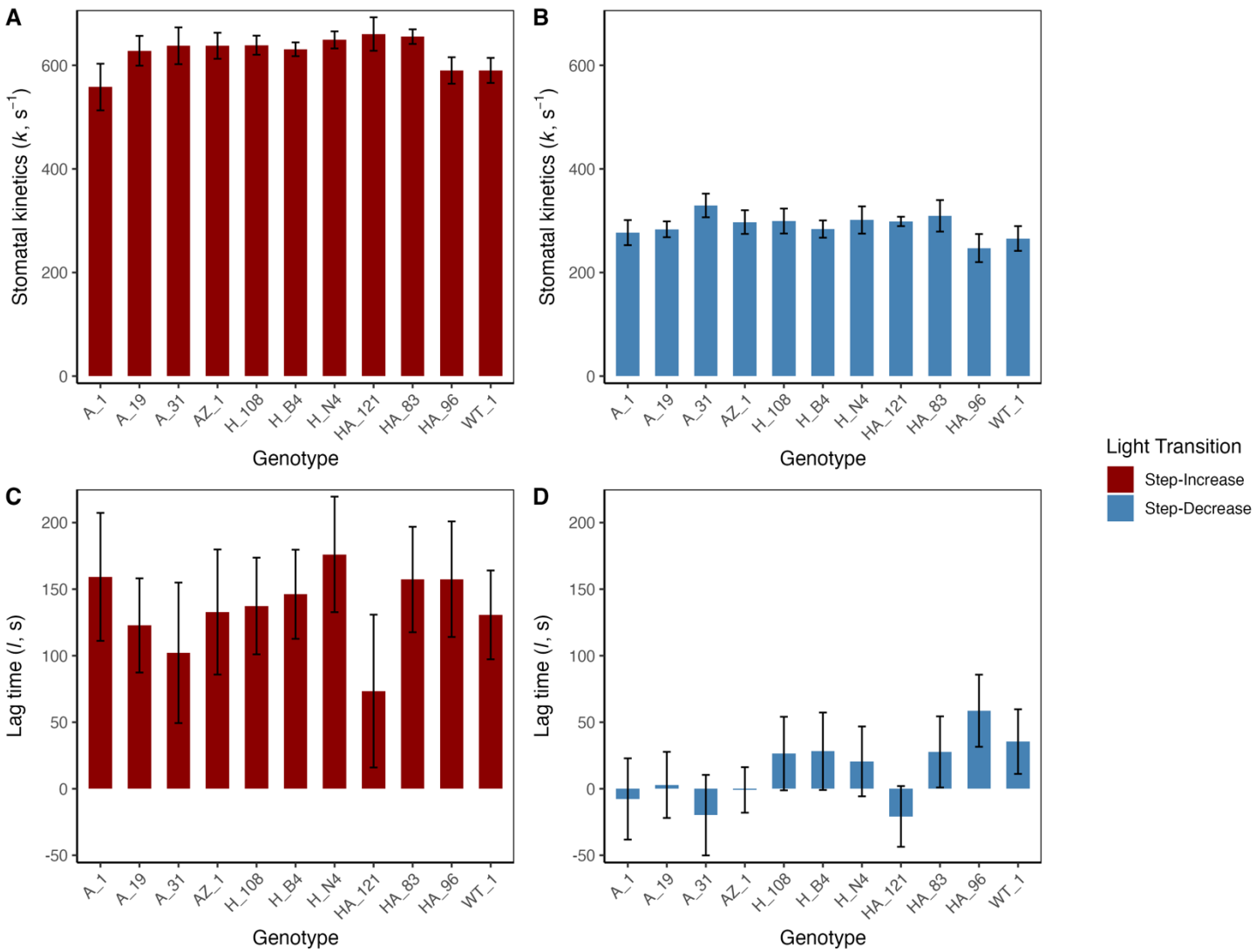

*Figure 5.17. Stomatal response kinetics across T2 genotypes during light step transitions. (A) Stomatal kinetics parameter (k) and (B) lag time (l) for transgenic tobacco genotypes during a step-increase and step-decrease in light intensity. Bars represent genotype means (± standard error) for each phase, with red bars indicating responses during light induction (Step-Increase) and blue bars during light reduction (Step-Decrease). Stomatal kinetics (k) reflects the rate of g_{sw} response to a light step change, while lag time (l) represents the temporal delay before the onset of response. Statistical differences are denoted by asterisks and brackets between comparisons (ANOVA with Tukey HSD, * $p < 0.05$, ** $p < 0.01$, *** $p < 0.001$) above the bar charts (n = 7-8). Environmental conditions: 25–30°C day and 20°C night, 60% RH and a 16-h photoperiod of 100-250 µmol photons m^{-2} s^{-1}. Measurements were performed on the youngest fully expanded leaf.*

To assess whether guard-cell-specific expression of KST1:AHA2 or KST1:HXK was associated with changes in stomatal conductance during dynamic light conditions, the relationship between transgene expression and the maximum stomatal conductance ($g_{sw\,max}$) achieved during the high-light phase of the step change was examined using linear regression analysis (Fig. 5.18). No significant relationship was seen between either the relative expression of either transgene and g_{swmax} (Pearson correlation, $p > 0.05$ in both cases). A slightly stronger negative relationship was seen between KST1:HXK expression and g_{swmax} than KST1:AHA2 ($R^2 = 0.45$ vs 0.31). These data suggesting that neither transgene exerts significant control over maximum stomatal conductance when responding to changes in light.

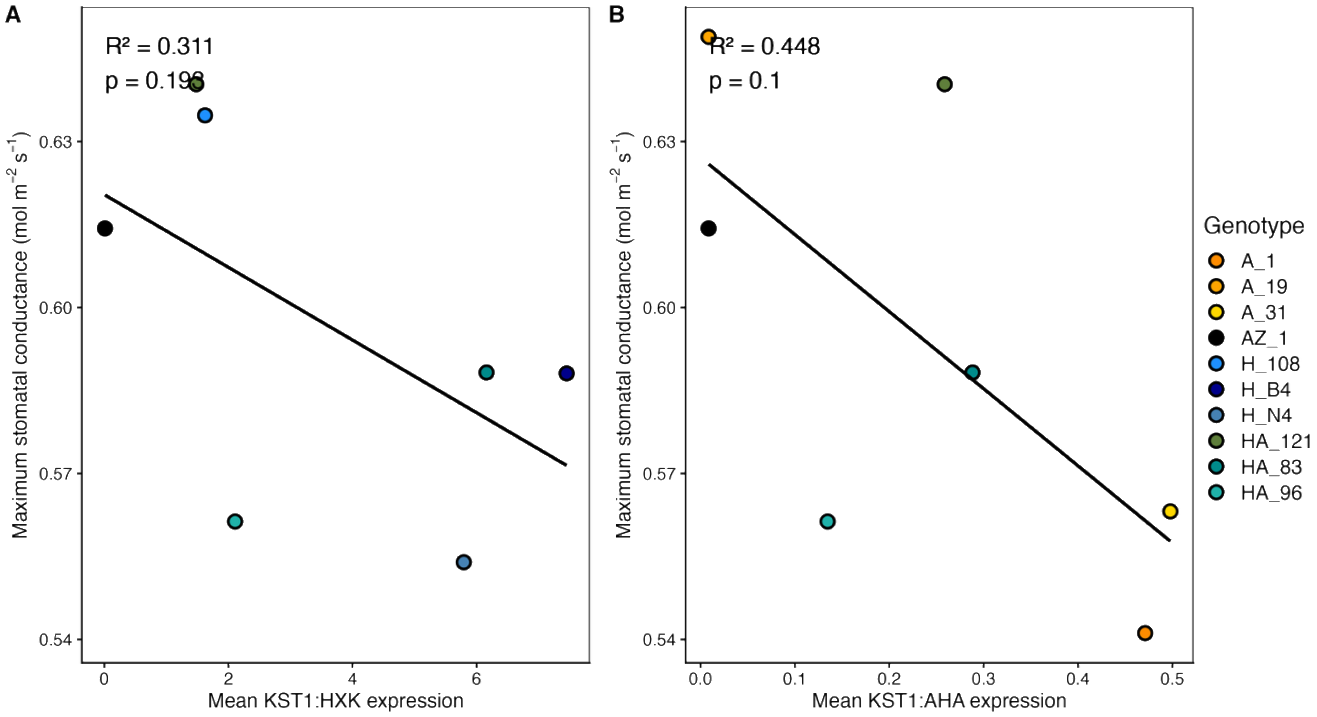

Figure 5.18. Relationship between guard-cell transgene expression and maximum stomatal conductance of T2 transgenic tobacco genotypes during a step increase in light intensity. A) Mean expression of KST1:HXK correlated with the maximum stomatal conductance (g_{swmax})reached during the high-light phase of the step change. B) Mean expression of KST1:AHA2 correlated with (g_{swmax})during the high-light phase. Linear regressions are shown, with R^2 and p values indicated in each panel.

5.2.9. Transgene Effect On Plant Growth

To assess the impact of transgene expression on plant growth and productivity, a harvest analysis was performed (Fig. 5.19). Genotypic differences were seen in fresh weight, leaf area and dry weight (Fig. 5.19A, B and C). AHA2 single lines A_1 and A19 and HXK single line H_B4, the HXK line with the highest relative transgene expression, had significantly lower fresh weight, leaf area and dry weight than the controls (Kruskal-Wallis, Dunn test, $p < 0.05$). AHA2 single line A_31 had only significantly reduced dry weight compared to the azygous control (Kruskal-Wallis, Dunn test, p = 0.026). The leaf area to fresh weight ratio was consistent across all lines, suggesting that the observed

reductions in both were uniform. The mass of the T2 seeds that were sown for this experiment was measured to see if that may explain some of the differences in T2 biomass. No significant differences were found between seed mass, despite the trend towards lower seed weight in the line with the lowest biomass, A_1. These data would suggest that high levels of relative expression of AHA2 and HXK resulted in lower biomass accumulation under low light conditions.

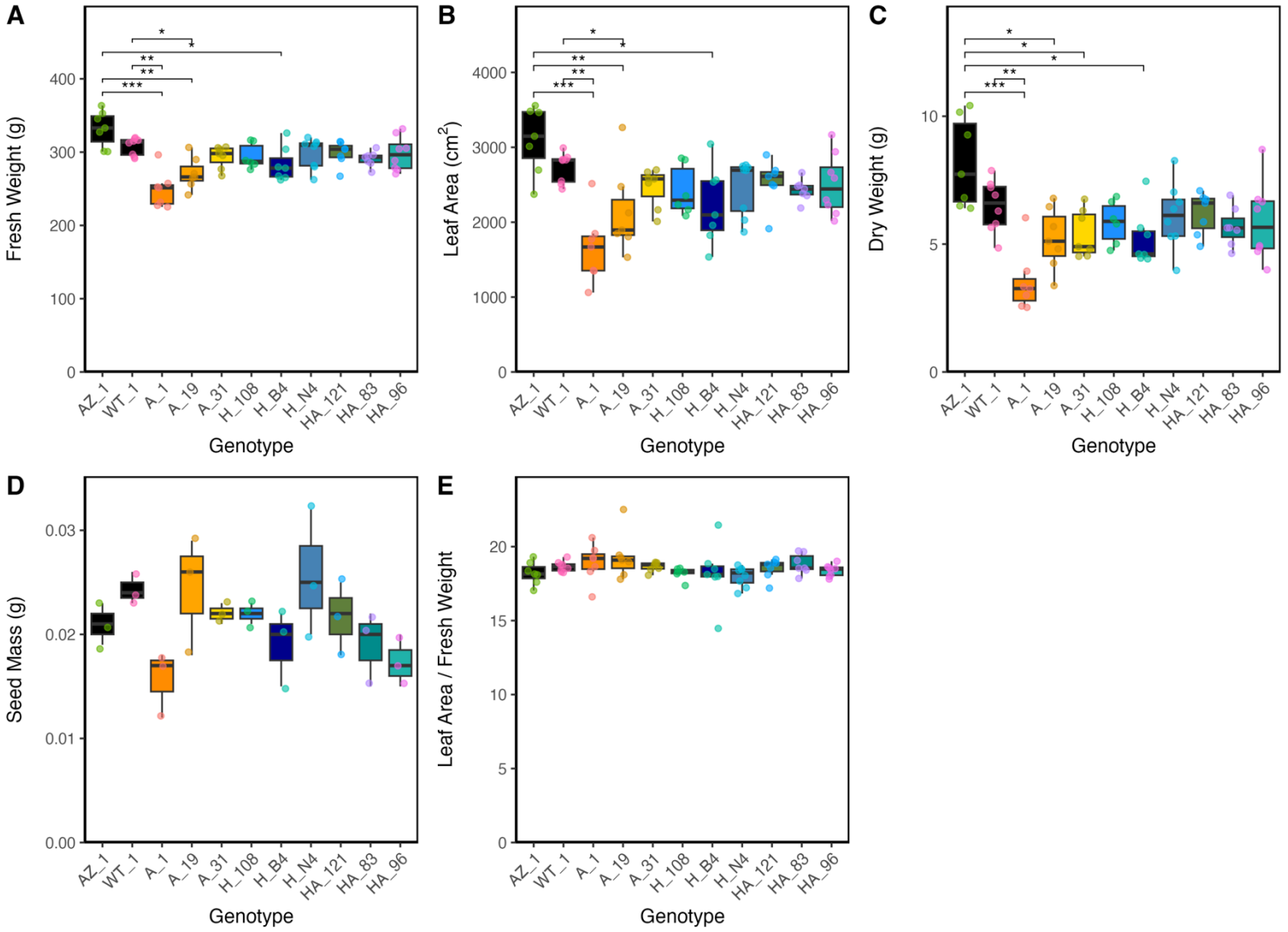

Figure 5.19. Comparison of destructive harvest data among T2 transgenic tobacco lines. (A) Fresh weight, (B) Leaf area and (E) Leaf Area to Fresh Weight ratio measurements were taken during destructive harvest. (C) Dry Weight was collected from oven-dried samples. D) Seed mass of 50 seeds collected pre-destructive harvest. Boxplots display the median (horizontal line), interquartile range (box), and whiskers extending to 1.5 × the interquartile range, with individual biological replicates shown as jitter points (n = 6 per line, for seed mass n = 3x 50 seeds). Environmental conditions: 25–30°C day and 20°C night, 60% RH and a 16-h photoperiod of 100-250 µmol photons m^{-2} s^{-1}.

To investigate whether variation in transgene expression was associated with differences in plant biomass accumulation, mean KST1:HXK and KST1:AHA expression levels were correlated with fresh and dry weight across genotypes (Fig. 5.20). For both HXK and AHA expression, negative relationships were observed with fresh and dry weight

(Fig. 5.20 A–D), indicating a trend towards reduced biomass accumulation at higher levels of transgene expression. No significant association was found between fresh weight or dry weight and KST1:AHA expression (Fig. 5.20A and B) (Pearson correlation, $p > 0.05$ in both cases), with weak- moderate coefficients of determination ($R^2 = 0.269–0.421$).

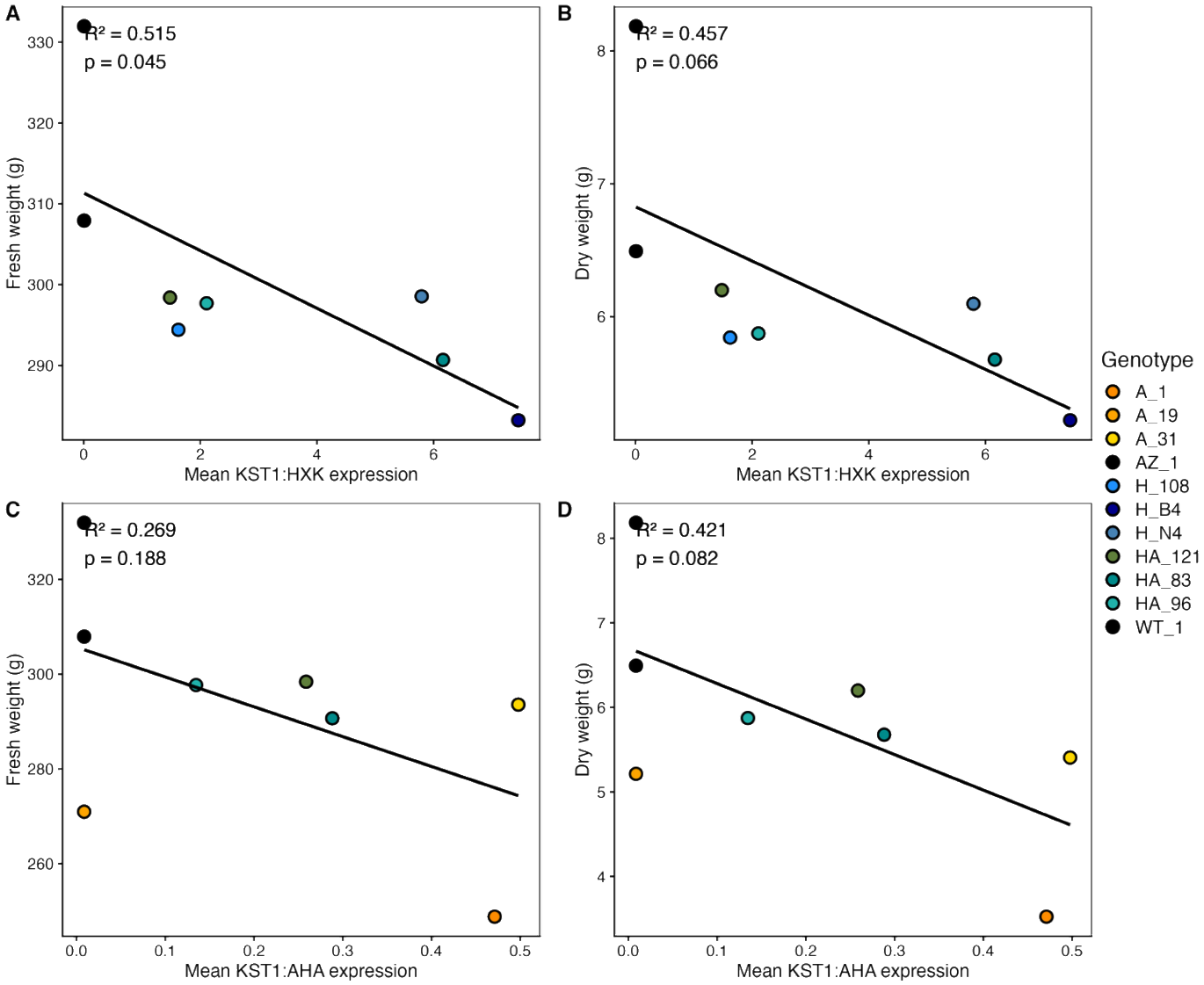

Figure 5.20 Relationship between transgene expression and biomass. A) Mean expression of KST1:HXK *correlated with fresh weight. B) Mean expression of* KST1:HXK *correlated with dry weight. C) Mean expression of* KST1:AHA *correlated with fresh weight. D) C) Mean expression of* KST1:AHA *correlated with fresh weight. Linear regressions are shown, with R^2 and p values indicated in each panel.*

For KST1:HXK, increased expression was significantly associated with lower fresh weight (R^2 = 0.515, p = 0.045) and near significant correlation with dry weight (R^2 = 0.457, p = 0.066) (Fig. 5.20A and B). These data suggest that KST1:HXK expression may contribute to reduced biomass accumulation.

Collectively, these analyses indicate that increased transgene expression was not associated with enhanced biomass accumulation under the growth conditions used in this study. While KST1:AHA expression showed no significant relationship with either fresh or dry weight, elevated KST1:HXK expression was associated with reduced biomass, with a significant negative correlation observed for fresh weight and a near-significant trend for dry weight. This suggests that high levels of guard-cell-specific HXK expression may impose a physiological cost that limits growth rather than conferring a benefit.

5.3. Discussion

Improving stomatal responses to environmental change can help to optimise both photosynthetic carbon gain and intrinsic water use efficiency. Under fluctuating light, slow stomatal opening imposes a restriction on carbon assimilation, and slow stomatal closure can lead to excess water loss (McAusland et al., 2016). In this study, the potential of manipulating the internal mechanics of stomatal behaviour was explored using the transgene AHA2, encoding a membrane-hyperpolarising H^+-ATPase proton pump, and HXK1, encoding a sugar-phosphorylating enzyme that senses carbohydrate status to trigger ABA-mediated stomatal closure. Both genes, when overexpressed in the guard cells, have previously been shown to impact stomatal behaviour. Both genes, when overexpressed in the guard cells, have previously been shown to impact stomatal behaviour. Specifically, AHA2 enhances stomatal opening, leading to increased CO_2 uptake and growth, while HXK1 promotes sugar- and ABA-mediated stomatal closure, improving water-use efficiency and stress tolerance (Kelly *et al.*, 2013, 2019; Wang *et al.*, 2013; Lugassi *et al.*, 2015, 2019). HXK and AHA2 were also shown not to have a detrimental effect on photosynthetic carbon assimilation or ABA-mediated stomatal closure, respectively. This lack of negative trade-offs suggests that combining both genes could provide additive benefits, enhancing CO_2 uptake through increased opening while simultaneously improving water-use efficiency via sugar- and ABA-mediated closure. In T1 line selection, HXK single lines exhibited faster photosynthetic induction due to higher gsw under high light, alongside significantly lower lag times (l) for both stomatal opening and closure. However, in the T2 experiment, which also included AHA2

single lines and was conducted under low light conditions, HXK single lines displayed reduced F_v/F_m, while high-expressing AHA2 lines suffered lower YII during photosynthetic induction and relaxation. *A/Ci* analyses revealed that AHA2 single lines had reduced A_{max}, whereas other genotypes were unaffected. Step-change in light intensity experiments showed no significant differences between lines, suggesting that the advantage conferred by HXK under high light is lost in low light. Notably, all AHA2 single lines, as well as one of three HXK single lines, exhibited reduced biomass (fresh weight, dry weight, and leaf area). HXK enhances stomatal responsiveness under high light, but this advantage disappears under low light, while AHA2 overexpression imposes penalties on photosynthetic efficiency and growth, and combining the two genes does not yield additive benefits.

5.3.1. Effect Of Hexokinase On Stomatal Behaviour

The guard-cell-specific overexpression of Hexokinase impacted stomatal dynamics and thus leaf gas exchange under fluctuating conditions during T1 selection. Most reports of HXK overexpression in guard cells have focused on steady-state stomatal behaviour. Across multiple species, including tomato, Arabidopsis, citrus and tobacco, HXK expression consistently reduced diurnal g_{sw} and transpiration without negatively affecting photosynthesis or growth (Kelly *et al.*, 2013, 2019; Lugassi *et al.*, 2015, 2019; Acevedo-Siaca *et al.*, 2022). This, alongside the molecular evidence of its function, led to the prevailing view of HXK as a sugar/ABA-mediated closure regulator, coordinating carbohydrate status with water conservation. In contrast, the dynamic measurements of step changes in irradiance here revealed that HXK single lines

maintained higher g_{sw} than azygous controls throughout both the light induction and relaxation phases, accompanied by accelerated photosynthetic induction. One likely explanation is that the lower diurnal g_{sw} typically observed in HXK lines enables greater soil water availability during growth, thereby relaxing water constraints under experimental conditions (Acevedo-Siaca *et al.*, 2022). This water-conservative baseline may allow stomata in HXK lines to open more readily during dynamic transitions, resulting in the consistently higher g_{sw} observed here under fluctuating light.

Beyond this physiological explanation, the findings presented here also highlight a mechanistic contrast with the existing literature. Previous studies have established a clear role for HXK in mediating sugar-induced stomatal closure. Guard cell-targeted HXK accelerates closure through an ABA- and NO-dependent pathway, reducing diurnal g_{sw} and transpiration in multiple species, including tomato, Arabidopsis, citrus, and tobacco (Kelly *et al.*, 2013, 2019; Lugassi *et al.*, 2015, 2019; Acevedo-Siaca *et al.*, 2022). This body of work emphasised HXK as a closure regulator, consistent with its function as a sugar sensor linking carbohydrate accumulation to stomatal restriction. By contrast, the dynamic light experiments reported in this study revealed that HXK single lines exhibited reduced lag times for both opening and closure, suggesting that HXK also enhances the sensitivity of stomata to environmental changes. One explanation lies in its dual catalytic–signalling role. While high sugar concentrations drive closure via ABA/NO signalling, at lower sugar levels, HXK activity may primarily serve a metabolic function, rapidly phosphorylating glucose to glucose-6-phosphate (Rolland, Baena-Gonzalez and Sheen, 2006; Granot, David-Schwartz and Kelly, 2013). This metabolite feeds directly into glycolysis and the oxidative pentose phosphate pathway, providing ATP and NADPH

to fuel guard-cell transport processes. Enhanced HXK expression would therefore ensure a faster energy supply to support plasma-membrane H^+-ATPase activity and K^+ uptake, thereby accelerating the onset of stomatal opening (Lawson and Blatt, 2014; Jezek and Blatt, 2017). A further, longer-term factor may be that HXK plants exhibit lower diurnal g_{sw}, as reported in steady-state studies (Kelly *et al.*, 2013, 2019; Lugassi *et al.*, 2019), leading to improved soil water conservation. This water-conservative background may relax hydraulic limitations during step-change measurements, enabling guard cells in HXK lines to build turgor more rapidly once the opening machinery is triggered. Together, these observations suggest a concentration- and context-dependent model: at low sugar, HXK enhances guard-cell metabolic readiness and speeds up opening, whereas at high sugar it engages the ABA/NO pathway to promote closure. This dual functionality reconciles the findings presented here with the established literature, reframing HXK not as a closure-specific regulator but as a broad modulator of stomatal sensitivity and kinetics.

By contrast, when HXK plants were grown under low light (T2), these advantages were lost, and HXK single lines even exhibited reduced F_v/F_m. This may be due to a shortfall in sugar availability before induction. Under low-light growth, photosynthetic capacity and carbohydrate reserves are diminished, leaving guard cells with insufficient substrate to activate HXK-driven metabolic priming (Lawson et al., 2014). Without an adequate sugar pool, HXK cannot provide the accelerated G6P flux required to support rapid ATP generation and turgor adjustments. Similarly, the closure advantage conferred by HXK under high-light growth is also absent, as limited photosynthate export and reduced phloem loading mean that sugar accumulation around guard cells is too low to

engage the HXK–ABA/NO closure pathway (Kelly *et al.*, 2013, 2019; Lugassi *et al.*, 2015, 2019; Acevedo-Siaca *et al.*, 2022). Thus, the discrepancy between high- and low-light-grown HXK plants highlights the context-dependence of HXK function: under high light, elevated sugar supply enables HXK to act both as a priming factor for faster induction and as a mediator of feedback closure; under low light, insufficient sugar prevents engagement of either pathway, erasing the dynamic advantage.

HXK lines grown under low irradiance displayed significantly lower F_v/F_m, indicating impaired PSII maximum efficiency. This contrasts with previous reports where guard-cell–targeted HXK reduced stomatal conductance and transpiration without negatively affecting photosynthesis or growth under normal or drought conditions (Kelly *et al.*, 2013, 2019; Lugassi *et al.*, 2019). HXK mediates sugar-induced stomatal closure through ABA and nitric oxide signalling (Kelly *et al.*, 2013), and its persistent activity may enhance ABA sensitivity even under low-light, non-stressful conditions. Elevated ABA signalling is known to restrict CO_2 supply by tightening stomatal closure and to increase excitation pressure at PSII, both of which enhance vulnerability to photodamage (Lawson, Kramer and Raines, 2012). Thus, the reduced F_v/F_m observed in HXK plants under low light reflects a depressed CO_2 availability due to stomatal closure in response to small sugar fluxes.

Importantly, these physiological effects were accompanied by a negative association between HXK expression level and whole-plant biomass accumulation. Across genotypes, increased KST1:HXK expression was associated with reduced fresh weight and showed a near-significant negative relationship with dry weight. While the limited number of genotypes precludes strong quantitative conclusions, this trend is

consistent with the known role of HXK in promoting a more conservative stomatal phenotype (Kelly et al., 2013, 2019; Lugassi et al., 2015, 2019; Acevedo-Siaca et al., 2022).

Under low irradiance, where photosynthetic capacity and carbohydrate availability are already constrained, even modest reductions in stomatal conductance can disproportionately limit cumulative carbon assimilation and growth (Walters and Horton, 1994; Evans and Poorter, 2001; Lawson, Kramer and Raines, 2012). Persistent HXK activity may therefore impose a growth penalty by restricting CO_2 supply during dynamic light transitions and by increasing the metabolic cost of guard-cell signalling (Rolland, Baena-Gonzalez and Sheen, 2006; Granot, David-Schwartz and Kelly, 2013; Jezek and Blatt, 2017).

Together, these findings suggest that while HXK-mediated stomatal regulation can be advantageous under conditions of high light or water limitation, its expression under low-light acclimation may inadvertently constrain carbon gain and biomass accumulation, highlighting the strong context-dependence of guard-cell metabolic engineering.

5.3.2. Effect Of AHA2 On Stomatal Behaviour

Despite its canonical role in promoting stomatal opening, AHA2 single lines in this study did not show any increase in g_{sw} during step-change measurements, nor differences in modelled stomatal kinetic parameters. Additionally, they suffered reduced YII during photosynthetic induction and relaxation, lower A_{max} in A/C_i curves, and decreased biomass. This indicates that enhanced proton pumping capacity in guard

cells does not necessarily translate into increased stomatal conductance or improved carbon gain, and instead imposes physiological costs in tobacco. This contrasts with Wang et al. (2013), who reported that guard-cell-specific overexpression of AHA2 in Arabidopsis promoted stomatal opening, CO_2 uptake, and biomass accumulation (Wang *et al.*, 2013). One explanation is a stoichiometric/regulatory mismatch: the activity of the plasma membrane H^+-ATPase depends on phosphorylation, 14-3-3 protein binding, and the coordination of downstream transporters(Palmgren, 2001; Haruta *et al.*, 2010; Falhof *et al.*, 2016; Inoue and Kinoshita, 2017). Overexpressing AHA2 without parallel upregulation of these cofactors may lead to pumps that are abundant but not properly activated in vivo, explaining the absence of higher g_{sw}. At the same time, mis-timed or constitutive proton pumping is energetically costly, diverting ATP from carbon assimilation and perturbing ion homeostasis (excess apoplastic acidification, disrupted K^+/anion fluxes).

Overexpression of AHA2 in guard cells imposes both production and operational costs. AHA2 is a large, multi-pass plasma membrane protein whose biosynthesis requires substantial investment of amino acids and lipids for folding, ER–Golgi trafficking, and membrane insertion, thereby diverting carbon and nitrogen resources from growth processes. Once incorporated into the plasma membrane, AHA2 activity is energetically expensive: each cycle of proton pumping consumes ATP, and guard-cell transport processes already account for one of the most energy-demanding cellular activities (Lawson and Blatt, 2014; Jezek and Blatt, 2017). Although guard-cell chloroplasts can generate ATP and reductants, their output is limited, and the majority of the energetic supply depends on sugars imported from mesophyll cells via apoplastic

transport (Outlaw, 2010). Under suboptimal light, when whole-plant carbon gain and ATP production are constrained, the increased energetic burden of sustaining elevated AHA2 levels is likely to exacerbate competition for resources, explaining the reductions in photochemical efficiency (YII), carboxylation capacity (A_{max}), and biomass observed in the KST1::AHA2 lines here. This interpretation is consistent with Wang et al. (2013), who reported that the benefits of AHA2 overexpression for stomatal conductance and CO_2 assimilation were only apparent under moderate-to-high irradiance, highlighting a strong dependency on light-driven energy supply (Wang *et al.*, 2013). Crucially, AHA2 activation is directly regulated by blue-light signalling through phototropins, which phosphorylate the C-terminal regulatory domain of the pump and promote 14-3-3 protein binding, locking the ATPase in an active conformation (Kinoshita and Shimazaki, 1999; Inoue and Kinoshita, 2017). Under low irradiance, limited blue-light signalling and low ATP availability would restrict the activation and fuelling of excess AHA2, explaining why the KST1::AHA2 lines did not display higher g_{sw} during step-change measurements yet still incurred metabolic costs. Thus, AHA2 overexpression without sufficient irradiance and regulatory capacity results in an energetic burden rather than a photosynthetic benefit.

5.3.3. The Combined Effect Of Hexokinase And AHA2 On Stomatal Behaviour

The combined guard-cell-specific overexpression of HXK and AHA2 produced outcomes distinct from either single transgene, reinforcing the idea that metabolic context and regulatory balance are crucial for guard-cell engineering. In the T1 high-light–

grown plants, HXK single lines displayed faster photosynthetic induction and reduced lag times for stomatal opening and closure, consistent with HXK's role in sugar phosphorylation and sensing to fine-tune guard-cell responsiveness (Kelly *et al.*, 2013, 2019; Lugassi *et al.*, 2015, 2019). However, the HXK::AHA2 double lines did not differ from the controls, indicating that AHA2 overexpression counteracted HXK's kinetic advantage. This suggests a form of metabolic antagonism, while HXK may enhance responsiveness through sugar signalling and metabolic priming, AHA2 may impose a significant ATP demand and regulatory bottleneck that may constrain the same transport machinery HXK accelerates. Since H^+-ATPase activity depends on phosphorylation, 14-3-3 binding, and adequate ATP supply (Palmgren, 2001; Falhof *et al.*, 2016), an oversupply of pumps without coordinated regulatory capacity may increase basal energetic cost without increasing g_{sw}. In this scenario, the system becomes energetically saturated, flattening the dynamic range of stomatal responses and erasing the kinetic improvements seen in HXK single lines grown under high light.

In contrast, T2 plants grown under low-light growth conditions, the double lines did not suffer the penalties seen in AHA2 single lines. AHA2 plants alone showed reduced YII, lower A_{max}, and diminished biomass, consistent with the high cost associated with producing and operating abundant H^+-ATPases under carbon-limiting conditions. The absence of these penalties in the HXK::AHA2 doubles suggests a compensatory role of HXK. By phosphorylating glucose to glucose-6-phosphate, HXK sustains glycolysis and the oxidative pentose phosphate pathway, providing ATP and reductants that may help buffer the additional metabolic burden of AHA2 expression (Kelly *et al.*, 2013). This energy supply could prevent the imbalances that lead to photochemical stress in AHA2

lines, explaining why the doubles performed comparably to controls rather than mirroring the negative phenotype of AHA2 singles. Moreover, HXK's sugar-sensing function could provide a closure bias that tempers AHA2-driven proton pumping, preventing runaway stomatal opening and excessive water loss under low light when photosynthate is scarce (Kelly *et al.*, 2013). This interpretation is also consistent with Wang et al. (2013), who showed that AHA2 overexpression did not interfere with ABA-mediated stomatal closure, indicating that the closure pathways remain intact (Wang *et al.*, 2013). In the double lines, HXK may therefore act through its sugar/ABA signalling to reinforce the closure response, effectively balancing AHA2-driven opening and reducing the risk of excessive conductance under conditions of limited carbon supply.

Together, these findings underscore that HXK and AHA2 interact in condition-dependent ways. Under high light, the interaction may be counterproductive, as the energetic burden of AHA2 and electrophysiological bias may neutralise the enhancements provided by HXK. Under low light, the interaction becomes compensatory, as the metabolic and signalling roles of HXK may offset the penalties of AHA2 overexpression. Crucially, in neither context did the double lines outperform HXK singles, suggesting that simple stacking of stomatal genes does not guarantee additive benefits. Instead, guard-cell engineering must account for the stoichiometric balance of transporters, the regulatory capacity of kinases and 14-3-3 proteins, and the availability of metabolic energy. The contrasting outcomes in HXK::AHA2 plants thus provide a cautionary example: single-gene manipulations can yield predictable improvements, but combining them may create emergent trade-offs unless the entire metabolic and regulatory framework is considered.

6. General discussion

Stomata are central regulators of plant productivity, acting as microscopic gateways that coordinate carbon assimilation with water loss. By modulating the diffusion of CO_2 into the mesophyll, stomata directly determine photosynthetic capacity, while their regulation of transpiration underpins plant water relations and evaporative cooling (Hetherington and Woodward, 2003; Lawson and Morison, 2004; Kirkham, 2005). At the global scale, the cumulative effect of stomatal behaviour influences both the terrestrial carbon sink and the hydrological cycle, linking leaf-level processes to climate regulation (Lawson and Blatt, 2014; Hatfield and Dold, 2019). Despite their central role in regulating gas exchange, stomata are not inherently optimised for maximising photosynthetic productivity. Instead, their behaviour is often biased toward minimising water loss, reflecting a conservative strategy shaped by the need to balance carbon gain with hydraulic safety (Bertolino, Caine and Gray, 2019; Henry, Grace P John, *et al.*, 2019; Yokoyama *et al.*, 2023; Fernández-Molano *et al.*, 2025). Mesophyll photosynthesis can respond to changes in light within seconds, yet stomatal movements typically lag by several minutes, creating a persistent temporal mismatch (Lawson and Blatt, 2014; McAusland et al., 2016). Under fluctuating environmental conditions, this lag imposes two major constraints: lost carbon gain during light increases, when stomata fail to open rapidly enough to meet mesophyll demand, and excess water loss during light decreases, when stomata remain open despite declining CO_2 assimilation (Lawson and Vialet-Chabrand, 2019). Improving stomatal capacity and responsiveness has therefore emerged as a promising target for enhancing photosynthetic efficiency and water-use efficiency in crops (Drake, Froend and Franks, 2013; Lawson and Matthews, 2020).

This thesis explored strategies to overcome stomatal limitations on photosynthesis through genetic manipulation. Using the model species *Nicotiana tabacum* (tobacco) and the commercial crop *Fragaria* × *ananassa* (strawberry), transgenic lines were generated to test how altering stomatal development and guard cell behaviour affects gas exchange, photosynthesis, and growth. These experiments examined three key avenues: (i) increasing stomatal density to enhance CO_2 uptake, (ii) improving stomatal responsiveness and kinetics through manipulation of guard cell metabolism, and (iii) assessing the feasibility of stacking multiple traits to achieve additive benefits. Across both species, these approaches revealed the potential for stomatal engineering to mitigate diffusional limitations on photosynthesis, while also highlighting the compensatory mechanisms, context-dependencies, and systemic trade-offs that constrain their effectiveness.

6.1. Increasing SD Through Genetic Manipulation

Stomatal conductance, a central determinant of plant gas exchange, is governed by a combination of anatomical traits, such as stomatal density, size, and pore geometry, and dynamic physiological responses that regulate stomatal aperture in response to environmental cues (Franks and Farquhar, 2007; Dow, Berry and Bergmann, 2014; Lawson and Blatt, 2014). One of the most direct approaches to alleviating diffusional constraints on photosynthesis is to increase stomatal density (SD), thereby providing more pores for CO_2 diffusion into the leaf. Experimental manipulations of the STOMAGEN/EPFL9 gene in *Arabidopsis thaliana* demonstrated that a two- to three-fold

increase in SD led to a ~30% enhancement in photosynthetic CO_2 assimilation under saturating light conditions, however, without greater biomass accumulation (Tanaka et al., 2013). Under fluctuating light conditions, plants with increased stomatal density, such as EPF1 knockout and STO-overexpressing lines, exhibited enhanced photosynthetic induction and higher cumulative CO_2 assimilation compared to wild-type controls. Notably, the moderate increase in SD seen in *epf1* conferred a significant biomass advantage, suggesting that enhancing stomatal density can improve carbon gain under dynamic light, though excessive increases, as in STO-overexpressing lines, may yield diminishing returns (Sakoda *et al.*, 2020).

These results firmly established stomatal development as a tractable genetic target for improving gas exchange. However, they also highlighted inherent trade-offs, as increased SD was accompanied by substantial increases in transpiration and reduced water-use efficiency (WUE) (Tanaka et al., 2013; Lawson and Blatt, 2014; Sakoda et al., 2020).

The work presented in this thesis tested whether similar gains could be achieved in both a model system (*Nicotiana tabacum*) and a commercially relevant crop (*Fragaria* × *ananassa*). In tobacco, constitutive overexpression of STO reliably produced significant increases in SD across both abaxial and adaxial surfaces, consistent with the expected phenotype (Chapter 4). Despite these increases, proportional improvements in stomatal conductance (g_{sw}) and CO_2 assimilation were not consistently observed, suggesting that compensatory processes may have limited the realised benefit. Potential mechanisms described in the literature, including reductions in stomatal size, restrictions on maximum aperture, or altered epidermal patterning, could help to explain why increases

in SD did not always translate into higher gas exchange (Büssis et al., 2006; Franks and Beerling, 2009; Drake, Froend and Franks, 2013). Amphistomatous leaves, having stomata on both adaxial and abaxial surfaces like those of *Nicotiana tobacum*, often exhibit reduced CO_2 diffusion path lengths and lower boundary layer resistance, which tends to increase internal CO_2 concentration (C_i) and chloroplast CO_2 concentration (C_c) compared to hypostomatous leaves (Parkhurst, 1978; Mott and Michaelson, 1991; Drake *et al.*, 2019; Harrison *et al.*, 2020; Xiong and Flexas, 2020; Triplett, Buckley and Muir, 2024; Watts *et al.*, 2024). Thus, due to already reduced diffusional constraints, increasing the SD of amphistomatous leaves may provide little to no additional benefit to alleviating diffusional constraints. Benefits may yet be reaped at higher temperatures, as elevated stomatal density can enhance evaporative cooling capacity, thereby mitigating the detrimental effects of supra-optimal temperatures on the heat-sensitive photosynthetic machinery. Increased transpirational water loss can reduce leaf temperature by several degrees, which helps preserve photosystem efficiency and enzymatic activity under thermal stress (Urban *et al.*, 2017; Diao *et al.*, 2024). Recent evidence further suggests that even when photosynthesis declines at high temperatures, stomatal conductance may remain elevated to facilitate evaporative cooling, effectively decoupling CO_2 uptake from water loss (Diao *et al.*, 2024). In Arabidopsis, mutants with extremely low SD suffered reduced cooling at 30°C but compensated via structural modifications, emphasising the importance of stomatal traits in thermal resilience (Pérez-Bueno *et al.*, 2022). These mechanisms may contribute to improved diurnal assimilation and thermal stability in high-SD genotypes exposed to episodic heat stress.

In strawberry, overexpression of STO similarly increased SD, but the gains were largely associated with the formation of stomatal clusters that violated the one-cell spacing rule (Chapter 3) (Geisler, Nadeau and Sack, 2000; Dow, Berry and Bergmann, 2014). This clustering impaired stomatal function, resulting in poor coordination of aperture dynamics and reduced responsiveness to fluctuating light (Dow, Berry and Bergmann, 2014). As a result, the anticipated increase in g_{sw} and A was not realised, and in some cases, clustered stomata were detrimental, resulting in reduced g_{sw} via compromised stomatal function (Dow, Berry and Bergmann, 2014). Stomatal clustering was also present in previous overexpressions of STO in Arabidopsis, yet still resulted in increases in g_{sw} and A (Tanaka et al., 2013; Sakoda et al., 2020). The contrasting outcomes of STO overexpression in *Arabidopsis* and strawberry may, in part, reflect differences in genome size and its constraints on stomatal dimensions. Genome size imposes a lower limit on guard cell size, with larger genomes producing larger minimum stomata (Jordan *et al.*, 2015; Roddy *et al.*, 2020). *Arabidopsis thaliana*, with a compact diploid genome of ~135 Mb (Lian *et al.*, 2024), can accommodate increases in stomatal density by producing smaller guard cells, thereby maintaining efficient packing with relatively little clustering. This allows STO overexpression in *Arabidopsis* to increase both stomatal conductance and photosynthetic assimilation despite some clustering (Tanaka et al., 2013; Sakoda et al., 2020). In contrast, the cultivated strawberry is an octoploid species with a haploid genome of ~805 Mb (Edger *et al.*, 2019). Such a large genome constrains the minimum size of guard cells, limiting the degree to which size can decrease in response to rising density. As a consequence, elevated SD in strawberry more readily leads to stomatal clustering, mechanical crowding, and overlapping substomatal airspaces, impairing aperture dynamics and reducing responsiveness

under fluctuating light (Chapter 3). These genome-imposed constraints may therefore help explain why Arabidopsis tolerates clustering without forfeiting gains in gas exchange, whereas strawberry exhibits functional penalties when SD is artificially increased. As both Arabidopsis and Strawberry are hypostomatous, species and perhaps even the genetic background must be taken into account when aiming to manipulate epidermal patterning and predictions of such outcomes from studies in model species may not so easily translate to complex crops.

Interestingly, in strawberry, the changes in SD were confined to the abaxial leaf surface, reinforcing the hypostomatal nature of this species. This asymmetry raises important questions about the developmental mechanisms that determine epidermal sensitivity to stomatal developmental signals. Because the STO construct was driven by the constitutive CaMV 35S promoter, the signal promoting stomatal development should have been present ubiquitously throughout the leaf (Benfey and Chua, 1990). The absence of any detectable changes on the adaxial surface, therefore, suggests that this epidermis is largely insensitive to STO-mediated signalling. Several mechanisms could underlie this insensitivity. Firstly, leaf polarity cues establish distinct developmental programs between adaxial and abaxial domains, with transcription factors such as PHABULOSA and KANADI shaping epidermal identity and potentially constraining responsiveness to stomatal signalling pathways (Eshed *et al.*, 2001; Emery *et al.*, 2003). Second, components of the EPF/TMM/ERECTA signalling module that regulate stomatal lineage divisions may be differentially expressed or functionally limited on the adaxial surface, thereby restricting the capacity for additional stomata to form (Shpak *et al.*, 2005; Hunt and Gray, 2009; Hunt, Bailey and Gray, 2010; J. S. J. Lee *et al.*, 2015). Finally,

although STO is normally expressed in the mesophyll and diffuses to the epidermis (Sugano *et al.*, 2009; Hunt, Bailey and Gray, 2010; J. S. J. Lee *et al.*, 2015), its perception may depend on receptor availability or cuticular properties that differ between surfaces, making the adaxial epidermis relatively insensitive. Together, these possibilities suggest that anatomical context and intrinsic epidermal polarity can strongly constrain the outcomes of developmental manipulations, even when transgenes are expressed constitutively.

Overall, these results highlight the difficulty of achieving consistent gains in carbon assimilation through SD manipulation alone. Compensatory mechanisms appear to act as a stabilising force, buffering the balance between carbon gain and water conservation.

6.2. Improving Stomatal Responsiveness And Kinetics Through Genetic Manipulation

While increasing stomatal density has the potential to enhance CO_2 diffusion, an equally important limitation arises from the inherently slow kinetics of stomatal movements. Mesophyll photosynthesis can respond to fluctuations in irradiance within seconds, yet stomatal opening and closure typically lag by several minutes (Lawson and Blatt, 2014; McAusland et al., 2016). This temporal mismatch leads to lost carbon assimilation during light increases and excess water loss during light decreases, representing a major constraint under dynamic environmental conditions (Lawson and Vialet-Chabrand, 2019). Engineering faster or more responsive stomata, therefore,

represents a promising avenue for improving photosynthetic efficiency and water-use efficiency in crops (Lawson and Matthews, 2020).

Guard cell–specific overexpression studies have demonstrated that manipulating sugar and ion transport pathways can produce distinct shifts in stomatal behaviour. Lines overexpressing *Arabidopsis* Hexokinase (HXK1) in guard cells consistently show reduced stomatal conductance and transpiration, leading to improved water-use efficiency and enhanced tolerance to drought and salt stress, often without compromising photosynthesis or growth (Kelly *et al.*, 2013, 2019; Lugassi *et al.*, 2015, 2019; Acevedo-Siaca *et al.*, 2022). By contrast, overexpression of the plasma membrane H^+-ATPase AHA2 in guard cells accelerates light-induced stomatal opening, enhancing photosynthetic rates and plant growth while retaining normal closure responses to ABA and darkness (Wang *et al.*, 2013; Toh *et al.*, 2021). Taken together, these studies illustrate that HXK and AHA2 manipulations yield complementary outcomes: HXK favouring tighter closure and water conservation, and AHA2 promoting faster opening and greater carbon assimilation. The combination of such traits could, in principle, generate stomata that balance both rapid responsiveness and reinforced closure, better aligning stomatal dynamics with mesophyll carbon demand under fluctuating environments.

In tobacco, guard cell-targeted expression of HXK reduced stomatal lag times to opening and closure, and accelerated the relative induction of CO_2 assimilation following step increases in light intensity, particularly in the T1 generation grown under high light conditions (Chapter 5). These benefits, however, were lost in the T2 generation grown under low light, emphasising that the effects of HXK are context dependent. In strawberry, HXK expression did not directly alter behaviour beyond the wild-type

response; rather, it appeared to rescue the innate low lag time seen in control lines when responding to decreases in light intensity in lines that had impaired stomatal response, likely due to stomatal clustering (Chapter 3). In both strawberry and tobacco, higher low-light g_{sw} in guard cell HXK overexpressors may reflect a combination of water-conservative growth, which relaxes hydraulic limits under experimental conditions, and the dual catalytic–signalling role of HXK (Discussed in Chapter 5). While high sugar concentrations activate ABA/NO-dependent closure (Kelly *et al.*, 2013; Lugassi *et al.*, 2015; Acevedo-Siaca *et al.*, 2022), at lower sugar levels, HXK may primarily fuel metabolism, enhancing guard-cell energy supply and thereby accelerating opening responses (Rolland, Baena-Gonzalez and Sheen, 2006; Granot, David-Schwartz and Kelly, 2013; Lawson and Blatt, 2014; Jezek and Blatt, 2017). Overall, HXK overexpression does not consistently enhance stomatal responsiveness, but it can accelerate dynamics under favourable conditions and mitigate impairments when stomatal function is compromised. This contrasts with much of the existing literature, where HXK expression typically depresses g_{sw}, suggesting that its effects may depend on whether its primary role is sugar sensing or hexose phosphorylation (Kelly *et al.*, 2013, 2019; Granot *et al.*, 2015; Lugassi *et al.*, 2015, 2019; Acevedo-Siaca *et al.*, 2022). In the latter case, HXK may provide additional G6P to fuel guard cell metabolism and facilitate opening (see Chapter 5). These observations highlight the need for further study into the catalytic role of HXK in guard cells, and how the balance between its enzymatic and signalling functions shapes stomatal behaviour.

The effects of AHA2 were more limited than anticipated. Guard cell-targeted overexpression of AHA2 in tobacco did not produce significant differences in stomatal

conductance, assimilation, or water-use efficiency under fluctuating light (Chapter 5). Instead, several AHA2 lines displayed reduced photosynthetic capacity and lower operating efficiency of photosystem II, particularly under low light conditions. These results contrast with earlier reports in *Arabidopsis*, where enhanced H^+-ATPase activity increased light-induced stomatal opening and boosted carbon gain (Wang *et al.*, 2013). One possible explanation is that the energetic costs of sustained H^+-ATPase activity in tobacco, especially under carbon-limited conditions, outweighed any benefit to CO_2 uptake. Alternatively, differences in promoter strength, species-specific guard cell signalling, or light environment may have contributed to the lack of a positive effect.

A broader trend across both species and genotypes was that stomatal behaviour leaned towards faster and more immediate closure than opening. Lag times and kinetic parameters consistently showed that stomata closed more rapidly following decreases in light intensity than they opened in response to increases (Chapters 3–5). This bias towards closure has been reported previously and is often interpreted as a conservative strategy to limit unnecessary water loss (McAusland et al., 2016; Matthews, Vialet-Chabrand and Lawson, 2018). From an ecological perspective, this asymmetry reflects the evolutionary prioritisation of water conservation over maximising instantaneous carbon gain, a trade-off that has enabled survival across diverse environments but also constrains primary productivity under fluctuating light (Anderegg *et al.*, 2018; Henry, Grace P. John, *et al.*, 2019; Lawson and Vialet-Chabrand, 2019; Zhu *et al.*, 2023). Engineering interventions such as HXK more often reinforced or, in the case of the clustered strawberries, rescued closure responses than accelerated opening highlights how deeply embedded this bias is in guard cell behaviour. Even when HXK did enhance

opening under favourable conditions, its stronger and more consistent effects were associated with closure, underlining the evolutionary prioritisation of water conservation over carbon gain.

Taken together, these findings highlight both the promise and the complexity of engineering stomatal kinetics. HXK manipulation can influence the coordination of photosynthesis and stomatal conductance, but its effects are highly context dependent and more often reinforce closure dynamics than accelerate opening. Previous studies have shown that AHA2 overexpression can promote rapid stomatal opening and enhance carbon assimilation (Wang *et al.*, 2013; Toh *et al.*, 2021); however, in the low-light–grown plants examined here, it proved to be net detrimental, with reductions in maximum photosynthesis and biomass. The lack of additive benefit when combined with HXK further underscores the difficulty of achieving predictable outcomes from guard cell engineering. More broadly, the intrinsic asymmetry of stomatal behaviour, faster and more consistent closure relative to opening, appears to impose a fundamental limit on the extent to which photosynthetic induction can be improved through guard cell manipulations alone. Future work may therefore need to identify targets that directly accelerate opening kinetics, or to combine guard cell interventions with mesophyll traits, to maximise carbon gain under dynamic light.

6.3. Feasibility Of Gene Stacking Stomatal Traits For Added Benefit

Multigene engineering has proven a powerful tool for enhancing photosynthesis when targets act on separate limitations. For example, simultaneous overexpression of

SBPase, FBPA and the putative bicarbonate transporter *ictB* in tobacco doubled biomass compared with WT, greatly exceeding the benefit of any single gene (Simkin *et al.*, 2015). Similar additive gains have been reported when combining CBC enzymes with photorespiratory bypasses (Simkin *et al.*, 2017) or with algal electron transport components under field conditions (López-Calcagno et al., 2020). These successes provided the foundation for testing whether stacking stomatal traits could produce complementary benefits.

The logic behind the combination of two stomatal traits, constitutive overexpression of STO alongside guard-cell-specific overexpression of HXK, appears to be sound. SD increases via STO increased g_{sw} and A at the cost of iWUE (Tanaka et al., 2013; Sakoda et al., 2020). The decrease in iWUE caused by STO could be offset by HXK, potentially without offsetting any of the gains in A (Kelly *et al.*, 2013, 2019; Lugassi *et al.*, 2015, 2019; Acevedo-Siaca *et al.*, 2022). The combination of these two traits was therefore expected to raise the potential for diffusion (via SD) while cushioning the water-use penalty (via HXK).

In strawberry, however, the anticipated complementarity between STO and HXK was not realised. The expression of neither transgene individually had its predicted effect, impaired stomatal function due to clustering via STO, and HXK did not enhance the innate stomatal kinetics. HXK alone did not surpass wild-type responses, but when overexpressed alongside STO in the double lines, it appeared to rescue the innate lag in closure in clustered lines, suggesting that its function in the guard cells could partially overcome the impaired response to stomatal closure when stomata cluster. HXK activity in guard cells may help overcome clustering-related limitations on closure by reinforcing

ABA-mediated sugar sensing and supplying additional metabolic drive. Overexpression of HXK accelerates sugar-induced closure via ABA signalling (Kelly *et al.*, 2013; Granot *et al.*, 2015), and its catalytic product glucose-6-phosphate (G6P) has been shown to directly induce stomatal closure in an irradiance-dependent manner, partly through ROS production (DI-An *et al.*, 2021). By amplifying closure signals and providing substrates for guard cell metabolism, HXK can compensate for impaired coordination in clustered stomata, enabling more uniform and rapid closure despite mechanical and hydraulic constraints (Lugassi *et al.*, 2019). However, strawberry stomata are already characterised by intrinsically conservative behaviour, with rapid and strong closure prioritised over opening (Yokoyama *et al.*, 2023). This likely makes additional HXK activity largely redundant under normal conditions, with its effects only evident as a rescue mechanism when clustering impairs function. When combined, the two traits failed to deliver additive gains in g_{sw}, A, or iWUE as the deleterious effects of clustering outweighed the potential gains from higher stomatal number and HXK's stabilisation.

The STO + ictB stack was designed to increase diffusion capacity and biochemical capacity in tandem: STO by increasing stomatal density, and ictB by enhancing photosynthetic performance through mechanisms that remain incompletely defined. Early studies reported ictB-associated increases in photosynthesis under limiting CO_2 (Lieman-Hurwitz *et al.*, 2003), and subsequent work in soybean and maize demonstrated gains in assimilation, biomass, and yield under both controlled and field conditions (Hay *et al.*, 2017; Koester *et al.*, 2021). In tobacco, ictB has shown variable effects, with strong additive gains when stacked with CBC enzymes (Simkin *et al.*, 2015), but negligible benefit under field conditions when expressed alone (Ruiz-Vera *et al.*, 2022). In this

study, the hypothesised complementarity between STO and ictB did not materialise: the stack showed no consistent increases in A, g_{sw}, or biomass relative to either single gene or wild type. A likely explanation is that both manipulations ultimately act to raise chloroplastic CO_2 concentration (C_c) via different mechanisms. ictB expression has been shown to lower CO_2 compensation points and enhance in vivo Rubisco activation, consistent with increased CO_2 availability at the enzyme site (Lieman-Hurwitz *et al.*, 2003). Similarly, increasing stomatal density through STO elevates g_{sw} and boosts CO_2 supply to the mesophyll, thereby raising C_c (Tanaka et al., 2013). When combined, these traits may therefore converge on the same limiting process, producing diminishing returns rather than additive benefits. Although ictB alone has been shown to enhance photosynthesis and biomass in tobacco (Simkin *et al.*, 2015), the largest gains occurred when it was combined with CBC enzymes such as SBPase and FBPA, which relieve distinct biochemical bottlenecks. In that study, the triple stack more than doubled biomass compared to WT, far exceeding the benefit of any single gene. By contrast, in the STO + ictB lines presented here, both manipulations potentially converged on C_c enhancement, restricting the potential for additive benefits. Furthermore, retransformation of plants with identical viral expression cassettes increased the risk of transgene silencing, which may have further limited ictB expression and reduced its impact in the stacked lines (Chapter 4). Finally, the low-light growth conditions used here likely accentuated these constraints, as photosynthesis was predominantly light-limited, reducing the potential for synergistic gains from traits that primarily enhance CO_2 supply and utilisation.

HXK and AHA2 were selected as a kinetic pair, with the rationale that HXK would promote faster or more stable closure while AHA2, a plasma membrane H^+-ATPase, would enhance light-induced opening. Both manipulations had previously been reported to confer benefits when tested individually: HXK improving water-use efficiency and closure dynamics (Kelly *et al.*, 2013, 2019; Lugassi *et al.*, 2015, 2019), and AHA2 increasing g_{sw} and *A* in *Arabidopsis*, albeit at the cost of WUE (Wang *et al.*, 2013; Toh *et al.*, 2021). The expectation was that combining them would improve synchronisation of stomatal movements from both ends, reducing induction lags and water loss under fluctuating light. In practice, HXK alone conferred reduced lag times and improved coordination with photosynthesis in T1 plants grown under high light (Chapter 5), while AHA2 single lines in tobacco showed no consistent benefit and, in some cases, reduced photosynthetic performance. The stacked HXK + AHA2 plants did not outperform HXK alone, and in some instances performed worse. The lack of synergy in the HXK + AHA2 lines may reflect intracellular interference when both constructs were targeted to the same guard cells. Guard-cell metabolism and ion transport operate as tightly integrated systems, and modelling studies have shown that simultaneous manipulation of multiple transporters can generate unanticipated trade-offs due to resource constraints and altered homeostasis (Wang, Hills and Blatt, 2014; Lawson and Matthews, 2020). Thus, although HXK and AHA2 individually have been shown to confer benefits in Arabidopsis, tobacco, and hybrid aspen (Wang *et al.*, 2013; Toh *et al.*, 2021; Acevedo-Siaca *et al.*, 2022), their combined overexpression in tobacco appears to have converged on overlapping mechanisms of ion transport and energetics, eroding the advantage conferred by HXK in single lines.

Across all three stacks tested, the intended complementarity was not realised. Unlike CBC and photorespiration stacks, where additive effects have been consistently achieved, stomatal trait combinations in this work were constrained by developmental and physiological trade-offs. In strawberry, clustering limited the benefits of increased SD; in tobacco, *ictB* and AHA2 did not provide strong enough individual gains to complement STO or HXK, respectively. As a result, additive improvements in photosynthesis or growth were not observed. These findings highlight the complexity of stacking stomatal traits, where interactions are less predictable than in linear biochemical pathways, and underscore the importance of validating single-gene benefits before expecting cumulative outcomes.

6.4. Context Matters

A consistent theme emerging from this and previous studies is that while some transgenic modifications to enhance photosynthesis have delivered clear and reproducible benefits in the field, others have proven more variable, highlighting the strong influence of environmental context. For example, synthetic photorespiratory bypasses increased tobacco biomass by more than 40% in replicated field trials (South *et al.*, 2019), faster relaxation of non-photochemical quenching boosted soybean seed yield by up to 33% (De Souza *et al.*, 2022), and SBPase overexpression improved growth and biomass in field-grown tobacco (López-Calcagno et al., 2020). By contrast, ictB produced gains under controlled conditions and in combination with CBC enzymes

(Simkin *et al.*, 2015), but has often failed to confer consistent benefits in the field, with no yield increases in tobacco (Ruiz-Vera *et al.*, 2022) and only modest, variable effects in maize (Koester *et al.*, 2021). These examples illustrate both the promise and the fragility of photosynthetic engineering, reinforcing the need for rigorous field validation across diverse environments.

The variability in performance reflects the difference between the environments where such lines are typically evaluated and the reality of crop production. In the field, light is rarely constant: fluctuations in irradiance occur across seconds to minutes due to sunflecks, canopy shading and cloud cover, while longer-term gradients of light penetration occur from the top to the base of the canopy (Lawson and Blatt, 2014; Kaiser, Morales and Harbinson, 2018). These dynamics mean that improvements to photosynthesis at steady state do not necessarily translate to cumulative carbon gain in the field (Slattery *et al.*, 2018; Long *et al.*, 2022). Assessing transgenic plants under low light and fluctuating light regimes, therefore, provides additional insight into crop performance under suboptimal and, in some ways, more realistic proxies for crop conditions than testing solely under optimal conditions. The present work demonstrated this clearly: benefits observed in T1 HXK lines under high light were not maintained when T2 generations were grown under low light (Chapter 5), while STO and ictB manipulations in tobacco showed little advantage under low light conditions, a useful proxy for shaded or deep canopy conditions (Chapter 4).

Promoter choice also strongly influenced outcomes. The CaMV 35S promoter is widely used in plant transformation for its strong constitutive expression, yet it has well-recognised limitations for field applications (Elmayan and Vaucheret, 1996; Thierry and

Vaucheret, 1996; Velten *et al.*, 2012; Amack and Antunes, 2020; Sherpa and Dey, 2024). Multiple studies have reported homology-dependent silencing of duplicated 35S elements, particularly in multigene constructs (Elmayan and Vaucheret, 1996; Thierry and Vaucheret, 1996; Kohli *et al.*, 2006), and suspected silencing of 35S-driven transgenes has been noted in field trials, including work with SBPase in wheat (Driever *et al.*, 2017). In this thesis, double 35S-driven constructs (STO + ictB) showed signs of reduced expression over generations (Chapter 4), and 35S-STO in strawberry produced maladaptive clustered stomata with diminished functionality (Chapter 3). More targeted promoter strategies may be better suited. STO is normally expressed in the mesophyll (Sugano *et al.*, 2009), and using a mesophyll-specific promoter could replicate endogenous signalling more faithfully than constitutive expression. Similarly, HXK expression under the guard-cell-specific KST1 promoter improved stomatal behaviour without the growth penalties reported under systemic expression (Dai et al., 2002; Kelly et al., 2012, 2013). Tissue-specific expression not only improves trait targeting but also reduces the risk of metabolic burden on the whole plant.

Finally, it is important to recognise that altering a single gene does not occur in isolation. Systemic changes can arise due to overexpression, often with unintended consequences that may not be obvious under controlled conditions. For instance, increased stomatal density can alter epidermal patterning and clustering, which in turn impairs function (Chapter 3), while guard-cell HXK affected lag times in environmentally contingent ways (Chapter 5). The case of STO further illustrates this complexity: although its signalling is likely restricted to the epidermis due to receptor localisation, constitutive production and secretion of the peptide represents a continuous metabolic drain, with

potential consequences for whole-plant carbon flux (Sugano *et al.*, 2009; Kondo *et al.*, 2010; Zhang *et al.*, 2025). This principle is echoed by AHA2 overexpression (Chapter 5), where transgenically enhanced production of a large, energetically expensive membrane protein was associated with reduced photosynthetic capacity and biomass under light-limited conditions (Wang *et al.*, 2013; Lawson and Matthews, 2020). More broadly, constitutive overexpression risks diverting carbon flux, perturbing signalling pathways, and influencing growth in ways that confound intended outcomes. A more nuanced approach, employing tissue-specific or inducible promoters, fine-tuning expression levels, and testing under fluctuating environments, is therefore essential if manipulations are to have utility in the field.

Together, these results emphasise that the context in which transgenes are expressed and evaluated matters as much as the genes themselves. Success in laboratory or glasshouse conditions does not guarantee benefits in the field, where fluctuating light, resource limitation, and stress interactions are the norm. Promoter design, expression stability, and systemic effects must be accounted for to ensure that photosynthetic engineering strategies translate beyond the bench to meaningful improvements in crop productivity.

6.5. Future Applications

While few obvious benefits from the stomatal manipulations presented in this thesis are presented, the stomatal limitations to productivity and slow responsiveness remain (Lawson and Blatt, 2014; McAusland et al., 2016). Thus, genetic manipulations of

stomatal patterning and behaviour have the potential to alleviate these constraints. The data presented in this thesis are informative, examining understudied crop species and exploring suboptimal conditions, and can help guide future manipulation strategies.

Focusing on the economically important crop species strawberry, stomatal limitation is one of the major constraints to carbon assimilation, particularly after midday and under stressful conditions (Yokoyama *et al.*, 2023). Repression of the innate midday depression may allow strawberries to achieve greater cumulative carbon gain as well as dissipate heat stress, as temperatures can easily exceed optimal conditions when grown in polytunnels or glasshouses. One obvious manipulation may be guard cell-targeted RNA interference of the endogenous strawberry HXK. As this gene is shown to play a role in stomatal closure under optimal conditions, it may play a very strong role in the midday depression in strawberries (Kelly *et al.*, 2013; Yokoyama *et al.*, 2023). Reducing the expression of HXK may help to maintain higher g_{sw} throughout the afternoon, providing evaporative cooling and greater diurnal carbon gain. Evaporative cooling via higher stomatal conductance may alleviate heat-induced declines in photosynthetic efficiency by lowering leaf temperature. Heat stress in strawberry reduces net CO_2 assimilation, PSII efficiency, and biomass, particularly above 35-40 °C, with evidence of irreversible photodamage to the photosystems (Kadir, Sidhu and Al-Khatib, 2006; Kesici *et al.*, 2013; Menzel, 2024). Increased transpiration can help dissipate excess heat, reducing midday depression of photosynthesis, a phenomenon also demonstrated in other fruit crops such as cranberry, where evaporative cooling lowered leaf temperature by 5-10 °C and improved carbon gain (Pelletier *et al.*, 2016). While this inevitably comes at the cost of greater water use, in strawberries grown in polytunnels or glasshouses under relatively controlled and irrigated conditions, the benefits of sustained photosynthesis, improved

thermal tolerance, and greater diurnal carbon gain may outweigh the penalties in water-use efficiency.

Increasing the SD of strawberry remains an effective method of alleviating stomatal diffusional resistances. To avoid aberrant stomatal clustering phenotypes, as displayed here (Chapter 3), targeted knock-outs of competitive antagonist ligands from EPF1 and EPF2 could be employed. Sakoda et al. (2020) used the targeted knock-out of EPF1 to produce moderate increases in SD (~50%), which resulted in greater biomass accumulation than the WT or STO overexpression (Sakoda *et al.*, 2020). The propensity for stomatal clustering in the 35S::STO strawberry lines produced here may suggest greater competition between STO and EPF1 than between STO and EPF2 for the binding of the ERECTA family receptors (ER, ERL1, ERL2) in complex with TMM, as EPF1 acts much later in development, acting to enforce the one-cell spacing rule (Hara et al., 2007; Sugano et al., 2009; Dow, Bergmann and Berry, 2014). Targeted KO of EPF1 in strawberry may, therefore, provide a way to increase SD moderately without incurring the extreme clustering penalties resulting from transgenic overexpression. Such an approach would offer a more precise means of enhancing stomatal conductance in strawberry, balancing gains in CO_2 diffusion with maintenance of functional stomatal patterning, and highlights the value of loss-of-function strategies in achieving more controlled trait improvements than constitutive overexpression.

6.6. Conclusion

This thesis demonstrates both the potential and the limitations of engineering stomatal traits to enhance photosynthesis. Across different genetic strategies and species, the outcomes revealed that while stomatal development and guard cell

metabolism can be effectively manipulated, the benefits are often constrained by developmental trade-offs, energetic costs, and environmental contingencies. Importantly, the work highlights that transgene effects are not expressed in isolation: their success depends on the cellular and developmental context, on promoter choice and stability, and on the environmental conditions in which they are tested. By examining these traits under fluctuating light, low-light, and in a complex polyploid crop, this study provides insights that extend beyond model species and optimal conditions, offering a more realistic perspective on the challenges of photosynthetic engineering. These findings emphasise the need for careful design of expression strategies, consideration of trait interactions, and rigorous testing under suboptimal environments. Future progress will depend on integrating stomatal engineering with complementary mesophyll and biochemical traits, while refining approaches to minimise unintended systemic costs. In doing so, the promise of enhancing photosynthetic efficiency through targeted manipulation of stomatal traits can be more fully realised in crops of agricultural importance.

7. References

Abrash, E.B. and Bergmann, D.C. (2010) 'Regional specification of stomatal production by the putative ligand CHALLAH', *Development (Cambridge, England)*, 137(3), pp. 447–455. Available at: https://doi.org/10.1242/DEV.040931.

Abrash, E.B., Davies, K.A. and Bergmann, D.C. (2011) 'Generation of signaling specificity in Arabidopsis by spatially restricted buffering of ligand-receptor interactions', *The Plant cell*, 23(8), pp. 2864–2879. Available at: https://doi.org/10.1105/TPC.111.086637.

Acevedo-Siaca, L.G. *et al.* (2022) 'Guard-cell-targeted overexpression of Arabidopsis Hexokinase 1 can improve water use efficiency in field-grown tobacco plants', *Journal of Experimental Botany*, 73(16), pp. 5745–5757. Available at: https://doi.org/10.1093/JXB/ERAC218.

Ainsworth, E.A. and Long, S.P. (2005) 'What have we learned from 15 years of free-air CO2 enrichment (FACE)? A meta-analytic review of the responses of photosynthesis, canopy properties and plant production to rising CO2', *New Phytologist*, 165(2), pp. 351–372. Available at: https://doi.org/10.1111/J.1469-8137.2004.01224.X.

Ainsworth, E.A. and Long, S.P. (2021) '30 years of free-air carbon dioxide enrichment (FACE): What have we learned about future crop productivity and its potential for adaptation?', *Global Change Biology*, 27(1), pp. 27–49. Available at: https://doi.org/10.1111/GCB.15375.

al Alawi, A.M., Majoni, S.W. and Falhammar, H. (2018) 'Magnesium and Human Health: Perspectives and Research Directions', *International Journal of Endocrinology*, 2018. Available at: https://doi.org/10.1155/2018/9041694.

Almari, A.M.S. (2021) *Role of Rieske FeS and SBPase in stomatal behaviour*. University of Essex.

Amack, S.C. and Antunes, M.S. (2020) 'CaMV35S promoter – A plant biology and biotechnology workhorse in the era of synthetic biology', *Current Plant Biology*, 24, p. 100179. Available at: https://doi.org/10.1016/J.CPB.2020.100179.

Anderegg, W.R.L. *et al.* (2018) 'Woody plants optimise stomatal behaviour relative to hydraulic risk', *Ecology Letters*, 21(7), pp. 968–977. Available at: https://doi.org/10.1111/ELE.12962;JOURNAL:JOURNAL:14610248;PAGE:STRING:ARTICLE/CHAPTER.

Antunes, W.C. *et al.* (2017) 'Guard cell-specific down-regulation of the sucrose transporter SUT1 leads to improved water use efficiency and reveals the interplay between carbohydrate metabolism and K+ accumulation in the regulation of stomatal opening', *Environmental and Experimental Botany*, 135, pp. 73–85. Available at: https://doi.org/10.1016/J.ENVEXPBOT.2016.12.004.

Aranda, I. *et al.* (2012) 'Limitaciones estomáticas y no-estomáticas en la asimilación foliar de carbono en brinzales de haya (Fagus sylvatica L.) bajo condiciones naturales', *Forest Systems*, 21(3), pp. 405–417. Available at: https://doi.org/10.5424/FS/2012213-02348.

Asseng, S. *et al.* (2015) 'Rising temperatures reduce global wheat production', *Nature Climate Change*, 5(2), pp. 143–147. Available at: https://doi.org/10.1038/NCLIMATE2470.

Assmann, S.M. and Jegla, T. (2016) 'Guard cell sensory systems: recent insights on stomatal responses to light, abscisic acid, and CO2', *Current Opinion in Plant Biology*, 33, pp. 157–167. Available at: https://doi.org/10.1016/J.PBI.2016.07.003.

Assmann, S.M., Simoncini, L. and Schroeder, J.I. (1985) 'Blue light activates electrogenic ion pumping in guard cell protoplasts of Vicia faba', *Nature*, 318(6043), pp. 285–287. Available at: https://doi.org/10.1038/318285A0.

Atkinson, C.J., Davies, W.J. and Mansfield, T.A. (1989) 'Changes in Stomatal Conductance in Intact Ageing Wheat Leaves in Response to Abscisic Acid', *Journal of Experimental Botany*, 40(9), pp. 1021–1028. Available at: https://doi.org/10.1093/JXB/40.9.1021.

Bailey, L.B. (2009) *Folate in health and disease*. CRC press.

Bailey, R.L., West, K.P. and Black, R.E. (2015) 'The Epidemiology of Global Micronutrient Deficiencies', *Annals of Nutrition and Metabolism*, 66(Suppl. 2), pp. 22–33. Available at: https://doi.org/10.1159/000371618.

Balasooriya, H.N. *et al.* (2018) 'Interaction of elevated carbon dioxide and temperature on strawberry (Fragaria× ananassa) growth and fruit yield', *International Journal of Biological, Biomolecular, Agricultural, Food and Biotechnological Engineering, World*

Academy of Science, Engineering and Technology, International Science Index, 12(9), pp. 279–287.

Balasooriya, H.N. *et al.* (2019) 'Impact of elevated carbon dioxide and temperature on strawberry polyphenols', *Journal of the Science of Food and Agriculture*, 99(10), pp. 4659–4669. Available at: https://doi.org/10.1002/JSFA.9706.

Barradas, V.L. and Jones, H.G. (1996) 'Responses of C0 2 assimilation to changes in irradiance: laboratory and field data and a model for beans [Phaseolus vulgaris L.)', *Journal of Experimental Botany*, 47(298), pp. 639–645. Available at: https://academic.oup.com/jxb/article/47/5/639/514355 (Accessed: 16 May 2022).

Barrett, C.B. (2014) 'Food Security and Sociopolitical Stability', *Food Security and Sociopolitical Stability* [Preprint]. Available at: https://doi.org/10.1093/ACPROF:OSO/9780199679362.001.0001.

Barrett, M.R. (1996) 'The Environmental Impact of Pesticide Degradates in Groundwater', *ACS Symposium Series*, 630, pp. 198–225. Available at: https://doi.org/10.1021/BK-1996-0630.CH016.

Bauwe, H., Hagemann, M. and Fernie, A.R. (2010) 'Photorespiration: players, partners and origin', *Trends in Plant Science*, 15(6), pp. 330–336. Available at: https://doi.org/10.1016/J.TPLANTS.2010.03.006.

Bendich, A. *et al.* (1986) 'The antioxidant role of vitamin C', *Advances in Free Radical Biology & Medicine*, 2(2), pp. 419–444. Available at: https://doi.org/10.1016/S8755-9668(86)80021-7.

Benfey, P.N. and Chua, N.-H. (1990) ‘ The Cauliflower Mosaic Virus 35 S Promoter: Combinatorial Regulation of Transcription in Plants ’, *Science*, 250(4983), pp. 959–966. Available at: https://doi.org/10.1126/SCIENCE.250.4983.959;PAGE:STRING:ARTICLE/CHAPTER.

de Benoist, B. (2008) ‘Conclusions of a WHO Technical Consultation on folate and vitamin B12 deficiencies’, *Food and Nutrition Bulletin*, 29(2 SUPPL.). Available at: https://doi.org/10.1177/15648265080292s129.

Berger, D. and Altmann, T. (2000) ‘A subtilisin-like serine protease involved in the regulation of stomatal density and distribution in Arabidopsis thaliana’, *Genes & Development*, 14(9), p. 1119. Available at: https://doi.org/10.1101/gad.14.9.1119.

Bergmann, D.C., Lukowitz, W. and Somerville, C.R. (2004) ‘Stomatal development and pattern controlled by a MAPKK kinase’, *Science (New York, N.Y.)*, 304(5676), pp. 1494–1497. Available at: https://doi.org/10.1126/SCIENCE.1096014.

Bergmann, D.C. and Sack, F.D. (2007) ‘Stomatal Development’, *Annual Review of Plant Biology*, 58, pp. 163–181. Available at: https://doi.org/10.1146/annurev.arplant.58.032806.104023.

Bertolino, L.T., Caine, R.S. and Gray, J.E. (2019) ‘Impact of stomatal density and morphology on water-use efficiency in a changing world’, *Frontiers in Plant Science*, 10, p. 427588. Available at: https://doi.org/10.3389/FPLS.2019.00225/BIBTEX.

Bhat, S.R. and Srinivasan, R. (2002) ‘Molecular and genetic analyses of transgenic plants:: Considerations and approaches’, *Plant Science*, 163(4), pp. 673–681. Available at: https://doi.org/10.1016/S0168-9452(02)00152-8.

Bhatt, I.D. and Dhar, U. (2000) ‘Micropropagation of Indian wild strawberry’, *Plant Cell, Tissue and Organ Culture 2000 60:2*, 60(2), pp. 83–88. Available at: https://doi.org/10.1023/A:1006471815566.

Bi, H. *et al.* (2013) ‘Cloning and expression analysis of transketolase gene in Cucumis sativus L.’, *Plant Physiology and Biochemistry*, 70, pp. 512–521. Available at: https://doi.org/10.1016/J.PLAPHY.2013.06.017.

Biswas, M.K. *et al.* (2009) ‘Development and evaluation of in vitro somaclonal variation in strawberry for improved horticultural traits’, *Scientia horticulturae*, 122(3), pp. 409–416.

Black, B.L., Enns, J.M. and Hokanson, S.C. (2002) ‘A Comparison of Temperate-climate Strawberry Production Systems Using Eastern Genotypes’, *HortTechnology*, 12(4), pp. 670–675. Available at: https://doi.org/10.21273/HORTTECH.12.4.670.

Black, C.C. (2018) “Effects of Herbicides on Photosynthesis,” *Weed Physiology*, pp. 1–36. Available at: https://doi.org/10.1201/9781351077736-1.

Black, R.E. *et al.* (2013) ‘Maternal and child undernutrition and overweight in low-income and middle-income countries’, *The Lancet*, 382(9890), pp. 427–451. Available at: https://doi.org/10.1016/S0140-6736(13)60937-X.

Blatt, M.R. (2000) ‘Cellular signaling and volume control in stomatal movements in plants’, *Annual review of cell and developmental biology*, 16, pp. 221–241. Available at: https://doi.org/10.1146/ANNUREV.CELLBIO.16.1.221.

Boardman, N.K. (1977) ‘Comparative Photosynthesis of Sun and Shade Plants’, *Annual Review of Plant Biology*, 28(Volume 28, 1977), pp. 355–377. Available at: https://doi.org/10.1146/ANNUREV.PP.28.060177.002035.

Bouis, H.E., Eozenou, P. and Rahman, A. (2011) ‘Food prices, household income, and resource allocation: Socioeconomic perspectives on their effects on dietary quality and nutritional status’, *Food and Nutrition Bulletin*, 32(1 SUPPL.). Available at: https://doi.org/10.1177/15648265110321s103.

Brodribb, T.J. *et al.* (2009) ‘Evolution of stomatal responsiveness to CO2 and optimization of water-use efficiency among land plants’, *New Phytologist*, 183(3), pp. 839–847. Available at: https://doi.org/10.1111/J.1469-8137.2009.02844.X.

Buckley, T.N. and Mott, K.A. (2013) ‘Modelling stomatal conductance in response to environmental factors’, *Plant, Cell and Environment*, 36, pp. 1691–1699. Available at: https://doi.org/10.1111/pce.12140.

Bunce, J.A. (2001) ‘Seasonal patterns of photosynthetic response and acclimation to elevated carbon dioxide in field-grown strawberry’, *Photosynthesis Research 2001 68:3*, 68(3), pp. 237–245. Available at: https://doi.org/10.1023/A:1012928928355.

Bushway, L.J. and Pritts, M.P. (2002) ‘Enhancing Early Spring Microclimate to Increase Carbon Resources and Productivity in June-bearing Strawberry’, *Journal of the*

American Society for Horticultural Science, 127(3), pp. 415–422. Available at: https://doi.org/10.21273/JASHS.127.3.415.

Büssis, D. *et al.* (2006) 'Stomatal aperture can compensate altered stomatal density in Arabidopsis thaliana at growth light conditions', *Functional Plant Biology*, 33(11), pp. 1037–1043. Available at: https://doi.org/10.1071/FP06078.

von Caemmerer, S. and Farquhar, G.D. (1981) 'Some relationships between the biochemistry of photosynthesis and the gas exchange of leaves', *Planta*, 153(4), pp. 376–387. Available at: https://doi.org/10.1007/BF00384257/METRICS.

Caine, R.S. *et al.* (2019) 'Rice with reduced stomatal density conserves water and has improved drought tolerance under future climate conditions', *New Phytologist*, 221(1), pp. 371–384. Available at: https://doi.org/10.1111/NPH.15344/FORMAT/PDF.

Cameron, J.S. and Hancock, J.F. (1986) 'Enhanced vigor in vegetative progeny of micropropagated strawberry plants', *HortScience*, 21(5), pp. 1225–1226.

Carr, A.C. and Maggini, S. (2017) 'Vitamin C and Immune Function', *Nutrients 2017, Vol. 9, Page 1211*, 9(11), p. 1211. Available at: https://doi.org/10.3390/NU9111211.

Casson, S. and Gray, J.E. (2008) 'Influence of environmental factors on stomatal development', *New Phytologist*, 178(1), pp. 9–23. Available at: https://doi.org/10.1111/J.1469-8137.2007.02351.X.

Casson, S.A. and Hetherington, A.M. (2010) 'Environmental regulation of stomatal development', *Current Opinion in Plant Biology*, 13(1), pp. 90–95. Available at: https://doi.org/10.1016/J.PBI.2009.08.005.

Centre for the Promotion of Imports, N. (2021) *The European market potential for strawberries | CBI*. Available at: https://www.cbi.eu/market-information/fresh-fruit-vegetables/strawberries/market-potential (Accessed: 22 November 2021).

Chen, Z.H. *et al.* (2012) 'Systems dynamic modeling of the stomatal guard cell predicts emergent behaviors in transport, signaling, and volume control', *Plant physiology*, 159(3), pp. 1235–1251. Available at: https://doi.org/10.1104/PP.112.197350.

Choi, H.W. *et al.* (2009) 'Stability and inheritance of endosperm-specific expression of two transgenes in progeny from crossing independently transformed barley plants', *Plant Cell Reports*, 28(8), pp. 1265–1272. Available at: https://doi.org/10.1007/S00299-009-0726-Y/FIGURES/5.

Crandon, J.H., Lund, C.C. and Dill, D.B. (2009) 'Experimental Human Scurvy', *The New England Journal of Medicine*, 223(10), pp. 353–369. Available at: https://doi.org/10.1056/NEJM194009052231001.

Crane, R. *et al.* (2023) 'Horticulture Production in England'.

Dai, N. *et al.* (2002) 'The tomato Hexokinase LeHXK1 cloning, mapping, expression pattern and phylogenetic relationships', *Plant Science*, 163(3), pp. 581–590. Available at: https://doi.org/10.1016/S0168-9452(02)00166-8.

Daloso, D.M. *et al.* (2016) 'Guard cell-specific upregulation of sucrose synthase 3 reveals that the role of sucrose in stomatal function is primarily energetic', *New Phytologist*, 209(4), pp. 1470–1483. Available at: https://doi.org/10.1111/nph.13704 (Accessed: 19 December 2023).

Darrow, G.M. (1966) *The Strawberry.*, *The Strawberry*. Holt, Rinehart and Winston New York.

Davis, T.M., Denoyes-Rothan, B. and Lerceteau-Köhler, E. (2007) 'Strawberry', *Fruits and Nuts*, pp. 189–205. Available at: https://doi.org/10.1007/978-3-540-34533-6_8.

Debnath, S.C. (2005) 'Strawberry sepal: Another explant for thidiazuron-induced adventitious shoot regeneration', *In Vitro Cellular & Developmental Biology - Plant 2005 41:5*, 41(5), pp. 671–676. Available at: https://doi.org/10.1079/IVP2005688.

Debnath, S.C. (2009) 'Characteristics of strawberry plants propagated by in vitro bioreactor culture and ex vitro propagation method', *Engineering in Life Sciences*, 9(3), pp. 239–246. Available at: https://doi.org/10.1002/ELSC.200800095.

Debnath, S.C. (2011) 'Developing a scale-up system for the in vitro multiplication of thidiazuron-induced strawberry shoots using a bioreactor', *https://doi.org/10.4141/CJPS07147*, 88(4), pp. 737–746. Available at: https://doi.org/10.4141/CJPS07147.

Debnath, S.C. (2012a) 'Propagation Strategies and Genetic Fidelity in Strawberries', *https://doi.org/10.1080/15538362.2012.696520*, 13(1–2), pp. 3–18. Available at: https://doi.org/10.1080/15538362.2012.696520.

Debnath, S.C. (2012b) 'Strategies approaches to propagate strawberry nuclear stocks using a bioreactor', in *VII International Strawberry Symposium 1049*, pp. 145–150.

Debnath, S.C. (2015) 'Zeatin overcomes thidiazuron-induced inhibition of shoot elongation and promotes rooting in strawberry culture in vitro',

https://doi.org/10.1080/14620316.2006.11512072, 81(3), pp. 349–354. Available at: https://doi.org/10.1080/14620316.2006.11512072.

Debnath, S.C. (2016) 'Molecular approaches for monitoring clonal fidelity and epigenetic variation in in vitro-derived strawberry plants', in *VIII International Strawberry Symposium 1156*, pp. 83–88.

Deng, X. and Woodward, F.I. (1998) 'The Growth and Yield Responses ofFragaria ananassato Elevated CO2and N Supply', *Annals of Botany*, 81(1), pp. 67–71. Available at: https://doi.org/10.1006/ANBO.1997.0535.

Department for Environment, F. and R.A. *et al.* (2019) *Agriculture in the United Kingdom 2019*. Available at: https://assets.publishing.service.gov.uk/government/uploads/system/uploads/attachment_data/file/950618/AUK-2019-07jan21.pdf (Accessed: 19 November 2021).

Dermody, O. *et al.* (2008) 'How do elevated CO2 and O3 affect the interception and utilization of radiation by a soybean canopy?', *Global Change Biology*, 14(3), pp. 556–564. Available at: https://doi.org/10.1111/J.1365-2486.2007.01502.X.

DI-An, N. *et al.* (2021) 'Glucose-6-phosphate induced changed of stomatal aperture in an irradiance dependent manner', *IOP Conference Series: Earth and Environmental Science*, 657(1), p. 012025. Available at: https://doi.org/10.1088/1755-1315/657/1/012025.

Diao, H. *et al.* (2024) 'Uncoupling of stomatal conductance and photosynthesis at high temperatures: mechanistic insights from online stable isotope techniques', *New*

Phytologist, 241(6), pp. 2366–2378. Available at: https://doi.org/10.1111/NPH.19558;WGROUP:STRING:PUBLICATION.

Dijkstra, J. (1993) 'DEVELOPMENT OF ALTERNATIVE METHODS FOR HEALTHY PROPAGATION OF STRAWBERRY PLANTS USING CUTTINGS', *Acta Horticulturae*, (348), pp. 234–236. Available at: https://doi.org/10.17660/ACTAHORTIC.1993.348.36.

Ding, F. *et al.* (2016) 'Changes in SBPase activity influence photosynthetic capacity, growth, and tolerance to chilling stress in transgenic tomato plants', *Scientific Reports*, 6. Available at: https://doi.org/10.1038/SREP32741.

Doheny-Adams, T. *et al.* (2012) 'Genetic manipulation of stomatal density influences stomatal size, plant growth and tolerance to restricted water supply across a growth carbon dioxide gradient', *Philosophical transactions of the Royal Society of London. Series B, Biological sciences*, 367(1588), pp. 547–555. Available at: https://doi.org/10.1098/RSTB.2011.0272.

Dow, G.J., Bergmann, D.C. and Berry, J.A. (2014) 'An integrated model of stomatal development and leaf physiology', *New Phytologist*, 201(4), pp. 1218–1226. Available at: https://doi.org/10.1111/NPH.12608.

Dow, G.J., Berry, J.A. and Bergmann, D.C. (2014) 'The physiological importance of developmental mechanisms that enforce proper stomatal spacing in Arabidopsis thaliana', *New Phytologist*, 201(4), pp. 1205–1217. Available at: https://doi.org/10.1111/NPH.12586.

Drake, P.L. *et al.* (2019) 'Two sides to every leaf: water and CO2 transport in hypostomatous and amphistomatous leaves', *New Phytologist*, 222(3), pp. 1179–1187. Available at: https://doi.org/10.1111/NPH.15652.

Drake, P.L., Froend, R.H. and Franks, P.J. (2013) 'Smaller, faster stomata: scaling of stomatal size, rate of response, and stomatal conductance', *Journal of Experimental Botany*, 64(2), pp. 495–505. Available at: https://doi.org/10.1093/JXB/ERS347.

Drewnowski, A. *et al.* (2012) 'Sweetness and Food Preference', *The Journal of Nutrition*, 142(6), pp. 1142S-1148S. Available at: https://doi.org/10.3945/JN.111.149575.

Driever, S.M. *et al.* (2017) 'Increased SBPase activity improves photosynthesis and grain yield in wheat grown in greenhouse conditions', *Philosophical Transactions of the Royal Society B: Biological Sciences*, 372(1730). Available at: https://doi.org/10.1098/RSTB.2016.0384.

Dunn, J. *et al.* (2019) 'Reduced stomatal density in bread wheat leads to increased water-use efficiency', *Journal of Experimental Botany*, 70(18), pp. 4737–4747. Available at: https://doi.org/10.1093/JXB/ERZ248.

Durner, E.F. *et al.* (1984) 'Photoperiod and temperature effects on flower and runner development in day-neutral, junebearing, and everbearing strawberries', *Journal of the American Society for Horticultural Science*, 109(3), pp. 396–400.

Dutton, C. *et al.* (2019) 'Bacterial infection systemically suppresses stomatal density', *Plant, Cell & Environment*, 42(8), pp. 2411–2421. Available at: https://doi.org/10.1111/PCE.13570.

Duursma, R.A. (2015) ‘Plantecophys - An R Package for Analysing and Modelling Leaf Gas Exchange Data’, *PLOS ONE*, 10(11), p. e0143346. Available at: https://doi.org/10.1371/JOURNAL.PONE.0143346.

Edger, P.P. *et al.* (2018) ‘Single-molecule sequencing and optical mapping yields an improved genome of woodland strawberry (Fragaria vesca) with chromosome-scale contiguity’, *GigaScience*, 7(2), pp. 1–7. Available at: https://doi.org/10.1093/GIGASCIENCE/GIX124.

Edger, P.P. *et al.* (2019) ‘Origin and evolution of the octoploid strawberry genome’, *Nature Genetics*, 51(3), p. 541. Available at: https://doi.org/10.1038/S41588-019-0356-4.

Elmayan, T. and Vaucheret, H. (1996) ‘Expression of single copies of a strongly expressed 35S transgene can be silenced post-transcriptionally’, *The Plant Journal*, 9(6), pp. 787–797. Available at: https://doi.org/10.1046/J.1365-313X.1996.9060787.X.

Emery, J.F. *et al.* (2003) ‘Radial Patterning of Arabidopsis Shoots by Class III HD-ZIP and KANADI Genes’, *Current Biology*, 13(20), pp. 1768–1774. Available at: https://doi.org/10.1016/j.cub.2003.09.035.

Enoch, H.Z., Rylski, I. and Spigelman, M. (1976) ‘CO2 enrichment of strawberry and cucumber plants grown in unheated greenhouses in Israel’, *Scientia Horticulturae*, 5(1), pp. 33–41. Available at: https://doi.org/10.1016/0304-4238(76)90020-0.

Eshed, Y. *et al.* (2001) 'Establishment of polarity in lateral organs of plants', *Current Biology*, 11(16), pp. 1251–1260. Available at: https://doi.org/10.1016/S0960-9822(01)00392-X.

Evans, J.R. and Poorter, H. (2001) 'Photosynthetic acclimation of plants to growth irradiance: The relative importance of specific leaf area and nitrogen partitioning in maximizing carbon gain', *Plant, Cell and Environment*, 24(8), pp. 755–767. Available at: https://doi.org/10.1046/J.1365-3040.2001.00724.X;CTYPE:STRING:JOURNAL.

Evenson, R.E. and Gollin, D. (2003) 'Assessing the impact of the Green Revolution, 1960 to 2000', *Science*, 300(5620), pp. 758–762. Available at: https://doi.org/10.1126/SCIENCE.1078710.

Falhof, J. *et al.* (2016) 'Plasma Membrane H+-ATPase Regulation in the Center of Plant Physiology', *Molecular Plant*, 9(3), pp. 323–337. Available at: https://doi.org/10.1016/J.MOLP.2015.11.002/ASSET/4D28EFF1-B373-4875-8FEA-A7E18CEB6293/MAIN.ASSETS/GR7.JPG.

Fanourakis, D. *et al.* (2011) 'Avoiding high relative air humidity during critical stages of leaf ontogeny is decisive for stomatal functioning', *Physiologia Plantarum*, 142(3), pp. 274–286. Available at: https://doi.org/10.1111/J.1399-3054.2011.01475.X.

FAO (2015) *State of Food Insecurity in the World 2015*, *Food and Agriculture Organization of the United Nations (FAO)*. Rome, Italy. Available at: https://www.fao.org/publications/sofi/2015/en/.

FAO (2020) *FAOSTAT- Crops and livestock products*, *Food and Agriculture Organisation of the United Nations*. Available at: https://www.fao.org/faostat/en/#data/QCL (Accessed: 5 January 2022).

Farooq, M. *et al.* (2009) 'Plant drought stress: effects, mechanisms and management', in *Sustainable agriculture*. Springer, pp. 153–188.

Farquhar, G.D. and Richards, R.A. (1984) 'Isotopic Composition of Plant Carbon Correlates With Water-Use Efficiency of Wheat Genotypes', *Functional Plant Biology*, 11(6), pp. 539–552. Available at: https://doi.org/10.1071/PP9840539.

Farquhar, G.D. and Sharkey, T.D. (1982) 'Stomatal Conductance and Photosynthesis', *Annual Review of Plant Physiology*, 33(1), pp. 317–345. Available at: https://doi.org/10.1146/ANNUREV.PP.33.060182.001533.

Feng, L., Wang, K., *et al.* (2007) 'Overexpression of SBPase enhances photosynthesis against high temperature stress in transgenic rice plants', *Plant Cell Reports*, 26(9), pp. 1635–1646. Available at: https://doi.org/10.1007/S00299-006-0299-Y/FIGURES/10.

Feng, L., Han, Y., *et al.* (2007) 'Overexpression of sedoheptulose-1,7-bisphosphatase enhances photosynthesis and growth under salt stress in transgenic rice plants', *Functional plant biology : FPB*, 34(9), pp. 822–834. Available at: https://doi.org/10.1071/FP07074.

Fernandez, G.E., Butler, L.M. and Louws, F.J. (2001) 'Strawberry Growth and Development in an Annual Plasticulture System', *HortScience*, 36(7), pp. 1219–1223. Available at: https://doi.org/10.21273/HORTSCI.36.7.1219.

Fernández-Molano, G.E. *et al.* (2025) 'Stomatal regulation, leaf water relations, and leaf phenology are coordinated in tree species from the Sonoran Desert', *AoB PLANTS*, 17(5), p. 41. Available at: https://doi.org/10.1093/AOBPLA/PLAF041.

Field, C.B. and Barros, V.R. (2014) *Climate change 2014–Impacts, adaptation and vulnerability: Regional aspects*. Cambridge University Press.

Fiola, J.A. *et al.* (1997) 'Cool climate strawberries fare well on plasticulture', *Fruit Grower. May*, pp. 41–42.

Fiola, J.A., Lengyen, R.J. and Reichert, D.A. (1995) 'Planting density and date affect productivity and profitability of "Chandler",'Tribute', and "Tristar" in strawberry plasticulture.', *Advances in strawberry research* [Preprint].

Fitzgerald, G.J. *et al.* (2016) 'Elevated atmospheric [CO2] can dramatically increase wheat yields in semi-arid environments and buffer against heat waves', *Global Change Biology*, 22(6), pp. 2269–2284. Available at: https://doi.org/10.1111/GCB.13263.

Foley, J.A. *et al.* (2011) 'Solutions for a cultivated planet', *Nature 2011 478:7369*, 478(7369), pp. 337–342. Available at: https://doi.org/10.1038/nature10452.

Franks, P.J. and Beerling, D.J. (2009) 'Maximum leaf conductance driven by CO2 effects on stomatal size and density over geologic time', *Proceedings of the National Academy of Sciences*, 106(25), pp. 10343–10347. Available at: https://doi.org/10.1073/PNAS.0904209106.

Franks, P.J., Drake, P.L. and Beerling, D.J. (2009) 'Plasticity in maximum stomatal conductance constrained by negative correlation between stomatal size and density:

An analysis using Eucalyptus globulus', *Plant, Cell and Environment*, 32(12), pp. 1737–1748. Available at: https://doi.org/10.1111/J.1365-3040.2009.002031.X;JOURNAL:JOURNAL:13653040;REQUESTEDJOURNAL:JOURNAL:13653040;WGROUP:STRING:PUBLICATION.

Franks, P.J. and Farquhar, G.D. (2007) 'The Mechanical Diversity of Stomata and Its Significance in Gas-Exchange Control', *Plant Physiology*, 143(1), pp. 78–87. Available at: https://doi.org/10.1104/PP.106.089367.

Froger, A. and Hall, J.E. (2007) 'Transformation of Plasmid DNA into E. coli Using the Heat Shock Method', *Journal of Visualized Experiments : JoVE*, 6(6). Available at: https://doi.org/10.3791/253.

Fujino, M. (1967) 'Role of adenosinetriphosphate and adenosinetriphosphatase in stomatal movement', *Sci. Bull. Fac. Educ. Nagasaki Univ*, 18(1).

Galmés, J. *et al.* (2007) 'Water relations and stomatal characteristics of Mediterranean plants with different growth forms and leaf habits: Responses to water stress and recovery', *Plant and Soil*, 290(1–2), pp. 139–155. Available at: https://doi.org/10.1007/S11104-006-9148-6/FIGURES/8.

Geisler, M., Nadeau, J. and Sack, F.D. (2000) 'Oriented Asymmetric Divisions That Generate the Stomatal Spacing Pattern in Arabidopsis Are Disrupted by the too many mouths Mutation', *The Plant Cell*, 12(11), pp. 2075–2086. Available at: https://doi.org/10.1105/TPC.12.11.2075.

Genty, B., Briantais, J.M. and Baker, N.R. (1989) 'The relationship between the quantum yield of photosynthetic electron transport and quenching of chlorophyll fluorescence', *Biochimica et Biophysica Acta (BBA) - General Subjects*, 990(1), pp. 87–92. Available at: https://doi.org/10.1016/S0304-4165(89)80016-9.

Giampieri, F. *et al.* (2012) 'The strawberry: Composition, nutritional quality, and impact on human health', *Nutrition*, 28(1), pp. 9–19. Available at: https://doi.org/10.1016/J.NUT.2011.08.009.

Gonzalez-Fuentes, J.A. *et al.* (2016) 'Diurnal root zone temperature variations affect strawberry water relations, growth, and fruit quality', *Scientia Horticulturae*, 203, pp. 169–177. Available at: https://doi.org/10.1016/J.SCIENTA.2016.03.039.

Graham, R.D., Welch, R.M. and Bouis, H.E. (2001) 'Addressing micronutrient malnutrition through enhancing the nutritional quality of staple foods: Principles, perspectives and knowledge gaps', *Advances in Agronomy*, 70, pp. 77–142. Available at: https://doi.org/10.1016/S0065-2113(01)70004-1.

Granot, D. *et al.* (2015) 'Sensing Sugar and Saving Water', *Procedia Environmental Sciences*, 29, p. 3. Available at: https://doi.org/10.1016/J.PROENV.2015.07.123.

Granot, D., David-Schwartz, R. and Kelly, G. (2013) 'Hexose kinases and their role in sugar-sensing and plant development', *Frontiers in Plant Science*, 4(MAR). Available at: https://doi.org/10.3389/FPLS.2013.00044,.

Grassi, G. and Magnani, F. (2005) 'Stomatal, mesophyll conductance and biochemical limitations to photosynthesis as affected by drought and leaf ontogeny in ash and oak

trees', *Plant, Cell and Environment*, 28(7), pp. 834–849. Available at: https://doi.org/10.1111/J.1365-3040.2005.01333.X;JOURNAL:JOURNAL:13653040;REQUESTEDJOURNAL:JOURNAL:13653040;WGROUP:STRING:PUBLICATION.

Gray, S.B. *et al.* (2016) 'Intensifying drought eliminates the expected benefits of elevated carbon dioxide for soybean', *Nature Plants 2016 2:9*, 2(9), pp. 1–8. Available at: https://doi.org/10.1038/nplants.2016.132.

Green, R.E. *et al.* (2005) 'Farming and the fate of wild nature', *Science*, 307(5709), pp. 550–555. Available at: https://doi.org/10.1126/SCIENCE.1106049/SUPPL_FILE/GREEN.SOM.PDF.

Gulati, A., Fan, S. and Dalafi, S. (2005) 'The dragon and the elephant: Agricultural and rural reforms in China and India'. Available at: https://doi.org/10.22004/AG.ECON.59826.

Guttridge, C.G. (1985) 'Fragaria ananassa', *CRC handbook of flowering*, 8, pp. 16–33.

Haake, V. *et al.* (1998) 'A moderate decrease of plastid aldolase activity inhibits photosynthesis, alters the levels of sugars and starch, and inhibits growth of potato plants', *The Plant Journal*, 14(2), pp. 147–157. Available at: https://doi.org/10.1046/J.1365-313X.1998.00089.X.

Haake, V. *et al.* (1999) 'Changes in aldolase activity in wild-type potato plants are important for acclimation to growth irradiance and carbon dioxide concentration, because plastid aldolase exerts control over the ambient rate of photosynthesis across

a range of growth conditions', *The Plant Journal*, 17(5), pp. 479–489. Available at: https://doi.org/10.1046/J.1365-313X.1999.00391.X.

Hamanishi, E.T., Thomas, B.R. and Campbell, M.M. (2012) 'Drought induces alterations in the stomatal development program in Populus', *Journal of Experimental Botany*, 63(13), pp. 4959–4971. Available at: https://doi.org/10.1093/JXB/ERS177.

Hancock, J.F. (1999) *Strawberries*. Wallingford, United Kingdom: CABI Publishing.

Hancock, J.F., Sjulin, T.M. and Lobos, G.A. (2008) 'Strawberries', *Temperate Fruit Crop Breeding: Germplasm to Genomics*, 9781402069079, pp. 393–437. Available at: https://doi.org/10.1007/978-1-4020-6907-9_13.

Handley, D.T. (2008) 'The strawberry plant: what you should know', *University of Marine Cooperative Extension, Highmoor Farm, PO Box*, 179.

Hara, K. *et al.* (2007) 'The secretory peptide gene EPF1 enforces the stomatal one-cell-spacing rule', *Genes & Development*, 21(14), p. 1720. Available at: https://doi.org/10.1101/GAD.1550707.

Hara, K. *et al.* (2009) 'Epidermal Cell Density is Autoregulated via a Secretory Peptide, EPIDERMAL PATTERNING FACTOR 2 in Arabidopsis Leaves', *Plant and Cell Physiology*, 50(6), pp. 1019–1031. Available at: https://doi.org/10.1093/PCP/PCP068.

Harrison, E.L. *et al.* (2020) 'The influence of stomatal morphology and distribution on photosynthetic gas exchange', *The Plant Journal*, 101(4), pp. 768–779. Available at: https://doi.org/10.1111/TPJ.14560.

Harrison, E.P. *et al.* (1997) 'Reduced sedoheptulose-1,7-bisphosphatase levels in transgenic tobacco lead to decreased photosynthetic capacity and altered carbohydrate accumulation', *Planta 1997 204:1*, 204(1), pp. 27–36. Available at: https://doi.org/10.1007/S004250050226.

Harrison, E.P. *et al.* (2001) 'Small decreases in SBPase cause a linear decline in the apparent RuBP regeneration rate, but do not affect Rubisco carboxylation capacity', *Journal of Experimental Botany*, 52(362), pp. 1779–1784. Available at: https://doi.org/10.1093/JEXBOT/52.362.1779.

Hartz, T.K., Baameur, A. and Holt, D.B. (1991) 'Carbon Dioxide Enrichment of High-value Crops under Tunnel Culture', *Journal of the American Society for Horticultural Science*, 116(6), pp. 970–973. Available at: https://doi.org/10.21273/JASHS.116.6.970.

Haruta, M. *et al.* (2010) 'Molecular characterization of mutant Arabidopsis plants with reduced plasma membrane proton pump activity', *Journal of Biological Chemistry*, 285(23), pp. 17918–17929. Available at: https://doi.org/10.1074/jbc.M110.101733.

Haruta, M., Gray, W.M. and Sussman, M.R. (2015) 'Regulation of the plasma membrane proton pump (H+-ATPase) by phosphorylation', *Current Opinion in Plant Biology*, 28, pp. 68–75. Available at: https://doi.org/10.1016/J.PBI.2015.09.005.

Hatfield, J.L. and Dold, C. (2019) 'Water-use efficiency: Advances and challenges in a changing climate', *Frontiers in Plant Science*, 10, p. 103. Available at: https://doi.org/10.3389/FPLS.2019.00103/BIBTEX.

Haworth, M. *et al.* (2018) 'Allocation of the epidermis to stomata relates to stomatal physiological control: Stomatal factors involved in the evolutionary diversification of the angiosperms and development of amphistomaty', *Environmental and Experimental Botany*, 151, pp. 55–63. Available at: https://doi.org/10.1016/J.ENVEXPBOT.2018.04.010.

Hay, W.T. *et al.* (2017) 'Enhancing soybean photosynthetic CO 2 assimilation using a cyanobacterial membrane protein, ictB', *Journal of Plant Physiology*, 212, pp. 58–68. Available at: https://doi.org/10.1016/j.jplph.2017.02.003.

Heath, O.V.S. (1938) 'An Experimental Investigation of the Mechanism of Stomatal Movement, with Some Preliminary Observations Upon the Response of the Guard Cells to" Shock"', *The New Phytologist*, 37(5), pp. 385–395.

Hedden, P. (2003) 'The genes of the Green Revolution', *Trends in Genetics*, 19(1), pp. 5–9. Available at: https://doi.org/10.1016/S0168-9525(02)00009-4.

Henry, C., John, Grace P, *et al.* (2019) 'A stomatal safety-efficiency trade-off constrains responses to leaf dehydration', *Nature Comminications* [Preprint]. Available at: https://doi.org/10.1038/s41467-019-11006-1.

Henry, C., John, Grace P., *et al.* (2019) 'A stomatal safety-efficiency trade-off constrains responses to leaf dehydration', *Nature Communications*, 10(1), pp. 1–9. Available at: https://doi.org/10.1038/S41467-019-11006-1;TECHMETA=14,63;SUBJMETA=158,1736,2455,449,631,704;KWRD=ECOPHYSIOLOGY,PLANT+PHYSIOLOGY.

Hess, F.D. (2018) “Herbicide Effects on Plant Structure, Physiology, and Biochemistry,” *Pesticide Interactions in Crop Production*, pp. 13–34. Available at: https://doi.org/10.1201/9781351075459-2.

Hetherington, A.M. and Woodward, F.I. (2003) ‘The role of stomata in sensing and driving environmental change’, *Nature 2003 424:6951*, 424(6951), pp. 901–908. Available at: https://doi.org/10.1038/nature01843.

HICKLENTON, P.R. and JOLLIFFE, P.A. (2011) ‘EFFECTS OF GREENHOUSE CO2 ENRICHMENT ON THE YIELD AND PHOTOSYNTHETIC PHYSIOLOGY OF TOMATO PLANTS’, *https://doi.org/10.4141/cjps78-119*, 58(3), pp. 801–817. Available at: https://doi.org/10.4141/CJPS78-119.

Hills, A. *et al.* (2012) ‘OnGuard, a computational platform for quantitative kinetic modeling of guard cell physiology’, *Plant physiology*, 159(3), pp. 1026–1042. Available at: https://doi.org/10.1104/PP.112.197244.

Hoagland, D.R. and Arnon, D.I. (1950) ‘The Water-Culture Method for Growing Plants without Soil. ’, *California Agricultural Experiment Station* [Preprint]. Available at: https://www.scirp.org/reference/referencespapers?referenceid=1850958 (Accessed: 7 August 2025).

Hodge, J. (2016) ‘Hidden hunger: Approaches to tackling micronutrient deficiencies’, *INTERNATIONAL FOOD POLICY RESEARCH INSTITUTE (IFPRI)* [Preprint]. Available at: https://doi.org/10.2499/9780896295889_04.

Hood, E.E. *et al.* (1993) 'New Agrobacterium helper plasmids for gene transfer to plants', *Transgenic Research 1993 2:4*, 2(4), pp. 208–218. Available at: https://doi.org/10.1007/BF01977351.

Hronková, M. *et al.* (2015) 'Light-induced STOMAGEN-mediated stomatal development in Arabidopsis leaves', *Journal of Experimental Botany*, 66(15), pp. 4621–4630. Available at: https://doi.org/10.1093/jxb/erv233.

Huang, S. *et al.* (2023) 'The CIPK23 protein kinase represses SLAC1-type anion channels in Arabidopsis guard cells and stimulates stomatal opening', *New Phytologist*, 238(1), pp. 270–282. Available at: https://doi.org/10.1111/NPH.18708.

Hulme, M.F. *et al.* (2013) 'Conserving the Birds of Uganda's Banana-Coffee Arc: Land Sparing and Land Sharing Compared', *PLOS ONE*, 8(2), p. e54597. Available at: https://doi.org/10.1371/JOURNAL.PONE.0054597.

Hummer, K.E., Nathewet, P. and Yanagi, T. (2009) 'Decaploidy in Fragaria iturupensis (Rosaceae)', *American Journal of Botany*, 96(3), pp. 713–716. Available at: https://doi.org/10.3732/AJB.0800285.

Hunt, L., Bailey, K.J. and Gray, J.E. (2010) 'The signalling peptide EPFL9 is a positive regulator of stomatal development', *The New phytologist*, 186(3), pp. 609–614. Available at: https://doi.org/10.1111/J.1469-8137.2010.03200.X.

Hunt, L. and Gray, J.E. (2009) 'The signaling peptide EPF2 controls asymmetric cell divisions during stomatal development', *Current biology : CB*, 19(10), pp. 864–869. Available at: https://doi.org/10.1016/J.CUB.2009.03.069.

IndexBox (2021) *Global Strawberry Market Overview 2021 - IndexBox*. Available at: https://www.indexbox.io/store/world-strawberries-market-report-analysis-and-forecast-to-2020/ (Accessed: 22 November 2021).

Inoue, S.I. and Kinoshita, T. (2017) 'Blue light regulation of stomatal opening and the plasma membrane H+-ATPase', *Plant Physiology*, 174(2), pp. 531–538. Available at: https://doi.org/10.1104/PP.17.00166,.

Ishikawa, C. *et al.* (2011) 'Functional incorporation of sorghum small subunit increases the catalytic turnover rate of Rubisco in transgenic rice', *Plant physiology*, 156(3), pp. 1603–1611. Available at: https://doi.org/10.1104/PP.111.177030.

Islam, M.S., Matsui, T. and Yoshida, Y. (1996) 'Effect of carbon dioxide enrichment on physico-chemical and enzymatic changes in tomato fruits at various stages of maturity', *Scientia Horticulturae*, 65(2–3), pp. 137–149. Available at: https://doi.org/10.1016/0304-4238(95)00867-5.

Jahn, O.L. and Dana, M.N. (1970) 'Crown and inflorescence development in the Strawberry, Fragaria ananassa', *American Journal of Botany*, 57(6Part1), pp. 605–612. Available at: https://doi.org/10.1002/J.1537-2197.1970.TB09855.X.

Jeanguenin, L., Mir, A.P. and Chaumont, F. (2017) 'Uptake, Loss and Control', *Encyclopedia of Applied Plant Sciences*, 1, pp. 135–140. Available at: https://doi.org/10.1016/B978-0-12-394807-6.00087-3.

Jezek, M. and Blatt, M.R. (2017) 'The membrane transport system of the guard cell and its integration for stomatal dynamics', *Plant Physiology*, 174(2), pp. 487–519. Available at: https://doi.org/10.1104/PP.16.01949,.

Johnson, A.L., Govindarajulu, R. and Ashman, T.L. (2014) 'Bioclimatic evaluation of geographical range in Fragaria (Rosaceae): consequences of variation in breeding system, ploidy and species age', *Botanical Journal of the Linnean Society*, 176(1), pp. 99–114. Available at: https://doi.org/10.1111/BOJ.12190.

Jordan, G.J. *et al.* (2015) 'Environmental adaptation in stomatal size independent of the effects of genome size', *New Phytologist*, 205(2), pp. 608–617. Available at: https://doi.org/10.1111/NPH.13076;PAGE:STRING:ARTICLE/CHAPTER.

Kadir, S., Sidhu, G. and Al-Khatib, K. (2006) 'Strawberry (Fragaria ×ananassa Duch.) Growth and Productivity as Affected by Temperature', *HortScience*, 41(6), pp. 1423–1430. Available at: https://doi.org/10.21273/HORTSCI.41.6.1423.

Kado, C.I., Lai, E.M. and Kelly, B. (2000) 'On the Mechanism of Horizontal Gene Transfer by Agrobacterium tumefaciens', *Developments in Plant Genetics and Breeding*, 5(C), pp. 68–75. Available at: https://doi.org/10.1016/S0168-7972(00)80010-9.

Kaiser, E., Morales, A. and Harbinson, J. (2018) 'Fluctuating light takes crop photosynthesis on a rollercoaster ride', *Plant Physiology*, 176(2), pp. 977–989. Available at: https://doi.org/10.1104/PP.17.01250,.

Kellerman, W.A. (1892) 'Interesting variations of the strawberry leaf', *Botanical Gazette*, 17, pp. 257–258.

Kelly, G. *et al.* (2012) 'The Pitfalls of Transgenic Selection and New Roles of AtHXK1: A High Level of AtHXK1 Expression Uncouples Hexokinase1-Dependent Sugar Signaling from Exogenous Sugar', *Plant Physiology*, 159(1), p. 47. Available at: https://doi.org/10.1104/PP.112.196105.

Kelly, G. *et al.* (2013) 'Hexokinase mediates stomatal closure', *The Plant journal : for cell and molecular biology*, 75(6), pp. 977–988. Available at: https://doi.org/10.1111/TPJ.12258.

Kelly, G *et al.* (2017) 'The Solanum tuberosum KST1 partial promoter as a tool for guard cell expression in multiple plant species', *Journal of experimental botany*, 68(11), pp. 2885–2897. Available at: https://doi.org/10.1093/JXB/ERX159.

Kelly, G. *et al.* (2019) 'Guard-Cell Hexokinase Increases Water-Use Efficiency Under Normal and Drought Conditions', *Frontiers in Plant Science*, 10, p. 1499. Available at: https://doi.org/10.3389/FPLS.2019.01499/BIBTEX.

Kesici, M. *et al.* (2013) 'Heat-stress Tolerance of Some Strawberry (Fragaria × ananassa) Cultivars', *Notulae Botanicae Horti Agrobotanici Cluj-Napoca*, 41(1), pp. 244–249. Available at: https://doi.org/10.15835/NBHA4119009.

Keutgen, N., Chen, K. and Lenz, F. (1997) 'Responses of strawberry leaf photosynthesis, chlorophyll fluorescence and macronutrient contents to elevated CO2', *Journal of Plant Physiology*, 150(4), pp. 395–400. Available at: https://doi.org/10.1016/S0176-1617(97)80088-0.

Khan, I., Azam, A. and Mahmood, A. (2013) 'The impact of enhanced atmospheric carbon dioxide on yield, proximate composition, elemental concentration, fatty acid and vitamin C contents of tomato (Lycopersicon esculentum)', *Environmental monitoring and assessment*, 185(1), pp. 205–214. Available at: https://doi.org/10.1007/S10661-012-2544-X.

Khan, K.M. and Jialal, I. (2021) 'Folic Acid Deficiency', *StatPearls* [Preprint]. Available at: https://www.ncbi.nlm.nih.gov/books/NBK535377/ (Accessed: 9 January 2022).

Kinoshita, T. and Shimazaki, K.I. (1999) 'Blue light activates the plasma membrane H+-ATPase by phosphorylation of the C-terminus in stomatal guard cells', *The EMBO Journal*, 18(20), pp. 5548–5558. Available at: https://doi.org/10.1093/EMBOJ/18.20.5548.

Kirkham, M.B. (2005) 'Principles of Soil and Plant Water Relations', *Principles of Soil and Plant Water Relations* [Preprint]. Available at: https://doi.org/10.1016/B978-0-12-409751-3.X5000-2.

Kirkham, M.B. (2014) 'Principles of soil and plant water relations, 2nd Edition', *Principles of Soil and Plant Water Relations, 2nd Edition*, pp. 1–579. Available at: https://doi.org/10.1016/C2013-0-12871-1.

Koester, R.P. *et al.* (2021) 'Transgenic insertion of the cyanobacterial membrane protein ictB increases grain yield in Zea mays through increased photosynthesis and carbohydrate production'. Available at: https://doi.org/10.1371/journal.pone.0246359.

Köhler, I.H. *et al.* (2017) 'Expression of cyanobacterial FBP/SBPase in soybean prevents yield depression under future climate conditions', *Journal of Experimental Botany*, 68(3), pp. 715–726. Available at: https://doi.org/10.1093/JXB/ERW435.

Kohli, A. *et al.* (2006) 'The Quest to Understand the Basis and Mechanisms that Control Expression of Introduced Transgenes in Crop Plants', *Plant Signaling & Behavior*, 1(4), pp. 185–195. Available at: http://www.landesbioscience.com/journals/psb/abstract.php?id=3195 (Accessed: 21 July 2025).

Kondo, T. *et al.* (2010) 'Stomatal density is controlled by a mesophyll-derived signaling molecule', *Plant & cell physiology*, 51(1), pp. 1–8. Available at: https://doi.org/10.1093/PCP/PCP180.

Konsin, M., Voipio, I. and Palonen, P. (2001) 'Influence of photoperiod and duration of short-day treatment on vegetative growth and flowering of strawberry (Fragaria3ananassa Duch.)', *http://dx.doi.org/10.1080/14620316.2001.11511330*, 76(1), pp. 77–82. Available at: https://doi.org/10.1080/14620316.2001.11511330.

Kramer, D.M. *et al.* (2004) 'New fluorescence parameters for the determination of QA redox state and excitation energy fluxes', *Photosynthesis Research*, 79(2), pp. 209–218. Available at: https://doi.org/10.1023/B:PRES.0000015391.99477.0D/METRICS.

Kwak, J.M. *et al.* (2001) 'Dominant negative guard cell K+ channel mutants reduce inward-rectifying K+ currents and light-induced stomatal opening in arabidopsis', *Plant Physiology*, 127(2), pp. 473–485. Available at: https://doi.org/10.1104/PP.010428.

Lake, J.A., Woodward, F.I. and Quick, W.P. (2002) 'Long-distance CO2 signalling in plants', *Journal of Experimental Botany*, 53(367), pp. 183–193. Available at: https://doi.org/10.1093/JEXBOT/53.367.183.

LaMondia, J.A. (2004) 'Strawberry black root rot', *Advances in strawberry research*, 23, pp. 1–10.

Lampard, G.R., MacAlister, C.A. and Bergmann, D.C. (2008) 'Arabidopsis stomatal initiation is controlled by MAPK-mediated regulation of the bHLH SPEECHLESS', *Science (New York, N.Y.)*, 322(5904), pp. 1113–1116. Available at: https://doi.org/10.1126/SCIENCE.1162263.

Larson, K.D. (1996) 'Challenges for annual strawberry production systems', in *Proc. IV North Amer. Strawberry Conf*, pp. 155–161.

Lau, O.S. *et al.* (2018) 'Direct Control of SPEECHLESS by PIF4 in the High-Temperature Response of Stomatal Development', *Current Biology*, 28(8), pp. 1273-1280.e3. Available at: https://doi.org/10.1016/J.CUB.2018.02.054.

Lau, O.S. and Bergmann, D.C. (2012) 'Stomatal development: a plant's perspective on cell polarity, cell fate transitions and intercellular communication', *Development (Cambridge, England)*, 139(20), pp. 3683–3692. Available at: https://doi.org/10.1242/DEV.080523.

Lawson, T. *et al.* (2006) 'Decreased SBPase activity alters growth and development in transgenic tobacco plants', *Plant, Cell & Environment*, 29(1), pp. 48–58. Available at: https://doi.org/10.1111/J.1365-3040.2005.01399.X.

Lawson, T. *et al.* (2014) 'Mesophyll photosynthesis and guard cell metabolism impacts on stomatal behaviour', *New Phytologist*, 203(4), pp. 1064–1081. Available at: https://doi.org/10.1111/NPH.12945.

Lawson, T. and Blatt, M.R. (2014) 'Stomatal Size, Speed, and Responsiveness Impact on Photosynthesis and Water Use Efficiency', *Plant Physiology*, 164(4), pp. 1556–1570. Available at: https://doi.org/10.1104/PP.114.237107.

Lawson, T., Caemmerer, S. von and Baroli, I. (2010) 'Photosynthesis and Stomatal Behaviour', pp. 265–304. Available at: https://doi.org/10.1007/978-3-642-13145-5_11.

Lawson, T., Kramer, D.M. and Raines, C.A. (2012) 'Improving yield by exploiting mechanisms underlying natural variation of photosynthesis', *Current Opinion in Biotechnology*, 23(2), pp. 215–220. Available at: https://doi.org/10.1016/J.COPBIO.2011.12.012.

Lawson, T. and Matthews, J. (2020) 'Guard Cell Metabolism and Stomatal Function', *https://doi.org/10.1146/annurev-arplant-050718-100251*, 71, pp. 273–302. Available at: https://doi.org/10.1146/ANNUREV-ARPLANT-050718-100251.

Lawson, T. and Morison, J.I.L. (2004) 'Stomatal function and physiology', *The Evolution of Plant Physiology*, pp. 217–242. Available at: https://doi.org/10.1016/B978-012339552-8/50013-5.

Lawson, T. and Vialet-Chabrand, S. (2019) 'Speedy stomata, photosynthesis and plant water use efficiency', *New Phytologist*, 221(1), pp. 93–98. Available at: https://doi.org/10.1111/NPH.15330.

Lawson, T. and Weyers, J. (1999) ‘Spatial and temporal variation in gas exchange over the lower surface of Phaseolus vulgaris L. primary leaves’, *Journal of Experimental Botany*, 50(337), pp. 1381–1391. Available at: https://doi.org/10.1093/JXB/50.337.1381.

Lawson, T., Weyers, J. and Brook, R.A.’ (1998) ‘The nature of heterogeneity in the stomatal behaviour of Phaseolus vulgaris L. primary leaves’, *Journal of Experimental Botany*, 49(325), pp. 1387–1395. Available at: https://academic.oup.com/jxb/article/49/325/1387/506284 (Accessed: 24 April 2025).

Lee, J. *et al.* (2015) ‘Competitive binding of antagonistic peptides fine-tunes stomatal patterning’, *Nature*, 522(7557), pp. 439–443. Available at: https://doi.org/10.1038/NATURE14561.

Lee, J.S. *et al.* (2012) ‘Direct interaction of ligand-receptor pairs specifying stomatal patterning’, *Genes & development*, 26(2), pp. 126–136. Available at: https://doi.org/10.1101/GAD.179895.111.

Lefebvre, S. *et al.* (2005) ‘Increased Sedoheptulose-1,7-Bisphosphatase Activity in Transgenic Tobacco Plants Stimulates Photosynthesis and Growth from an Early Stage in Development’, *Plant Physiology*, 138(1), pp. 451–460. Available at: https://doi.org/10.1104/PP.104.055046.

Léger, D. (2008) ‘Scurvy’, *Canadian Family Physician*, 54(10).

Li, S. *et al.* (2021) ‘Role of Hydraulic Signal and ABA in Decrease of Leaf Stomatal and Mesophyll Conductance in Soil Drought-Stressed Tomato’, *Frontiers in Plant Science*, 12, p. 653186. Available at: https://doi.org/10.3389/FPLS.2021.653186/FULL.

Li, X. *et al.* (2020) 'Physiological and molecular basis of promoting leaf growth in strawberry (Fragaria ananassa Duch.) by CO2 enrichment', *http://mc.manuscriptcentral.com/tbeq*, 34(1), pp. 905–917. Available at: https://doi.org/10.1080/13102818.2020.1811766.

Li, Yuanyuan *et al.* (2017) 'Combining genetic and evolutionary engineering to establish C4 metabolism in C3 plants', *Journal of Experimental Botany*, 68(2), pp. 117–125. Available at: https://doi.org/10.1093/JXB/ERW333.

Li, Yongping *et al.* (2017) 'Global identification of alternative splicing via comparative analysis of SMRT- and Illumina-based RNA-seq in strawberry', *The Plant Journal*, 90(1), pp. 164–176. Available at: https://doi.org/10.1111/TPJ.13462.

Lian, Q. *et al.* (2024) 'A pan-genome of 69 Arabidopsis thaliana accessions reveals a conserved genome structure throughout the global species range', *Nature Genetics 2024 56:5*, 56(5), pp. 982–991. Available at: https://doi.org/10.1038/s41588-024-01715-9.

Lieman-Hurwitz, J. *et al.* (2003) 'Enhanced photosynthesis and growth of transgenic plants that express ictB , a gene involved in HCO 3-accumulation in cyanobacteria', *Plant Biotechnology Journal*, 1, pp. 43–50. Available at: https://doi.org/10.1046/j.1467-7652.2003.00003.x.

Lin, G. *et al.* (2017) 'A receptor-like protein acts as a specificity switch for the regulation of stomatal development', *Genes & development*, 31(9), pp. 927–938. Available at: https://doi.org/10.1101/GAD.297580.117.

Lin, Y. *et al.* (2021) 'Genome-wide identification of GMP genes in Rosaceae and functional characterization of FaGMP4 in strawberry (Fragaria × ananassa)', *Genes and Genomics*, 43(6), pp. 587–599. Available at: https://doi.org/10.1007/S13258-021-01062-7/METRICS.

Liston, A., Cronn, R. and Ashman, T.L. (2014) 'Fragaria: A genus with deep historical roots and ripe for evolutionary and ecological insights', *American Journal of Botany*, 101(10), pp. 1686–1699. Available at: https://doi.org/10.3732/AJB.1400140.

Liu, T. *et al.* (2021) 'Reannotation of the cultivated strawberry genome and establishment of a strawberry genome database', *Horticulture Research*, 8(1), p. 41. Available at: https://doi.org/10.1038/S41438-021-00476-4/42041633/41438_2021_ARTICLE_476.PDF.

Livak, K.J. and Schmittgen, T.D. (2001) 'Analysis of relative gene expression data using real-time quantitative PCR and the 2-ΔΔCT method', *Methods*, 25(4), pp. 402–408. Available at: https://doi.org/10.1006/meth.2001.1262.

Long, S.P. *et al.* (2006) 'Can improvement in photosynthesis increase crop yields?', *Plant, Cell & Environment*, 29(3), pp. 315–330. Available at: https://doi.org/10.1111/J.1365-3040.2005.01493.X.

Long, S.P. *et al.* (2022) 'Into the Shadows and Back into Sunlight: Photosynthesis in Fluctuating Light', *Annual Review of Plant Biology*, 73(Volume 73, 2022), pp. 617–648. Available at: https://doi.org/10.1146/ANNUREV-ARPLANT-070221-024745/CITE/REFWORKS.

Longhi, S. *et al.* (2014) ‘Molecular genetics and genomics of the Rosoideae: state of the art and future perspectives’, *Horticulture Research 2013 1:1*, 1(1), pp. 1–18. Available at: https://doi.org/10.1038/hortres.2014.1.

López-Calcagno, P.E. *et al.* (2020) ‘Stimulating photosynthetic processes increases productivity and water-use efficiency in the field’, *Nature Plants 2020 6:8*, 6(8), pp. 1054–1063. Available at: https://doi.org/10.1038/s41477-020-0740-1.

Lu, S. *et al.* (2013) ‘Increased expression of phospholipase Dα1 in guard cells decreases water loss with improved seed production under drought in Brassica napus’, *Plant Biotechnology Journal*, 11(3), pp. 380–389. Available at: https://doi.org/10.1111/PBI.12028.

Lugassi, N. *et al.* (2015) ‘Expression of Arabidopsis Hexokinase in Citrus Guard Cells Controls Stomatal Aperture and Reduces Transpiration’, *Frontiers in Plant Science*, 0(DEC), p. 1114. Available at: https://doi.org/10.3389/FPLS.2015.01114.

Lugassi, N. *et al.* (2019) ‘Expression of Arabidopsis Hexokinase in Tobacco Guard Cells Increases Water-Use Efficiency and Confers Tolerance to Drought and Salt Stress’, *Plants*, 8(12). Available at: https://doi.org/10.3390/plants8120613.

Lunn, D. *et al.* (2024) ‘Greater aperture counteracts effects of reduced stomatal density on water use efficiency: a case study on sugarcane and meta-analysis’, *Journal of Experimental Botany*, 75(21), pp. 6837–6849. Available at: https://doi.org/10.1093/JXB/ERAE271.

Maggini, S., Wenzlaff, S. and Hornig, D. (2010) ‘Essential role of vitamin c and zinc in child immunity and health’, *Journal of International Medical Research*, 38(2), pp. 386–414. Available at: https://doi.org/10.1177/147323001003800203.

Mano, N.A., Madore, B. and Mickelbart, M. V. (2023) ‘Different Leaf Anatomical Responses to Water Deficit in Maize and Soybean’, *Life*, 13(2), p. 290. Available at: https://doi.org/10.3390/LIFE13020290/S1.

Martín-Pizarro, C., Triviño, J.C. and Posé, D. (2019) ‘Functional analysis of the TM6 MADS-box gene in the octoploid strawberry by CRISPR/Cas9-directed mutagenesis’, *Journal of Experimental Botany*, 70(3), pp. 885–895. Available at: https://doi.org/10.1093/JXB/ERY400.

Matson, P.A. *et al.* (1997) ‘Agricultural Intensification and Ecosystem Properties’, *Science*, 277(5325), pp. 504–509. Available at: https://doi.org/10.1126/SCIENCE.277.5325.504.

Matson, P.A. and Vitousek, P.M. (2006) ‘Agricultural Intensification: Will Land Spared from Farming be Land Spared for Nature?’, *Conservation Biology*, 20(3), pp. 709–710. Available at: https://doi.org/10.1111/J.1523-1739.2006.00442.X.

Matthews, J.S.A., Vialet-Chabrand, S. and Lawson, T. (2018) ‘Acclimation to Fluctuating Light Impacts the Rapidity of Response and Diurnal Rhythm of Stomatal Conductance’, *Plant Physiology*, 176(3), pp. 1939–1951. Available at: https://doi.org/10.1104/PP.17.01809.

Mayer, J.E., Pfeiffer, W.H. and Beyer, P. (2008) 'Biofortified crops to alleviate micronutrient malnutrition', *Current Opinion in Plant Biology*, 11(2), pp. 166–170. Available at: https://doi.org/10.1016/J.PBI.2008.01.007.

McAusland, L. *et al.* (2016) 'Effects of kinetics of light-induced stomatal responses on photosynthesis and water-use efficiency', *New Phytologist*, 211(4), pp. 1209–1220. Available at: https://doi.org/10.1111/NPH.14000.

McElwain, J.C., Yiotis, C. and Lawson, T. (2016) 'Using modern plant trait relationships between observed and theoretical maximum stomatal conductance and vein density to examine patterns of plant macroevolution', *New Phytologist*, 209(1), pp. 94–103. Available at: https://doi.org/10.1111/NPH.13579;WGROUP:STRING:PUBLICATION.

Mehta, D. (2018) 'The Green Revolution did not increase poverty and hunger for millions', *Nature Plants 2018 4:10*, 4(10), pp. 736–736. Available at: https://doi.org/10.1038/s41477-018-0240-8.

Menzel, C.M. (2024) 'Climate change increases net CO2 assimilation in the leaves of strawberry, but not yield', *Journal of Horticultural Science and Biotechnology*, 99(3), pp. 233–266. Available at: https://doi.org/10.1080/14620316.2023.2263773;WGROUP:STRING:PUBLICATION.

Mineau, P. (2005) 'A review and analysis of study endpoints relevant to the assessment of "long term" pesticide toxicity in avian and mammalian wildlife', *Ecotoxicology*, 14(8), pp. 775–799. Available at: https://doi.org/10.1007/S10646-005-0028-2/TABLES/3.

Mitra, M.L. (1971) ‘Confusional states in relation to vitamin deficiencies in the elderly’, *Journal of the American Geriatrics Society*, 19(6), pp. 536–545. Available at: https://doi.org/10.1111/J.1532-5415.1971.TB01213.X.

Mohammed, U. *et al.* (2019) ‘Rice plants overexpressing OsEPF1 show reduced stomatal density and increased root cortical aerenchyma formation’, *Scientific Reports*, 9(1). Available at: https://doi.org/10.1038/S41598-019-41922-7.

Moore, B. *et al.* (2003) ‘Role of the Arabidopsis glucose sensor HXK1 in nutrient, light, and hormonal signaling’, *Science (New York, N.Y.)*, 300(5617), pp. 332–336. Available at: https://doi.org/10.1126/SCIENCE.1080585.

Morgan, P.B. *et al.* (2005) ‘Smaller than predicted increase in aboveground net primary production and yield of field-grown soybean under fully open-air [CO2] elevation’, *Global change biology*, 11(10), pp. 1856–1865. Available at: https://doi.org/10.1111/J.1365-2486.2005.001017.X.

Morison, J.I.L., Stewart, B.A. and Howell, T. (2003) ‘Plant water use, stomatal control’, *Encyclopedia of Water Science. Marcel Dekker, New York*, pp. 680–685.

Mosier, A., Syers, J.K. and Freney, J.R. (2013) *Agriculture and the nitrogen cycle: assessing the impacts of fertilizer use on food production and the environment*. Island Press.

Mott, K.A. and Michaelson, O. (1991) ‘AMPHISTOMY AS AN ADAPTATION TO HIGH LIGHT INTENSITY IN AMBROSIA CORDIFOLIA (COMPOSITAE)’, *American Journal of*

Botany, 78(1), pp. 76–79. Available at: https://doi.org/10.1002/J.1537-2197.1991.TB12573.X.

Müller-Röber, B. *et al.* (1994) 'A truncated version of an ADP-glucose pyrophosphorylase promoter from potato specifies guard cell-selective expression in transgenic plants.', *The Plant Cell*, 6(5), p. 601. Available at: https://doi.org/10.2307/3869866.

Müller-Röber, B. *et al.* (1995) 'Cloning and electrophysiological analysis of KST1, an inward rectifying K+ channel expressed in potato guard cells.', *The EMBO Journal*, 14(11), p. 2409. Available at: /pmc/articles/PMC398354/?report=abstract.

Murashige, T. and Skoog, F. (1962) 'A Revised Medium for Rapid Growth and Bio Assays with Tobacco Tissue Cultures', *Physiologia Plantarum*, 15(3), pp. 473–497. Available at: https://doi.org/10.1111/J.1399-3054.1962.TB08052.X.

Na, J.K. and Metzger, J.D. (2017) 'Guard-cell-specific expression of Arabidopsis ABF4 improves drought tolerance of tomato and tobacco', *Molecular Breeding*, 37(12), p. 154. Available at: https://doi.org/10.1007/s11032-017-0758-x.

Nadeau, J.A. (2009) 'Stomatal development: new signals and fate determinants', *Current Opinion in Plant Biology*, 12(1), pp. 29–35. Available at: https://doi.org/10.1016/J.PBI.2008.10.006.

Nadeau, J.A. and Sack, F.D. (2002) 'Control of stomatal distribution on the Arabidopsis leaf surface', *Science (New York, N.Y.)*, 296(5573), pp. 1697–1700. Available at: https://doi.org/10.1126/SCIENCE.1069596.

Nagaya, S. *et al.* (2010) 'The HSP Terminator of Arabidopsis thaliana Increases Gene Expression in Plant Cells', *Plant and Cell Physiology*, 51(2), pp. 328–332. Available at: https://doi.org/10.1093/PCP/PCP188.

Naing, A.H. *et al.* (2019) 'In vitro propagation method for production of morphologically and genetically stable plants of different strawberry cultivars', *Plant Methods*, 15(1), pp. 1–10. Available at: https://doi.org/10.1186/S13007-019-0421-0/FIGURES/10.

National Institute of Health (2021a) *Folate - Health Professional Fact Sheet*, *NIH: Office of Dietary Supplements*. Available at: https://ods.od.nih.gov/factsheets/Folate-HealthProfessional/ (Accessed: 2 December 2021).

National Institute of Health (2021b) *Magnesium - Health Professional Fact Sheet*, *NIH: Office of Dietary Supplements*. Available at: https://ods.od.nih.gov/factsheets/Magnesium-HealthProfessional/ (Accessed: 2 December 2021).

National Institute of Health (2021c) *Vitamin C - Health Professional Fact Sheet*. Available at: https://ods.od.nih.gov/factsheets/VitaminC-HealthProfessional/ (Accessed: 25 November 2021).

Nishi, S. and Ohsawa, K. (1973) 'Mass production method of virus-free strawberry plants through meristem callus', *Japan Agricultural Research Quarterly*, 7, pp. 189–194.

Nunes, T.D.G. *et al.* (2022) 'Quantitative effects of environmental variation on stomatal anatomy and gas exchange in a grass model', *Quantitative Plant Biology*, 3, p. e6. Available at: https://doi.org/10.1017/QPB.2021.19.

O'Dell, C.R. and Williams, J. (2009) 'Hill system plastic mulched strawberry production guide for colder areas'.

Ohki, S., Takeuchi, M. and Mori, M. (2011) 'The NMR structure of stomagen reveals the basis of stomatal density regulation by plant peptide hormones', *Nature communications*, 2(1). Available at: https://doi.org/10.1038/NCOMMS1520.

Ölçer, H., Lloyd, J.C. and Raines, C.A. (2001) 'Photosynthetic Capacity Is Differentially Affected by Reductions in Sedoheptulose-1,7-Bisphosphatase Activity during Leaf Development in Transgenic Tobacco Plants', *Plant Physiology*, 125(2), pp. 982–989. Available at: https://doi.org/10.1104/PP.125.2.982.

Ooms, G. *et al.* (1982) 'Octopine Ti-plasmid deletion mutants of Agrobacterium tumefaciens with emphasis on the right side of the T-region', *Plasmid*, 7(1), pp. 15–29. Available at: https://doi.org/10.1016/0147-619X(82)90023-3.

Orcaray, L. *et al.* (2012) "Impairment of carbon metabolism induced by the herbicide glyphosate," *Journal of Plant Physiology*, 169(1), pp. 27–33. Available at: https://doi.org/10.1016/J.JPLPH.2011.08.009.

Outlaw, W.H. (2010) 'Integration of Cellular and Physiological Functions of Guard Cells', *https://doi.org/10.1080/713608316*, 22(6), pp. 503–529. Available at: https://doi.org/10.1080/713608316.

Ouyang, W. *et al.* (2017) 'Stomatal conductance, mesophyll conductance, and transpiration efficiency in relation to leaf anatomy in rice and wheat genotypes under

drought', *Journal of Experimental Botany*, 68(18), pp. 5191–5205. Available at: https://doi.org/10.1093/JXB/ERX314.

Palmgren, M.G. (2001) 'Plant plasma membrane H+-ATPases: Powerhouses for nutrient uptake', *Annual Review of Plant Biology*, 52(Volume 52, 2001), pp. 817–845. Available at: https://doi.org/10.1146/ANNUREV.ARPLANT.52.1.817/CITE/REFWORKS.

Papanatsiou, M. *et al.* (2019) 'Optogenetic manipulation of stomatal kinetics improves carbon assimilation,water use, and growth', *Science*, 363(6434), pp. 1456–1459. Available at: https://doi.org/10.1126/SCIENCE.AAW0046/SUPPL_FILE/AAW0046_PAPANATSIOU_SM.PDF.

Parkhurst, D.F. (1978) 'The Adaptive Significance of Stomatal Occurrence on One or Both Surfaces of Leaves', *The Journal of Ecology*, 66(2), p. 367. Available at: https://doi.org/10.2307/2259142.

Parlange, J.-Y. and Waggoner, P.E. (1970) 'Stomatal Dimensions and Resistance to Diffusion', *Plant Physiology*, 46(2), p. 337. Available at: https://doi.org/10.1104/PP.46.2.337.

Parry, M.A.J. *et al.* (2013) 'Rubisco activity and regulation as targets for crop improvement', *Journal of Experimental Botany*, 64(3), pp. 717–730. Available at: https://doi.org/10.1093/JXB/ERS336.

Parry, M.L. *et al.* (2004) 'Effects of climate change on global food production under SRES emissions and socio-economic scenarios', *Global Environmental Change*, 14(1), pp. 53–67. Available at: https://doi.org/10.1016/J.GLOENVCHA.2003.10.008.

Pelletier, V. *et al.* (2016) 'Reducing cranberry heat stress and midday depression with evaporative cooling', *Scientia Horticulturae*, 198, pp. 445–453. Available at: https://doi.org/10.1016/J.SCIENTA.2015.12.028.

Pérez-Bueno, M.L. *et al.* (2022) 'An extremely low stomatal density mutant overcomes cooling limitations at supra-optimal temperature by adjusting stomatal size and leaf thickness', *Frontiers in Plant Science*, 13, p. 919299. Available at: https://doi.org/10.3389/FPLS.2022.919299/BIBTEX.

Peterhansel, C. *et al.* (2010) 'Photorespiration', *The Arabidopsis Book / American Society of Plant Biologists*, 8, p. e0130. Available at: https://doi.org/10.1199/TAB.0130.

Phalan, B., Balmford, A., *et al.* (2011) 'Minimising the harm to biodiversity of producing more food globally', *Food Policy* [Preprint]. Available at: https://doi.org/10.1016/j.foodpol.2010.11.008.

Phalan, B., Onial, M., *et al.* (2011) 'Reconciling food production and biodiversity conservation: Land sharing and land sparing compared', *Science*, 333(6047), pp. 1289–1291. Available at: https://doi.org/10.1126/SCIENCE.1208742/SUPPL_FILE/PHALAN.SOM.PDF.

Pillitteri, L.J. and Torii, K.U. (2012) 'Mechanisms of stomatal development', *Annual Review of Plant Biology*, 63(Volume 63, 2012), pp. 591–614. Available at: https://doi.org/10.1146/ANNUREV-ARPLANT-042811-105451/CITE/REFWORKS.

Pimentel, D. *et al.* (1992) 'Environmental and Economic Costs of Pesticide Use', *BioScience*, 42(10), pp. 750–760. Available at: https://doi.org/10.2307/1311994.

Pingali, P.L. (2012) 'Green Revolution: Impacts, limits, and the path ahead', *Proceedings of the National Academy of Sciences*, 109(31), pp. 12302–12308. Available at: https://doi.org/10.1073/PNAS.0912953109.

Plesch, G., Ehrhardt, T. and Mueller-Roeber, B. (2001) 'Involvement of TAAAG elements suggests a role for Dof transcription factors in guard cell-specific gene expression', *The Plant journal : for cell and molecular biology*, 28(4), pp. 455–464. Available at: https://doi.org/10.1046/J.1365-313X.2001.01166.X.

Poling, E.B. (1993) 'Strawberry Plasticulture in North Carolina: II. Preplant, Planting, and Postplant Considerations for Growing ` Chandler' Strawberry on Black Plastic Mulch', *HortTechnology*, 3(4), pp. 383–393. Available at: https://doi.org/10.21273/HORTTECH.3.4.383.

Poling, E.B. (1996) 'Challenges for annual production systems in cool climates', in *Proceedings of the IV North American Strawberry Conference. University of Florida, Orlando, FL*, pp. 162–170.

Poling, E.B. (2012) 'Strawberry plant structure and growth habit', *New York State Berry Growers Association, Berry EXPO* [Preprint].

Pospíšilová, J. (1996) ‘Effect of air humidity on the development of functional stomatal apparatus’, *Biologia Plantarum*, 38(2), pp. 197–204. Available at: https://doi.org/10.1007/BF02873846/METRICS.

Pritts, M. *et al.* (1998) ‘Strawberry Production Guide for the Northeast, Midwest, and Eastern Canada (NRAES-88)’. Available at: https://ecommons.cornell.edu/handle/1813/66932 (Accessed: 22 November 2021).

Pritts, M. and Dale, A. (1989) ‘Dayneutral Strawberry Production Guide’, *Information bulletin 215 Cornell Cooperative Extension* [Preprint]. Available at: https://ecommons.cornell.edu/handle/1813/3275 (Accessed: 18 November 2021).

Prohens, J. *et al.* (2022) ‘Stability of Transgene Inheritance in Progeny of Field-Grown Pear Trees over a 7-Year Period’, *Plants 2022, Vol. 11, Page 151*, 11(2), p. 151. Available at: https://doi.org/10.3390/PLANTS11020151.

Qi, X. *et al.* (2017) ‘Autocrine regulation of stomatal differentiation potential by EPF1 and ERECTA-LIKE1 ligand-receptor signaling’, *eLife*, 6. Available at: https://doi.org/10.7554/ELIFE.24102.

Qu, M. *et al.* (2016) ‘Rapid stomatal response to fluctuating light: an under-explored mechanism to improve drought tolerance in rice’, *Functional Plant Biology*, 43(8), pp. 727–738. Available at: https://doi.org/10.1071/FP15348.

Qu, M. *et al.* (2020) ‘Alterations in stomatal response to fluctuating light increase biomass and yield of rice under drought conditions’, *The Plant Journal*, 104(5), pp. 1334–1347. Available at: https://doi.org/10.1111/TPJ.15004.

le Quéré, C. *et al.* (2009) 'Trends in the sources and sinks of carbon dioxide', *Nature Geoscience 2009 2:12*, 2(12), pp. 831–836. Available at: https://doi.org/10.1038/ngeo689.

Ray, D.K. *et al.* (2013) 'Yield Trends Are Insufficient to Double Global Crop Production by 2050', *PLOS ONE*, 8(6), p. e66428. Available at: https://doi.org/10.1371/JOURNAL.PONE.0066428.

Ritchie, H. and Roser, M. (2017) 'Micronutrient Deficiency', *Our World in Data* [Preprint]. Available at: https://ourworldindata.org/micronutrient-deficiency (Accessed: 9 January 2022).

Riu, Y.-S. *et al.* (2021) 'Guard-cell-specific expression of phototropin2 C-terminal fragment enhances leaf transpiration', *Plants*, 11(1), p. 65.

Roddy, A.B. *et al.* (2020) 'The Scaling of Genome Size and Cell Size Limits Maximum Rates of Photosynthesis with Implications for Ecological Strategies', *https://doi.org/10.1086/706186*, 181(1), pp. 75–87. Available at: https://doi.org/10.1086/706186.

Rolland, F., Baena-Gonzalez, E. and Sheen, J. (2006) 'Sugar sensing and signaling in plants: conserved and novel mechanisms', *Annual review of plant biology*, 57, pp. 675–709. Available at: https://doi.org/10.1146/ANNUREV.ARPLANT.57.032905.105441.

Ruiz-Vera, U.M. *et al.* (2022) 'Field-grown ictB tobacco transformants show no difference in photosynthetic efficiency for biomass relative to the wild type', *Journal of*

Experimental Botany, 73(14), pp. 4897–4907. Available at: https://doi.org/10.1093/JXB/ERAC193.

Rutherford, A.W. and Krieger-Liszkay, A. (2001) "Herbicide-induced oxidative stress in photosystem II," *Trends in Biochemical Sciences*, 26(11), pp. 648–653. Available at: https://doi.org/10.1016/S0968-0004(01)01953-3.

Sachs, T. (1991) *Pattern formation in plant tissues*. Cambridge University Press.

Sade, N. *et al.* (2014) 'Differential tissue-specific expression of NtAQP1 in Arabidopsis thaliana reveals a role for this protein in stomatal and mesophyll conductance of CO_2 under standard and salt-stress conditions', *Planta*, 239(2), pp. 357–366. Available at: https://doi.org/10.1007/S00425-013-1988-8.

Sage, R.F., Way, D.A. and Kubien, D.S. (2008) 'Rubisco, Rubisco activase, and global climate change', *Journal of Experimental Botany*, 59(7), pp. 1581–1595. Available at: https://doi.org/10.1093/JXB/ERN053.

Sakoda, K. *et al.* (2020) 'Higher Stomatal Density Improves Photosynthetic Induction and Biomass Production in Arabidopsis Under Fluctuating Light', *Frontiers in Plant Science*, 0, p. 1609. Available at: https://doi.org/10.3389/FPLS.2020.589603.

Sakoda, K. *et al.* (2021) 'Stomatal, mesophyll conductance, and biochemical limitations to photosynthesis during induction', *Plant Physiology*, 185(1), pp. 146–160. Available at: https://doi.org/10.1093/PLPHYS/KIAA011.

Sargent, D.J. *et al.* (2016) 'HaploSNP affinities and linkage map positions illuminate subgenome composition in the octoploid, cultivated strawberry (Fragaria×ananassa)', *Plant science : an international journal of experimental plant biology*, 242, pp. 140–150. Available at: https://doi.org/10.1016/J.PLANTSCI.2015.07.004.

Schaart, J.G. (2014) 'Agrobacterium-mediated transformation of strawberry', *Bio-protocol*, 4(1), p. e1022. Available at: https://doi.org/10.21769/BIOPROTOC.1022.

Schlüter, U. *et al.* (2003) 'Photosynthetic performance of an Arabidopsis mutant with elevated stomatal density (sdd1-1) under different light regimes', *Journal of Experimental Botany*, 54(383), pp. 867–874. Available at: https://doi.org/10.1093/JXB/ERG087.

Schnell, J. *et al.* (2014) 'A comparative analysis of insertional effects in genetically engineered plants: considerations for pre-market assessments', *Transgenic Research*, 24(1), p. 1. Available at: https://doi.org/10.1007/S11248-014-9843-7.

Schroeder, J.I. *et al.* (2001) 'Guard cell signal transduction', *Annual Review of Plant Biology*, 52(Volume 52, 2001), pp. 627–658. Available at: https://doi.org/10.1146/ANNUREV.ARPLANT.52.1.627/CITE/REFWORKS.

Schroeder, J.I., Hedrich, R. and Fernandez, J.M. (1984) 'Potassium-selective single channels in guard cell protoplasts of Vicia faba', *Nature 1984 312:5992*, 312(5992), pp. 361–362. Available at: https://doi.org/10.1038/312361a0.

Schroeder, J.I., Raschke, K. and Neher, E. (1987) 'Voltage dependence of K+ channels in guard-cell protoplasts', *Proceedings of the National Academy of Sciences of the United*

States of America, 84(12), pp. 4108–4112. Available at: https://doi.org/10.1073/PNAS.84.12.4108.

Schuler, M.L., Mantegazza, O. and Weber, A.P.M. (2016) 'Engineering C4 photosynthesis into C3 chassis in the synthetic biology age', *The Plant Journal*, 87(1), pp. 51–65. Available at: https://doi.org/10.1111/TPJ.13155.

Sherpa, T. and Dey, N. (2024) 'Development of robust constitutive synthetic promoter using genetic resources of plant pararetroviruses', *Frontiers in Plant Science*, 15, p. 1515921. Available at: https://doi.org/10.3389/FPLS.2024.1515921/FULL.

Shimazaki, K., Iino, M. and Zeiger, E. (1986) 'Blue light-dependent proton extrusion by guard-cell protoplasts of Vicia faba', *Nature 1986 319:6051*, 319(6051), pp. 324–326. Available at: https://doi.org/10.1038/319324a0.

Shpak, E.D. *et al.* (2005) 'Stomatal patterning and differentiation by synergistic interactions of receptor kinases', *Science (New York, N.Y.)*, 309(5732), pp. 290–293. Available at: https://doi.org/10.1126/SCIENCE.1109710.

Shulaev, V. *et al.* (2010) 'The genome of woodland strawberry (Fragaria vesca)', *Nature Genetics 2010 43:2*, 43(2), pp. 109–116. Available at: https://doi.org/10.1038/ng.740.

Simkin, A.J. *et al.* (2015) 'Multigene manipulation of photosynthetic carbon assimilation increases CO2 fixation and biomass yield in tobacco', *Journal of Experimental Botany*, 66(13), pp. 4075–4090. Available at: https://doi.org/10.1093/JXB/ERV204.

Simkin, A.J. *et al.* (2017) 'Simultaneous stimulation of sedoheptulose 1,7-bisphosphatase, fructose 1,6-bisphophate aldolase and the photorespiratory glycine

decarboxylase-H protein increases CO2 assimilation, vegetative biomass and seed yield in Arabidopsis', *Plant Biotechnology Journal*, 15(7), pp. 805–816. Available at: https://doi.org/10.1111/PBI.12676.

Simkin, A.J. (2019) 'Genetic Engineering for Global Food Security: Photosynthesis and Biofortification', *Plants 2019, Vol. 8, Page 586*, 8(12), p. 586. Available at: https://doi.org/10.3390/PLANTS8120586.

Simkin, A.J., López-Calcagno, P.E. and Raines, C.A. (2019) 'Feeding the world: improving photosynthetic efficiency for sustainable crop production', *Journal of Experimental Botany*, 70(4), pp. 1119–1140. Available at: https://doi.org/10.1093/JXB/ERY445.

Skelton, R.P. *et al.* (2017) 'Gas exchange recovery following natural drought is rapid unless limited by loss of leaf hydraulic conductance: evidence from an evergreen woodland', *New Phytologist*, 215(4), pp. 1399–1412. Available at: https://doi.org/10.1111/NPH.14652.

Slattery, R.A. *et al.* (2018) 'The Impacts of Fluctuating Light on Crop Performance', *Plant Physiology*, 176(2), pp. 990–1003. Available at: https://doi.org/10.1104/PP.17.01234.

Solomon, S. *et al.* (2007) *Climate change 2007-the physical science basis: Working group I contribution to the fourth assessment report of the IPCC*. Cambridge university press.

South, P.F. *et al.* (2018) ‘Optimizing photorespiration for improved crop productivity’, *Journal of Integrative Plant Biology*, 60(12), pp. 1217–1230. Available at: https://doi.org/10.1111/JIPB.12709.

South, P.F. *et al.* (2019) ‘Synthetic glycolate metabolism pathways stimulate crop growth and productivity in the field’, *Science*, 363(6422). Available at: https://doi.org/10.1126/SCIENCE.AAT9077/SUPPL_FILE/DATASETS_S1-S11_S16-S20.PDF.

De Souza, A.P. *et al.* (2022) ‘Soybean photosynthesis and crop yield are improved by accelerating recovery from photoprotection’, *Science*, 377(6608), pp. 851–854. Available at: https://doi.org/10.1126/SCIENCE.ADC9831/SUPPL_FILE/SCIENCE.ADC9831_MDAR_REPRODUCIBILITY_CHECKLIST.PDF.

Stevens, J., Jones, M.A. and Lawson, T. (2021) ‘Diverse physiological and physical responses among wild, landrace and elite barley varieties point to novel breeding opportunities’, *Agronomy*, 11(5). Available at: https://doi.org/10.3390/AGRONOMY11050921.

Stevens, M.D. *et al.* (2011) ‘Horticultural and Economic Considerations in the Sustainability of Three Cold-climate Strawberry Production Systems’, *HortScience*, 46(3), pp. 445–451. Available at: https://doi.org/10.21273/HORTSCI.46.3.445.

Sugano, S.S. *et al.* (2009) ‘Stomagen positively regulates stomatal density in Arabidopsis’, *Nature 2009 463:7278*, 463(7278), pp. 241–244. Available at: https://doi.org/10.1038/nature08682.

Sun, P. *et al.* (2012) 'Effects of Elevated CO2 and Temperature on Yield and Fruit Quality of Strawberry (Fragaria × ananassa Duch.) at Two Levels of Nitrogen Application', *PLOS ONE*, 7(7), p. e41000. Available at: https://doi.org/10.1371/JOURNAL.PONE.0041000.

Sung, F.J.M. and Chen, J.J. (1991) 'Gas exchange rate and yield response of strawberry to carbon dioxide enrichment', *Scientia Horticulturae*, 48(3–4), pp. 241–251. Available at: https://doi.org/10.1016/0304-4238(91)90132-I.

Suzuki, Y. *et al.* (2007) 'Increased Rubisco Content in Transgenic Rice Transformed with the "Sense" rbcS Gene', *Plant and Cell Physiology*, 48(4), pp. 626–637. Available at: https://doi.org/10.1093/PCP/PCM035.

Swartz, H.J., Galetta, G. and Zimmerman, R. (1981) 'Field performance and phenotypic stability of tissue culture-propagated strawberries'.

Takahashi, S. *et al.* (2015) 'Natural Variation in Stomatal Responses to Environmental Changes among Arabidopsis thaliana Ecotypes', *PLOS ONE*, 10(2), p. e0117449. Available at: https://doi.org/10.1371/JOURNAL.PONE.0117449.

Takayama, K *et al.* (2003) "Fluorescence image sensing is an active sensing technique, for example laser-induced fluorescence (LIF) imaging and chlorophyll fluorescence imaging," *Govindjee and Nedbal* [Preprint].

Tamura, T. *et al.* (2010) 'Folate in Health and Disease'.

Tanaka, Yoko *et al.* (2013) 'ABA inhibits entry into stomatal-lineage development in Arabidopsis leaves', *The Plant Journal*, 74(3), pp. 448–457. Available at: https://doi.org/10.1111/TPJ.12136.

Tanaka, Y *et al.* (2013) 'Enhancement of leaf photosynthetic capacity through increased stomatal density in Arabidopsis', *The New phytologist*, 198(3), pp. 757–764. Available at: https://doi.org/10.1111/NPH.12186.

Tennessen, J.A. *et al.* (2013) 'Targeted sequence capture provides insight into genome structure and genetics of male sterility in a gynodioecious diploid strawberry, fragaria vesca ssp. bracteata (rosaceae)', *G3: Genes, Genomes, Genetics*, 3(8), pp. 1341–1351. Available at: https://doi.org/10.1534/G3.113.006288/-/DC1.

Tennessen, J.A. *et al.* (2014) 'Evolutionary Origins and Dynamics of Octoploid Strawberry Subgenomes Revealed by Dense Targeted Capture Linkage Maps', *Genome Biology and Evolution*, 6(12), pp. 3295–3313. Available at: https://doi.org/10.1093/GBE/EVU261.

Thierry, D. and Vaucheret, H. (1996) 'Sequence homology requirements for transcriptional silencing of 35S transgenes and post-transcriptional silencing of nitrite reductase (trans)genes by the tobacco 271 locus', *Plant Molecular Biology*, 32(6), pp. 1075–1083. Available at: https://doi.org/10.1007/BF00041391/METRICS.

Thomas, W.R. and Holt, P.G. (1978) 'Vitamin C and immunity: an assessment of the evidence.', *Clinical and Experimental Immunology*, 32(2), p. 370. Available at: /pmc/articles/PMC1541262/?report=abstract (Accessed: 9 January 2022).

Tichá, I. (1982) ‘PHOTOSYNTHETIC CHARACTERISTICS DURING ONTOGENESIS OF LEAVES. VII: STOMATA DENSITY AND SIZES’.

Tilman, D. and Clark, M. (2015) ‘Food, Agriculture & the Environment: Can We Feed the World & Save the Earth?’, *Daedalus*, 144(4), pp. 8–23. Available at: https://doi.org/10.1162/DAED_A_00350.

Tizaoui, K. and Kchouk, M.E. (2012) ‘Genetic approaches for studying transgene inheritance and genetic recombination in three successive generations of transformed tobacco’. Available at: www.sbg.org.br (Accessed: 21 July 2025).

Toh, S. *et al.* (2021) ‘Overexpression of Plasma Membrane H+-ATPase in Guard Cells Enhances Light-Induced Stomatal Opening, Photosynthesis, and Plant Growth in Hybrid Aspen’, *Frontiers in Plant Science*, 12, p. 766037. Available at: https://doi.org/10.3389/FPLS.2021.766037/BIBTEX.

Triplett, G., Buckley, T.N. and Muir, C.D. (2024) ‘Amphistomy increases leaf photosynthesis more in coastal than montane plants of Hawaiian ‘ilima (Sida fallax)’, *American Journal of Botany*, 111(2), p. e16284. Available at: https://doi.org/10.1002/AJB2.16284;PAGEGROUP:STRING:PUBLICATION.

Tscharntke, T. *et al.* (2012) ‘Global food security, biodiversity conservation and the future of agricultural intensification’, *Biological Conservation*, 151(1), pp. 53–59. Available at: https://doi.org/10.1016/J.BIOCON.2012.01.068.

Tsuzuki, T. *et al.* (2013) ‘Overexpression of the Mg-chelatase H subunit in guard cells confers drought tolerance via promotion of stomatal closure in Arabidopsis thaliana’,

Frontiers in Plant Science, 4(OCT), p. 65554. Available at: https://doi.org/10.3389/FPLS.2013.00440/ABSTRACT.

Uematsu, K. *et al.* (2012) 'Increased fructose 1,6-bisphosphate aldolase in plastids enhances growth and photosynthesis of tobacco plants', *Journal of experimental botany*, 63(8), pp. 3001–3009. Available at: https://doi.org/10.1093/JXB/ERS004.

Ueno, K. *et al.* (2005) 'Biochemical Characterization of Plasma Membrane H+-ATPase Activation in Guard Cell Protoplasts of Arabidopsis thaliana in Response to Blue Light', *Plant and Cell Physiology*, 46(6), pp. 955–963. Available at: https://doi.org/10.1093/PCP/PCI104.

United Nations (2019) 'Department of Economic and Social Affairs, Population Division. World Population Prospects 2019: Data Booklet (ST/ESA/SER. A/424)'.

Urban, J. *et al.* (2017) 'Increase in leaf temperature opens stomata and decouples net photosynthesis from stomatal conductance in Pinus taeda and Populus deltoides x nigra', *Journal of Experimental Botany*, 68(7), pp. 1757–1767. Available at: https://doi.org/10.1093/JXB/ERX052.

U.S. Department of Agriculture (2018) *Strawberries, raw Nutritional Information*, *FoodData Central*. Available at: https://fdc.nal.usda.gov/fdc-app.html#/food-details/167762/nutrients (Accessed: 22 November 2021).

Velten, J. *et al.* (2012) 'Transgene Silencing and Transgene-Derived siRNA Production in Tobacco Plants Homozygous for an Introduced AtMYB90 Construct', *PLOS ONE*, 7(2), p. e30141. Available at: https://doi.org/10.1371/JOURNAL.PONE.0030141.

Vialet-Chabrand, S.R.M. *et al.* (2017) 'Temporal Dynamics of Stomatal Behavior: Modeling and Implications for Photosynthesis and Water Use', *Plant Physiology*, 174(2), pp. 603–613. Available at: https://doi.org/10.1104/PP.17.00125.

Vico, G. *et al.* (2011) 'Effects of stomatal delays on the economics of leaf gas exchange under intermittent light regimes', *New Phytologist*, 192, pp. 640–652. Available at: https://doi.org/10.1111/j.1469-8137.2011.03847.x.

Walters, R.G. and Horton, P. (1994) 'Acclimation of Arabidopsis thaliana to the light environment: Changes in composition of the photosynthetic apparatus', *Planta*, 195(2), pp. 248–256. Available at: https://doi.org/10.1007/BF00199685/METRICS.

Wang, H. *et al.* (2007) 'Stomatal development and patterning are regulated by environmentally responsive mitogen-activated protein kinases in Arabidopsis', *The Plant cell*, 19(1), pp. 63–73. Available at: https://doi.org/10.1105/TPC.106.048298.

Wang, R. *et al.* (2015) 'Latitudinal variation of leaf stomatal traits from species to community level in forests: Linkage with ecosystem productivity', *Scientific Reports*, 5(1), pp. 1–11. Available at: https://doi.org/10.1038/SREP14454;SUBJMETA=158,2445,2455,631;KWRD=ECOPHYSIOLOGY,ECOSYSTEM+ECOLOGY.

Wang, S.Y. and Bunce, J.A. (2004) 'Elevated carbon dioxide affects fruit flavor in field-grown strawberries (Fragaria × ananassa Duch)', *Journal of the Science of Food and Agriculture*, 84(12), pp. 1464–1468. Available at: https://doi.org/10.1002/JSFA.1824.

Wang, S.Y., Bunce, J.A. and Maas, J.L. (2003) 'Elevated Carbon Dioxide Increases Contents of Antioxidant Compounds in Field-Grown Strawberries', *Journal of Agricultural and Food Chemistry*, 51(15), pp. 4315–4320. Available at: https://doi.org/10.1021/JF021172D.

Wang, Y. *et al.* (2013) 'Overexpression of plasma membrane H+-ATPase in guard cells promotes light-induced stomatal opening and enhances plant growth', *Proceedings of the National Academy of Sciences of the United States of America*, 111(1), pp. 533–538. Available at: https://doi.org/10.1073/PNAS.1305438111/SUPPL_FILE/PNAS.201305438SI.PDF.

Wang, Y., Hills, A. and Blatt, M.R. (2014) 'Systems Analysis of Guard Cell Membrane Transport for Enhanced Stomatal Dynamics and Water Use Efficiency', *Plant Physiology*, 164(4), pp. 1593–1599. Available at: https://doi.org/10.1104/PP.113.233403.

Wang, Z. *et al.* (2014) 'Improving Storability of Fresh Strawberries with Controlled Release Chlorine Dioxide in Perforated Clamshell Packaging', *Food and Bioprocess Technology*, 7(12), pp. 3516–3524. Available at: https://doi.org/10.1007/S11947-014-1364-0.

Watts, J.L. *et al.* (2024) 'Does stomatal patterning in amphistomatous leaves minimize the CO2 diffusion path length within leaves?', *AoB Plants*, 16(2), p. plae015. Available at: https://doi.org/10.1093/AOBPLA/PLAE015.

Weber, A.P.M. and Bar-Even, A. (2019) 'Update: Improving the Efficiency of Photosynthetic Carbon Reactions', *Plant Physiology*, 179(3), pp. 803–812. Available at: https://doi.org/10.1104/PP.18.01521.

Weber, E. *et al.* (2011) 'A Modular Cloning System for Standardized Assembly of Multigene Constructs', *PLOS ONE*, 6(2), p. e16765. Available at: https://doi.org/10.1371/JOURNAL.PONE.0016765.

Welch, R.M. and Graham, R.D. (2004) 'Breeding for micronutrients in staple food crops from a human nutrition perspective', *Journal of Experimental Botany*, 55(396), pp. 353–364. Available at: https://doi.org/10.1093/JXB/ERH064.

Weyers, J.D.B. (1990) *Methods in stomatal research*.

Weyers, J.D.B. and Lawson, T. (1997) 'Heterogeneity in Stomatal Characteristics', *Advances in Botanical Research*, 26(C), pp. 317–352. Available at: https://doi.org/10.1016/S0065-2296(08)60124-X.

Weyers, J.D.B., Lawson, T. and Peng, Z.Y. (1997) 'Variation in stomatal characteristics at the whole-leaf level', *Scaling-up: from cell to landscape* [Preprint].

Whitehouse, A.B. *et al.* (2011) 'Meristem culture for the elimination of the strawberry crown rot pathogen Phytophthora cactorum', *Journal of Berry Research*, 1(3), pp. 129–136.

Willmer, C. and Fricker, M. (1996) 'The distribution of stomata', *Stomata*, pp. 12–35. Available at: https://doi.org/10.1007/978-94-011-0579-8_2.

Wilson, F.M. *et al.* (2019) 'CRISPR/Cas9-mediated mutagenesis of phytoene desaturase in diploid and octoploid strawberry', *Plant Methods*, 15(1), pp. 1–13. Available at: https://doi.org/10.1186/S13007-019-0428-6/TABLES/2.

Wong, S.C., Cowan, I.R. and Farquhar, G.D. (1979) 'Stomatal conductance correlates with photosynthetic capacity', *Nature 1979 282:5737*, 282(5737), pp. 424–426. Available at: https://doi.org/10.1038/282424a0.

Woodward, F.I., Lake, J.A. and Quick, W.P. (2002) 'Stomatal development and CO2: Ecological consequences', *New Phytologist*, 153(3), pp. 477–484. Available at: https://doi.org/10.1046/J.0028-646X.2001.00338.X.

Xiong, D. and Flexas, J. (2020) 'From one side to two sides: the effects of stomatal distribution on photosynthesis', *New Phytologist* [Preprint]. Available at: https://doi.org/10.1111/nph.16801.

Xu, Z. and Zhou, G. (2008) 'Responses of leaf stomatal density to water status and its relationship with photosynthesis in a grass', *Journal of Experimental Botany*, 59(12), pp. 3317–3325. Available at: https://doi.org/10.1093/JXB/ERN185.

Yin, Q. *et al.* (2020) 'The relationships between photosynthesis and stomatal traits on the Loess Plateau', *Global Ecology and Conservation*, 23, p. e01146. Available at: https://doi.org/10.1016/J.GECCO.2020.E01146.

Yokoyama, G. *et al.* (2023) 'Diurnal changes in the stomatal, mesophyll, and biochemical limitations of photosynthesis in well-watered greenhouse-grown

strawberries', *Photosynthetica*, 61(1), pp. 1–12. Available at: https://doi.org/10.32615/PS.2023.001.

Yoo, C.Y. *et al.* (2012) 'The Arabidopsis GTL1 Transcription Factor Regulates Water Use Efficiency and Drought Tolerance by Modulating Stomatal Density via Transrepression of SDD1', *The Plant Cell*, 22(12), pp. 4128–4141. Available at: https://doi.org/10.1105/TPC.110.078691.

Yu Gong, H. *et al.* (2015) 'Transgenic Rice Expressing Ictb and FBP/ Sbpase Derived from Cyanobacteria Exhibits Enhanced Photosynthesis and Mesophyll Conductance to CO 2'. Available at: https://doi.org/10.1371/journal.pone.0140928.

Zhang, Z. *et al.* (2025) 'Peptide hormones in plants', *Molecular Horticulture 2025 5:1*, 5(1), pp. 1–50. Available at: https://doi.org/10.1186/S43897-024-00134-Y.

Zhu, R. *et al.* (2023) 'A stomatal optimization model adopting a conservative strategy in response to soil moisture stress', *Journal of Hydrology*, 617, p. 128931. Available at: https://doi.org/10.1016/J.JHYDROL.2022.128931.

Zhu, X.G., Long, S.P. and Ort, D.R. (2010) 'Improving Photosynthetic Efficiency for Greater Yield', *Annual Review of Plant Biology*, 61, pp. 235–261. Available at: https://doi.org/10.1146/ANNUREV-ARPLANT-042809-112206.

Zhu, X.G., de Sturler, E. and Long, S.P. (2007) 'Optimizing the Distribution of Resources between Enzymes of Carbon Metabolism Can Dramatically Increase Photosynthetic Rate: A Numerical Simulation Using an Evolutionary Algorithm', *Plant Physiology*, 145(2), pp. 513–526. Available at: https://doi.org/10.1104/PP.107.103713.

Zimmerli, C. *et al.* (2012) ‘PHO1 expression in guard cells mediates the stomatal response to abscisic acid in Arabidopsis’, 72(2), pp. 199–211. Available at: https://doi.org/10.1111/J.1365-313X.2012.05058.X.

Zoulias, N. *et al.* (2018) ‘Molecular control of stomatal development’, *Biochemical Journal*, 475(2), p. 441. Available at: https://doi.org/10.1042/BCJ20170413.